Metabolomic Analysis of Human Plasma during Acute Myocardial Ischemia and Reperfusion. A Non-targeted and Targeted Approach.

by

Arun Surendran

A Thesis submitted to the Faculty of Graduate Studies of
The University of Manitoba
in partial fulfilment of the requirements of the degree of

DOCTOR OF PHILOSOPHY

Department of Physiology and Pathophysiology,
Max Rady College of Medicine,
Rady Faculty of Health Science,
University of Manitoba
Winnipeg, Manitoba

CONTENTS

ACKNOWLEDGEMENTS

I want to express my heartfelt gratitude to my Ph.D. supervisor Dr. Amir Ravandi, for his continuous support and assistance during my research and writing this thesis. His patience and unconditional guidance throughout this journey always helped to bring out the best in me. I also appreciate my co-supervisor, Dr. Michel Aliani, whose constructive feedback and helpful advice helped me become a better researcher.

Besides my supervisors, I would like to thank my committee members, Dr. Grant Pierce and Dr. Harold Aukema, for their guidance and insightful comments. As a research institute director, Dr. Pierce provided the most excellent working environment for all students, particularly international students, to feel welcomed and supported. I appreciate Dr. Aukema for his persistent help and valuable input during my past years as a graduate student. I would also like to thank my mentors in India, Professor M. Radhakrishna Pillai and Dr. Abdul Jaleel, for encouraging me and providing me the opportunity to come to Canada and pursue Ph.D. at St. Boniface Hospital Research Centre, Winnipeg, Manitoba.

I would also extend my sincere thanks to current and past members of Dr. Ravandi's lab: Dr. Aleksandra Stamenkovic, Dr. Zahra Solati, and Dr. Andrea Edel for their assistance, encouragement, and never-ending support during the highs and lows of my journey. Moreover, I would like to thank all the summer trainees, Pascal, Shubh, Negar, and Hannah, for all the help, long conversations, laugh, and pleasant times we had together. I am grateful to all the research and non-research staff for making my days brighter with their beautiful smiles and helpful nature. My special thanks to Mahesh, Prathap, Mihir, Pema, Raghu, Keshav, Nikita, David, Glen, Nagakannan, and Abhay, whose friendship and support during my journey have been invaluable.

Lastly, I would like to thank my family for their generous support and love throughout my entire life. I thank them all; my father (Mr. Kadakampally Surendran), mother (Ms. Sulekha), wife (Ms. Smrithy), son (Master Ethan), brother (Mr. Anoop), and my in-laws for believing in me and always encouraging me to pursue my dreams. Thank you for all the love, care, and sacrifices you made for my happiness.

Thank you all for helping me to follow my dreams.

CONTRIBUTIONS OF AUTHORS

This thesis includes four multi-authored manuscripts. The list below outlines the type of contributions made by each author to manuscripts in order of appearance in the thesis.

PAPER 1:

Surendran, A., Atefi, N., Zhang, H., Aliani, M., & Ravandi, A. (2021). Defining Acute Coronary Syndrome through Metabolomics. *Metabolites, 11(10), 685.*

Conceptualization: A.R. and A.S.; literature collection: A.S., N.A., H.Z.; data curation, original draft writing: A.S.; reviewing, editing, and finalizing the manuscript: A.S., M.A., A.R.

PAPER 2:

Surendran, A., Aliani, M., & Ravandi, A. (2019). Metabolomic characterization of myocardial ischemia-reperfusion injury in ST-segment elevation myocardial infarction patients undergoing percutaneous coronary intervention. *Scientific reports, 9(1), 11742.*

Data curation: A.S., M.A., A.R.; formal analysis: A.S., M.A., A.R.; methodology: A.S., M.A., A.R.; supervision: M.A., A.R.; writing ± review & editing: A.S., M.A., A.R.

PAPER 3:

Surendran, A., Atefi, N., Ismail, U., Shah, A., & Ravandi, A. (2022). Impact of myocardial reperfusion on human plasma lipidome. *iScience, 25(2), 103828.*

Conceptualization, A.R. and A.S.; methodology, A.R. and A.S.; sample preparation, A.S. and N.A.; statistics, A.S.; formal analysis, A.S, U.I.; visualization, A.S.; writing - original draft, A.S.; writing - review & editing, A.S, A.Shah A.R. and.; supervision, A.R.

PAPER 4:

Surendran A, Ismail U, Atefi N, Bagchi AK, Singal PK, Shah A, Aliani M, Ravandi A. (2023). Lipidomic Predictors of Coronary No-Reflow. *Metabolites, 13(1), 79.*

Conceptualization, A.R.; methodology, A.R., U.I., A.B., A.S.; sample preparation, A.S., N.A.; statistics, A.S., M.A.; formal analysis, A.S, U.I.; visualization, A.S.; writing - original draft, A.S.; writing - review & editing, A.S, A.R. and M.A.; supervision, A.R., A.Shah, M.A., and P.S.

LIST OF TABLES

LIST OF FIGURES

ABSTRACT

Revascularization of the infarct vessel by the primary percutaneous coronary intervention (PCI) is the treatment of choice for patients presenting with ST-segment elevation myocardial infarction (STEMI). However, myocardial reperfusion can paradoxically augment the injury to the myocardium through a process known as ischemia/reperfusion (IR) injury, which reduces the benefits of blood flow restoration. The pathophysiological mechanism underlying the development of I/R injury remains poorly understood. Herein, we employed a comprehensive metabolomics platform integrating non-targeted and targeted approaches to help us better understand the metabolic and lipid pathways impacted during I/R.

Our non-targeted metabolomics analysis discovered 130 circulating metabolites that were significantly altered ($p<0.001$) in the setting of I/R injury during the first 48 hours post-reperfusion. Lipid molecules formed the largest pool of metabolites changing over the first 48 h after reperfusion. The pathway enrichment analysis identified the altered metabolic pathways indicative of the early reaction to reperfusion and late response to reperfusion. Also, we identified a select group of lipid species that can predict the extent of myocardial infarction based on the initial blood sample.

Based on our above findings, we selected a targeted lipidomics approach to confirm our findings from the initial untargeted metabolomic analysis regarding the changes in plasma lipidome following reperfusion. We found that except for oxidized phospholipids (OxPL), the total amount of most of the lipid classes was markedly reduced immediately after reperfusion. The circulating free fatty acids (FA) exhibited the most extensive change in the first 24 h after PCI. We found that specific lipid species (acylcarnitine 18:2, TG 51:0, and LPC 17:1) could also distinguish STEMI

patients with less cardiac injury from those with sizeable cardiac injury. These lipids were also associated with future cardiovascular events.

Given the vital role played by lipids in the onset and progression of reperfusion injury, we next explored the role of lipids in the no-reflow phenomenon, which sets out during the ischemic period and then progresses during the reperfusion phase. Our analysis showed that the baseline levels of specific lipid species mainly belonging to the phosphatidylcholine (PC), alkylphosphatidylcholine (PC(O)), and sphingomyelin (SM) species were elevated in no-reflow patients. The fatty acid levels were markedly reduced ($p<0.05$) in no-reflow patients following reperfusion. We also found that sphingomyelin species (SM 41:1 and SM 41:2) were positively correlated with markers of no-reflow at pre-PCI and post-PCI.

To summarize, we have developed the most detailed metabolomics and lipidomics atlas of human plasma during I/R injury. The results from this study will move us closer to our ultimate goal of devising therapeutic options to mitigate myocardial damage following acute myocardial infarction.

CHAPTER 1. Review of literature

Published: Metabolites (2021), 11(10), 685

Defining acute coronary syndrome through metabolomics

Arun Surendran BE, MBA[1,2,3], Negar Atefi BSc[1], Hannah Zhang MSc[1], Michel Aliani PhD[4], Amir Ravandi MD PhD[1,3,5]

[1]Cardiovascular Lipidomics Laboratory, St. Boniface Hospital, Albrechtsen Research Centre, [2]Mass Spectrometry and Proteomics Core Facility, Rajiv Gandhi Centre for Biotechnology, Kerala, India, [3]Department of Physiology and Pathophysiology, [4]Faculty of Agricultural and Food Sciences, Rady Faculty of Health Sciences, University of Manitoba, [5]Section of Cardiology, Department of Medicine, Rady Faculty of Health Sciences, University of Manitoba

Corresponding author
Dr. Amir Ravandi MD PhD FRCPC
Interventional Cardiology
Cardiovascular Lipidomics Laboratory,
St. Boniface Hospital,
409 Tache Ave,
Winnipeg, MB Canada R2H 2A6

Phone.204-235-3206 and 204-235-3414
Fax.204-235-0793 and 204-235-0793

Email: aravandi@sbgh.mb.ca

1.1 Abstract

As an emerging platform technology, metabolomics offers new insights into the pathomechanisms associated with complex disease conditions, including cardiovascular diseases. It also facilitates assessing the risk of developing the disease before its clinical manifestation. For this reason, metabolomics is of growing interest for understanding the pathogenesis of acute coronary syndromes (ACS), finding new biomarkers of ACS, and its associated risk management. Metabolomics-based studies in ACS have already demonstrated immense potential for biomarker discovery and mechanistic insights by identifying metabolomic signatures (e.g., branched-chain amino acids, acylcarnitines, lysophosphatidylcholines) associated with disease progression. Herein, we discuss the various metabolomics approaches and the challenges involved in metabolic profiling focusing on ACS. Special attention has been paid to the clinical studies of metabolomics and lipidomics in ACS, with an emphasis on ischemia/reperfusion injury.

Keywords: metabolomics, lipidomics, acute coronary syndrome, ischemia/reperfusion injury

1.2 Graphical abstract

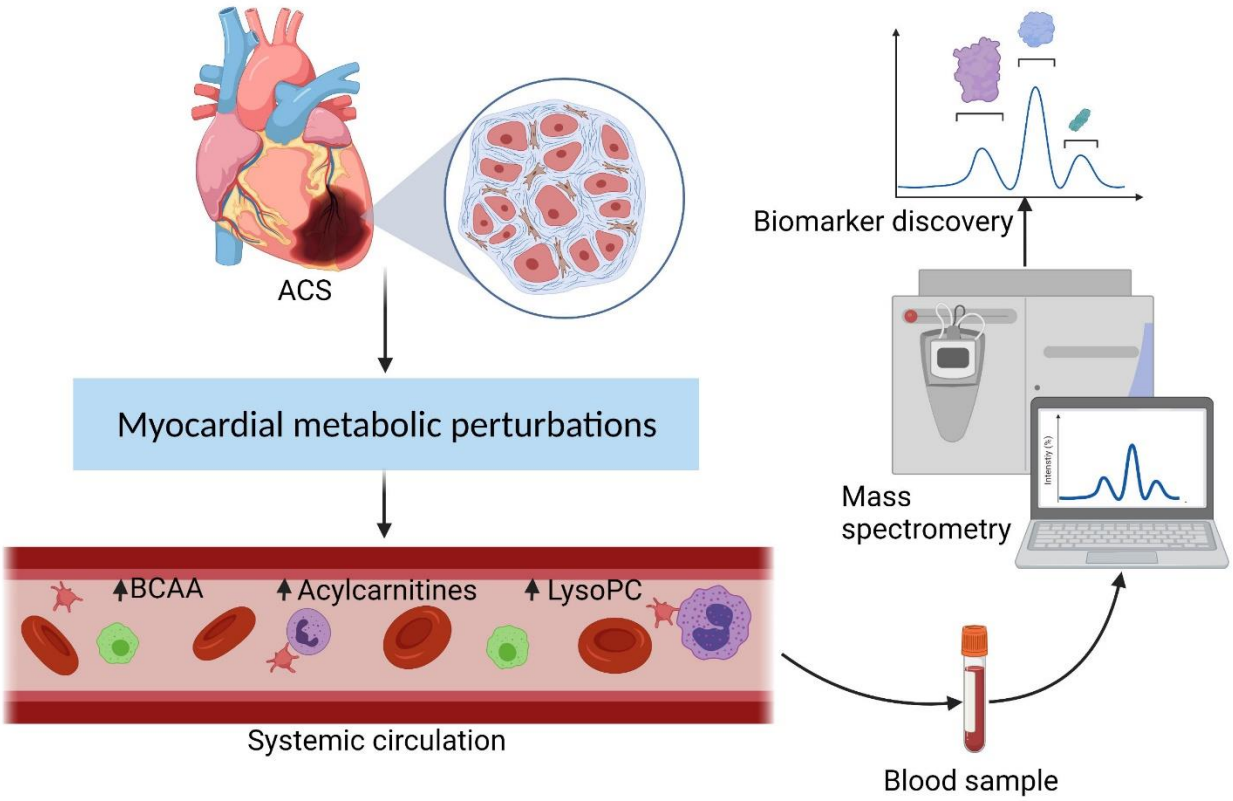

Defining acute coronary syndrome through metabolomics.

1.3 Abbreviations

ACS, acute coronary syndrome; AMI, acute myocardial infarction; BCAA, branched chain amino acids; CAD, coronary artery disease; CE/MS, capillary electrophoresis and mass spectrometry; CVD, cardiovascular disease; GC/MS, gas chromatography and mass spectrometry; I/R, ischemia/reperfusion; LC/MS, liquid chromatography and mass spectrometry; LDL, low density lipoprotein; HDL, high density lipoprotein; MACE, major adverse cardiac events; MS, mass spectrometry; NMR, nuclear magnetic resonance; NSTEMI, non-ST-segment elevation myocardial infarction; PCI, percutaneous coronary intervention; ROS, reactive oxygen species; STEMI, ST-segment elevation myocardial infarction; UA, unstable angina

1.4 Introduction

Coronary Artery Disease (CAD) continues to be a major public health concern with considerable morbidity and mortality in developed countries[1]. CAD includes chronic coronary artery disease (stable angina), and acute coronary syndrome (ACS), which almost invariably presents as chest discomfort with or without dyspnea. It is estimated that in the United States alone, 720,000 people experience a new episode of ACS every year[2]. The costs and resource utilization associated with ACS also place an enormous economic burden on the health care system[2-4]. For instance, in a retrospective single-cohort study, it was found that the average one-year cost per patient associated with ACS was around 32,000 US dollars[4]. The term ACS refers to a spectrum of conditions in which myocardial ischemia or infarction develops due to acute occlusion of coronary blood flow to any part of the heart. The usual cause of acute occlusion is coronary artery thrombosis caused by rupture or erosion of a high-risk, lipid-laden, atheromatous plaque[5]. This sudden, reduced blood flow to the heart results in an imbalance between myocardial metabolic demands and blood supply leading to myocardial ischemia, which is the hallmark of ACS[3,6]. The imbalance may also be caused by several other cardiac abnormalities, including coronary artery embolism, coronary spasm, coronary dissection, severe anemia, and calcific aortic valve stenosis[3]. Depending upon the range of ischemic state, location of the occlusion, cardiac biomarker levels (e.g., troponin), and ST-segment elevation on the electrocardiogram (ECG), ACS is mainly categorized into three types (**Figure-1.1**), namely unstable angina (UA), non-ST-segment elevation myocardial infarction (NSTEMI), and ST-segment elevation myocardial infarction (STEMI)[5]. Typically, a complete coronary artery occlusion leading to myocardial tissue injury and elevated cardiac troponin level results in STEMI. Partial occlusion or occlusion with collateral circulation may lead to NSTEMI or UA, depending on the presence or absence of cardiac troponin level, respectively[5,7]. Troponins

are released into the bloodstream when there is any damage to the heart muscle[8]. Due to its high sensitivity and specificity, cardiac troponin measurement is an essential element in diagnosing and managing ACS.

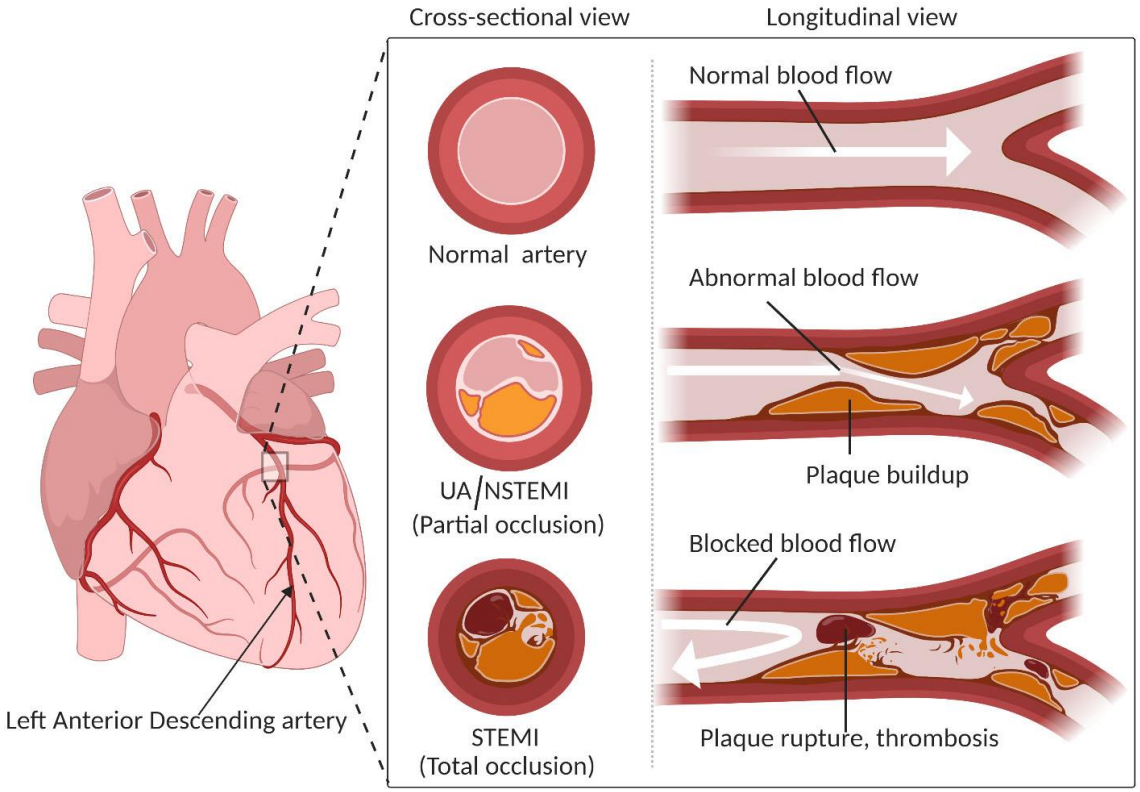

Figure-1.1: Classification of acute coronary syndromes. Acute coronary syndromes are categorized into unstable angina (UA), non-ST-segment elevation myocardial infarction (NSTEMI), and ST-segment elevation myocardial infarction (STEMI). A complete coronary artery occlusion due to thrombus formation results in STEMI, where the coronary blood flow is completely obstructed. A partial occlusion of the artery (blood flow is not entirely restricted) can result in NSTEMI or UA.

The human heart is the most metabolically active organ and under normal conditions, cardiac metabolism is tightly regulated by oxygen availability, substrate oxidation, hormonal and neurohumoral signals, among other factors[9]. The primary substrates for cardiac ATP production are lipids, carbohydrates, lactate, and glycogen[9]. Of these, lipids alone contribute to 60-90% of ATP production in the heart *via* oxidation of fatty acids[10]. Due to its exuberant use in the myocardium and its role in maintaining the myocardial cell structure and cardiac function, alterations in lipid metabolism contribute to many cardiovascular pathologies, including atherosclerosis, insulin resistance, hypertension, and type 2 diabetes mellitus[11]. A fall in oxygen level and substrate availability during myocardial ischemic conditions alters the dynamic equilibrium state of cardiac metabolism and leads to loss of homeostasis[12]. Hence, it is not surprising that ACS involves changes in cardiac metabolism. While some of the metabolic changes help the heart adjust to the altering substrate needs and physiological demands, most changes are maladaptive and initiate other cardiac abnormalities, including myocardial stunning, cell death, and contractile dysfunction[13]. Recent findings suggest that alterations in the cardiac metabolism alone can also perpetuate disturbances in systemic metabolism[14]. Hence, blood-derived plasma or serum metabolic profile could provide insights into the pathophysiological processes happening within the heart in the event of an ACS.

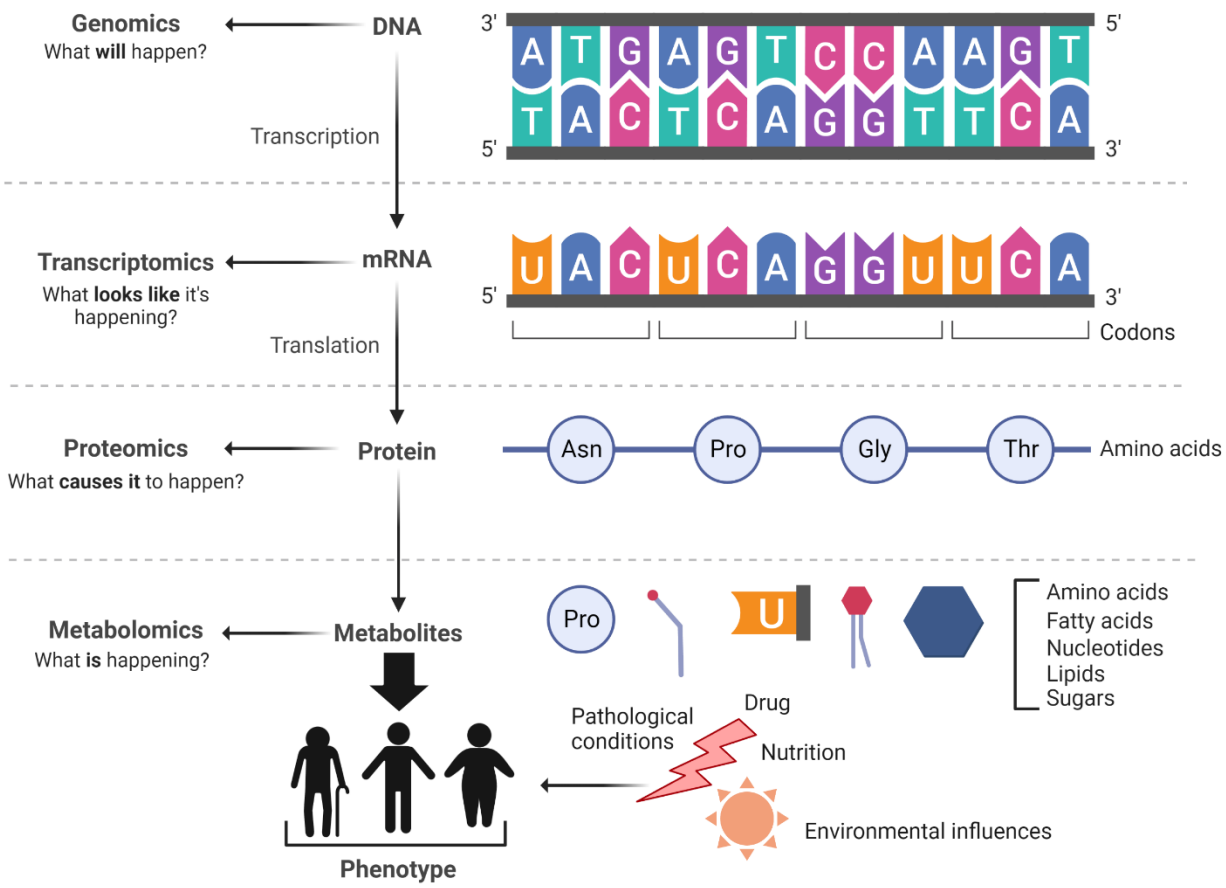

Figure-1.2: The 'omics cascade'. It depicts the directional flow of biological information from genes to metabolites. Metabolomics is at the end of the cascade and is closer to the phenotype of an organism than proteomics or genomics.

Metabolomics is the new entrant in the 'omics' cascade in systems biology (genomics, transcriptomics, and proteomics) approach (**Figure-1.2**). It involves high-throughput identification and quantification of small chemical compounds (<1000 to 1500 Da), commonly known as metabolites, present in a variety of biological systems such as a cell, an organism, or biological fluids[15-17]. The complete set of these small-molecule metabolites and their interactions within the biological system are known as the metabolome. The metabolome includes endogenous (e.g., amino acids, fatty acids, sugars, carbohydrates, vitamins, lipids, and their derivatives) as well as exogenous (e.g., pollutants, pharmaceuticals, food additives, xenobiotics) compounds. Lipidomics

is a novel subdivision of metabolomics, dedicated to the detailed analysis of complex lipid mixtures found in biological materials[18]. The metabolome composition is inherently dynamic and flexible due to its continuous interaction within the biological system and also with the outside environment, including the effects of drugs, nutrition, lifestyle, or therapeutics[19]. Hence, any perturbations in metabolite levels are a true reflection of the phenotype and function of the developmental or pathological state of the biological system. Recent advancements in 'omics' technology platforms, particularly genomics and proteomics technologies, have enabled us to assess the changes within the genome and the proteome in cardiovascular diseases (CVD), including ACS. Metabolomics and lipidomics are required to bridge the knowledge gap between phenotype and metabolic abnormalities in CVD.

Given that ACS is a multifactorial phenomenon, it requires a global assessment of molecular/cellular pathological functions from both untargeted and targeted approaches. Recognizing this, the American Heart Association recently released a scientific statement highlighting the potential impact of metabolomics in cardiovascular health and disease[20]. Thus, metabolomics and lipidomics are now evolving as essential tools in cardiovascular research (i) to gain a better understanding of the mechanisms underlying CVD, (ii) to determine the clinically relevant metabolomic perturbations, and (iii) to identify novel biomarkers involved in various cardiovascular disease conditions.

1.5 Analytical tools in metabolomics

Though metabolomics research is considered a relatively new field, the initial report of screening metabolites in body fluids for diagnostic purposes can be traced back to ancient China (1500 – 2000 BC), where traditional Chinese physicians used ants to diagnose diabetes by evaluating the smell, taste, and color of urine samples from patients[21]. However, the pioneering work done by the

laboratories of Robinson and Pauling research groups in the early 1970s[22-24] laid the foundation for a new era in metabolomics research. They successfully quantitated metabolites from various biofluids, including human blood and urine vapor, by applying gas chromatography coupled with mass spectrometry (GC/MS) technique. The first printed reference to the word 'metabolic profile' appeared in the literature in 1971[25,26], when Horning and Horning used GC/MS platform to profile different human metabolic products, including sugars, alcohols, and drug metabolites from blood and urine samples. Since these initial efforts, several investigators have contributed in parallel to develop this naive concept into a format that is on par with the other established 'omics' approaches, namely genomics and proteomics. The word 'metabolome' was first used by Oliver Fiehn, a key metabolomics researcher, in 1998[27] to denote the changes in relative concentrations of metabolites due to the deletion or overexpression of a gene. Due to the metabolome's vast complexity and dynamic nature, no single instrument platform currently available can simultaneously analyze all the metabolites present in a biological sample. For example, within lipids alone, diverse lipid classes and lipid molecular species are categorized based on their structural and chemical properties. Moreover, while some lipids such as cholesteryl esters and triglycerides are usually present in high concentrations (1-10 mmol/L) in samples such as plasma, others such as eicosanoids derived from arachidonic acid are present only in trace amounts (1-10 pmol/L)[28]. Numerous analytical platforms with varying degrees of specificity and sensitivity have been developed in the last two decades to measure specific portions of the complex metabolome. Presently, nuclear magnetic resonance (NMR) spectroscopy and mass spectrometry (MS), coupled with gas or liquid chromatography (GC/MS or LC/MS, respectively), are the most widely used analytical tools in metabolomics investigations[15]. In addition, analytical platforms such as MS coupled with capillary electrophoresis (CE/MS), shotgun lipidomics, and direct MS infusion

methods are also used to fully understand the broad spectrum of metabolites[15,29]. For instance, while NMR makes the study of different isomers possible, GC/MS or LC/MS can analyze a large variety of molecules with high sensitivity, and CE/MS can provide data of high resolution. **Table-1.1** summarizes the main advantages and disadvantages of using MS and NMR techniques.

Table-1.1: A summary of the important advantages and limitations of NMR and MS techniques

Technique	Advantages	Disadvantages
NMR	Highly reproducible results	Relatively low sensitivity compared to MS
	Provides structural information about the compounds	Only suited for medium to high abundant metabolites (micro molar range)
	Minimal requirement for sample preparation	Relatively longer data acquisition times compared to MS
	Non-destructive in nature and suitable for multiple analysis of the same sample	Highly pH sensitive
	Allows investigation of tissue energetics and *in vivo* metabolism	
	Suitable for compounds which are otherwise difficult to ionize or derivatize	
	Appropriate to use with samples with high salt content including urine	
	Well-established NMR spectra library to aid data analysis	
	Ability to detect different isomeric products	
GC/MS	Method of choice for the analysis of volatile/non-polar metabolites	Detection of polar metabolites is difficult and needs chemical derivatization.
	Increased signal-to-noise (S/N) ratios and relatively better resolution	Limited metabolome coverage
	Publicly available spectral libraries for compound identification	The high temperature applied in GC/MS can cause degradation or transformation of compounds.
LC/MS	Ability to analyze metabolites with wide range of polarity including thermally unstable ones	Not suitable for the analysis of gaseous mixtures
	Quicker and less extensive sample extraction procedures	Decreased sensitivity due to ion suppression

	Suitable for measurement of compounds of lower volatility	Difficulty in distinguishing isomers (both structural and positional) of molecules
	Requires little sample volume	

Abbreviations: NMR, nuclear magnetic resonance spectroscopy; GC/MS, gas chromatography/ mass spectrometry; LC/MS, liquid chromatography/mass spectrometry

1.5.1 NMR spectroscopy

NMR spectroscopy is one of the most prevalent techniques used in metabolomics research for structural elucidation of both pure compounds and mixtures. This technique relies on the magnetic spin properties (nuclear magnetic moment and angular momentum) of protons and neutrons in the nucleus of an atom to provide information on molecular structures. It is based on the principle that any nucleus possessing a (non-zero) nuclear spin can release characteristic radiofrequency waves when placed in an external magnetic field. The resonance frequency of the released energy is affected by the chemical microenvironment of these atoms and the coupling effect with nearby nuclei. The resulting frequencies are recorded as chemical shifts, and their patterns can be used for compound identification[15]. The most commonly used nuclei for analysis are ^{1}H, ^{13}C, and ^{31}P isotopes. The proton NMR spectroscopy (^{1}H-NMR) has the advantage of having greater relative sensitivity and a short acquisition time. For this reason, ^{1}H-NMR is widely used to identify and quantify a large number of small molecules coexisting in biological material, such as tissues, whole cells, and biofluids. The major disadvantage of traditional one-dimensional (1D) ^{1}H-NMR is that the spectrum became very complex for larger, more complex molecules, making interpretation difficult as most of the signals overlap heavily. However, two-dimensional (2D) NMR helps circumvent this challenge by resolving signals that usually overlap in ^{1}H-NMR. In short, 2D-NMR provides extra information about a molecule than traditional ^{1}H-NMR spectra, thereby making

spectral interpretation easy. Current practice requires 1D ^{1}H-NMR to complement 2D-NMR or mass spectrometer for molecular identity confirmation. Carbon-13 NMR spectroscopy (^{13}C-NMR) and phosphorous-31 NMR spectroscopy (^{31}P-NMR) predominantly find applications in cellular energetics, particularly in tracking cellular changes in cardiac metabolism under normoxic and ischemic conditions[30-32].

^{1}H-NMR spectroscopy is routinely used to analyze several low-molecular-weight molecules, including branched-chain amino acids (e.g., valine, isoleucine) and ketone bodies from plasma and serum to find biomarkers for ACS[33-35]. In a study looking at potential candidate biomarkers for UA from plasma samples, ^{1}H-NMR NMR spectroscopy identified ten steroid metabolites belonging to the steroid hormone biosynthesis pathway, including one mineralocorticoid (deoxycorticosterone) and nine sex hormone metabolites (e.g., estradiol, 2-hydroxyestradiol)[36]. Also, NMR has become the primary tool for analyzing urinary metabolites. In a study involving UA patients[37], ^{1}H-NMR NMR analysis could successfully identify and quantitate waste metabolites such as trimethylamine-N-oxide (TMAO) and trimethylamine (TMA) from urine specimens in addition to short-chain fatty acids (e.g., 3-hydroxybutyrate), organic acids (e.g., indol-3-acetate, methylmalonate) and amino acids (e.g., lysine, proline).

The main advantages of NMR are its non-destructive nature and higher reproducibility[38,39]. However, it is often limited by its requirement of a larger sample amount (2–50 mg) and therefore reduced sensitivity for low abundant compounds[40]. An early metabolomics study showed that ^{1}H-NMR spectroscopy could correctly diagnose the presence of CAD and assess its severity[41]. Other applications of NMR based metabolic profiling in ACS mainly include analysis of both urine[37] and serum[34,35] metabolites for unstable angina pectoris disease, investigating the serum metabolic characteristics of acute myocardial infarction (AMI) patients in comparison with those of chest

pain controls[42], and deciphering the metabolomic fingerprint of coronary blood in STEMI patients[43]. **Table-1.2** shows that in ACS metabolomics studies, ^{1}H-NMR spectroscopy is the most used NMR technique for analyzing biofluids, including plasma, serum, and urine.

1.5.2 Mass spectrometry

Mass spectrometry (MS) provides accurate weight measurements of one or more molecules within a sample of interest. MS separates the molecules based on their specific mass-to-charge ratio (*m/z*) by converting them into ions in the gas phase[44]. The separated ions are then sorted according to their acceleration and deflection in an external electromagnetic field. The final output is presented as the relative abundance of each ion as an *m/z* spectrum. MS is extensively used in the field due to its wide dynamic range, speed, high sensitivity, and the ability to identify and quantify more metabolites in a single measurement relative to NMR.

The MS essentially has three main components; 1) the ion source, where the sample gets ionized; 2) the mass analyzer, where the ions get separated according to their mass to charge (*m/z*) values; and 3) the detector, which provides a count of the intensity of separated ions[45]. The most commonly used mass analyzers are Time-of-Flight (TOF), magnetic sector, and quadrupole, each with its own set of strengths and limitations[46]. Time-of-Flight, as the name implies, uses a flight tube of known length, where the ions get separated based on the flight time (time taken for the ions to travel through the flight tube). TOF MS consists of a pulsed ion source and therefore is best suited with ionization methods that ionize molecules in pulses, such as laser ionization. TOF systems have an excellent mass range and are generally utilized for high-resolution MS. Unlike TOF systems, magnetic sector mass analyzers use a magnetic field to sort ions of different mass to charge ratios. The key advantages of magnetic sector mass analyzers are their high sensitivity and high resolution. As its name suggests, quadrupole consists of four parallel cylindrical or hyperbolic

rods. The opposite rods are connected electrically inside a vacuum chamber. By changing the electrical potential, ions with different *m/z* values can be 'filtered' through the quadrupole to the detector one after another. The quadrupole mass analyzers are usually compact and have good scan speed, durability, and reliability. However, they usually have a limited mass range.

MS uses various ionization methods for mass analysis. The classic methods include matrix assisted laser desorption ionization (MALDI) and electrospray ionization (ESI), in addition to other methods such as electron impact (EI) ionization, chemical ionization, and atmospheric pressure chemical ionization (APCI)[47]. ESI is based on the evaporation of charged droplets and is notable for being the softest ionization method, allowing for generating ions with multiple charges with great sensitivity and no matrix interference[48]. However, some of the pitfalls of ESI include incompatibility with salts, complex mixtures, and impure samples. On the other hand, MALDI functions by proton absorption and transfer and can ionize metabolites with much higher masses (up to 300,000 Da). MALDI is also compatible with both salts in millimolar concentration as well as complex samples. One disadvantage of using MALDI is the potential for the degeneration of metabolites due to the acidic matrix or photogeneration via laser ionization. Also, MALDI is also not suitable to analyze low molecular weight compounds (<1,000 m/z) because of the matrix background interferences in this mass range[49]. Overall, it has been shown that using multiple ionization approaches with mass spectrometry can enhance the detection of global metabolome for complex samples[50].

A separation technique in a time dimension (GC, LC, or CE) is often employed before MS analysis to isolate the individual components from complex samples containing hundreds to thousands of small molecules[51]. The chromatographic separation techniques use the physicochemical properties of the compounds in a sample, such as polarity, size, presence of double bonds, to separate the

molecules inside the medium[52]. Hence, combinations of separation and MS, usually either GC/MS or LC/MS, have become the preferred analytical choice for small-molecule analysis from complex biological samples. The application of MS-based metabolic fingerprinting in ACS mainly includes investigating biomarkers for ACS[53-56], characterizing the metabolic difference between different types of ACS,[57-59] and identifying the molecular differences between patients with ACS and healthy controls[60,61].

For minimally complex samples such as synthetic peptides or pure compounds, direct infusion mass spectrometry (DIMS) or shotgun lipidomics (for lipid samples) are used. The samples are introduced directly into the MS without prior chromatographic separation. Though suited for high throughput metabolomics analysis, DIMS often suffers from matrix effect and ion suppression since all the sample components are infused simultaneously[62,63]. Direct infusion also leads to ion source contamination which usually takes a long time to recover. Recently introduced chip-based direct-infusion nano electrospray interfaces were successful in resolving this problem to a great extent[64]. Due to the lack of chromatographic separation, DIMS also cannot separate isomeric compounds. One approach to achieving isomeric separation is incorporating ion mobility spectrometry (IMS) as the separation process before MS[65]. Another drawback of DIMS system is that multiple ions of the same molecule, such as its molecular ions, adducts, and in-source fragments, can present in the mass spectrum and thus making interpretation of the data very difficult.

Compared to NMR, MS is the method of choice for global metabolite profiling and identifying unknown compounds within samples. MS can detect various metabolite classes (polar, non-polar, and neutral) depending on the choice of ionization mode (positive/negative). For instance, positive ESI mode works well with medium-sized polar molecules, whereas negative ESI mode is suitable

for carbohydrates and organic acids. It is worth mentioning that all clinical studies of lipidomics in ACS mentioned in **Table-1.3** were done using LC/MS platform. Also, MS also provides an excellent analytical platform for profiling the molecular composition of lipoprotein complexes. For example, multiple clinical studies[66-68] employed the LC/MS platform to highlight the changes in lipidome composition of HDL (high-density lipoprotein) during ACS pathogenesis.

NMR and MS primarily use two strategies to conduct metabolomics and lipidomics studies, i.e., untargeted, and targeted approaches[69,70]. The untargeted approach, also called open profiling, aims to analyze the most comprehensive set of metabolites from biological samples and is non-selective and non-discriminative towards metabolites screening. It is mainly used for the discovery of novel biomarkers or to generate a specific hypothesis. Usually, no pre-existing knowledge about the metabolic profile of the sample is required for this type of analysis. The untargeted approach usually compares metabolite levels between different groups (e.g., healthy control *vs*. disease) under similar conditions[69,71]. A schematic showing the different steps in untargeted metabolomics is shown in **Figure-1.3**.

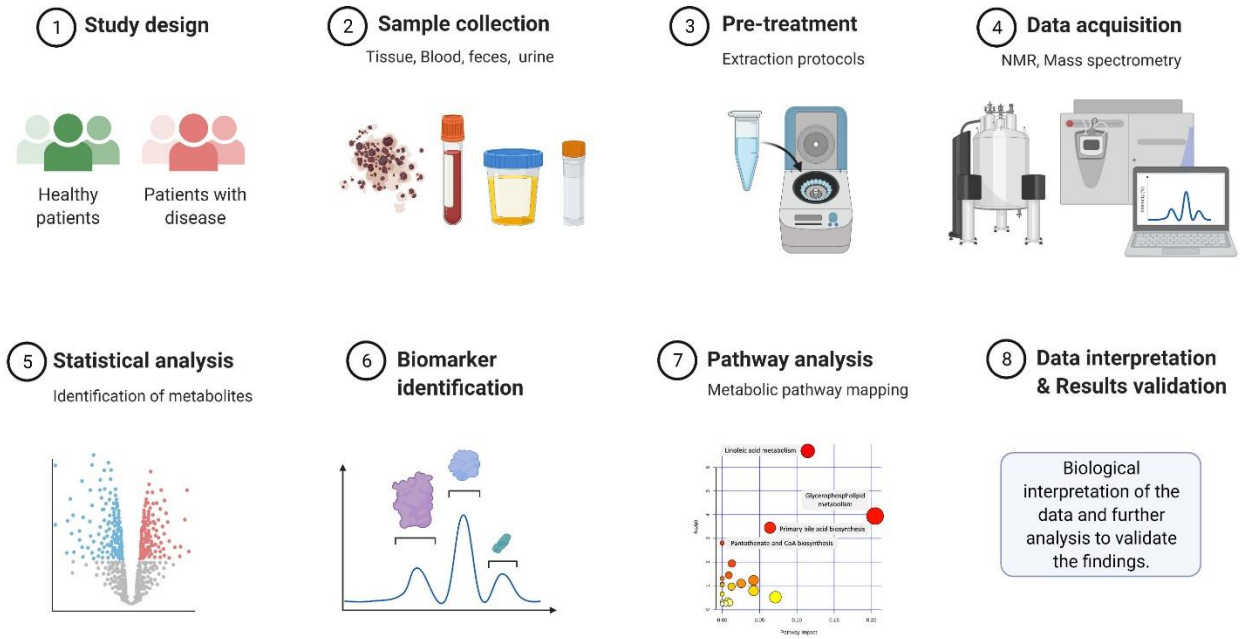

Figure-1.3: A standard workflow for untargeted metabolomics. After sample collection and extraction, the samples are analyzed by NMR spectroscopy or mass spectrometry. The raw data is then analyzed using appropriate software followed by statistical analysis to identify metabolites of interest or potential candidate biomarkers. Adapted from "Untargeted Metabolomics for Discovery of Disease Biomarkers", by BioRender.com (2021). Retrieved from https://app.biorender.com/biorender-templates

On the other hand, the targeted approach or closed profiling focuses on a limited number of known metabolites, such as 10-20 lipids, and seeks to quantify them. A hypothesis is being tested in this approach, and often the sample preparation and analytical techniques are more sophisticated. In the case of ACS, the most commonly used approach so far has been untargeted metabolomics to differentiate ACS profile from healthy controls. However, most ACS studies complement their untargeted analysis by performing a targeted analysis of those compounds that exhibited a significant difference between various groups for further quantitation and identity confirmation using the suitable internal standards. In a study to understand the underlying mechanisms associated with CAD progression, Zhang and colleagues initially performed an untargeted analysis of metabolites in plasma of 2324 patients who underwent coronary angiography[72]. They identified a total of 36 differential metabolites across different CAD types, including N-acetylneuraminic acid (a ligand for many hormones and lectins), whose levels were elevated in plasma during CAD progression. Subsequently, a targeted quantification was performed using isotope-labeled N-acetylneuraminic acid to confirm its vital role in CAD progression.

1.6 Pre-analytical considerations in metabolomics studies

The analytical quality of both untargeted and targeted metabolomics approaches is mainly dependent on the various pre-analytical steps involved in sample handling, sample collection, centrifugation, aliquoting, transportation, freezing, and storage[73]. Even minor discrepancies in any of these pre-analytical factors can greatly influence metabolomic assessments. Discrepancies may include, but are not limited to, choice of anticoagulants or preservatives added to the sample specimen, time delay, and storage temperature during blood preprocessing[74], diet and time of sampling in urinalysis[75,76], metabolite degradation or aggregation induced by air oxidation and light exposure[77,78], number of freeze-thaw cycles before aliquoting biological fluids[79], and time delay in transportation and sample storage[80]. Therefore, knowledge about different sample collection procedures and preparation protocols is essential to ensure reliable and reproducible results in a metabolomics study. A variety of biological fluids, including plasma, serum, urine, saliva, cerebrospinal fluid, bronchoalveolar lavage fluid, and cell and tissue extracts, are used in metabolomics studies depending upon the biological question under study and the pathophysiological nature of the disease process[81].

1.6.1 Serum vs. Plasma

Notably, most of the metabolomics studies in ACS have been done using either plasma or serum as the sample source[34,35,53-55]. The general theme of most of these plasma or serum-based studies is to find biomarkers associated with ACS and its subtypes, compared to healthy controls. Though both plasma and serum matrices provide an excellent functional readout of an organism's metabolic activity, the question regarding which is more suitable is still highly debatable. Both plasma and serum are derived from the liquid portion of the blood. The serum is the liquid part that remains after the blood has clotted, and it is obtained by centrifugation after clotting. Plasma

is not coagulated and is obtained by adding an appropriate anticoagulant (heparin, citrate, or Ethylenediaminetetraacetic acid (EDTA)) to the whole blood, followed by centrifugation and aliquoting[81]. Typically, plasma makes up to 55% of the total volume of blood, and it contains dissolved proteins, clotting factors, salts, lipids, and other suspended materials in water. The serum is similar to plasma, except it lacks fibrinogen (clotting factor). Contrary to serum, plasma has the advantage that it can be immediately placed on ice, thereby avoiding the possible loss of labile metabolites due to enzymatic conversion or other degradation processes during clot formation at room temperature[81]. Several studies have tested the role of pre-analytical factors on the metabolic composition of serum and plasma[82-84]. Teahan et al. showed that variations in certain pre-analytical factors such as clotting time and temperature, the presence/absence of anticoagulant, and storage conditions including repeated freeze−thaw cycles, can introduce bias into metabolic data[84]. Also, recent data suggests that it is not advisable to combine serum samples exposed to different clotting procedures (e.g., thrombin *vs.* silicate-enhanced) or different clotting times into a single sample set for biomarker analysis, as coagulation and associated processes can alter metabolite concentrations[85]. This limitation can be highly challenging, particularly in multicentric clinical studies involving humans, where samples are collected from different hospital sites and transported to a centralized facility for further processing and analysis.

Besides assessing various pre-analytical factors, numerous studies have also investigated the difference in metabolic profile generated by serum and plasma samples[85-87]. In a study comparing serum and plasma metabolic profiles[85], it was found out that 46% out of the 216 identified metabolites were significantly different between the two, and except for three (methionine, C2:0- and C3:0-carnitine), the levels of all other metabolites were higher in serum. In line with this, in another metabolomics study comprising 377 individuals[87], it was reported that although the

reproducibility was slightly better in plasma than serum, the concentrations of analytes were generally higher in serum with an average relative difference of 11.7%. In another study involving 29 small-cell lung cancer patients[86], it was shown that neither fluid is superior to the other, and the two metabolomes were markedly similar in terms of reproducibility, specificity, and metabolic coverage. These studies suggest that even though both biofluids are comparable in terms of analytical throughput, serum may provide better sensitivity than plasma.

1.6.2 Polar vs. Non-polar metabolites

Due to the enormous diversity in the physicochemical properties of metabolites, especially polar (including amino acids, nucleic acids, and sugars) and non-polar (including fatty acids and other lipids) metabolite classes, no ideal extraction protocol exists that can extract both polar and non-polar metabolites from the same sample. Accordingly, a comprehensive analysis of the entire metabolome in a biological sample requires multiple extraction strategies to cover different metabolite classes. Hence, multiple aliquots of the same sample with specific extraction procedures, such as using a modified Bligh-Dyer protocol for extracting polar metabolites[88], are required to obtain extensive coverage of the entire cellular metabolome, which in turn facilitates the need to have a larger sample amount. In studies where sample amount is a limiting factor, this approach might not be feasible. Of late, efforts have been made to develop extraction protocols that can extract both polar and non-polar analytes from the same sample[89]. Selecting the proper extraction protocol is critical in all metabolomics studies as the metabolite extraction step directly affects all downstream steps of metabolomics data analysis.

1.7 Extraction procedures for metabolomics

The reliability and accuracy of metabolic data also depend upon the sample preparation strategy. Ideally, the sample processing should be fast, easy, minimal, and tailored to the analytical scheme.

Common approaches include homogenization, dialysis, fractionation, extraction, distillation, centrifugation, and concentration. Critically, these approaches should be compatible with the nature of the biological matrix, chemical/physical properties of analyte of interest, and the final detection technology. For example, in a typical LC/MS platform, sample preparation is usually the most time-consuming and error-prone step of the chromatographic assay. The inherent 'matrix effect' on different samples such as plasma, serum, urine, and tissue lysate, presents significant analytical challenges during LC/MS analysis[90]. Matrix effects are caused by co-eluting endogenous components and preservative agents in the same matrix,[91] which often lead to material buildup on the analytical column and ion source in LC and MS, respectively. This can cause ion suppression or enhancement, drift in chromatographic response, increased or reduced analytical signal, reduced column life, and frequent MS cleaning[92]. Cumulatively, these issues may compromise analytical accuracy and increase the total analysis time, in addition to significantly affecting the cost of MS analysis[90]. Therefore, thoughtful selection and optimizing sample preparation procedures are essential to minimize variability and improve analytical performance in metabolomics studies.

The three most popular sample preparation techniques in metabolomics analysis include protein precipitation (PPT), liquid-liquid extraction (LLE), and solid-phase extraction (SPE)[93,94]. PPT generally begins with adding organic solvents such as methanol, acetonitrile, or a combination thereof to the sample, followed by agitation and centrifugation[95]. Its 'nonselective' nature makes it well suited for global metabolomics analysis. Adding an ice-cold organic solvent is beneficial as it may improve the efficiency of protein removal and prevent metabolite degradation as the sample warms up from its stored frozen state[96]. While agitation increases the protein accumulation rate, centrifugation helps separate the supernatant holding analytes from the protein pellets[97].

Though this method provides high metabolite coverage, PPT is often time-consuming, particularly while dealing with hundreds of samples manually, as in large-scale epidemiological studies. Robotic systems capable of performing automated protein precipitation such as membrane-based protein precipitation filter plates have been developed recently to address this issue[93,98,99].

Another classic method used for the qualitative/quantitative identification of metabolites is biphasic LLE. LLE utilizes two immiscible liquids for the extraction of analytes. In LLE, the analyte is differentially distributed between the aqueous matrix and water-immiscible organic solvent[93]. Traditionally, LLE is most preferred for doing comprehensive lipid analysis[100] (i.e., global lipidomics). Apart from enriching analytes of interest (here, lipids) and improving signal-to-noise ratios, any extraction protocol used in lipidomics should also remove any non-lipid compounds. Being insoluble in water, lipids are extracted from a biological matrix, such as blood plasma or tissue, using organic solvents. The most widely used method for isolating lipids from biological samples was devised by Folch et al. more than 60 years ago using 2:1 chloroform/methanol (v/v) as the solvent mixture[101]. In this two-phase LLE procedure, most lipids get dispersed into the lower chloroform phase and is clearly separated from the upper methanolic phase holding non-lipid substances. To enhance recovery, Bligh and Dyer later revised Folch's method by combining chloroform, methanol, and water[102]. The disadvantage of these two methods is that the recovery of the lower lipid fraction is often cumbersome, resulting in contamination of the isolate and blockage of the analytical column. In 2008, Matyash and co-workers[103] showed that an extraction procedure using methyl-*tert*-butyl ether (MTBE) could solve this problem as the lipid-containing organic layer settles at the top during phase separation thereby enabling a much cleaner lipid extraction. More recently, a chloroform free one-phase lipid extraction protocol based on a mixture of butanol and methanol (BUME) was described by Löfgren and coworkers[104]. This

novel approach is rapid and shows similar extraction efficiency compared to the Folch and the Bligh and Dyer procedures.

In SPE, samples are loaded onto a solid sorbent held primarily on a cartridge device (SPE cartridge). The analyte of interest present in samples is selectively retained by the sorbent material[105]. The retained analyte is then eluted with a suitable solvent[106]. Different SPE types include reverse, normal, anion, cation, and mixed-mode sorbents[93]. Due to its highly selective nature, SPE is not recommended for global metabolomics profiling[107]. It is mainly used to concentrate analytes present at low levels and purify analytes from matrix interferences. There exist contradictory reports regarding the analytical reproducibility using the SPE procedure. In a study comparing PPT and SPE procedures, SPE showed improved repeatability than PPT for human plasma metabolic profiling[108]. However, in another similar study evaluating different human plasma preparation protocols, the metabolome coverage and repeatability of the SPE procedure is reported to be lower than PPT protocols[109]. Once an extraction procedure is selected, caution should be taken to ensure that the same procedure is repeated consistently throughout the entire study. For large-scale cohort studies, maintaining this consistency presents a real challenge. Inconsistency in extraction procedures is a source of variation in the dataset and may compromise the robustness and accuracy of final results.

1.8 Data processing in metabolomics

As with genomics platform, metabolomics studies generate a large amount of multidimensional, non-linear, and non-normal data[110]. Due to its sheer complexity, metabolomics data-analytical approaches rely heavily on advanced computational approaches. Many instrument-specific and open-source software solutions are available, such as MetaboAnalyst[111] and XCMS[112], that can do the critically important steps in metabolomics data analysis, such as run alignment, peak picking,

data preprocessing (e.g., deconvolution, scaling, and normalization), annotation, and compound identification. However, selecting a suitable approach or software is often confusing and depends upon the separation technique, detection mode and output file format (e.g., mzXML, mzML, NetCDF) generated by each instrument. Also, there remains little accord or harmonization among different software in handling various cross-vendor file formats. Recently, much effort has been made to address this issue, and new software platform such as Progenesis QI[113] has been developed that is compatible with a wide variety of instruments and can perform platform-independent metabolomics data analysis.

1.8.1 Handling unwanted variances in metabolomics data

Analytical and biological variability issues are critical in human metabolomics studies. If these unwanted variations are not accounted for, it may affect the statistical power of detecting metabolites that are characteristic of, for example, a disease state such as ACS. Laboratory procedures or technological platforms primarily introduce analytical variability. Typical example includes matrix effects, temperature changes, solvent pH changes, sample degradation over time in extended sample runs spanning weeks or months, fluctuation in instrumental sensitivity, and personal errors[114]. One way to combat these analytical errors is by employing suitable sample normalization strategies such as data-driven normalizations, internal standards-based normalization, or quality control (QC)-based normalization[115]. These strategies help to standardize metabolite abundances before statistical analyses and improve the quality of metabolomics data. Of these, QC-based normalization approaches are gaining more popularity of late[114,116]. Several QC-based normalization algorithms have been developed in recent times including batch-ratio[117], LOESS[118], and SERFF[115]. The QC samples are injected at regular intervals along with the study samples in every batch. Ideally, the QC sample should have the same matrix composition as that

of study samples and is usually obtained by pooling multiple aliquots. After QC-based batch correction, those metabolites which exhibited poor repeatability across QC samples were often removed based on specific cut-off criteria to assure an expected level of data quality. For example, after batch correction, only those metabolites satisfying the cut-off criteria were often retained for subsequent data analysis[119], such as 1) metabolites present in > 50% of QC samples, 2) metabolites with a coefficient of variation for QC samples <20%.

Though the above mentioned approaches can largely eliminate unwanted analytical variations from the dataset, the inherent biological variability induced by factors such as diet, ethnicity, physical activity, circadian rhythm, and medications still poses a significant challenge in interpreting the real physiological variations due to disease status or interventions[120]. To overcome these challenges, several strategies have been proposed, including cross-validation of results using an appropriate proportion of test and validation sets (e.g., 30%, the 'test set'), validation of identified biomarkers using large cohorts of multi-centric samples (validation set), reporting results in relative amounts rather than absolute amounts of metabolites, and finally validation of candidate biomarkers based on comparison to an isotopically labeled internal standards. Current practice involves using different software for different tasks in the metabolomics workflow, such as one for peak picking, another one for normalization, and another one for metabolite annotations. This is a very tedious process and also a time-consuming one. As we move forward, particular emphasis should be given to developing software that can automate everything from aligning runs to peak picking to batch correction to metabolite annotations, which may become "current practices" in the immediate future.

1.9 Metabolomics in ACS

Recently, there has been a growing appreciation for metabolomics as a promising approach for investigating cardiovascular diseases, including CAD to allow for better mechanistic understanding and also biomarker discovery. The studies in the 2000s by Sabatine and colleagues initially demonstrated the application of a blood-based metabolomics platform to identify markers associated with myocardial injury. In a study comprising 36 subjects who underwent exercise stress testing (inducible ischemia), Sabatine et al. showed that myocardial ischemia is characterized by significant changes in the circulating levels of multiple metabolites, including lactic acid (final product of glycolysis)[121]. The pathway analysis identified a key role for the TCA cycle (regulator of oxidative phosphorylation) during myocardial ischemia. Moreover, they identified a panel of six metabolites, including citric acid, which could accurately stratify patients with myocardial ischemia from control subjects. Following this study, in a human model of planned myocardial infarction, via alcohol septal ablation, the same group identified metabolic changes as early as 10 minutes after myocardial injury[122]. They reported that perturbations in pyrimidine metabolism, the TCA cycle, and the pentose phosphate pathway were associated with myocardial injury. Importantly, these perturbations were observed in both coronary sinus and peripheral blood and were further validated in an independent clinical cohort.

A comprehensive overview of the clinical studies of metabolomics in ACS is provided in **Table-1.2**. Only those studies which explicitly discuss any of the ACS subtypes were included in the table. As evident from **Table-1.2**, blood-derived plasma and serum from veins are the most preferred biological fluids, and LC/MS is the favored technique being used in these studies. However, the sampling time varies greatly between these studies. First-morning collection, collection after overnight fasting, spot sampling at the time of admission (non-fasting), and timed

collection at different sampling time points are the various sampling modes employed in these studies. The ideal sampling time is when the rate of metabolic flow, or flux, is constant, i.e., a steady metabolic state. However, ACS always involves 'metabolic shifts', and thus there is no steady metabolic state available in ACS events. Under these circumstances, time-series analyses could provide a better insight into the molecules and pathways with clinical relevance.

The initial clinical studies of metabolomics in ACS made use of GC/MS to identify biomarkers for the early diagnosis of ACS. Utilizing GC/MS, Vallejo et al. and Laborde et al. elucidated the metabolic differences in plasma of non-ST elevation ACS patients relative to healthy subjects[123,124]. These studies collectively identified tricarboxylic acid (TCA) cycle intermediates along with 4-hydroxyproline, tryptophan, 3-OH-butyric acid, and 2-OH-butyric acid as key players in ACS pathophysiology. Subsequent studies employed NMR, LC/MS, and CE/MS approaches, shifting focus from the broad spectrum of ACS towards various ACS subtypes. Using CE/MS and hydrophilic interaction chromatography/MS targeted analysis, Naz et al. found increased acylcarnitines (associated with defective mitochondrial β-oxidation) and amino acids (involved in myocardial energy metabolism) levels in STEMI patients compared to NSTEMI patients[58]. Another study used a combination of different metabolomics approaches, including GC/MS, and H-NMR, and confirmed the presence of elevated hydrogen sulfide (an endogenous gasotransmitter) levels in STEMI patients compared to UA patients[125]. In a large study comprising 2,324 patients from 4 independent centers[57], Fan et al. evaluated the diagnostic value of plasma metabolomics to characterize different types of CAD. Based on CAD severity, patients were divided into five groups of those with the normal coronary artery, nonobstructive coronary atherosclerosis, stable angina, UA, and AMI. They found 89 differential metabolites across different CAD types. Additionally, they identified glycerophospholipid metabolism, amino acids,

acylcarnitines, TCA cycle, and bile acid biosynthesis as the main metabolic pathways associated with CAD progression. Importantly, these findings were replicated in a validation cohort.

Metabolomics has also been used to explore biomarkers predictive of adverse cardiovascular events following ACS. For instance, Du et al. performed LC/MS analysis of 26 amino acids in a cohort of 138 STEMI patients with acute heart failure to find metabolites predictive of adverse cardiovascular events[126]. They found that elevated plasma branched-chain amino acids (BCAA) levels on admission are associated with adverse cardiovascular events. In another study comprising 978 patients[127], Vignoli et al. used NMR-based metabolomics to identify prognostic markers of two-year mortality after AMI. They showed that elevated levels of amino acids including mannose, formate, acetone, proline, creatinine, acetate, and 3-hydroxybutyrate were associated with mortality following AMI. Another study used an untargeted LC/MS approach and showed that six metabolic pathways, namely urea cycle, tyrosine, lysine, tryptophan, aspartate/asparagine, and carnitine shuttle, are associated with mortality in patients with CAD[128]. More recently, Chorell et al. showed that lysophospholipids (involved in inflammation, arteriosclerosis) are associated with future cardiovascular risk in STEMI and NSTEMI patients[129]. They reported that while STEMI is characterized by a higher ratio of lysophosphatidylcholine to lysophosphatidylethanolamine, NSTEMI is characterized by a lower ratio of these two lipids[129].

In recent times, lipid molecules and their associated pathways gained particular interest in the setting of ACS. In 2018, Wang et al. demonstrated that in addition to TCA cycle intermediates and amino acid metabolism, other lipid-associated pathways, including fatty acid metabolism and fatty acid β‑oxidation, also play important roles in ACS[130]. During the same time, Goulart et al. showed that the most perturbed metabolites associated with STEMI were primarily lipid species, including

phosphatidylcholines, lysophosphatidylcholines, and sphingomyelins[131]. These results underscore the need for comprehensive lipid profiling to provide insight into ACS pathogenesis.

One of the most consistent findings in these clinical studies has been the link between carnitine (short-chain and long-chain) and lysophosphatidylcholine (LPC) species with ACS. Carnitines play a critical role in transporting long-chain fatty acids from the cytoplasm into the mitochondria, where they undergo β-oxidation to produce energy. Accumulating evidence suggests that elevated levels of carnitines reflect impaired β-oxidation and mitochondrial dysfunction[132] and are associated with a wide variety of disorders, including type 2 diabetes[133], and cardiovascular diseases[134]. Since long-chain fatty acylcarnitines are produced from fatty acid metabolism and are primarily synthesized in the mitochondria, their levels indicate mitochondrial fatty acid oxidation[135]. On the other hand, LPC is a group of proinflammatory lipids, which is primarily derived from phosphatidylcholine (PC) by the enzymatic action of phospholipase A2 (PLA2). LPC has been linked to the pathogenesis of atherosclerosis and the progression of various diseases[136], including cardiovascular diseases, renal failure[137], ovarian cancer[138], and diabetes[139]. Among other properties, LPC also activates several signaling pathways such as oxidative stress and inflammatory responses, contributing to endothelial cell injury in atherosclerosis and cardiovascular disorders[140].

Table-1.2: Main findings from the clinical studies of metabolomics in acute coronary syndrome

No	First Author, year	Sample size	Sampling time	Specimen/ Technique	Main findings
1	W Zhong[141], 2021	284 ACS; 130 HC	At the time of hospital admission	Plasma LC/MS	Phenylalanine, arginine, and proline metabolism and synthesis and degradation of ketone bodies are involved in ACS pathogenesis.
2	E Chorell[129], 2021	50 STEMI; 50 NSTEMI; 100 HC	After fasting for 4 h	Plasma GC/MS, LC/MS	Plasma lysophospholipids ratio (LPC: LPE) could predict future risk in STEMI and NSTEMI patients.
3	N Aa[142], 2021	85 MI; 61 non-MI chest pain; 84 HC	Within 6 h of the initial symptom attack	Plasma GC/MS, LC/MS	Patients with MI had elevated plasma levels of deoxyuridine, methionine, and homoserine.
4	H Chen[143], 2021	Discovery: 942 Validation: 493	After fasting for 8 h	Plasma LC/MS	Perturbations in cysteine and methionine metabolism and glycerophospholipid metabolism are associated with CAD severity.
5	A Mehta[144], 2020	Discovery: 454 Validation: 322	After overnight fasting	Plasma LC/MS	Perturbations in tryptophan, lysine, tyrosine, asparagine/aspartate, urea cycle, and the carnitine shuttle metabolism are associated with mortality in CAD patients.
6	J Li[145], 2020	136 NOCAD; 118 AMI	After overnight fasting	Serum LC/MS	23 differential metabolites were identified between AMI and NOCAD, including 12 acylcarnitines, seven fatty acids, three glycerophospholipids, and L-tryptophan.
7	H Jiang[146], 2020	252 ACS	After initial diagnosis of ACS	Serum LC/MS	A total of four metabolites including isoundecylic acid, betaine, 1-heptadecanoyl-sn-glycero-3-phosphocholine, and acetylcarnitine could discriminate stable and vulnerable plaques.

8	A Khan[147], 2020	112 patients at AMI risk; 89 HC	During routine blood collection after overnight fasting	Serum LC/MS	L-homocysteine sulfinic acid, cysteic acid, and carnitine could serve as predictive markers for AMI risk.
9	M Pouralijan Amiri[36], 2020	94 UA; 32 controls (angina, but no CAD)	After coronary angiography	Plasma H-NMR	17 metabolites involved in pathways such as steroid hormone biosynthesis, aminoacyl-tRNA biosynthesis, and lysine degradation could serve as promising biomarkers for UA diagnosis.
10	A Vignoli[33], 2020	825 total, 702 survivors and 123 deceased	24–48 h after the PCI and overnight fasting	Serum H-NMR	Characterization of metabolite–metabolite association, can be used as a potential tool to predict mortality in AMI patients.
11	G Gundogdu[60], 2020	20 STEMI; 15 HC	Within an hour of the initial symptom attack	Serum LC/MS	Malonic acid, maleic acid, fumaric acid and palmitic acid could be used for the diagnosis of STEMI.
12	A Surendran[148], 2019	27 STEMI	Pre-PCI, 2 h, 24 h and 48 h post-PCI	Plasma LC/MS	Identified lipids and lipid-derived molecules as the major constituents of the altered metabolomic profile prior to PCI and in the follow up time intervals post PCI.
13	J Wang[149], 2019	40 UA; 39 HC	Blood samples taken at the same day of inclusion in the study	Plasma LC/MS	27 metabolites, including free fatty acids, amino acids, LPE, LPC, and organic acids, can be used to diagnose UA patients.
14	M Deidda[43], 2019	15 STEMI	Coronary artery blood sampling during PCI	Plasma H-NMR	Coronary blood fingerprint in STEMI patients was represented by choline, phosphocholine, myo-inositol, lysine, ornithine, and 2-phosphoglycerate metabolites.

15	A Vignoli[127], 2019	Training: 80 survivors and 40 deceased Validation: 752 survivors and 106 deceased	24–48 h after the PCI and overnight fasting	Serum H-NMR	Mortality in AMI patients were associated with elevated serum levels of acetone, 3-hydroxybutyrate, mannose, creatinine, acetate, formate, proline, and lower serum levels of valine and histidine.
16	VAM Goulart[150], 2019	15 STEMI; 19 HC	Within 7 h after hospitalization	Plasma LC/MS	STEMI metabolic fingerprint includes perturbations associated with phosphatidylcholines, lysophosphatidylcholines, sphingomyelins, and biogenic amine species.
17	Y Wang[130], 2018	36 ACS; 30 HC	Not specified	Urine LC/MS	Identified fatty acid metabolism, fatty acid β-oxidation, amino acid metabolism, and TCA cycle as critical pathways associated with ACS pathogenesis
18	X Du[151], 2018	96 STEMI with post-PCI AEs; 96 without AEs	Arterial blood before coronary angiography	Plasma LC/MS	Circulating levels of branched chain amino acids (BCAAs) were associated with the risk of adverse cardiovascular events in STEMI patients.
19	X Du[126], 2018	138 STEMI with AHF; 138 STEMI without AHF	At the time of hospital admission	Plasma LC/MS	Elevated plasma BCAA levels were associated with long-term adverse cardiovascular events in patients with STEMI and AHF.
20	L Huang[152], 2018	44 STEMI (22 LMCAD and 22 non-LMCAD); 22 HC	At the time of hospital admission	Plasma LC/MS	Retinol metabolism was the most perturbed metabolic pathway for the LMCAD phenotype.

21	D Dazhi[42], 2018	45 AMI;45 chest pain controls (CPCS)	At the time of hospital admission and prior to any medication	Serum H-NMR	Multiple altered metabolic pathways, including the TCA cycle, lipoprotein changes, anaerobic glycolysis, gluconeogenesis, and fatty acid metabolism, characterize AMI patients compared to CPCS.
22	M Kohlhauer[153], 2018	115 STEMI; 26 control patients (SA/NSTEMI)	Immediately after stent deployment	Plasma LC/MS	Increased levels of myocardial succinate are found in STEMI patients.
23	L Zhang[154], 2018	2,324 patients who underwent coronary angiography	Before coronary angiography	Plasma LC/MS	N-acetylneuraminic acid plays a key role during CAD progression.
24	X Yin[61], 2018	20 STEMI; 20 non-ACS patients	Pre-PCI	Plasma LC/MS, ICP/MS	ACS patients are characterized by disturbances in LPC, caffeine, glycolysis, tryptophan, and sphingomyelin metabolism.
25	W Yao[34], 2017	22 UA; 22 HC	Within 24 h after overnight fasting	Serum H-NMR	UA patients are characterized by perturbations in phospholipid and amino acid metabolism.
26	SE Ali[125], 2016	30 STEMI; 15 UA; 15 HC	1–2 h post chest pain for STEMI patients, before and after angioplasty for UA patients	Serum GC/MS, SPME-GC/MS, H-NMR	Elevated levels of serum hydrogen sulfide could discriminate STEMI patients from UA patients.
27	Y Fan[57], 2016	Discovery: 1,086 Validation: 933	Before coronary angiography	Plasma LC/MS	89 differential metabolites were identified between and within different CAD subtypes.
28	X Xu[59], 2015	38 SA; 34 AMI; 71 HC	After overnight fasting	Serum LC/MS	Different lipid classes, including fatty acids, steroids, phospholipids, sphingolipids, and glycerolipids, are associated with CAD progression.

29	L Huang[155], 2016	47 STEMI (23 youth, 24 elderly), 48 healthy controls (24 youth, 24 elderly)	Post-PCI	Plasma LC/MS	The most perturbed metabolic pathway in young STEMI patients was sphingolipid metabolism.
30	K Ameta[35], 2016	65 UA; 62 HC	Within 4 h of onset of angina	Serum H-NMR	Five significantly altered metabolites, namely valine, alanine, glutamine, inosine, and adenine, differentiate UA patients from HC.
31	Z Li[37], 2015	27 UA; 20 HC	In the morning after fasting for 12 h	Urine H-NMR	20 metabolites, including energy metabolism-related metabolites and amino acids, could discriminate UA patients from HC.
32	S Naz[58], 2015	Discovery: 16 STEMI; 16 NSTEMI Validation: 20 STEMI; 28 NSTEMI	Pre-PCI	Serum LC/MS	Carnitine-related compounds and amino acids were differentially present in STEMI and NSTEMI conditions.
33	CM Laborde[56], 2013	Discovery: 35 NSTEACS; 35 HC Validation: 15 NSTEACS; 15 HC	At the onset of the syndrome	Plasma GC/MS, LC/MS	A panel of metabolites consisting of 5-OH-tryptophan, 2-OH-butyric acid, and 3-OH-butyric acid could serve as markers for the early diagnosis of ACS.
34	M Sun[55], 2013	45 UA; 43 atherosclerosis controls	In the morning after overnight fasting	Plasma LC/MS	16 potential endogenous biomarkers for UA were identified including kynurenine.

35	J Teul[54], 2011	19 NSTEACS; 6 HC	Immediately before coronary angiography, day 4, 2 months and 6 months after diagnosis	Plasma GC/MS	27 metabolites including glucose, fructose, myoinositol, pyruvate, lactate, and succinate varied with time following an ACS event.
36	M Vallejo[53], 2009	9 NSTEACS; 10 stable atherosclerosis ; 10 HC	In the morning after fasting on the 4th day of hospital stay	Plasma GC/MS	Plasma fingerprinting characterizes a key role for 4-hydroxyproline in ACS.

Abbreviations: STEMI, ST-elevation myocardial infarction; NSTEMI , non-ST-elevation myocardial infarction; NSTEACS, non-ST-elevation ACS; NOCAD, nonobstructive coronary artery disease; AMI, acute myocardial infarction; AHF, acute heart failure; MI, myocardial infarction; SA, stable angina pectoris; UA, unstable angina pectoris; PCI, percutaneous coronary intervention; ACS, acute coronary syndromes; CAD, coronary artery disease; HC, healthy control; LC/MS, liquid chromatography/mass spectrometry; GC/MS, gas chromatography/mass spectrometry; H-NMR, proton nuclear magnetic resonance; SPME, solid-phase microextraction; LPC, lysophosphatidylcholine; LPE, lysophosphatidylethanolamine; TCA, tricarboxylic acid cycle

1.10 Lipidomics in ACS

Apart from their primary role as the structural components of cells, lipids exert indispensable functionalities as cell signaling molecules and energy sources. Evidence from genomics studies and large randomized controlled trials has established the link between the dysregulated lipid metabolism and CAD progression, including ACS. The results from clinical trials of lipid-modifying therapy demonstrated that lowering the levels of serum lipids (especially cholesterol) reduces the risk of cardiovascular events[156]. Given the crucial role of lipids in regulating health and disease states, elucidating the lipid composition at the molecular and system level is essential to characterize the molecular basis of ACS. Therefore, there is a growing interest in lipidomics as a promising approach to reveal lipid alterations in ACS progression and to find new biomarkers for early ACS diagnosis. **Table-1.3** summarizes the applications of lipidomics on ACS in clinical settings. From **Table-1.3**, it is evident that MS has been the dominating technique for lipid profiling, and blood-derived plasma is the most preferred biospecimen.

Traditional clinical lipid biomarkers for the development and progression of CAD, including elevated serum low-density lipoprotein (LDL), decreased high-density lipoprotein (HDL), or increased triglycerides levels, often fail to distinguish ACS from stable coronary artery disease correctly. Using plasma lipid profiling on 220 individuals Meikle and colleagues showed that multivariate models incorporating both lipids and conventional risk factors could stratify unstable CAD from stable CAD patients with better accuracy than models with conventional risk factors alone[157]. The plasma levels of many lipids, including alkylphosphatidylcholine and phosphatidylcholine plasmalogen (these species are susceptible to oxidative stress), displayed a significant association with disease severity, suggesting their part in the onset and progression of ACS. In a report to characterize lipid species within lipoprotein particles, Meikle also reported

that the levels of phospholipids, including lysophospholipids and plasmalogens, were significantly lower within the HDL of the ACS group relative to the CAD group[158]. In line with this finding, Sutter et al. and Rached et al. showed the contribution of alterations in the HDL lipidome to the disease severity of ACS[66,67]. Similarly, looking at 365 lipids, Lee et al. demonstrated that the levels of saturated lysophosphatidylcholine (LPC) species (16:0 and 18:0) were increased only in the HDL fraction of the ACS group, indicating an intermediate link between LPC species and progression of ACS[68]. In another study using a targeted lipidomics approach, Garcia et al. showed that the HDL2 subclass of ACS patients is enriched with oxidized fatty acids compared to non-ACS subjects, which may modulate platelet-dependent thrombotic risk[159]. Together these studies demonstrate the ability of whole-plasma and lipoprotein-specific lipidomics for the early detection of ACS and discriminating stable CAD from ACS.

Recently, several studies have looked at the association between molecular lipid species and clinical outcomes in patients with ACS. In a study comprising 581 patients with ACS or stable CAD, Cheng et al. investigated the association of plasma lipids with 1-year clinical outcome[160]. They showed that plasma concentration of ceramides (involved in inflammation, membrane integrity and apoptosis), particularly, Cer(d18:1/16:0), is strongly associated with 1-year major adverse cardiac events (MACE) and plaque vulnerability, independent of statin usage and LDL levels. The prognostic value of these high-risk circulating ceramide species was further probed in the prospective ATHEROREMO cohort of 581 patients with stable angina pectoris or ACS and a median follow-up of 4.7 years[161]. Multivariable analyses showed that the circulating levels of Cer(d18:1/16:0), Cer(d18:1/20:0), Cer(d18:1/24:1), and their ratios were associated with adverse cardiac outcomes independent of the established clinical risk factors. A recent lipidomics analysis by Carvalho et al. employing paired tissue-plasma samples in human and animal models took these

results a step forward[162]. They showed that arterial and myocardial tissue ceramide levels also correlate with MACE in patients with AMI. Collectively, these data suggest a predictive role of plasma ceramide species in patients with ACS.

Table-1.3: Main findings from the clinical studies of lipidomics in acute coronary syndrome					
No	**First Author, year**	**Sample size**	**Sampling time**	**Specimen/ Technique**	**Main findings**
1	L Zhang[163], 2021	20 STEMI	30 min before PCI; 6, 12, 24, and 72 h after PCI; 1 day before discharge; and 28 days after PCI	Plasma LC/MS	The circulating levels of PGE2, PGD2, and TXA2 were significantly lower at 6 h post-PCI in STEMI patients. The levels of 20-HETE content were significantly higher at 12–72 h post-PCI.
2	J Burrello[164], 2020	7 STEMI; 9 controls	Pre-PCI, and 24 h post-PCI	Isolated EV Plasma LC/MS	The levels of ceramides, dihydroceramides, and sphingomyelins in extracellular vesicles increased in STEMI compared to matched controls and decreased post-PCI.
3	PJ Meikle[158], 2019	47 ACS; 83 stable CAD	Before coronary catheterization	Plasma LC/MS	Venous plasma lipid species was better than traditional risk factors in discriminating ACS from stable CAD.
4	JH Lee[68], 2018	30 CAD, 10 ACS, 10 with stable CAD without ACS	Not specified	Plasma LC/MS	Two LPC species (16:0 and 18:0) were significantly elevated only in the HDL of the ACS group *vs.* stable CAD group, whereas PE species (38:5 and 40:5) were elevated in ACS by >2-fold in both HDL and LDL.
5	MJ Gerl[165], 2018	74 ACS, 78 SA, 21 IS, 52 HC	Within the first 24 h of hospital admission	Plasma LC/MS	The levels of LPC and ratios of CE to free cholesterol were decreased in the CVD subjects compared to control subjects.
6	S Anroedh[166], 2018	581 ACS; 155 MACEs	Prior to coronary angiography or PCI	Plasma LC/MS	The circulating ceramides were associated with MACEs independent of clinical risk factors in CAD patients.
7	L Feng[167], 2018	40 STEMI	Pre-PCI, 2 h and 24 h post-PCI	Plasma LC/MS	16 circulating fatty acids were associated with myocardial reperfusion injury.

8	C Garcia[159], 2018	30 ACS; 30 No CAD	Before hospital discharge	Plasma LC/MS	HDL2 subclass from ACS patients was enriched with oxidized polyunsaturated fatty acids.
9	LP de Carvalho[162], 2018	Discovery: 337 Validation: 119	Pre-angiography and within 24 h post-angiography	Tissue, Plasma LC/MS	11 ceramides (C14 to C26) and 1 dihydroceramide (C16) were associated with MACEs in patients with AMI.
10	M Chatterjee[168], 2017	175 symptomatic CAD; 15 HC	During coronary angiography	Platelet LC/MS	Symptomatic CAD patients were characterized by a perturbed platelet lipidome.
11	L Zu[169], 2016	39 MACE; 39 Non-MACE; 39 controls	During coronary angiography	Plasma LC/MS	The plasma level of 19-HETE is useful for the prognosis of ACS after adjustment for clinical risk factors.
12	JM Cheng[160], 2015	162 STEMI; 151 NSTEACS; 261 stable CAD	Prior to coronary angiography	Plasma LC/MS	Plasma ceramide (d18:1/16:0) was associated with vulnerable plaque and 1-year MACE.
13	F Rached[67], 2015	16 STEMI; 10 controls	Within 24h after diagnosis	Plasma LC/MS	The lipidome of HDL particles were markedly altered in STEMI.
14	I Sutter[66], 2015	23 stable CAD; 22 ACS; 22 HC	Within 12 h of the initial symptom attack	Plasma LC/MS	HDL-plasmalogen levels were inversely associated with both stable and acute CAD.
15	JY Park[170], 2015	140 CAD; 70 HC	After fasting for 12 h	Serum LC/MS	PC containing palmitic acid, DG, SM, and Cer were associated with an increased risk of MI, whereas PE-plasmalogen and PI were associated with a decreased risk.
16	PJ Meikle[157], 2011	60 SA; 80 UA; 80 HC	Not specified	Plasma LC/MS	The study showed that multivariate models using multiple lipid species can stratify unstable and stable CAD patients with improved accuracy than traditional risk factors.

Abbreviations: MACE, major adverse cardiac events; STEMI, ST-elevation myocardial infarction; NSTEACS, non-ST-elevation ACS; AMI, acute myocardial infarction; MI, myocardial infarction; SA, stable angina pectoris; UA, unstable angina pectoris; IS, ischemic stroke; PCI, percutaneous coronary intervention; ACS, acute coronary syndromes; CAD, coronary artery disease; HC, healthy control; LC/MS, liquid chromatography/mass spectrometry; LPC, lysophosphatidylcholine; PE, phosphatidylethanolamine; CE, cholesteryl ester; PC, phosphatidylcholine; DG, diacylglycerol; SM, sphingomyelin; Cer, ceramide; PI, phosphatidylinositol; HDL, high-density lipoprotein

1.11 Metabolomics of ischemia/reperfusion injury

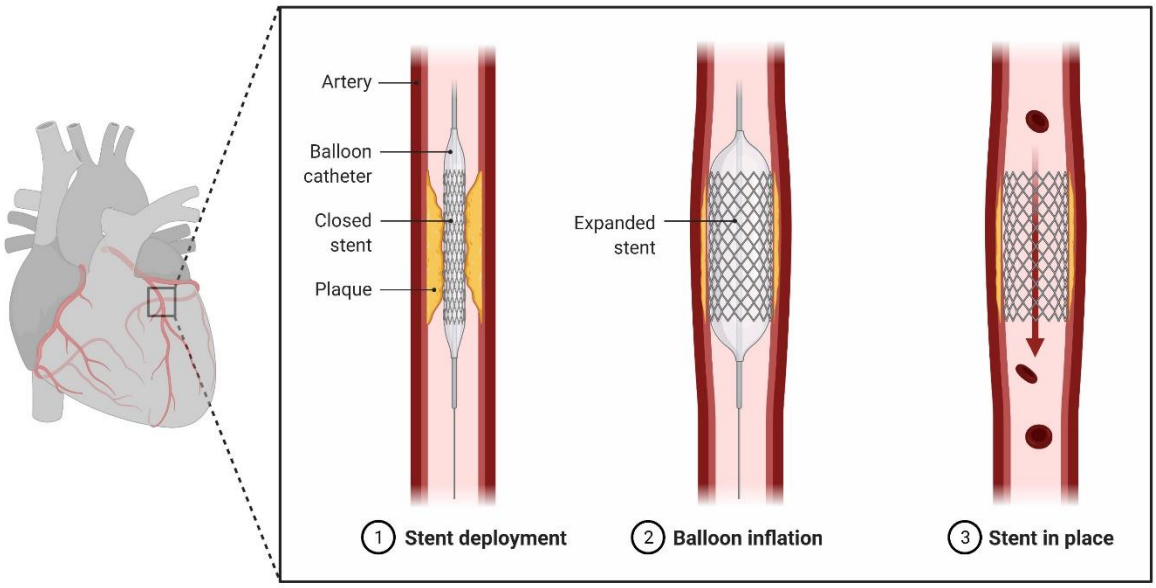

Figure-1.4: Percutaneous Coronary Intervention (PCI). PCI widens the blocked or narrow coronary arteries, thereby allowing reperfusion of the ischemic myocardium. Adapted from "Percutaneous Coronary Intervention", by BioRender.com (2021). Retrieved from https://app.biorender.com/biorender-templates

Timely myocardial reperfusion strategies employing fibrinolytic therapy or percutaneous coronary intervention (PCI) are the treatment of choice for acute STEMI patients. Besides salvaging viable cardiomyocytes from ischemic death, reperfusion profoundly limits the infarct size following a prolonged ischemic insult and improves the clinical outcome. However, pre-clinical and clinical data show that this sudden reintroduction of oxygen and nutrients during reperfusion by itself induces cardiomyocyte death, a phenomenon termed myocardial reperfusion injury[13,171]. Clinically, the largest effect of ischemia/reperfusion (I/R) injury is during PCI of STEMI patients.

In STEMI patients, once the coronary artery is opened by PCI (**Figure-1.4**), it allows for reperfusion of the ischemic myocardium. Despite rapid and successful reperfusion, the mortality rate after an AMI is nearly 10%[172].

Low blood flow during acute ischemia switches cell metabolism to anaerobic metabolism, resulting in lactate accumulation and lowering of intracellular pH[173]. Also, there is a decrease in cellular ATP, which results in Ca^{2+}overload[173]. These processes disturb cell volume regulatory mechanisms, leading to disrupted cellular structure and cell lysis. Thus, it is essential to restore tissue oxygen supply. However, reperfusion leads to a sudden increase in the amount of oxygen available that causes an intense burst of mitochondrial reactive oxygen species (ROS), resulting in cellular dysfunction by modifying intracellular molecules[173]. Reperfusion also restores the physiological pH, which releases the inhibitory effect on mitochondrial permeability transition pores (mPTP) opening. Moreover, reperfusion results in intracellular Ca^{2+}overload due to the dysfunction of the sarcoplasmic reticulum. Reperfusion also initiates endoplasmic reticulum stress, a pro-inflammatory response, and pro-thrombogenic pathway activation in ischemic tissues[171,173]. The excess Ca^{2+} and enhanced ROS production trigger mPTP opening, resulting in ATP depletion and, ultimately, cellular death. A graphic indicating the main proponents of myocardial I/R injury is shown in **Figure-1.5**. In brief, reperfusion is associated with an additional injury that extends the ischemic damage. As a result of this puzzling problem between ischemic injury versus reperfusion injury, there is significant interest in finding ways to protect against and treat the latter.

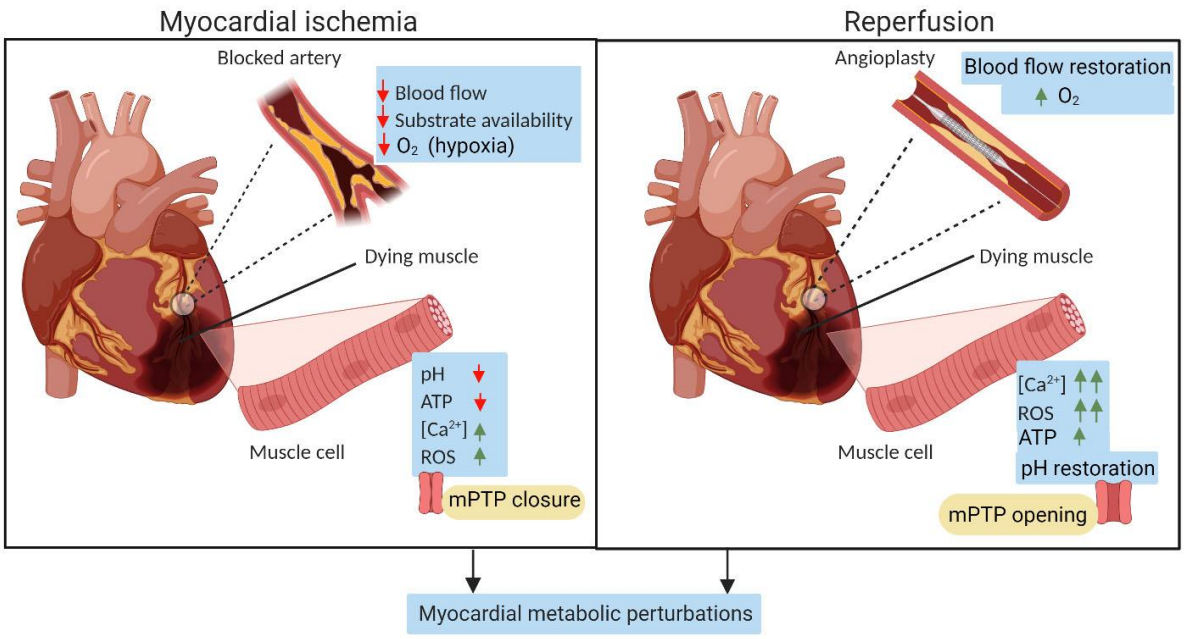

Figure-1.5: Myocardial ischemia/reperfusion (I/R) injury. Schematic showing the main events in myocardial I/R injury. Abbreviations: Ca2+, Calcium ion; ROS, reactive oxygen species; mPTP, mitochondrial permeability transition pore

The ROS generation during reperfusion was previously thought of as a non-specific response to reoxygenation of ischemic tissue. However, a recent comparative *in vivo* metabolomic analysis in a mouse model of I/R injury has revealed that the TCA cycle intermediate, succinate accumulates during ischemia and the oxidation of succinate during reperfusion drives mitochondrial ROS accumulation and reperfusion injury[174]. A later study used a targeted LC/MS approach to analyze plasma metabolites in 115 STEMI patients undergoing PCI and revealed that myocardial succinate accumulation is an early marker of human I/R injury[175]. They reported an association between myocardial content of succinate and the magnitude of ischemic injury in STEMI patients.

Recent metabolomics studies have also implicated the role of BCAAs in the development of I/R injury. In a metabolomics study utilizing a KO mouse model (2C-type ser/thr protein phosphatase (PP2Cm) deficient), Li et al. showed that impaired BCAA catabolism suppresses glucose uptake

and worsens the I/R injury[176]. A few studies have also explored the time-course changes in circulating metabolic profile following reperfusion. Based on a time-series analysis before and after PCI comprising 40 STEMI patients, Feng et al. showed that the fatty acid content in the circulating blood gradually decreases with an increase in reperfusion time[167]. In another study monitoring the changes in eicosanoid profile before and after PCI in 20 STEMI patients, Zhang et al. found that the levels of some bioactive eicosanoids, including PGE2, PGD2, TXA2, and 20-HETE were significantly decreased after PCI. Interestingly, these molecules are pro-inflammatory and are associated with platelet aggregation[177].

There are currently no therapeutic options for I/R injury in patients presenting with STEMI who undergo revascularization. Given the complex metabolic changes within the myocardium and hence within the circulation during I/R injury, it is necessary to identify the metabolic and lipidomic pathway(s) that impact clinical outcomes. There are many limitations to the current studies in the setting of I/R injury, including focussing on a single metabolite (e.g., succinate), a specific metabolite class (e.g., fatty acids or eicosanoids), a single pathway (e.g., BCAA metabolism), or having small sample sizes. Animal studies and planned strategies (e.g., inducible ischemia) are helpful to understand pathological mechanisms. Nevertheless, more clinical investigations incorporating time course analyses in large cohorts are needed to understand better the dynamic changes and metabolic pathways involved in human I/R injury.

1.12 Translational metabolomics and future directions

Despite showing substantial potential for biomarker discovery and a more detailed understanding of the pathogenesis of ACS, few findings from metabolomics studies have made it to clinical practice. One main reason for this is the concerns regarding the validity and reliability of new marker/cluster of metabolites[178]. The main challenge in biomarker validation is the difficulty in

measuring subtle differences in metabolite fluctuations associated with different disease status or interventions. Also, as evident from **Table-1.2** and **Table-1.3**, barring a few, most of the clinical metabolomics studies on ACS are small-scale preliminary-type studies done with a limited sample size (n<100), which lack the required statistical robustness and validity. We believe this also hindered the successful translation of metabolomics to clinics. In addition, as discussed in **section 1.7.1,** the inter-individual variation induced by diet, genetic and environmental exposures, coupled with technical variability, also diminishes metabolomics studies' power to detect actual physiological variations associated with different ACS subtypes and, eventually, to provide clinical biomarkers[179]. One way to overcome this is by conducting follow-up metabolomics experiments using a large validation cohort consisting of diverse patient groups (multi-centric) with suitable control cohorts. However, large-scale multi-cohort studies are usually laborious, expensive, and time-consuming. Once validated appropriately, there are increased prospects of translating these biomarkers towards disease diagnostics and risk prediction. Another potential challenge in translational metabolomics is that most of the metabolomics studies in ACS published thus far were focused on generating data and interpreting them without paying much attention to finding the mechanistic link underlying the association between the identified metabolites and ACS pathogeneses[180]. Finding the relation between candidate biomarkers and their biological role is the next important step after biomarker discovery. This can be done by employing suitable *in vitro* and animal model experiments. Importantly, in the future, the metabolomics community should work in tandem with other omics communities such as genomics and transcriptomics to gain more insights on cellular processes represented by a candidate marker[181]. This will bring us closer to a mechanistic understanding of physiological and pathophysiological conditions associated with various disease states including ACS.

Conclusions

Over the past decade, metabolomics has become a powerful investigative tool to elucidate the underlying metabolic mechanisms of cardiovascular diseases. Most of the metabolomics studies in ACS have focused on biomarker identification to differentiate ACS from healthy controls, to differentiate ACS subtypes (UA, NSTEMI, and STEMI), and to find predictive molecules of mortality or adverse events following an ACS incident. Several studies also performed pathway analysis for finding the biological pathways that contribute to disease pathogenesis. Many of these studies have already shown substantial potential for discovery and understanding. However, as discussed above, attempts to translate these study results into clinical practice have resulted in contradictory results. Considering metabolomics is still early in its scientific evolution, the future is promising with the ongoing technological advances in the field. More importantly, more clinical studies aiming at a systems-wide understanding of ACS pathogenesis rather than risk prediction models are the need of the hour.

1.13 References

1 Sanchis-Gomar, F., Perez-Quilis, C., Leischik, R. & Lucia, A. Epidemiology of coronary heart disease and acute coronary syndrome. *Ann Transl Med* **4**, 256-256, doi:10.21037/atm.2016.06.33 (2016).

2 Virani, S. S. *et al.* Heart Disease and Stroke Statistics-2020 Update: A Report From the American Heart Association. *Circulation* **141**, e139-e596, doi:10.1161/cir.0000000000000757 (2020).

3 Amsterdam, E. A. *et al.* 2014 AHA/ACC Guideline for the Management of Patients with Non-ST-Elevation Acute Coronary Syndromes: a report of the American College of Cardiology/American Heart Association Task Force on Practice Guidelines. *J Am Coll Cardiol* **64**, e139-e228, doi:10.1016/j.jacc.2014.09.017 (2014).

4 Menzin, J., Wygant, G., Hauch, O., Jackel, J. & Friedman, M. One-year costs of ischemic heart disease among patients with acute coronary syndromes: findings from a multi-employer claims database. *Curr Med Res Opin* **24**, 461-468, doi:10.1185/030079908x261096 (2008).

5 Anderson, J. L. & Morrow, D. A. Acute Myocardial Infarction. *N Engl J Med* **376**, 2053-2064, doi:10.1056/NEJMra1606915 (2017).

6 Moore, A. *et al.* Acute Myocardial Infarct. *Radiol Clin North Am* **57**, 45-55, doi:10.1016/j.rcl.2018.08.006 (2019).

7 Makki, N., Brennan, T. M. & Girotra, S. Acute coronary syndrome. *J Intensive Care Med* **30**, 186-200, doi:10.1177/0885066613503294 (2015).

8 Mahajan, V. S. & Jarolim, P. How to Interpret Elevated Cardiac Troponin Levels. *Circulation* **124**, 2350-2354, doi:doi:10.1161/CIRCULATIONAHA.111.023697 (2011).

9 Taegtmeyer, H. *A Primer on Carbohydrate Metabolism in the Heart*. Vol. 11 (Springer, 2014).

10 Goldberg, K. D. a. I. J. *Lipoproteins: A Source of Cardiac Lipids*. (Springer).

11 Burnett, J. R. Lipids, lipoproteins, atherosclerosis and cardiovascular disease. *Clin Biochem Rev* **25**, 2-2 (2004).

12 Rosano, G. M., Fini, M., Caminiti, G. & Barbaro, G. Cardiac metabolism in myocardial ischemia. *Curr Pharm Des* **14**, 2551-2562, doi:10.2174/138161208786071317 (2008).

13 Yellon, D. M. & Hausenloy, D. J. Myocardial Reperfusion Injury. *New England Journal of Medicine* **357**, 1121-1135, doi:10.1056/NEJMra071667 (2007).

14 Riehle, C. & Abel, E. D. Insulin Signaling and Heart Failure. *Circ Res* **118**, 1151-1169, doi:10.1161/circresaha.116.306206 (2016).

15 Griffin, J. L., Atherton, H., Shockcor, J. & Atzori, L. Metabolomics as a tool for cardiac research. *Nat Rev Cardiol* **8**, 630-643, doi:10.1038/nrcardio.2011.138 (2011).

16 Senn, T., Hazen, S. L. & Tang, W. H. W. Translating metabolomics to cardiovascular biomarkers. *Prog Cardiovasc Dis* **55**, 70-76, doi:10.1016/j.pcad.2012.06.004 (2012).

17 Dunn, W. B., Goodacre, R., Neyses, L. & Mamas, M. Integration of metabolomics in heart disease and diabetes research: current achievements and future outlook. *Bioanalysis* **3**, 2205-2222, doi:10.4155/bio.11.223 (2011).

18 Li, M., Zhou, Z., Nie, H., Bai, Y. & Liu, H. Recent advances of chromatography and mass spectrometry in lipidomics. *Anal Bioanal Chem* **399**, 243-249, doi:10.1007/s00216-010-4327-y (2011).

19 Courant, F., Antignac, J. P., Dervilly-Pinel, G. & Le Bizec, B. Basics of mass spectrometry based metabolomics. *Proteomics* **14**, 2369-2388, doi:10.1002/pmic.201400255 (2014).

20 Cheng, S. *et al.* Potential Impact and Study Considerations of Metabolomics in Cardiovascular Health and Disease: A Scientific Statement From the American Heart Association. *Circ Cardiovasc Genet* **10**, e000032, doi:10.1161/HCG.0000000000000032 (2017).

21 van der Greef, J. & Smilde, A. K. Symbiosis of chemometrics and metabolomics: past, present, and future. *Journal of Chemometrics* **19**, 376-386, doi:10.1002/cem.941 (2005).

22 Pauling, L. Orthomolecular psychiatry. Varying the concentrations of substances normally present in the human body may control mental disease. *Science* **160**, 265-271, doi:10.1126/science.160.3825.265 (1968).

23 Pauling, L., Robinson, A. B., Teranishi, R. & Cary, P. Quantitative analysis of urine vapor and breath by gas-liquid partition chromatography. *Proc Natl Acad Sci U S A* **68**, 2374-2376, doi:10.1073/pnas.68.10.2374 (1971).

24 Robinson, A. B., Westall, F. C. & Ellison, G. W. Multiple sclerosis: urinary amine measurement for orthomolecular diagnosis. *Life Sci* **14**, 1747-1753, doi:10.1016/0024-3205(74)90276-8 (1974).

25 Horning, E. C. & Horning, M. G. Metabolic profiles: gas-phase methods for analysis of metabolites. *Clin Chem* **17**, 802-809 (1971).

26 Horning, E. C. & Horning, M. G. Human Metabolic Profiles Obtained by GC and GC/MS. *Journal of Chromatographic Science* **9**, 129-140, doi:10.1093/chromsci/9.3.129 (1971).

27 Oliver, S. G., Winson, M. K., Kell, D. B. & Baganz, F. Systematic functional analysis of the yeast genome. *Trends Biotechnol* **16**, 373-378, doi:10.1016/s0167-7799(98)01214-1 (1998).

28 Burla, B. *et al.* MS-based lipidomics of human blood plasma: a community-initiated position paper to develop accepted guidelines. *J Lipid Res* **59**, 2001-2017, doi:10.1194/jlr.S087163 (2018).

29 Pouralijan Amiri, M. *et al.* Metabolomics in early detection and prognosis of acute coronary syndrome. *Clin Chim Acta* **495**, 43-53, doi:10.1016/j.cca.2019.03.1632 (2019).

30 Gadian, D. G. *et al.* Phosphorus nuclear magnetic resonance studies on normoxic and ischemic cardiac tissue. *Proc Natl Acad Sci U S A* **73**, 4446-4448, doi:10.1073/pnas.73.12.4446 (1976).

31 Ackerman, J. J., Bore, P. J., Gadian, D. G., Grove, T. H. & Radda, G. K. N.m.r. studies of metabolism in perfused organs. *Philos Trans R Soc Lond B Biol Sci* **289**, 425-436, doi:10.1098/rstb.1980.0059 (1980).

32 Bailey, I. A., Williams, S. R., Radda, G. K. & Gadian, D. G. Activity of phosphorylase in total global ischaemia in the rat heart. A phosphorus-31 nuclear-magnetic-resonance study. *Biochem J* **196**, 171-178, doi:10.1042/bj1960171 (1981).

33 Vignoli, A. *et al.* Differential Network Analysis Reveals Metabolic Determinants Associated with Mortality in Acute Myocardial Infarction Patients and Suggests Potential Mechanisms Underlying Different Clinical Scores Used To Predict Death. *Journal of proteome research* **19**, 949-961, doi:10.1021/acs.jproteome.9b00779 (2020).

34 Yao, W., Gao, Y. & Wan, Z. Serum Metabolomics Profiling to Identify Biomarkers for Unstable Angina. *BioMed Research International* **2017**, 7657306, doi:10.1155/2017/7657306 (2017).

35 Ameta, K. *et al.* 1H NMR-derived metabolomics of filtered serum of myocardial ischemia in unstable angina patients. *Clin Chim Acta* **456**, 56-62, doi:10.1016/j.cca.2016.02.020 (2016).

36 PouralijanAmiri, M. *et al.* NMR-based plasma metabolic profiling in patients with unstable angina. *Iran J Basic Med Sci* **23**, 311-320, doi:10.22038/IJBMS.2020.39979.9475 (2020).

37 Li, Z. *et al.* Analysis of urinary metabolomic profiling for unstable angina pectoris disease based on nuclear magnetic resonance spectroscopy. *Mol Biosyst* **11**, 3387-3396, doi:10.1039/c5mb00489f (2015).

38 Takis, P. G., Ghini, V., Tenori, L., Turano, P. & Luchinat, C. Uniqueness of the NMR approach to metabolomics. *TrAC Trends in Analytical Chemistry* **120**, 115300, doi:https://doi.org/10.1016/j.trac.2018.10.036 (2019).

39 Emwas, A.-H. *et al.* NMR Spectroscopy for Metabolomics Research. *Metabolites* **9**, 123 (2019).

40 Senn, T., Hazen, S. L. & Tang, W. H. Translating metabolomics to cardiovascular biomarkers. *Prog Cardiovasc Dis* **55**, 70-76, doi:10.1016/j.pcad.2012.06.004 (2012).

41 Brindle, J. T. *et al.* Rapid and noninvasive diagnosis of the presence and severity of coronary heart disease using 1H-NMR-based metabonomics. *Nat Med* **8**, 1439-1444, doi:10.1038/nm1202-802 (2002).

42 Deng, D. *et al.* Epidemiology and Serum Metabolic Characteristics of Acute Myocardial Infarction Patients in Chest Pain Centers. *Iran J Public Health* **47**, 1017-1029 (2018).

43 Deidda, M. *et al.* Metabolomic fingerprint of coronary blood in STEMI patients depends on the ischemic time and inflammatory state. *Scientific Reports* **9**, 312, doi:10.1038/s41598-018-36415-y (2019).

44 Griffiths, W. J. & Wang, Y. Mass spectrometry: from proteomics to metabolomics and lipidomics. *Chem Soc Rev* **38**, 1882-1896, doi:10.1039/b618553n (2009).

45 Griffiths, J. A Brief History of Mass Spectrometry. *Analytical Chemistry* **80**, 5678-5683, doi:10.1021/ac8013065 (2008).

46 Haag, A. M. in *Modern Proteomics – Sample Preparation, Analysis and Practical Applications* (eds Hamid Mirzaei & Martin Carrasco) 157-169 (Springer International Publishing, 2016).

47 Siuzdak, G. An Introduction to Mass Spectrometry Ionization: An Excerpt from The Expanding Role of Mass Spectrometry in Biotechnology, 2nd ed.; MCC Press: San Diego, 2005. *JALA: Journal of the Association for Laboratory Automation* **9**, 50-63, doi:10.1016/j.jala.2004.01.004 (2004).

48 Wilm, M. Principles of electrospray ionization. *Mol Cell Proteomics* **10**, M111.009407, doi:10.1074/mcp.M111.009407 (2011).

49 Peterson, D. S. Matrix-free methods for laser desorption/ionization mass spectrometry. *Mass Spectrom Rev* **26**, 19-34, doi:10.1002/mas.20104 (2007).

50 Nordström, A., Want, E., Northen, T., Lehtiö, J. & Siuzdak, G. Multiple ionization mass spectrometry strategy used to reveal the complexity of metabolomics. *Anal Chem* **80**, 421-429, doi:10.1021/ac701982e (2008).

51 Gowda, G. A. & Djukovic, D. Overview of mass spectrometry-based metabolomics: opportunities and challenges. *Methods Mol Biol* **1198**, 3-12, doi:10.1007/978-1-4939-1258-2_1 (2014).

52 Ding, M. & Rexrode, K. M. A Review of Lipidomics of Cardiovascular Disease Highlights the Importance of Isolating Lipoproteins. *Metabolites* **10**, doi:10.3390/metabo10040163 (2020).

53 Vallejo, M. *et al.* Plasma fingerprinting with GC-MS in acute coronary syndrome. *Anal Bioanal Chem* **394**, 1517-1524, doi:10.1007/s00216-009-2610-6 (2009).

54 Teul, J. *et al.* Targeted and non-targeted metabolic time trajectory in plasma of patients after acute coronary syndrome. *J Pharm Biomed Anal* **56**, 343-351, doi:10.1016/j.jpba.2011.05.020 (2011).

55 Sun, M. *et al.* Identification of biomarkers for unstable angina by plasma metabolomic profiling. *Mol Biosyst* **9**, 3059-3067, doi:10.1039/c3mb70216b (2013).

56 Laborde, C. M. *et al.* Plasma metabolomics reveals a potential panel of biomarkers for early diagnosis in acute coronary syndrome. *Metabolomics* **10**, 414-424, doi:10.1007/s11306-013-0595-9 (2014).

57 Fan, Y. *et al.* Comprehensive Metabolomic Characterization of Coronary Artery Diseases. *J Am Coll Cardiol* **68**, 1281-1293, doi:10.1016/j.jacc.2016.06.044 (2016).

58 Naz, S. *et al.* Unveiling differences between patients with acute coronary syndrome with and without ST elevation through fingerprinting with CE-MS and HILIC-MS targeted analysis. *Electrophoresis* **36**, 2303-2313, doi:10.1002/elps.201500169 (2015).

59 Xu, X. *et al.* Metabolomic profile for the early detection of coronary artery disease by using UPLC-QTOF/MS. *J Pharm Biomed Anal* **129**, 34-42, doi:10.1016/j.jpba.2016.06.040 (2016).

60 Gundogdu, G. *et al.* Serum metabolite profiling of ST-segment elevation myocardial infarction using liquid chromatography quadrupole time-of-flight mass spectrometry. *Biomed Chromatogr* **34**, e4738, doi:10.1002/bmc.4738 (2020).

61 Yin, X., de Carvalho, L. P., Chan, M. Y. & Li, S. F. Y. Integrated metabolomics and metallomics analyses in acute coronary syndrome patients. *Metallomics* **9**, 734-743, doi:10.1039/C7MT00071E (2017).

62 Chekmeneva, E. *et al.* Optimization and Application of Direct Infusion Nanoelectrospray HRMS Method for Large-Scale Urinary Metabolic Phenotyping in Molecular Epidemiology. *Journal of proteome research* **16**, 1646-1658, doi:10.1021/acs.jproteome.6b01003 (2017).

63 Ren, J.-L., Zhang, A.-H., Kong, L. & Wang, X.-J. Advances in mass spectrometry-based metabolomics for investigation of metabolites. *RSC Advances* **8**, 22335-22350, doi:10.1039/C8RA01574K (2018).

64 Kapron, J. T., Pace, E., Van Pelt, C. K. & Henion, J. Quantitation of midazolam in human plasma by automated chip-based infusion nanoelectrospray tandem mass spectrometry. *Rapid Communications in Mass Spectrometry* **17**, 2019-2026, doi:https://doi.org/10.1002/rcm.1145 (2003).

65 Li, H., Bendiak, B., Siems, W. F., Gang, D. R. & Hill, H. H., Jr. Ion mobility mass spectrometry analysis of isomeric disaccharide precursor, product and cluster ions. *Rapid Commun Mass Spectrom* **27**, 2699-2709, doi:10.1002/rcm.6720 (2013).

66 Sutter, I. *et al.* Plasmalogens of high-density lipoproteins (HDL) are associated with coronary artery disease and anti-apoptotic activity of HDL. *Atherosclerosis* **241**, 539-546, doi:10.1016/j.atherosclerosis.2015.05.037 (2015).

67 Rached, F. *et al.* Defective functionality of small, dense HDL3 subpopulations in ST segment elevation myocardial infarction: Relevance of enrichment in lysophosphatidylcholine, phosphatidic acid and serum amyloid A. *Biochim Biophys Acta* **1851**, 1254-1261, doi:10.1016/j.bbalip.2015.05.007 (2015).

68 Lee, J. H., Yang, J. S., Lee, S. H. & Moon, M. H. Analysis of lipoprotein-specific lipids in patients with acute coronary syndrome by asymmetrical flow field-flow fractionation and nanoflow liquid chromatography-tandem mass spectrometry. *J Chromatogr B Analyt Technol Biomed Life Sci* **1099**, 56-63, doi:10.1016/j.jchromb.2018.09.016 (2018).

69 Au, A. Metabolomics and Lipidomics of Ischemic Stroke. *Adv Clin Chem* **85**, 31-69, doi:10.1016/bs.acc.2018.02.002 (2018).

70 Dunn, W. B., Broadhurst, D. I., Atherton, H. J., Goodacre, R. & Griffin, J. L. Systems level studies of mammalian metabolomes: the roles of mass spectrometry and nuclear magnetic resonance spectroscopy. *Chem Soc Rev* **40**, 387-426, doi:10.1039/b906712b (2011).

71 Wishart, D. S. Metabolomics for Investigating Physiological and Pathophysiological Processes. *Physiol Rev* **99**, 1819-1875, doi:10.1152/physrev.00035.2018 (2019).

72 Zhang, L. *et al.* Functional Metabolomics Characterizes a Key Role for N-Acetylneuraminic Acid in Coronary Artery Diseases. *Circulation* **137**, 1374-1390, doi:doi:10.1161/CIRCULATIONAHA.117.031139 (2018).

73 Stevens, V. L., Hoover, E., Wang, Y. & Zanetti, K. A. Pre-Analytical Factors that Affect Metabolite Stability in Human Urine, Plasma, and Serum: A Review. *Metabolites* **9**, doi:10.3390/metabo9080156 (2019).

74 Kamlage, B. *et al.* Quality markers addressing preanalytical variations of blood and plasma processing identified by broad and targeted metabolite profiling. *Clin Chem* **60**, 399-412, doi:10.1373/clinchem.2013.211979 (2014).

75 Liu, X. *et al.* Which is the urine sample material of choice for metabolomics-driven biomarker studies? *Anal Chim Acta* **1105**, 120-127, doi:10.1016/j.aca.2020.01.028 (2020).

76 Giskeødegård, G. F., Andreassen, T., Bertilsson, H., Tessem, M. B. & Bathen, T. F. The effect of sampling procedures and day-to-day variations in metabolomics studies of biofluids. *Anal Chim Acta* **1081**, 93-102, doi:10.1016/j.aca.2019.07.026 (2019).

77 van de Merbel, N. C. Quantitative determination of endogenous compounds in biological samples using chromatographic techniques. *TrAC Trends in Analytical Chemistry* **27**, 924-933, doi:https://doi.org/10.1016/j.trac.2008.09.002 (2008).

78 Siegel, D., Permentier, H., Reijngoud, D. J. & Bischoff, R. Chemical and technical challenges in the analysis of central carbon metabolites by liquid-chromatography mass spectrometry. *J Chromatogr B Analyt Technol Biomed Life Sci* **966**, 21-33, doi:10.1016/j.jchromb.2013.11.022 (2014).

79 Zivkovic, A. M. *et al.* Effects of sample handling and storage on quantitative lipid analysis in human serum. *Metabolomics* **5**, 507-516, doi:10.1007/s11306-009-0174-2 (2009).

80 Jobard, E. *et al.* A Systematic Evaluation of Blood Serum and Plasma Pre-Analytics for Metabolomics Cohort Studies. *Int J Mol Sci* **17**, doi:10.3390/ijms17122035 (2016).

81 Vuckovic, D. Current trends and challenges in sample preparation for global metabolomics using liquid chromatography-mass spectrometry. *Anal Bioanal Chem* **403**, 1523-1548, doi:10.1007/s00216-012-6039-y (2012).

82 Bowen, R. A. *et al.* Effect of blood collection tubes on total triiodothyronine and other laboratory assays. *Clin Chem* **51**, 424-433, doi:10.1373/clinchem.2004.043349 (2005).

83 Clark, S. *et al.* Stability of plasma analytes after delayed separation of whole blood: implications for epidemiological studies. *Int J Epidemiol* **32**, 125-130, doi:10.1093/ije/dyg023 (2003).

84 Teahan, O. *et al.* Impact of analytical bias in metabonomic studies of human blood serum and plasma. *Anal Chem* **78**, 4307-4318, doi:10.1021/ac051972y (2006).

85 Liu, X. *et al.* Serum or plasma, what is the difference? Investigations to facilitate the sample material selection decision making process for metabolomics studies and beyond. *Anal Chim Acta* **1037**, 293-300, doi:10.1016/j.aca.2018.03.009 (2018).

86 Wedge, D. C. *et al.* Is serum or plasma more appropriate for intersubject comparisons in metabolomic studies? An assessment in patients with small-cell lung cancer. *Anal Chem* **83**, 6689-6697, doi:10.1021/ac2012224 (2011).

87 Yu, Z. *et al.* Differences between human plasma and serum metabolite profiles. *PLoS One* **6**, e21230, doi:10.1371/journal.pone.0021230 (2011).

88 Malik, D. M., Rhoades, S. & Weljie, A. Extraction and Analysis of Pan-metabolome Polar Metabolites by Ultra Performance Liquid Chromatography-Tandem Mass Spectrometry (UPLC-MS/MS). *Bio Protoc* **8**, e2715, doi:10.21769/BioProtoc.2715 (2018).

89 Tambellini, N. P., Zaremberg, V., Turner, R. J. & Weljie, A. M. Evaluation of extraction protocols for simultaneous polar and non-polar yeast metabolite analysis using multivariate projection methods. *Metabolites* **3**, 592-605, doi:10.3390/metabo3030592 (2013).

90 Hyötyläinen, T. Critical evaluation of sample pretreatment techniques. *Anal Bioanal Chem* **394**, 743-758, doi:10.1007/s00216-009-2772-2 (2009).

91 Panuwet, P. *et al.* Biological Matrix Effects in Quantitative Tandem Mass Spectrometry-Based Analytical Methods: Advancing Biomonitoring. *Crit Rev Anal Chem* **46**, 93-105, doi:10.1080/10408347.2014.980775 (2016).

92 Tsakelidou, E. *et al.* Sample Preparation Strategies for the Effective Quantitation of Hydrophilic Metabolites in Serum by Multi-Targeted HILIC-MS/MS. *Metabolites* **7**, doi:10.3390/metabo7020013 (2017).

93 Kole, P. L., Venkatesh, G., Kotecha, J. & Sheshala, R. Recent advances in sample preparation techniques for effective bioanalytical methods. *Biomed Chromatogr* **25**, 199-217, doi:10.1002/bmc.1560 (2011).

94 Alshammari, T. M., Al-Hassan, A. A., Hadda, T. B. & Aljofan, M. Comparison of different serum sample extraction methods and their suitability for mass spectrometry analysis. *Saudi Pharm J* **23**, 689-697, doi:10.1016/j.jsps.2015.01.023 (2015).

95 Rico, E., González, O., Blanco, M. E. & Alonso, R. M. Evaluation of human plasma sample preparation protocols for untargeted metabolic profiles analyzed by UHPLC-ESI-TOF-MS. *Anal Bioanal Chem* **406**, 7641-7652, doi:10.1007/s00216-014-8212-y (2014).

96 Heather, L. C., Wang, X., West, J. A. & Griffin, J. L. A practical guide to metabolomic profiling as a discovery tool for human heart disease. *J Mol Cell Cardiol* **55**, 2-11, doi:10.1016/j.yjmcc.2012.12.001 (2013).

97 Chang, M. S., Ji, Q., Zhang, J. & El-Shourbagy, T. A. Historical review of sample preparation for chromatographic bioanalysis: pros and cons. *Drug Development Research* **68**, 107-133, doi:10.1002/ddr.20173 (2007).

98 Biddlecombe, R. A. & Pleasance, S. Automated protein precipitation by filtration in the 96-well format. *J Chromatogr B Biomed Sci Appl* **734**, 257-265, doi:10.1016/s0378-4347(99)00355-2 (1999).

99 Ma, J. *et al.* A fully automated plasma protein precipitation sample preparation method for LC-MS/MS bioanalysis. *J Chromatogr B Analyt Technol Biomed Life Sci* **862**, 219-226, doi:10.1016/j.jchromb.2007.12.012 (2008).

100 Li, M., Yang, L., Bai, Y. & Liu, H. Analytical methods in lipidomics and their applications. *Anal Chem* **86**, 161-175, doi:10.1021/ac403554h (2014).

101 Folch, J., Lees, M. & Sloane Stanley, G. H. A simple method for the isolation and purification of total lipides from animal tissues. *J Biol Chem* **226**, 497-509 (1957).

102 Bligh, E. G. & Dyer, W. J. A rapid method of total lipid extraction and purification. *Can J Biochem Physiol* **37**, 911-917, doi:10.1139/o59-099 (1959).

103 Matyash, V., Liebisch, G., Kurzchalia, T. V., Shevchenko, A. & Schwudke, D. Lipid extraction by methyl-tert-butyl ether for high-throughput lipidomics. *J Lipid Res* **49**, 1137-1146, doi:10.1194/jlr.D700041-JLR200 (2008).

104 Löfgren, L. *et al.* The BUME method: a novel automated chloroform-free 96-well total lipid extraction method for blood plasma. *J Lipid Res* **53**, 1690-1700, doi:10.1194/jlr.D023036 (2012).

105 Barnes, B. B. & Snow, N. H. in *Comprehensive Sampling and Sample Preparation* (ed Janusz Pawliszyn) 893-926 (Academic Press, 2012).

106 Poole, C. F. in *Comprehensive Analytical Chemistry* Vol. 37 341-387 (Elsevier, 2002).

107 Sitnikov, D. G., Monnin, C. S. & Vuckovic, D. Systematic Assessment of Seven Solvent and Solid-Phase Extraction Methods for Metabolomics Analysis of Human Plasma by LC-MS. *Scientific Reports* **6**, 38885, doi:10.1038/srep38885 (2016).

108 Michopoulos, F., Lai, L., Gika, H., Theodoridis, G. & Wilson, I. UPLC-MS-Based Analysis of Human Plasma for Metabonomics Using Solvent Precipitation or Solid Phase Extraction. *Journal of Proteome Research* **8**, 2114-2121, doi:10.1021/pr801045q (2009).

109 Rico, E., González, O., Blanco, M. E. & Alonso, R. M. Evaluation of human plasma sample preparation protocols for untargeted metabolic profiles analyzed by UHPLC-ESI-TOF-MS. *Anal Bioanal Chem* **406**, 7641-7652, doi:10.1007/s00216-014-8212-y (2014).

110 Kordalewska, M. & Markuszewski, M. J. Metabolomics in cardiovascular diseases. *Journal of Pharmaceutical and Biomedical Analysis* **113**, 121-136, doi:https://doi.org/10.1016/j.jpba.2015.04.021 (2015).

111 Xia, J., Psychogios, N., Young, N. & Wishart, D. S. MetaboAnalyst: a web server for metabolomic data analysis and interpretation. *Nucleic Acids Res* **37**, W652-W660, doi:10.1093/nar/gkp356 (2009).

112 Forsberg, E. M. *et al.* Data processing, multi-omic pathway mapping, and metabolite activity analysis using XCMS Online. *Nat Protoc* **13**, 633-651, doi:10.1038/nprot.2017.151 (2018).

113 Zhang, X., Dong, J. & Raftery, D. Five Easy Metrics of Data Quality for LC-MS-Based Global Metabolomics. *Analytical chemistry* **92**, 12925-12933, doi:10.1021/acs.analchem.0c01493 (2020).

114 Livera, A. M. D. *et al.* Statistical Methods for Handling Unwanted Variation in Metabolomics Data. *Analytical Chemistry* **87**, 3606-3615, doi:10.1021/ac502439y (2015).

115 Fan, S. *et al.* Systematic Error Removal Using Random Forest for Normalizing Large-Scale Untargeted Lipidomics Data. *Analytical Chemistry* **91**, 3590-3596, doi:10.1021/acs.analchem.8b05592 (2019).

116 Kamleh, M. A., Ebbels, T. M. D., Spagou, K., Masson, P. & Want, E. J. Optimizing the Use of Quality Control Samples for Signal Drift Correction in Large-Scale Urine Metabolic Profiling Studies. *Analytical Chemistry* **84**, 2670-2677, doi:10.1021/ac202733q (2012).

117 Wang, S. Y., Kuo, C. H. & Tseng, Y. J. Batch Normalizer: a fast total abundance regression calibration method to simultaneously adjust batch and injection order effects in liquid chromatography/time-of-flight mass spectrometry-based metabolomics data and comparison with current calibration methods. *Anal Chem* **85**, 1037-1046, doi:10.1021/ac302877x (2013).

118 Cleveland, W. S. & Devlin, S. J. Locally Weighted Regression: An Approach to Regression Analysis by Local Fitting. *Journal of the American Statistical Association* **83**, 596-610, doi:10.2307/2289282 (1988).

119 McGarrah, R. W., Crown, S. B., Zhang, G.-F., Shah, S. H. & Newgard, C. B. Cardiovascular Metabolomics. *Circulation Research* **122**, 1238-1258, doi:doi:10.1161/CIRCRESAHA.117.311002 (2018).

120 De Livera, A. M. *et al.* Normalizing and Integrating Metabolomics Data. *Analytical Chemistry* **84**, 10768-10776, doi:10.1021/ac302748b (2012).

121 Sabatine, M. S. *et al.* Metabolomic Identification of Novel Biomarkers of Myocardial Ischemia. *Circulation* **112**, 3868-3875, doi:doi:10.1161/CIRCULATIONAHA.105.569137 (2005).

122 Lewis, G. D. *et al.* Metabolite profiling of blood from individuals undergoing planned myocardial infarction reveals early markers of myocardial injury. *J Clin Invest* **118**, 3503-3512, doi:10.1172/jci35111 (2008).

123 Vallejo, M. *et al.* Plasma fingerprinting with GC-MS in acute coronary syndrome. *Anal Bioanal Chem* **394**, 1517-1524, doi:10.1007/s00216-009-2610-6 (2009).

124 Laborde, C. M. *et al.* Plasma metabolomics reveals a potential panel of biomarkers for early diagnosis in acute coronary syndrome. *Metabolomics : Official journal of the Metabolomic Society* **10**, 414-424, doi:10.1007/s11306-013-0595-9 (2014).

125 Ali, S. E., Farag, M. A., Holvoet, P., Hanafi, R. S. & Gad, M. Z. A Comparative Metabolomics Approach Reveals Early Biomarkers for Metabolic Response to Acute Myocardial Infarction. *Scientific Reports* **6**, 36359, doi:10.1038/srep36359 (2016).

126 Du, X. *et al.* Increased branched-chain amino acid levels are associated with long-term adverse cardiovascular events in patients with STEMI and acute heart failure. *Life Sciences* **209**, 167-172, doi:https://doi.org/10.1016/j.lfs.2018.08.011 (2018).

127 Vignoli, A. *et al.* NMR-based metabolomics identifies patients at high risk of death within two years after acute myocardial infarction in the AMI-Florence II cohort. *BMC Medicine* **17**, 3, doi:10.1186/s12916-018-1240-2 (2019).

128 Mehta, A. *et al.* Untargeted high-resolution plasma metabolomic profiling predicts outcomes in patients with coronary artery disease. *PLOS ONE* **15**, e0237579, doi:10.1371/journal.pone.0237579 (2020).

129 Chorell, E., Olsson, T., Jansson, J. H. & Wennberg, P. Lysophospholipids as Predictive Markers of ST-Elevation Myocardial Infarction (STEMI) and Non-ST-Elevation Myocardial Infarction (NSTEMI). *Metabolites* **11**, doi:10.3390/metabo11010025 (2020).

130 Wang, Y. *et al.* Urinary metabonomic study of patients with acute coronary syndrome using UPLC-QTOF/MS. *J Chromatogr B Analyt Technol Biomed Life Sci* **1100-1101**, 122-130, doi:10.1016/j.jchromb.2018.10.005 (2018).

131 Goulart, V. A. M. *et al.* Metabolic Disturbances Identified in Plasma Samples from ST-Segment Elevation Myocardial Infarction Patients. *Dis Markers* **2019**, 7676189-7676189, doi:10.1155/2019/7676189 (2019).

132 Cao, B. *et al.* Characterizing acyl-carnitine biosignatures for schizophrenia: a longitudinal pre- and post-treatment study. *Transl Psychiatry* **9**, 19-19, doi:10.1038/s41398-018-0353-x (2019).

133 Diamanti, K. *et al.* Intra- and inter-individual metabolic profiling highlights carnitine and lysophosphatidylcholine pathways as key molecular defects in type 2 diabetes. *Scientific reports* **9**, 9653-9653, doi:10.1038/s41598-019-45906-5 (2019).

134 Guasch-Ferré, M. *et al.* Plasma acylcarnitines and risk of cardiovascular disease: effect of Mediterranean diet interventions. *Am J Clin Nutr* **103**, 1408-1416, doi:10.3945/ajcn.116.130492 (2016).

135 Makrecka-Kuka, M. *et al.* Plasma acylcarnitine concentrations reflect the acylcarnitine profile in cardiac tissues. *Scientific Reports* **7**, 17528, doi:10.1038/s41598-017-17797-x (2017).

136 Law, S.-H. *et al.* An Updated Review of Lysophosphatidylcholine Metabolism in Human Diseases. *International journal of molecular sciences* **20**, 1149, doi:10.3390/ijms20051149 (2019).

137 Sasagawa, T., Suzuki, K., Shiota, T., Kondo, T. & Okita, M. The significance of plasma lysophospholipids in patients with renal failure on hemodialysis. *J Nutr Sci Vitaminol (Tokyo)* **44**, 809-818, doi:10.3177/jnsv.44.809 (1998).

138 Okita, M., Gaudette, D. C., Mills, G. B. & Holub, B. J. Elevated levels and altered fatty acid composition of plasma lysophosphatidylcholine(lysoPC) in ovarian cancer patients. *Int J Cancer* **71**, 31-34, doi:10.1002/(sici)1097-0215(19970328)71:1<31::aid-ijc7>3.0.co;2-4 (1997).

139 Rabini, R. A. *et al.* Reduced Na(+)-K(+)-ATPase activity and plasma lysophosphatidylcholine concentrations in diabetic patients. *Diabetes* **43**, 915-919, doi:10.2337/diab.43.7.915 (1994).

140 Tan, S. T., Ramesh, T., Toh, X. R. & Nguyen, L. N. Emerging roles of lysophospholipids in health and disease. *Progress in Lipid Research* **80**, 101068, doi:https://doi.org/10.1016/j.plipres.2020.101068 (2020).

141 Zhong, W., Deng, Q., Deng, X., Zhong, Z. & Hou, J. Plasma Metabolomics of Acute Coronary Syndrome Patients Based on Untargeted Liquid Chromatography–Mass Spectrometry. *Frontiers in Cardiovascular Medicine* **8**, doi:10.3389/fcvm.2021.616081 (2021).

142 Aa, N. *et al.* Plasma Metabolites Alert Patients With Chest Pain to Occurrence of Myocardial Infarction. *Frontiers in Cardiovascular Medicine* **8**, doi:10.3389/fcvm.2021.652746 (2021).

143 Chen, H. *et al.* Comprehensive Metabolomics Identified the Prominent Role of Glycerophospholipid Metabolism in Coronary Artery Disease Progression. *Frontiers in Molecular Biosciences* **8**, doi:10.3389/fmolb.2021.632950 (2021).

144 Mehta, A. *et al.* Untargeted high-resolution plasma metabolomic profiling predicts outcomes in patients with coronary artery disease. *PLoS One* **15**, e0237579, doi:10.1371/journal.pone.0237579 (2020).

145 Li, J. *et al.* Metabolomics Study Revealing the Potential Risk and Predictive Value of Fragmented QRS for Acute Myocardial Infarction. *J Proteome Res* **19**, 3386-3395, doi:10.1021/acs.jproteome.0c00247 (2020).

146 Jiang, H. *et al.* The Serum Metabolic Biomarkers in Early Diagnosis and Risk Stratification of Acute Coronary Syndrome. *Front Physiol* **11**, 776-776, doi:10.3389/fphys.2020.00776 (2020).

147 Khan, A. *et al.* High-resolution metabolomics study revealing l-homocysteine sulfinic acid, cysteic acid, and carnitine as novel biomarkers for high acute myocardial infarction risk. *Metabolism* **104**, 154051, doi:10.1016/j.metabol.2019.154051 (2020).

148 Surendran, A., Aliani, M. & Ravandi, A. Metabolomic characterization of myocardial ischemia-reperfusion injury in ST-segment elevation myocardial infarction patients undergoing percutaneous coronary intervention. *Scientific Reports* **9**, 11742, doi:10.1038/s41598-019-48227-9 (2019).

149 Wang, J. *et al.* Identification of potential plasma biomarkers and metabolic dysfunction for unstable angina pectoris and its complication based on global metabolomics. *Biosci Rep* **39**, BSR20181658, doi:10.1042/BSR20181658 (2019).

150 Goulart, V. A. M. *et al.* Metabolic Disturbances Identified in Plasma Samples from ST-Segment Elevation Myocardial Infarction Patients. *Dis Markers* **2019**, 7676189, doi:10.1155/2019/7676189 (2019).

151 Du, X. *et al.* Relationships between circulating branched chain amino acid concentrations and risk of adverse cardiovascular events in patients with STEMI treated with PCI. *Scientific Reports* **8**, 15809, doi:10.1038/s41598-018-34245-6 (2018).

152 Huang, L. *et al.* Human Plasma Metabolomics Implicates Modified 9-cis-Retinoic Acid in the Phenotype of Left Main Artery Lesions in Acute ST-Segment Elevated Myocardial Infarction. *Scientific Reports* **8**, 12958, doi:10.1038/s41598-018-30219-w (2018).

153 Kohlhauer, M. *et al.* Metabolomic Profiling in Acute ST-Segment-Elevation Myocardial Infarction Identifies Succinate as an Early Marker of Human Ischemia-Reperfusion Injury. *J Am Heart Assoc* **7**, doi:10.1161/jaha.117.007546 (2018).

154 Zhang, L. *et al.* Functional Metabolomics Characterizes a Key Role for N-Acetylneuraminic Acid in Coronary Artery Diseases. *Circulation* **137**, 1374-1390, doi:10.1161/circulationaha.117.031139 (2018).

155 Huang, L. *et al.* Plasma Metabolic Profile Determination in Young ST-segment Elevation Myocardial Infarction Patients with Ischemia and Reperfusion: Ultra-performance Liquid Chromatography and Mass Spectrometry for Pathway Analysis. *Chin Med J (Engl)* **129**, 1078-1086, doi:10.4103/0366-6999.180527 (2016).

156 Carneiro, A. V., Costa, J. & Borges, M. Statins for primary and secondary prevention of coronary heart disease. A scientific review. *Rev Port Cardiol* **23**, 95-122 (2004).

157 Meikle, P. J. *et al.* Plasma Lipidomic Analysis of Stable and Unstable Coronary Artery Disease. *Arteriosclerosis, Thrombosis, and Vascular Biology* **31**, 2723-2732, doi:doi:10.1161/ATVBAHA.111.234096 (2011).

158 Meikle, P. J. *et al.* HDL Phospholipids, but Not Cholesterol Distinguish Acute Coronary Syndrome From Stable Coronary Artery Disease. *J Am Heart Assoc* **8**, e011792, doi:10.1161/jaha.118.011792 (2019).

159 Garcia, C. *et al.* Acute coronary syndrome remodels the antiplatelet aggregation properties of HDL particle subclasses. *J Thromb Haemost* **16**, 933-945, doi:10.1111/jth.14003 (2018).

160 Cheng, J. M. *et al.* Plasma concentrations of molecular lipid species in relation to coronary plaque characteristics and cardiovascular outcome: Results of the ATHEROREMO-IVUS study. *Atherosclerosis* **243**, 560-566, doi:10.1016/j.atherosclerosis.2015.10.022 (2015).

161 Anroedh, S. *et al.* Plasma concentrations of molecular lipid species predict long-term clinical outcome in coronary artery disease patients. *Journal of lipid research* **59**, 1729-1737, doi:10.1194/jlr.P081281 (2018).

162 de Carvalho, L. P. *et al.* Plasma Ceramides as Prognostic Biomarkers and Their Arterial and Myocardial Tissue Correlates in Acute Myocardial Infarction. *JACC Basic Transl Sci* **3**, 163-175, doi:10.1016/j.jacbts.2017.12.005 (2018).

163 Zhang, L. *et al.* Metabolomics reveal dynamic changes in eicosanoid profile in patients with ST-elevation myocardial infarction after percutaneous coronary intervention. *Clin Exp Pharmacol Physiol* **48**, 463-470, doi:10.1111/1440-1681.13435 (2021).

164 Burrello, J. *et al.* Sphingolipid composition of circulating extracellular vesicles after myocardial ischemia. *Scientific Reports* **10**, 16182, doi:10.1038/s41598-020-73411-7 (2020).

165 Gerl, M. J. *et al.* Cholesterol is Inefficiently Converted to Cholesteryl Esters in the Blood of Cardiovascular Disease Patients. *Scientific Reports* **8**, 14764, doi:10.1038/s41598-018-33116-4 (2018).

166 Anroedh, S. *et al.* Plasma concentrations of molecular lipid species predict long-term clinical outcome in coronary artery disease patients. *J Lipid Res* **59**, 1729-1737, doi:10.1194/jlr.P081281 (2018).

167 Feng, L. *et al.* Lipid Biomarkers in Acute Myocardial Infarction Before and After Percutaneous Coronary Intervention by Lipidomics Analysis. *Med Sci Monit* **24**, 4175-4182, doi:10.12659/msm.908732 (2018).

168 Chatterjee, M. *et al.* Regulation of oxidized platelet lipidome: implications for coronary artery disease. *Eur Heart J* **38**, 1993-2005, doi:10.1093/eurheartj/ehx146 (2017).

169 Zu, L., Guo, G., Zhou, B. & Gao, W. Relationship between metabolites of arachidonic acid and prognosis in patients with acute coronary syndrome. *Thrombosis Research* **144**, 192-201, doi:https://doi.org/10.1016/j.thromres.2016.06.031 (2016).

170 Park, J. Y., Lee, S. H., Shin, M. J. & Hwang, G. S. Alteration in metabolic signature and lipid metabolism in patients with angina pectoris and myocardial infarction. *PLoS One* **10**, e0135228, doi:10.1371/journal.pone.0135228 (2015).

171 Hausenloy, D. J. & Yellon, D. M. Myocardial ischemia-reperfusion injury: a neglected therapeutic target. *J Clin Invest* **123**, 92-100, doi:10.1172/jci62874 (2013).

172 Keeley, E. C., Boura, J. A. & Grines, C. L. Primary angioplasty versus intravenous thrombolytic therapy for acute myocardial infarction: a quantitative review of 23 randomised trials. *The Lancet* **361**, 13-20, doi:10.1016/S0140-6736(03)12113-7 (2003).

173 Kalogeris, T., Baines, C. P., Krenz, M. & Korthuis, R. J. Cell biology of ischemia/reperfusion injury. *Int Rev Cell Mol Biol* **298**, 229-317, doi:10.1016/B978-0-12-394309-5.00006-7 (2012).

174 Chouchani, E. T. *et al.* Ischaemic accumulation of succinate controls reperfusion injury through mitochondrial ROS. *Nature* **515**, 431-435, doi:10.1038/nature13909 (2014).

175 Kohlhauer, M. *et al.* Metabolomic Profiling in Acute ST‐Segment–Elevation Myocardial Infarction Identifies Succinate as an Early Marker of Human Ischemia–Reperfusion Injury. *Journal of the American Heart Association* **7**, e007546, doi:doi:10.1161/JAHA.117.007546 (2018).

176 Li, T. *et al.* Defective Branched-Chain Amino Acid Catabolism Disrupts Glucose Metabolism and Sensitizes the Heart to Ischemia-Reperfusion Injury. *Cell Metab* **25**, 374-385, doi:10.1016/j.cmet.2016.11.005 (2017).

177 Dennis, E. A. & Norris, P. C. Eicosanoid storm in infection and inflammation. *Nat Rev Immunol* **15**, 511-523, doi:10.1038/nri3859 (2015).

178 Li-Gao, R. *et al.* Assessment of reproducibility and biological variability of fasting and postprandial plasma metabolite concentrations using 1H NMR spectroscopy. *PLOS ONE* **14**, e0218549, doi:10.1371/journal.pone.0218549 (2019).

179 Sampson, J. N. *et al.* Metabolomics in epidemiology: sources of variability in metabolite measurements and implications. *Cancer Epidemiol Biomarkers Prev* **22**, 631-640, doi:10.1158/1055-9965.EPI-12-1109 (2013).

180 Johnson, C. H., Ivanisevic, J. & Siuzdak, G. Metabolomics: beyond biomarkers and towards mechanisms. *Nat Rev Mol Cell Biol* **17**, 451-459, doi:10.1038/nrm.2016.25 (2016).

181 Pinu, F. R., Goldansaz, S. A. & Jaine, J. Translational Metabolomics: Current Challenges and Future Opportunities. *Metabolites* **9**, 108, doi:10.3390/metabo9060108 (2019).

OVERALL RATIONALE AND HYPOTHESIS

After an acute myocardial infarction (AMI), timely reperfusion of coronary blood flow is vital to rescue the ischemic myocardium. Nonetheless, rapid restoration of oxygenated coronary blood flow to the myocardium (reperfusion) may result in further myocardial cell death and injury, a phenomenon termed myocardial ischemia/reperfusion (I/R) injury. The underlying pathophysiological mechanisms responsible for the development of myocardial I/R injury remain unclear. Given that the heart muscle is one of the most metabolically demanding organs, understanding myocardial metabolomics will allow a better understanding of the mechanisms involved in reperfusion injury. To this end, we have performed a comprehensive metabolomics analysis employing non-targeted and targeted approaches to investigate the changes in the plasma metabolome during human I/R injury.

Why is it important to understand the metabolomic changes during myocardial reperfusion injury? **We currently have no therapies available to attenuate the damaging effects of I/R injury. We can find new therapeutic approaches by understanding the metabolites and metabolomic pathways that are impacted during I/R.**

Hypothesis:

1) There is a large metabolomic shift during human myocardial reperfusion injury.

2) Plasma metabolites can serve as biomarkers of I/R injury and will offer insight into the mechanism of I/R injury.

Objectives:

1) Discover the metabolomic perturbations in plasma before and after primary PCI in the setting of human I/R injury.

2) To complete the first detailed lipidomics assessment of human plasma in the setting of human I/R injury.

3) To investigate the changes within human plasma lipidome during coronary no-reflow in STEMI patients and to correlate these changes with clinical parameters that represent no-reflow in the clinical setting.

CHAPTER 2. Metabolomic characterization of myocardial ischemia-reperfusion injury in ST-segment elevation myocardial infarction patients undergoing percutaneous coronary intervention

Rationale

The heart is the most metabolically demanding organ in the body. Hence, it is likely that during acute myocardial infarction, there are significant metabolism abnormalities. Considering the global and cardiac-specific metabolism changes accompanying myocardial ischemia/reperfusion (I/R) injury, a metabolomics approach can be used to determine if any metabolic patterns may highlight a metabolic pathway during I/R and also determine its clinical relevance. We aim to conduct a non-targeted metabolomics analysis (serial blood sampling) to identify and characterize perturbed metabolic pathways and circulating metabolites in the setting of I/R injury in STEMI patients undergoing PCI.

Published: Scientific Reports (2019), 9(1), 11742

Metabolomic characterization of myocardial ischemia-reperfusion injury in ST-segment elevation myocardial infarction patients undergoing percutaneous coronary intervention

Arun Surendran[1, 3], Michel Aliani[2, 3#] and Amir Ravandi[1, 3#]

Cardiovascular Lipidomics Laboratory, St. Boniface Hospital, Albrechtsen Research Centre[1], Department of Human Nutritional Sciences, University of Manitoba[2], Department of Physiology and Pathophysiology, Faculty of Health Sciences, University of Manitoba[3], Winnipeg, Canada

Disclosures
The authors declare that they have no competing interests.

Corresponding authors[#]:

Michel Aliani PhD
Department of Human Nutritional Sciences, University of Manitoba
Albrechtsen Research Centre, Winnipeg, Manitoba, Canada, R2H 2A6
R4024, 351 Tache Avenue
Winnipeg, MB, R2H 2A6 Canada
michel.aliani@umanitoba.ca

Amir Ravandi MD PhD, FRCPC
Albrechtsen Research Centre
Y3508, Bergen Cardiac Care Centre, 409 Tache Avenue
Winnipeg, Manitoba, Canada, R2H 2A6
aravandi@sbgh.mb.ca

2.1 Abstract

Background: The aim of the study was to discover the metabolomic changes in plasma that occur during human Ischemia-Reperfusion (I/R) injury and to evaluate the diagnostic utility of plasma metabolomic biomarkers for determination of myocardial injury. Deciphering the details of plasma metabolome in ST-segment elevation myocardial infarction (STEMI) patients before and after primary percutaneous coronary interventions (PCI) would allow for better understanding of the mechanisms involved during acute myocardial ischemia and reperfusion in humans.

Method: We performed a detailed non-targeted metabolomic analysis of plasma from 27 STEMI patients who had undergone primary PCI in the first 48 hrs employing a LC/MS approach. Plasma metabolome at ischemic condition was compared to multiple time points after PCI which allowed us to focus on changes in the reperfusion phase.

Results: Classification of the differential metabolites based on chemical taxonomy identified a major role for lipids and lipid-derived molecules. Biochemical pathway analysis identified valine, leucine and isoleucine biosynthesis, vitamin B6 metabolism and glutathione metabolism as the most significant metabolic pathways representing early response to I/R injury. We also identified phenylalanine, tyrosine, linoleic acid and glycerophospholipid metabolism as the most significant pathways representing late response to I/R injury. A panel of three metabolites pentadecanoic acid, linoleoyl carnitine and 1-linoleoylglycerophosphocholine was discovered to have diagnostic value in determining the extent of I/R injury based on cardiac biomarkers.

Conclusions: Using a non-targeted LC/MS approach, we have successfully generated the most comprehensive data to date on significant changes in the plasma metabolome in STEMI patients who underwent primary PCI in the first 48 hrs showing that lipid metabolites represent the largest cohort of molecules undergoing significant change.

Keywords: ischemia reperfusion injury, altered metabolic pathways, coronary artery disease, myocardial infarction, plasma, mass spectrometry

2.2 Abbreviations

CAD, coronary artery disease; MI, myocardial infarction; PCI, percutaneous coronary interventions; I/R, ischemia/reperfusion; STEMI, ST elevation myocardial infarction; LC/MS, Liquid chromatography–mass spectrometry; PCA, principal component analysis; PLS-DA, partial least squares-discriminant analysis; ROC, Receiver Operating Characteristic

2.3 Introduction

Despite considerable improvements in mortality rates over the past two decades, coronary artery disease (CAD) remains the leading cause of morbidity and mortality worldwide, with myocardial infarction (MI) a common manifestation of this disease[1]. After an acute myocardial infarction, early and successful myocardial reperfusion by means of primary percutaneous coronary interventions (PCI) is the treatment of choice for limiting the size of myocardial infarction and improving clinical outcomes. But the process of rapid restoration of blood flow to myocardium (reperfusion) can lead to additional injury, a phenomenon known as myocardial ischemia/reperfusion (I/R) injury[2]. The largest impact of I/R in the clinical setting is during percutaneous coronary intervention of patients presenting with an occluded coronary artery known as STEMI[3] (ST elevation myocardial infarction). Even with the best clinical care, the 30-day rate of Major Adverse Cardiac Events (MACE) for these patients is 10%[4].

Although there have been extensive *in vitro* and *in vivo* studies on the concept of I/R injury, there has yet to be a therapeutic option available to minimize the harmful effects of reperfusion injury. Many studies have investigated a single molecule or a single pathway as a potential therapeutic avenue. As in many other pathological processes there are multiple pathways involved in reperfusion injury. The numerous advancements in "omics" technology platforms in recent years have allowed us to determine the changes at the genome and proteome level. However, only changes in the metabolite level will allow us to understand the downstream effects of perturbed cellular pathways[5]. The heart is the most metabolically demanding organ in the body and its metabolic perturbation leads to changes in the metabolome of body fluids including plasma[6]. Therefore, changes in plasma metabolites may reflect underlying cardiac diseases progression. Previous studies have reported individual metabolic biomarkers for heart failure, myocardial

infarction, and CAD[7-9]. However, there is little information available on the metabolomic changes in human plasma during I/R injury.

In this study we did a detailed non-targeted plasma metabolomic analysis employing a liquid chromatography coupled with mass spectrometry (LC/MS) platform. We investigated the time-effect changes in human plasma metabolome before and after primary PCI during the first 48 hours in the setting of I/R injury in patients presenting with STEMI. We also identified a panel of plasma metabolite markers with potential for determining the extent of I/R injury.

2.4 Materials and methods

2.4.1 Patients and study design

A total of 108 plasma samples from 27 patients presenting with STEMI enrolled from St. Boniface Hospital, Canada between June 2014 and July 2015 formed the study cohort. Both verbal and written consent were obtained from all subjects.

Inclusion criteria were: ages between 18 and 75, confirmation of STE (ST segment elevation) on 12 lead ECG, presentation with chest pain and documentation of occluded coronary artery with coronary angiography. The overall study design is shown in **Figure-2.1A**. The samples were collected by venipuncture at four different time intervals including the time of arrival at the cardiac catheterization laboratory for primary PCI (0 h, time-1), 2 h post angioplasty (time-2), 24 h post angioplasty (time-3), and 48 h post angioplasty (time-4). Blood samples were collected in EDTA-treated tubes and immediately centrifuged at 2500 x g for 10 minutes at 4^{o}C in a refrigerated centrifuge to harvest plasma. To avoid frequent retrieval of the aliquot box from the -80^{o}C freezer that can cause small scale thawing, exactly 100 microliters of plasma samples required for sample preparation was aliquoted in cryogenic vials, (Fisher Scientific, NY, USA) snap-frozen in liquid nitrogen and sealed under a stream of nitrogen gas and frozen at -80^{o}C prior to metabolite

extraction. Average time of sample collection to plasma separation and aliquoting were less than 30 min. Approval for this study was obtained from both the University of Manitoba and the St. Boniface Hospital research ethics boards. Clinical data was reviewed retrospectively.

2.4.2 Sample size calculation

To determine the necessary number of subjects needed to ensure the detection of a true statistical difference across different time intervals, we performed a power analysis (**Supplementary Figure.1**). The power analysis indicated that we would have over 80% power to detect discriminating metabolites using approximately 25 subjects in each group. By considering the results from power analysis and effort required, we confined our study with 27 subjects. A detailed procedure for sample size consideration employed was provided under the heading '**1.1 Sample size calculation**' in the **Supplementary Data**.

2.4.3 Extraction of plasma metabolites

Extraction of low-molecular-weight (< 1500 Da) metabolites in plasma samples was done by as previously described[10]. Briefly, a volume of 100 microliters of plasma was mixed with a volume of 200 microliters of acetonitrile. The sample was centrifuged, and supernatant of the mixture was collected and then analysed. Each plasma sample was extracted in duplicate. Also, a quality control (QC) mixture made of pooled plasma samples were used to validate the extraction and LC-MS method[11]. More detail regarding blood sample collection, metabolite extraction and QC runs were provided under the heading '**1.3 Extraction of plasma metabolites'** in the **Supplementary Data**. The metabolites were separated on a 1290 Infinity Agilent HPLC system from Agilent Technologies (CA, USA) using a Zorbax Extend-C18 analytical column (2.1 mm × 50 mm I.D., particle size 1.8 µm, Agilent Technologies, USA). Mass spectral analysis of eluting peptides from

the analytical column was carried out on a 6538 UHD Accurate Q-TOF LC/MS from Agilent Technologies (CA, USA) controlled by MassHunter Workstation Software (v 7.0). All analyses were performed in both positive and negative mode ESI employing a dual ionization source. The acquired raw LC/MS data ('. d files') was preprocessed using Agilent MassHunter Qualitative Analysis (MHQ, vB.07) and Profinder (vB.06) software. Agilent Mass Profiler Professional (MPP, v12.6), MetaboAnalyst[12] software v3.0 and v4.0 (McGill University, Quebec, Canada), MetScape software v3.0 (http://metscape.ncibi.org), and R statistical software v3.5.2 (https://www.r-project.org) were used for data processing and statistical analysis. In addition, receiver operating characteristic (ROC) analysis was used to evaluate the diagnostic capability of metabolites which can serve as potential biomarkers. Detailed description of LC conditions, MS parameters, compound identification, data processing and statistical analysis were provided in the sections 1.4 to 1.6 in the **Supplementary Data.** Also, a summary of the metabolomic workflow was provided in **Supplementary Table.1.**

2.5 Results

Table-2.1 shows the demographic and laboratory data of the patients. We have also collected data on biochemical and cardiac markers including creatine kinase (CK) and high sensitivity troponin (TnT) for these patients. The mean age of our population was 61 years with 40% female and 15% had a diagnosis of type 2 diabetes. The prevalence of hypertension, dyslipidemia and smokers were 30%, 37% and 22% respectively and only a few (7%) had a previous history of known CAD. In our patients, 37% had occlusion in the left anterior descending (LAD) coronary artery, 48% in the right coronary artery (RCA) and 19% in the circumflex coronary artery. Based on patient's characteristics, our study cohort is similar to previous STEMI studies as shown by patients in the

FAST-MI Program (French Registry of Acute ST-Elevation or Non-ST-elevation Myocardial Infarction)[13].

Table-2.1 Demographic and laboratory characteristics of STEMI patients		
Characteristics (n=27)		**Results**
Age, yrs.		61.55±14.51
Female (%)		44
LVEF		59.29±13.07
Body mass index, kg/m2		28.48±5.08
Comorbidity (%)		
	Hypertension (%)	30
	Diabetes mellitus (%)	15
	Current smoker (%)	22
	Dyslipidemia (%)	37
	Hx of CAD (%)	7
Laboratory data		
	TG, mmol/l	1.9±1.65
	TC, mmol/l	4.69±1.27
	HDL-C, mmol/l	1.14±0.33
	LDL-C, mmol/l	2.84±1.06
	CR, mmol/l	92.33±43.97
Additional parameters*		
	Minutes from onset of chest pain to reperfusion	140 [50 – 360]
	Peak CK (Units/L)	1017 [136 – 7028]
	Peak TnT (ng/L)	1862 [503 – 10000]
Culprit vessel (%)		
	LAD Infarct (%)	37
	RCA Infarct (%)	48
	Circumflex Infarct (%)	19

Medications at baseline (%)		
	ASA	100
	Intravenous heparin	100
	ACEI/ARB	15
	Beta blocker	7
	Statin	15
	Ticagrelor	96
	Clopidorgrel	4

Values are mean ± SD or percent of patients otherwise specified.

* Median [Range]

GP IIb/IIIa inhibitors were not used in this cohort.

LVEF, left ventricular ejection fraction; Hx of CAD, history of coronary artery disease; TG, triglyceride; TC, total cholesterol; HDL-C, high-density lipoprotein cholesterol; LDL-C, low-density lipoprotein cholesterol; CR, creatinine; CK, creatine kinase; TnT, troponin; LAD, Left Anterior Descending coronary artery; RCA, Right coronary artery; ASA, Acetylsalicylic acid; ACEI, Angiotensin-converting enzyme (ACE) inhibitors; ARB, Angiotensin II receptor blockers.

Utilizing "Find by Formula" (FBF) algorithm, by searching against the database, resulted in the identification of 765 and 670 compounds in positive and negative modes, respectively in plasma from patients presenting with STEMI undergoing primary PCI. The endogenously present metabolites which are detected and quantified in blood from Human Metabolome Database[14] (HMDB) served as the database. We enlarged the scope of this database by adding further 350 metabolites from published literature known to be associated with cardiac diseases. In order to find missing features and to give higher confident identifications by further minimizing the false positives and false negatives identifications, batch recursive analysis was done on the already identified compounds. After recursive analysis, the list was further reduced to 69 and 82 compounds in positive and negative modes, respectively. After adjusting for p-value after

'Bonferroni FWER' correction, only those features satisfying $p<0.001$ were considered as significantly differential metabolites across all the four time intervals. The final annotated list contained 130 significantly differential metabolites ($p<0.001$) across all the four time intervals. Of these, 55 elements compounds were identified exclusively in "Positive" ESI mode, 64 compounds were identified exclusively in "Negative" ESI mode and 11 compounds were identified in both the modes (**Supplementary Figure.2 and Supplementary Table.2**). A total of 59 metabolites from this list were already recognized metabolic signatures of ischemia, myocardial infarction or other forms of CAD including non-obstructive coronary atherosclerosis, stable angina pectoris or unstable angina pectoris. The details of the significant compounds with their associated pathways and respective references from literature are shown in **Supplementary Table.3**.

2.5.1 Taxonomy of significant metabolites

Classification of significant metabolites ($p<0.001$) based on chemical taxonomy showed that lipids and lipid-derived molecules (38%) formed the major constituents of the altered metabolomic profile followed by organic acids, organo heterocyclic compounds, benzenoids, nucleotides and phytochemical compounds **(Figure-2.1B)**. These represent compounds with significant change amongst the four time points.

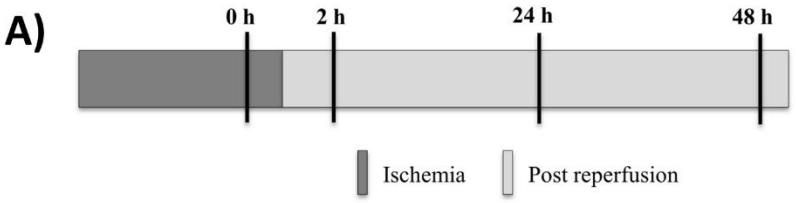
A)
0 h
2 h
24 h
48 h
Ischemia
Post reperfusion

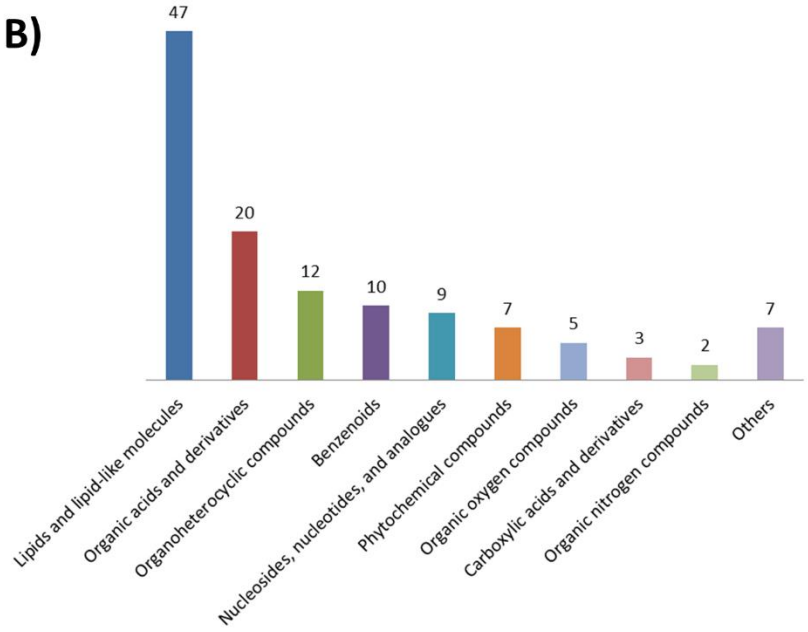
B)
47
20
12
10
9
7
5
3
2
7
Lipids and lipid-like molecules
Organic acids and derivatives
Organoheterocyclic compounds
Benzenoids
Nucleosides, nucleotides, and analogues
Phytochemical compounds
Organic oxygen compounds
Carboxylic acids and derivatives
Organic nitrogen compounds
Others

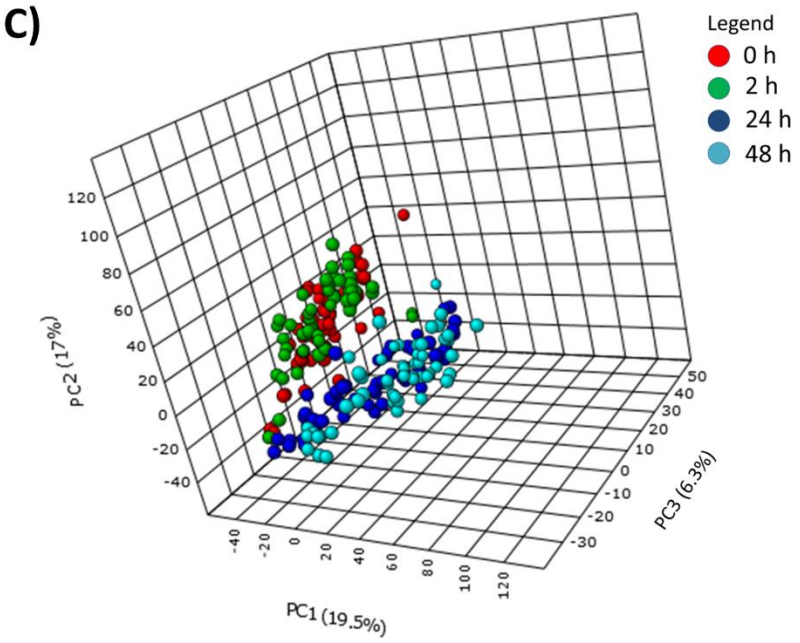
C)
Legend
0 h
2 h
24 h
48 h
PC2 (17%)
PC1 (19.5%)
PC3 (6.3%)

Figure-2.1:

Figure-2.1A: Overall study design. The samples were collected by venipuncture at four different time intervals including the time of arrival at the cardiac catheterization laboratory for primary PCI (0 h ischemic condition (pre angioplasty)), 2 h post angioplasty (time-2), 24 h post angioplasty (time-3), and 48 h post angioplasty (time-4).

Figure-2.1B: Metabolite classification based on chemical taxonomy. The number of metabolites from each metabolite super family of those identified ($p<0.001$) in the analysis.

Figure-2.1C: PCA plot of samples across different time intervals. PCA score plot showing a clear separation between samples from initial time points (0 h, 2 h) and final time points (24 h, 48 h). Also, it shows a close association among the samples of initial time points (0 h, 2 h) and final time points (24 h, 48 h).

2.5.2 Changes in metabolic profile before and after the reperfusion

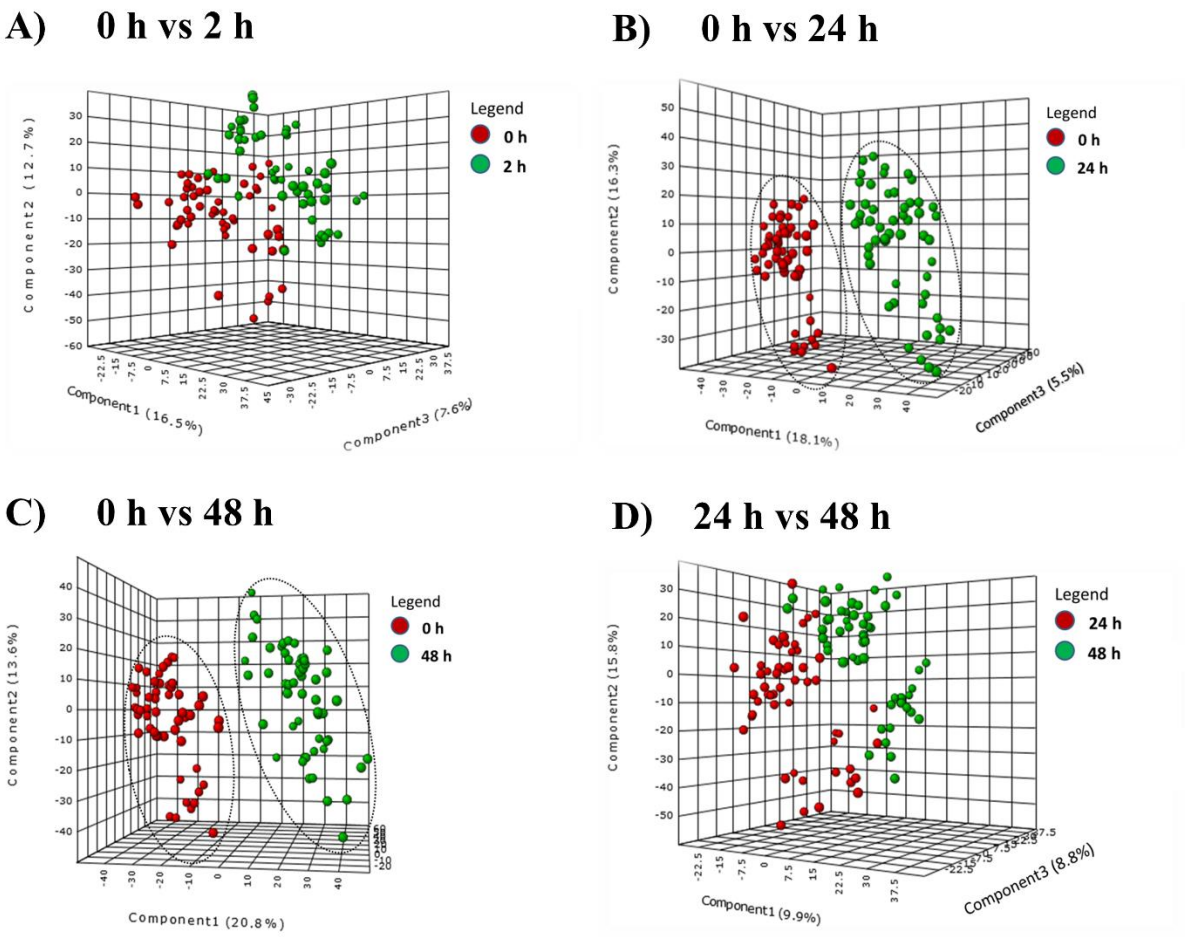

Figure-2.2: PLS-DA scores plot for comparison of the metabolic profiles: The partial least squares analysis (PLS-DA) score plots compared **(A)** '0 h ischemic' time point to '2 h post reperfusion' time point **(B)** '0 h ischemic' time point to '24 h post reperfusion' time point, **(C)** '0 h ischemic' time point to '48 h post reperfusion' time point and **(D)** '24 h post reperfusion' time point to '48 h post reperfusion' time point. The different colours, red and green correspond to different time points.

To understand the changes in plasma metabolome before and after the PCI, we employed multivariate pattern recognition tools such as principal component analysis (PCA) and partial least squares-discriminant analysis (PLS-DA). These visualizing plots were built based on the metabolite concentrations of 130 differential metabolites at each time interval. The PCA plot **(Figure-2.1C)** revealed that not only there was a clear separation in metabolic profile between initial time intervals (0 h, 2 h) and final time intervals (24 h, 48 h) but also, there was a close association existed among the initial time intervals (0 h, 2 h) and final time intervals (24 h, 48 h). In line with the PCA plot, PLS-DA plot **(Figure-2.2)** also confirmed a clear separation between '24 h post reperfusion' time point and baseline (0 h, ischemic condition) **(Figure-2.2B)** and a tight clustering between the '2 h post reperfusion' time point and baseline **(Figure-2.2A)**.

2.5.3 Early and late response to reperfusion

Metabolites showing significant changes were analyzed using Metabolomics Pathway Analysis[15] (MetPA) analysis to understand the metabolic pathways that were impacted due to primary PCI (**Figure-2.3).** Based on impact scores, the most significant pathways (FDR<=1) representing early response to reperfusion immediately after PCI (2 h after reperfusion) **(Figure-2.3A)** were found to be associated with valine, leucine and isoleucine biosynthesis, vitamin B6 metabolism and glutathione metabolism. Likewise, the most significant pathways (FDR<1) after PCI (24 h and 48 h after reperfusion) representing late response to reperfusion were found to be associated with the metabolism of following compounds: (1) phenylalanine, (2) tyrosine, (3) linoleic acid and (4) glycerophospholipid **(Figure-2.3B and Figure-2.3C)**. The number of metabolites involved at each time point were shown in **Supplementary Figure.3**.

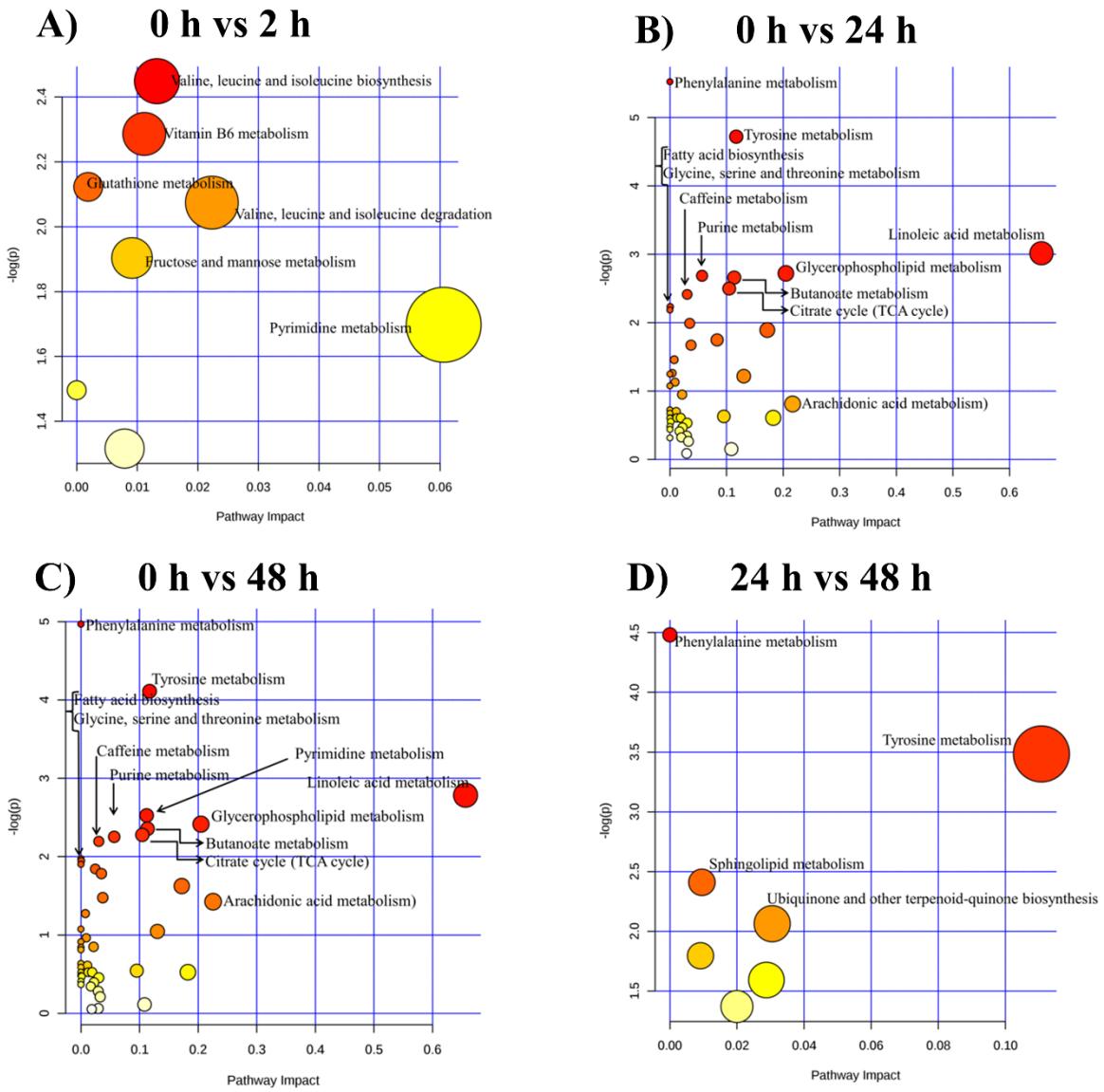

Figure-2.3: MetPA analysis of metabolic changes: TheMetPA analysis shows metabolic pathways of differential metabolites by comparing **(A)** '0 h ischemic' time point to '2 h post reperfusion' time point **(B)** '0 h ischemic' time point to '24 h post reperfusion' time point, **(C)**'0 h ischemic' time point to '48 h post reperfusion' time point and **(D)** '24 h post reperfusion' time point to '48 h post reperfusion' time point. The size and color of each circle indicate the significance of the pathway ranked by p-value (red: higher p-values and yellow: lower p-values) and pathway impact score (the larger the circle the higher the impact score), respectively.

2.5.4 Highly correlated metabolites

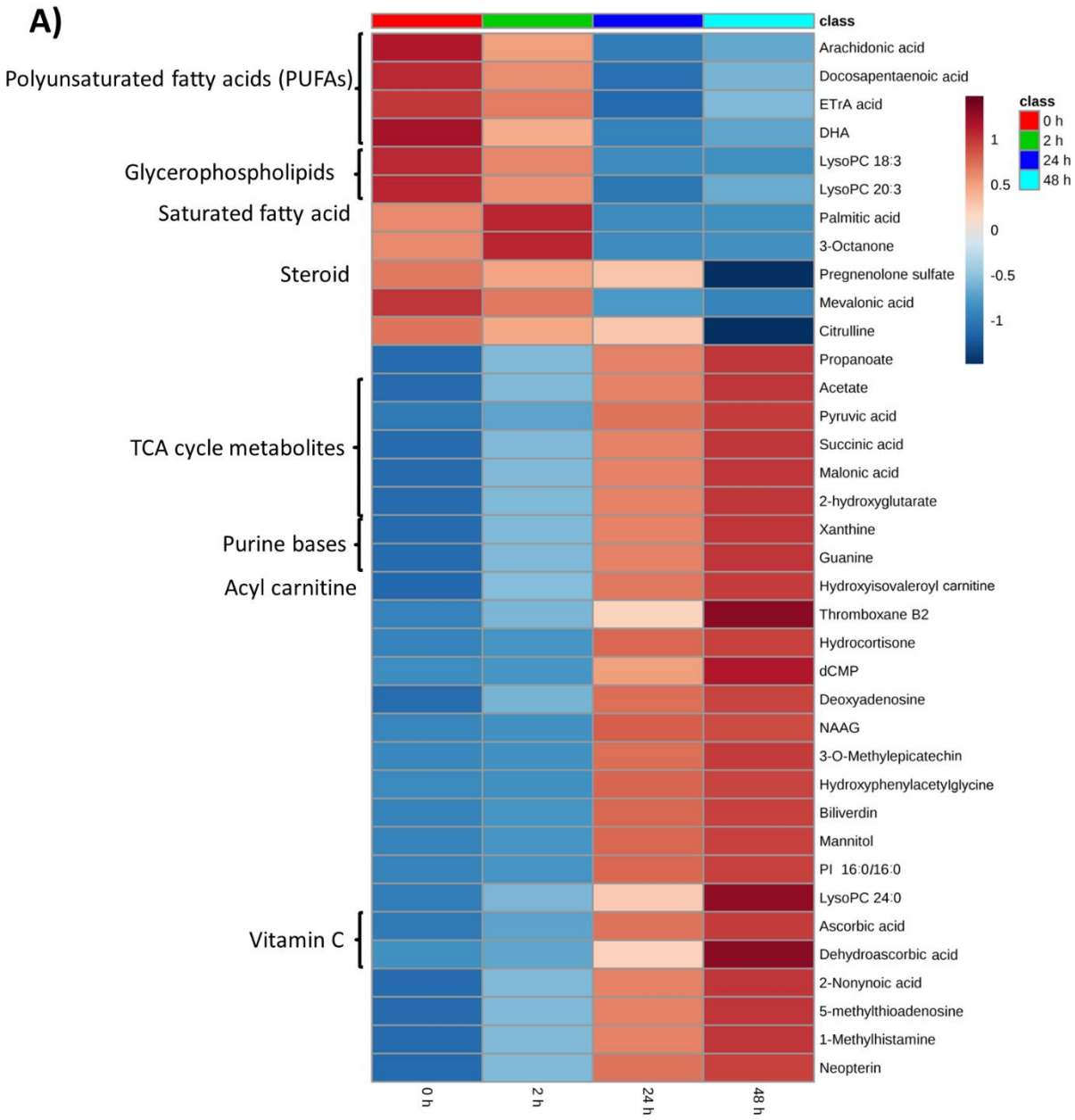

Figure-2.4A: Heat map of significant metabolites obtained from correlation analysis. The heat map constructed with highly correlated metabolites (n=37), |r| >0.9. The colors ranging from blue to orange indicates more concentration of metabolites. ETrA acid = 5,8,11-Eicosatrienoic acid; DHA = docosahexaenoic acid; NAAG = N-Acetylaspartylglutamic acid; LysoPC = lysophosphatidylcholine; PI = phosphatidylinositol; TCA = tricarboxylic acid**.**

B)

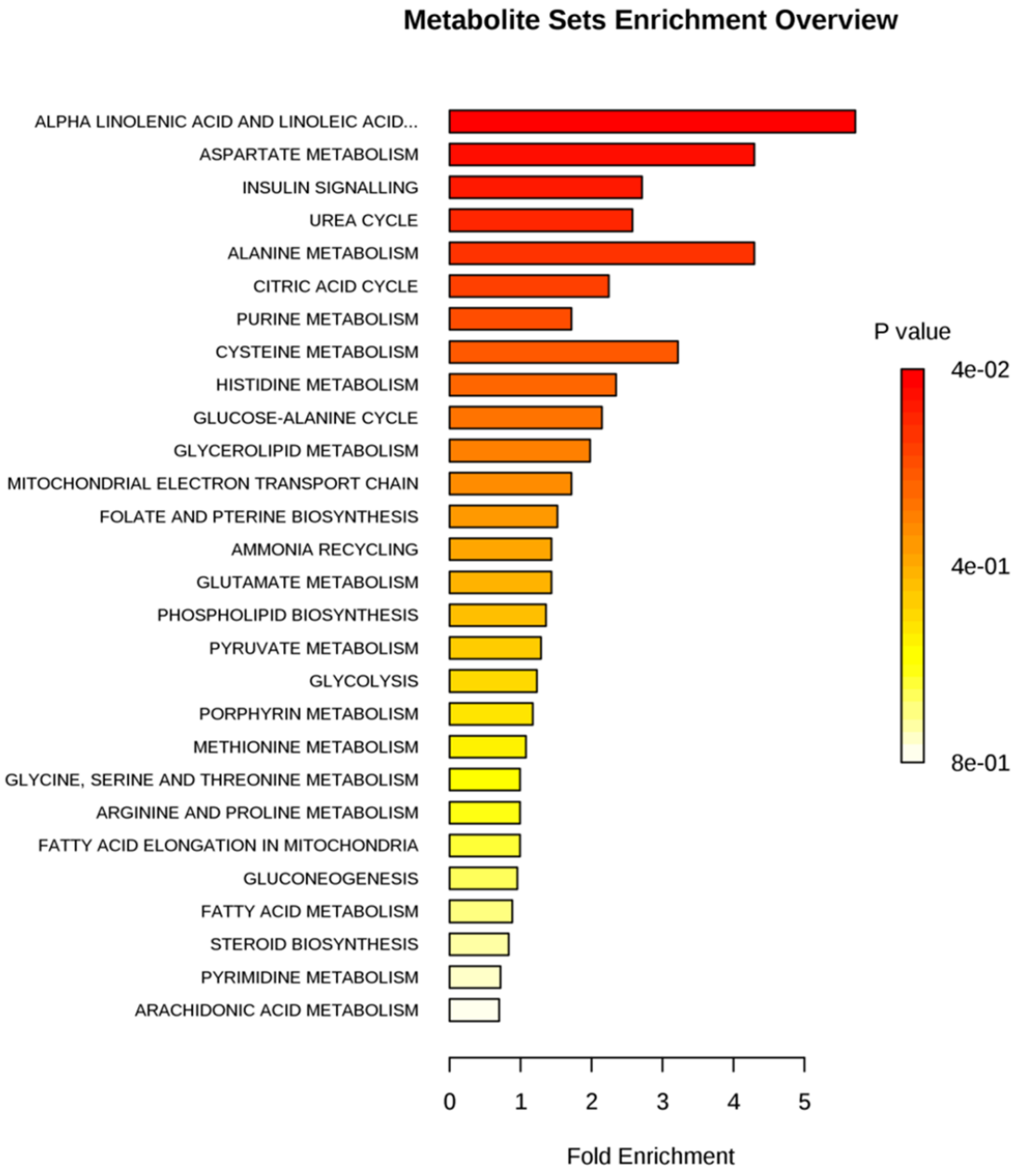

Figure-2.4B: Summary plot of metabolite set enrichment analysis (MSEA) of highly correlated metabolites. The horizontal bar graph summarizes the metabolic pathways that were significantly enriched by this group of functionally related metabolites (n=37) during the setting of I/R injury. The color code corresponds to the calculated p-values (red: $p = 4 \times 10^{-2}$ to white: $p = 8 \times 10^{-1}$).

Finding the highly correlated metabolites in the metabolite set becomes imperative as most of the high correlations may be due to either (1) stronger mutual control by a single enzyme or (2) variation of a single enzyme level much above others[16]. This can also help unravel the biological basis of underlying phenotypic or disease conditions[17,18]. To envisage this metabolite correlation, a heat map **(Figure-2.4A)** was made with only highly correlated metabolites (n=37) amongst 4 time points based on Pearson correlation (coefficient value, |r| >0.9). This heat map shows the relative concentration of 37 highly correlated metabolites across different time intervals. To identify subtle but substantial changes among these correlated compounds, Metabolite Set Enrichment Analysis (MSEA) was performed on these functionally related metabolites (n=37) along with their relative concentrations by using the web-based platform MetaboAnalyst (**Figure-2.4B**). The pathways significantly enriched by these related compounds were (FDR<=1) were (1) linoleic acid and alpha linolenic acid metabolism, (2) aspartate metabolism, (3) insulin signaling, (4) urea cycle, (5) alanine metabolism and (6) citric acid cycle. A correlation network plot showing connectivity and information flow was depicted in **Figure-2.5.** This metabolic network plot depicts the connection between highly correlated metabolites based on STITCH ('search tool for interactions of chemicals')[19] database, such that only highly confident interactions are shown. In this metabolite – metabolite network presentation, the most significant 'hub nodes' or metabolites that were involved in the flow of information between the different pathways were pyruvic acid, succinic acid, malonic acid, palmitic acid and arachidonic acid.

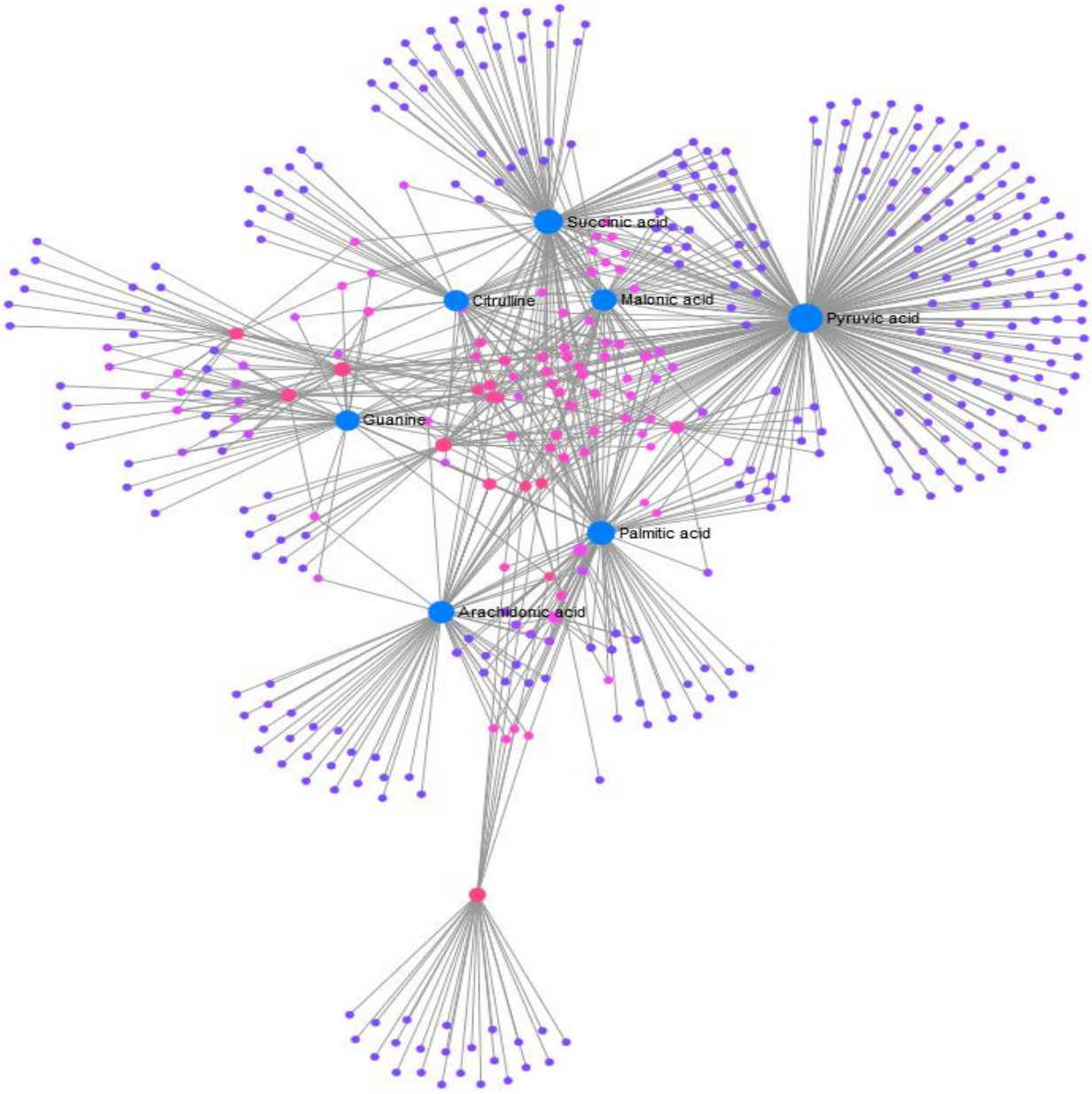

Figure-2.5: Network plot highlighting the highly correlated metabolites: The nodes represent metabolites and edges represent biochemical reactions. Only significant (|r| >0.9) correlations are drawn. The blue nodes represent the most significant hub nodes in establishing connection between the sub-networks in the flow of information. Pyruvic acid, Succinic acid, Malonic acid, Palmitic acid, and Arachidonic acid constitute the most significant sub nodes.

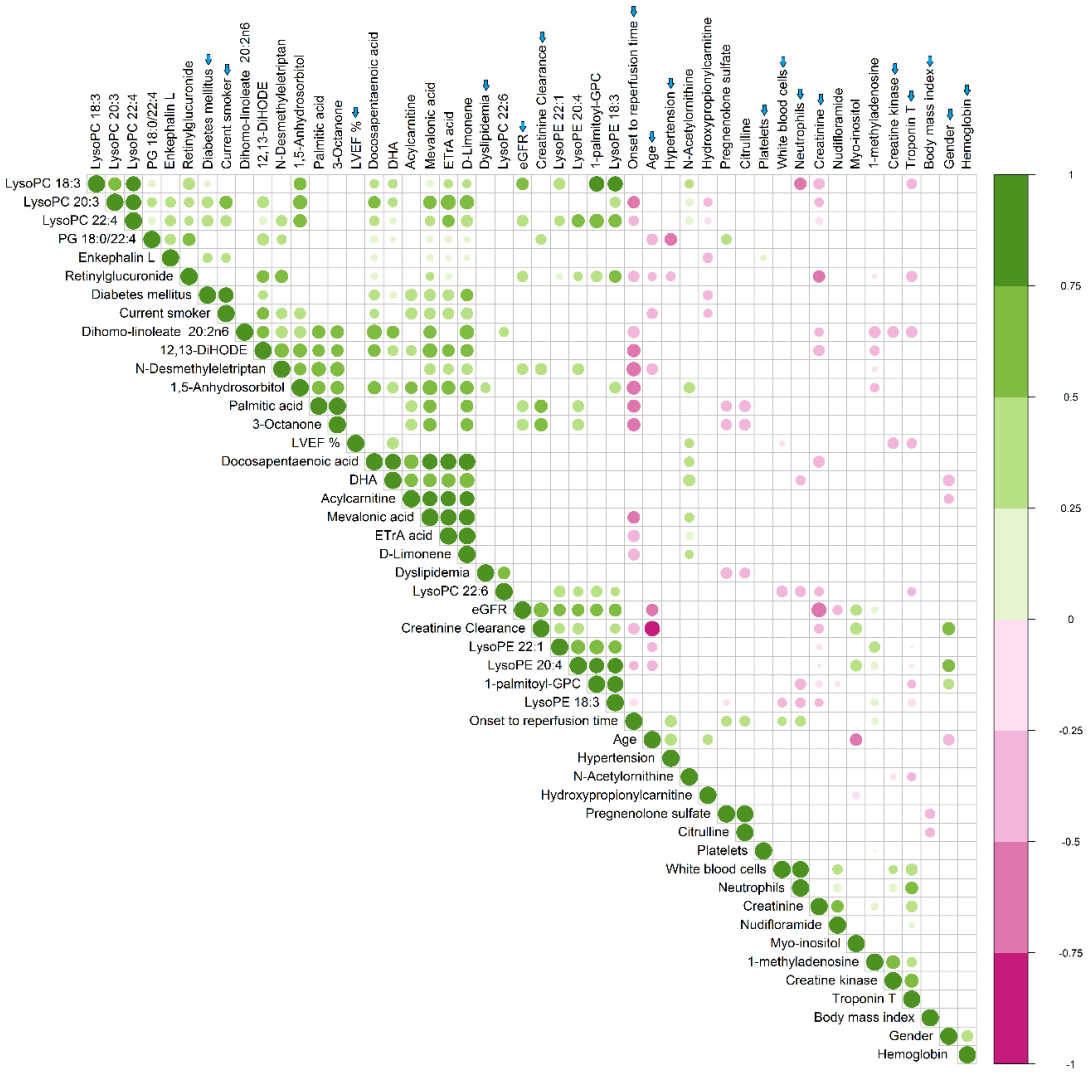

Figure-2.6: Correlation between clinical parameters and plasma metabolites at baseline: The figure shows the correlation matrix ordered by hierarchical clustering between the important clinical parameters and plasma metabolites at baseline (0 h, time-1). Positive correlations are displayed in green; negative correlations are displayed in pink; blue arrow indicates the clinical factors. Color intensity and the size of the circle are proportional to the correlation coefficients. In the right side of the correlogram, the legend color shows the correlation coefficients and the corresponding colors. Correlations with p-value > 0.05 as computed by Spearman correlations

were considered as insignificant and were left blank. Only those metabolites factors (30 metabolites) having more than two significant correlations ($p<0.05$) with any of the clinical parameters were used to construct the correlogram. ETrA acid, 5,8,11-Eicosatrienoic acid; DHA, docosahexaenoic acid; LVEF, left ventricular ejection fraction; 1-palmitoyl –GPC, 1-palmitoyl glycerophosphocholine

To further investigate the relationship between the plasma metabolites and important clinical factors at baseline (0 h, time-1), correlations were also calculated for all pairs of metabolite-clinical factors using the R statistical package 'corrplot'. The resulting correlation plot (**Figure-2.6**) was presented as a clustered matrix in which rows and columns are ordered such that correlated variables are close to each other. At baseline (**Figure-2.6**), the plasma concentrations of Lyso PE (18:3), Lyso PE (20:4), Lyso PE (22:1) showed a strong positive correlation with Glomerular Filtration Rate (eGFR), as were a number of other metabolites. Likewise, the plasma concentrations of 3-Octanone, palmitic acid, 12,13 DiHODE and few other metabolites were negatively correlated with duration of ischemia since onset of chest pain to reperfusion. In the full dataset, though there are a few clusters of correlated metabolites and clinical parameters, the overall correlation between the metabolites and clinical parameters is comparably weak.

2.5.5 Metabolites and clinical biomarkers of cardiac cell death

To find the links between changes in metabolite concentrations in plasma with STEMI patient physiology/pathology, we sought to find metabolites that are closely related to myocardial cell death and clinical outcomes. For that plasma metabolites were further evaluated for predictive accuracy for discriminating large infarct size patients from small infarct size patients based on troponin[20] and creatine kinase[21] (CK) concentrations which are the 'gold standard' biomarkers of cardiac cell death. The sample population was classified into two groups as '*Above median*

Troponin' group and '*Below median* Troponin' group centered on the median troponin value (peak TnT, 1862 ng/L) of the cohort. Based on univariate analysis, (area under the curve (AUC) > 75%, p-value < 0.01), we selected three metabolites namely pentadecanoic acid, 1-linoleoylglycerophosphocholine and linoleoyl carnitine to create a biomarker model to distinguish between these two groups using RF (random forest) algorithm[22] . This biomarker model was built using the metabolic profile at the time of admission. In order to produce a smooth ROC curve, 100 cross validations (CV) were performed, and the results were averaged to generate the plot (**Figure-2.7A**). From the ROC plot, it was evident that the combination of these 3 metabolites was a good classifier with an area under the curve (AUC) equal to 86%. The sample population was again classified into two groups centred on median CK value (peak CK, 1017 Units/L) of the cohort. The resulting ROC plot (**Figure-2.7B**) with an AUC value of 82%, further reinforced the diagnostic ability of these 3 metabolites to serve as potential biomarkers in determining the impact of myocardial injury. To deal with the problem of over-fitting and to assess the statistical significance of our biomarker model with this relatively smaller sample size, permutation tests were performed using 100 cross-validations on the metabolite data. The resulting empirical p-value obtained (p-value<0.05) shows the statistical significance of this biomarker model. The **Figure-2.7C** shows the change in concentration of these 3 metabolites across different time intervals.

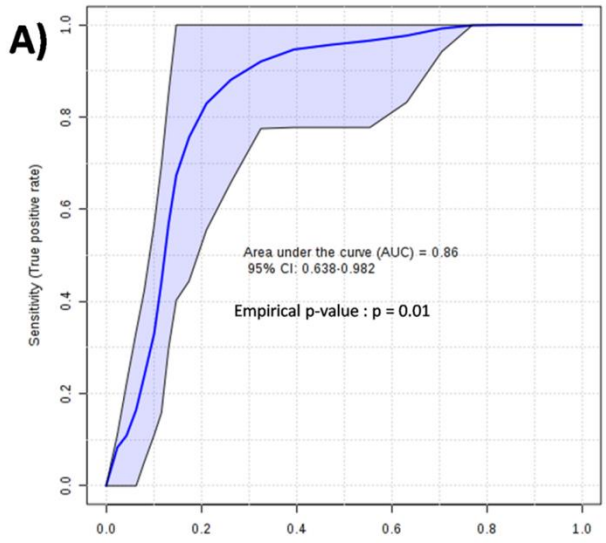
A)
Sensitivity (True positive rate)
Area under the curve (AUC) = 0.86
95% CI: 0.638-0.982
Empirical p-value : p = 0.01

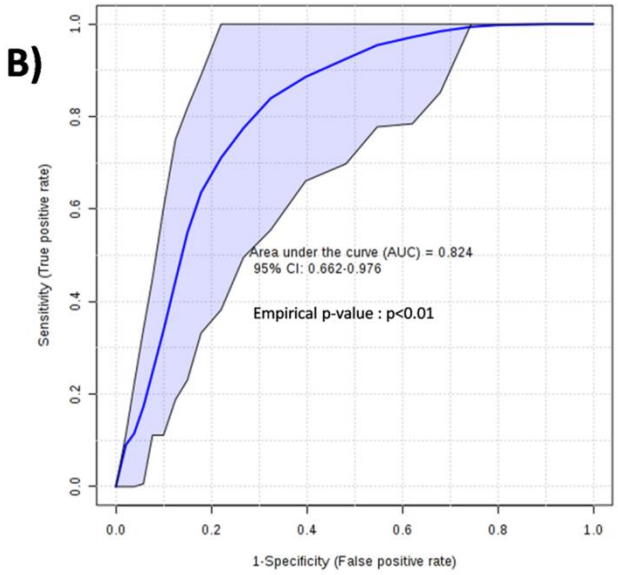
B)
Sensitivity (True positive rate)
Area under the curve (AUC) = 0.824
95% CI: 0.662-0.976
Empirical p-value : p<0.01
1-Specificity (False positive rate)

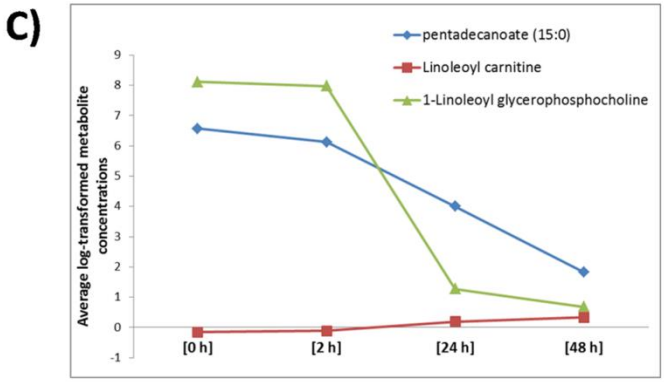
C)
pentadecanoate (15:0)
Linoleoyl carnitine
1-Linoleoyl glycerophosphocholine
Average log-transformed metabolite concentrations
[0 h]
[2 h]
[24 h]
[48 h]

Figure-2.7: Multivariate ROC plots based on the troponin and creatine kinase (CK) concentration A) Receiver operating characteristic (ROC) plot obtained by combining three metabolites namely pentadecanoic acid, linoleoyl carnitine and 1-linoleoylglycerophosphocholine. The curve is based on the median troponin value of the cohort (Peak TnT) and is represented by an area under the curve (AUC) of 0.86 indicating good predictive ability. B) The multivariate ROC curve discriminates individuals based on the median creatine kinase value (Peak CK). The curve is represented by area under the curve (AUC) of 0.82 indicating good predictive ability. The empirical p-value (p-value<0.05) shows the statistical significance of these biomarker models. C) The line plot shows the relative concentration of three potential metabolic biomarkers across different time intervals.

2.6 Discussion

A handful of metabolomic studies have been conducted in patients presenting with STEMI[23-25]. But none of these studies have investigated the time-effect changes in plasma metabolome before and after PCI which is crucial to provide insights into the altered metabolic pathways with clinical relevance during I/R injury. The main objective of our study was to characterize the altered metabolic pathway(s) in the first 48 hours after primary PCI which represent the reperfusion phase. To our knowledge, our study is the most comprehensive metabolomic analysis of human plasma ever undertaken during the first 48 hrs in the setting myocardial I/R injury in patients presenting with STEMI. In this study, we employed a repeated-measure research design by doing serial blood sampling from all STEMI patients both pre and post angioplasty. In repeated measures designs, each subject serves as their own biological control[26] thereby reducing the intra patient variability. This allows the analysis to focus precisely on intervention effects and allows for fewer subjects to detect a desired effect size[27] with increased statistical power.

Our study had three major findings. Firstly, we identified a total of 130 plasma metabolites (**Supplementary Table.3)** which were significantly ($p<0.001$) affected prior to coronary intervention and in the follow up time intervals in the setting myocardial I/R injury as outlined. Secondly, we used metabolic profiling to identify early and late response in plasma metabolome in response to I/R injury. Notably, linoleic acid and alpha linolenic acid metabolism pathway represent the most significant change in plasma metabolome among the related metabolites. Thirdly, classification using ROC analysis identified pentadecanoic acid, linoleoyl carnitine and 1-linoleoylglycerophosphocholine as the top discriminating metabolites in determining the extent of myocardial injury.

The lipids and lipid-derived molecules formed the major components (38%) of the altered metabolomic profile (**Figure-2.1B**) in the setting of I/R injury during the first 48 hours. Our previous work on *in vivo* models of I/R injury have also shown that during reperfusion, there are significant changes within bioactive lipid molecules[28,29]. The multivariate PCA and PLS-DA plots (**Figure-2.1C and Figure-2.2**), showed that the underlying plasma metabolomic change was progressive after 24 hours post primary PCI, with a comprehensive change in the plasma metabolome compared to baseline (0 h, ischemic condition).

The pathway impact analysis revealed key metabolites and perturbed pathways (**Figure-2.3**) that shed light on the early and late changes in plasma metabolome during I/R injury. Immediately post PCI **(Figure-2.3A)**, when compared to pre-PCI, metabolic pathways for valine, leucine and isoleucine biosynthesis, vitamin B6 metabolism and glutathione metabolism were observed to have significant change. Among the metabolites in these altered pathways, the three intermediaries of glutathione metabolism namely glutathione, oxidized (GSSG), ascorbic acid and dehydroascorbic acid are of significant importance in the setting of myocardial reperfusion

injury[30]. The extent of myocardial injury sustained during reperfusion is very dependent on the effectiveness of its antioxidant defenses[31]. Compared to ischemic period (0 h), there were marked increase in levels of ascorbic acid and oxidized forms of ascorbate and glutathione namely dehydroascorbic acid and GSSG, following reperfusion. This suggests that these tissue hydrophilic antioxidants may be the first line of antioxidant defences to curb the generation of reactive oxygen species (ROS) following reperfusion[31]. The most significant pathways (**Figure-2.3B and Figure-2.3C**) representing late response in plasma metabolism at 24 h and 48 h post PCI were phenylalanine metabolism, tyrosine metabolism, linoleic acid metabolism and glycerophospholipid metabolism which were different from those seen immediately post PCI.

Measures of correlation between metabolites in replicate profiles can be very informative about the underlying biological system[16]. From the heat map (**Figure-2.4A**) constructed with highly correlated metabolites (n=37), it was evident that the concentration levels of certain free fatty acids (FFA) such as arachidonic acid (AA), docosapentaenoic acid (DPA), eicosatrienoic acid, docosahexaenoic acid (DHA), which are intermediaries of linoleic acid and alpha linolenic acid metabolism, and certain lysophospholipids such as lysoPC (18:3), lysoPC (20:3) were elevated at ischemic time point (0 h, pre angioplasty), but decreased progressively following reperfusion. The enzyme phospholipases A_2 (PLA_2) is known to play an important role in the hydrolysis of phospholipids[32] especially phosphatidylcholines (PC), which leads to accumulation of FFA including (non-esterified) AA and DHA[33]. This non-esterified AA is then rapidly esterified to available lysophospholipids, or is converted into bioactive arachidonic acid metabolites, i.e., eicosanoids via cyclooxygenase (COX), lipoxygenase (LOX), or cytochrome P450 (CYP) epoxygenase enzymes[34]. From our study, the observed progressive decrease in the concentration levels of AA, DHA, DPA, and lysophospholipids after reperfusion strongly endorses the possible

part that PLA_2 plays in disturbed phospholipid homeostasis during the transition from reversible to irreversible ischemic myocardial injury. This evidence also underlines the current understanding that lipoprotein associated PLA_2 is a significant predictor of cardiovascular outcome independent of traditional clinical risk factors[35]. In addition, few other metabolites like citrulline (a participant in urea cycle), mevalonic acid, 3-octanone and pregnenolone sulfate also exhibited the same co-variation (initially increases with subsequent decline) as the above metabolites.

Amongst highly correlated metabolites, several metabolites exhibited a pattern (**Figure-2.4A**) which is different from the metabolites discussed above. The abundance levels of these metabolites declined at ischemic condition (0 h) compared to post reperfusion time intervals but elevated noticeably following reperfusion. These include pyruvate, succinate, malonic acid, 2-hydroxyglutarate, acetate and propanoate which are known to involve directly or indirectly with TCA cycle metabolism. The variation in the metabolic concentrations of these compounds before and after reperfusion suggests an impaired TCA cycle metabolism and subsequent energy metabolism in the setting of I/R injury. The heat map (**Figure-2.4A**) also shows that the concentration levels of certain other highly correlated metabolites, like deoxyadenosine, N-acetylaspartylglutamic acid (NAAG), 3-O-methylepicatechin, 2-nonynoic acid, 5-methylthioadenosine, 1-methylhistamine and neopterin also exhibited the same co-variation (initially low, but finally high) as the above metabolites.

Previous studies have shown that elevations in troponin (Troponin T) and creatine kinase (CK) or its specific MB (CKMB) isoform after primary PCI represent larger infarct size and are clearly associated with increased early and late mortality[36-38]. In our study cohort, a combination of three metabolites namely pentadecanoic acid (15:0), linoleoyl carnitine (18:2 carnitine) and 1-linoleoylglycerophosphocholine (18:2 lysoPC) exhibited good separating capability in

discriminating small and large infarct size patients with an AUC value of 86 based on peak troponin concentration (**Figure-2.7A**) and with an AUC value of 82 (**Figure-2.7B**) based on peak CK concentration. The **Figure-2.7C** shows the relative concentration of these three molecules across the four time points. For pentadecanoic acid and 18:2 lysoPC, their amount is high before reperfusion and their amount decreases considerably 2 h post reperfusion. In the case of 18:2 carnitine, its amount is negligible before reperfusion, but increases progressively post reperfusion. Thus, our data suggest that determining the concentration level of these three metabolites at the time of admission is a good indicator of myocardial infarct size following coronary angioplasty and subsequent increased late morbidity and mortality.

Until recently it was assumed that the existence of straight chain odd number fatty acids such as pentadecanoic acid (15:0) in normal physiological conditions were rare. Recent analytical instrumentation has proven this to be a misconception, since the presence of odd number carbon fatty acids such as 15:0 and 17:0 have been shown to occur as minor constituents in practically every natural fat and carry out many roles like synthesis of very-long-chain odd-numbered fatty acids, replenish the TCA cycle with anaplerotic intermediates and, hence, improve mitochondrial energy metabolism in nature[39]. But whether one or all of these known metabolic roles of 15:0 has a link to CVD risk is still debated. Though certain studies have reported the association of 15:0 with greater risk of CVD[40], many studies like Elwood et al[41] showed that, in relation to coronary artery disease, it is inappropriate to accept an estimate of CVD risk based on plasma concentrations of 15:0 alone. Also, earlier studies have reported that lower serum levels of 18:2 lysoPC, a lysophospholipid, has a tight relationship with increased arterial stiffness, increased resting heart rate and occurrence of silent myocardial ischemia[42,43]. Linoleoyl carnitine is a long-chain acyl fatty acid derivative ester of carnitine. Ischemic condition inhibits beta oxidation of fatty acids and leads

to accumulation of toxic intermediates of beta oxidation, particularly long-chain acyl carnitine compounds like linoleoyl carnitine. These compounds are detrimental to cellular function and are known to enhance myocardial injury by inducing structural damage in ischemic myocytes[44,45]. From our study these three molecules were proved to be promising molecular markers for the determination of myocardial injury. To our knowledge, this is the first published report of a blood-based biomarker panel for the prediction of I/R injury following coronary intervention in patients presenting with STEMI. This has the capacity to identify novel pathways impaired during reperfusion injury and identify patients at high risk for myocardial damage after primary PCI allowing for development of therapeutic intervention to minimize I/R injury.

2.7 Study limitations

Our study has several potential limitations that should be considered. First, though serial sampling performed in all STEMI patients both before and after PCI helped minimize inter-individual variability and clinical confounders such as diet, drug effects, age, sex, and other co morbidities, our study population was comparatively small to identify metabolites that failed to reach minimal significance. But these metabolites which fail to reach minimum significance might be scientifically relevant. So, it is important to adequately validate the identified metabolites in a relatively larger patient cohort. Second, though ROC analysis with 100 CV exhibited good prediction accuracy (better than 80%); these findings are exploratory in nature and should be confirmed in an independent patient cohort. Moreover, as with any untargeted metabolomic study, samples were analysed without authentic standards. This calls for further confirmation of these identified metabolites by employing a targeted metabolomic analysis.

Conclusions

Using a non-targeted LC-QTOF-MS methodology, we have successfully generated the most comprehensive data to date on significant changes in the plasma metabolome in STEMI patients undergoing primary PCI. The role of lipids and lipid metabolism pathways in the pathogenesis of atherosclerosis is already well understood. But there is little information about their role in reperfusion and I/R injury. From our study, we elucidated that lipid metabolism in general and phospholipid, linoleic acid and alpha linolenic acid metabolism in particular represent the largest change in the plasma metabolome post PPCI. We also identified a panel of three metabolites namely pentadecanoic acid, linoleoyl carnitine and 1-linoleoylglycerophosphocholine that could serve as plasma biomarkers in determining the extent of myocardial injury after PCI. This knowledge could help to predict the response to PCI and how to limit complications in STEMI patients after reperfusion. Given that there is currently no therapy available for I/R injury, we consider our results as a major step toward moving us closer to our ultimate goal of developing therapies to prevent myocardial reperfusion injury and improve clinical outcomes in patients with STEMI.

2.8 References

1 Global, regional, and national incidence, prevalence, and years lived with disability for 328 diseases and injuries for 195 countries, 1990-2016: a systematic analysis for the Global Burden of Disease Study 2016. *Lancet (London, England)* **390**, 1211-1259, doi:10.1016/s0140-6736(17)32154-2 (2017).

2 Yellon , D. M. & Hausenloy , D. J. Myocardial Reperfusion Injury. *New England Journal of Medicine* **357**, 1121-1135, doi:10.1056/NEJMra071667 (2007).

3 Hausenloy, D. J. & Yellon, D. M. Myocardial ischemia-reperfusion injury: a neglected therapeutic target. *The Journal of Clinical Investigation* **123**, 92-100, doi:10.1172/JCI62874 (2013).

4 Lambert, L. *et al.* Association between timeliness of reperfusion therapy and clinical outcomes in ST-elevation myocardial infarction. *Jama* **303**, 2148-2155, doi:10.1001/jama.2010.712 (2010).

5 Dettmer, K., Aronov, P. A. & Hammock, B. D. MASS SPECTROMETRY-BASED METABOLOMICS. *Mass spectrometry reviews* **26**, 51-78, doi:10.1002/mas.20108 (2007).

6 Sabatine, M. S. *et al.* Metabolomic identification of novel biomarkers of myocardial ischemia. *Circulation* **112**, 3868-3875, doi:10.1161/circulationaha.105.569137 (2005).

7 Fan, Y. *et al.* Comprehensive Metabolomic Characterization of Coronary Artery Diseases. *Journal of the American College of Cardiology* **68**, 1281-1293, doi:10.1016/j.jacc.2016.06.044 (2016).

8 Sansbury, B. E. *et al.* Metabolomic Analysis of Pressure-overloaded and Infarcted Mouse Hearts. *Circulation. Heart failure* **7**, 634-642, doi:10.1161/CIRCHEARTFAILURE.114.001151 (2014).

9 Cheng, M. L. *et al.* Metabolic disturbances identified in plasma are associated with outcomes in patients with heart failure: diagnostic and prognostic value of metabolomics. *Journal of the American College of Cardiology* **65**, 1509-1520, doi:10.1016/j.jacc.2015.02.018 (2015).

10 Mayengbam, S., House, J. D. & Aliani, M. Investigation of vitamin B(6) inadequacy, induced by exposure to the anti-B(6) factor 1-amino D-proline, on plasma lipophilic metabolites of rats: a metabolomics approach. *European journal of nutrition* **55**, 1213-1223, doi:10.1007/s00394-015-0934-x (2016).

11 Hanson, M., Zahradka, P., Taylor, C. G. & Aliani, M. Identification of urinary metabolites with potential blood pressure-lowering effects in lentil-fed spontaneously hypertensive rats. *European journal of nutrition*, doi:10.1007/s00394-016-1319-5 (2016).

12 Xia, J. & Wishart, D. S. in *Current protocols in bioinformatics* (John Wiley & Sons, Inc., 2002).

13 Puymirat, E. *et al.* Acute Myocardial Infarction: Changes in Patient Characteristics, Management, and 6-Month Outcomes Over a Period of 20 Years in the FAST-MI

Program (French Registry of Acute ST-Elevation or Non-ST-elevation Myocardial Infarction) 1995 to 2015. *Circulation*, doi:10.1161/circulationaha.117.030798 (2017).

14 Wishart, D. S. *et al.* HMDB: the Human Metabolome Database. *Nucleic acids research* **35**, D521-526, doi:10.1093/nar/gkl923 (2007).

15 Xia, J. & Wishart, D. S. MetPA: a web-based metabolomics tool for pathway analysis and visualization. *Bioinformatics* **26**, 2342-2344, doi:10.1093/bioinformatics/btq418 (2010).

16 Camacho, D., de la Fuente, A. & Mendes, P. The origin of correlations in metabolomics data. *Metabolomics* **1**, 53-63, doi:10.1007/s11306-005-1107-3 (2005).

17 Ursem, R., Tikunov, Y., Bovy, A., van Berloo, R. & van Eeuwijk, F. A correlation network approach to metabolic data analysis for tomato fruits. *Euphytica* **161**, 181, doi:10.1007/s10681-008-9672-y (2008).

18 Hu, T. *et al.* METABOLOMICS DIFFERENTIAL CORRELATION NETWORK ANALYSIS OF OSTEOARTHRITIS. *Pacific Symposium on Biocomputing. Pacific Symposium on Biocomputing* **21**, 120-131 (2016).

19 Kuhn, M., von Mering, C., Campillos, M., Jensen, L. J. & Bork, P. STITCH: interaction networks of chemicals and proteins. *Nucleic acids research* **36**, D684-D688, doi:10.1093/nar/gkm795 (2008).

20 Babuin, L. & Jaffe, A. S. Troponin: the biomarker of choice for the detection of cardiac injury. *CMAJ : Canadian Medical Association Journal* **173**, 1191-1202, doi:10.1503/cmaj.050141 (2005).

21 Blomberg, D. J., Kimber, W. D. & Burke, M. D. Creatine kinase isoenzymes. Predictive value in the early diagnosis of acute myocardial infarction. *The American journal of medicine* **59**, 464-469 (1975).

22 Breiman, L. Random Forests. *Machine Learning* **45**, 5-32, doi:10.1023/a:1010933404324 (2001).

23 Deidda, M. *et al.* Metabolomic fingerprint of coronary blood in STEMI patients depends on the ischemic time and inflammatory state. *Sci Rep* **9**, 312, doi:10.1038/s41598-018-36415-y (2019).

24 Kohlhauer, M. *et al.* Metabolomic Profiling in Acute ST-Segment-Elevation Myocardial Infarction Identifies Succinate as an Early Marker of Human Ischemia-Reperfusion Injury. *J Am Heart Assoc* **7**, doi:10.1161/jaha.117.007546 (2018).

25 Ali, S. E., Farag, M. A., Holvoet, P., Hanafi, R. S. & Gad, M. Z. A Comparative Metabolomics Approach Reveals Early Biomarkers for Metabolic Response to Acute Myocardial Infarction. *Sci Rep* **6**, 36359, doi:10.1038/srep36359 (2016).

26 Park, E., Cho, M. & Ki, C. S. Correct use of repeated measures analysis of variance. *The Korean journal of laboratory medicine* **29**, 1-9, doi:10.3343/kjlm.2009.29.1.1 (2009).

27 Morgan, T. M. & Case, L. D. Conservative Sample Size Determination for Repeated Measures Analysis of Covariance. *Annals of biometrics & biostatistics* **1**, 1002 (2013).

28 Hasanally, D. *et al.* Increased Oxidized Phosphatidylcholines During Global Cardiac Ischemia Correlates to Reduced Cardiac Function: Implications as Potential Target for Ischemia Reperfusion Injury. *Canadian Journal of Cardiology* **29**, S344, doi:10.1016/j.cjca.2013.07.587.

29 Yeang, C. *et al.* Reduction of Myocardial Ischemia-Reperfusion Injury by Inactivating Oxidized Phospholipids. *Cardiovascular research*, doi:10.1093/cvr/cvy136 (2018).

30 Gao, F. *et al.* Enhancement of glutathione cardioprotection by ascorbic acid in myocardial reperfusion injury. *The Journal of pharmacology and experimental therapeutics* **301**, 543-550 (2002).

31 Haramaki, N. *et al.* Networking antioxidants in the isolated rat heart are selectively depleted by ischemia-reperfusion. *Free radical biology & medicine* **25**, 329-339 (1998).

32 De Windt, L. J., Reneman, R. S., Van der Vusse, G. J. & Van Bilsen, M. Phospholipase A2-mediated hydrolysis of cardiac phospholipids: the use of molecular and transgenic techniques. *Molecular and cellular biochemistry* **180**, 65-73 (1998).

33 Farias, S. E. *et al.* Formation of eicosanoids, E(2)/D(2) isoprostanes, and docosanoids following decapitation-induced ischemia, measured in high-energy-microwaved rat brain. *Journal of Lipid Research* **49**, 1990-2000, doi:10.1194/jlr.M800200-JLR200 (2008).

34 Spector, A. A., Fang, X., Snyder, G. D. & Weintraub, N. L. Epoxyeicosatrienoic acids (EETs): metabolism and biochemical function. *Progress in lipid research* **43**, 55-90 (2004).

35 Sabatine, M. S. *et al.* Prognostic utility of lipoprotein-associated phospholipase A2 for cardiovascular outcomes in patients with stable coronary artery disease. *Arteriosclerosis, thrombosis, and vascular biology* **27**, 2463-2469, doi:10.1161/atvbaha.107.151670 (2007).

36 Novack, V., Pencina, M., Cohen, D. J. & et al. Troponin criteria for myocardial infarction after percutaneous coronary intervention. *Archives of Internal Medicine* **172**, 502-508, doi:10.1001/archinternmed.2011.2275 (2012).

37 Okamatsu, K. *et al.* Elevated troponin T levels and lesion characteristics in non-ST-elevation acute coronary syndromes. *Circulation* **109**, 465-470, doi:10.1161/01.cir.0000109696.92474.92 (2004).

38 Jeremias, A. *et al.* Differential mortality risk of postprocedural creatine kinase-MB elevation following successful versus unsuccessful stent procedures. *Journal of the American College of Cardiology* **44**, 1210-1214, doi:10.1016/j.jacc.2004.06.051 (2004).

39 Pfeuffer, M. & Jaudszus, A. Pentadecanoic and Heptadecanoic Acids: Multifaceted Odd-Chain Fatty Acids. *Advances in Nutrition* **7**, 730-734, doi:10.3945/an.115.011387 (2016).

40 Sun, Q., Ma, J., Campos, H. & Hu, F. B. Plasma and erythrocyte biomarkers of dairy fat intake and risk of ischemic heart disease. *The American journal of clinical nutrition* **86**, 929-937 (2007).

41 Elwood, P. C., Pickering, J. E., Hughes, J., Fehily, A. M. & Ness, A. R. Milk drinking, ischaemic heart disease and ischaemic stroke II. Evidence from cohort studies. *European journal of clinical nutrition* **58**, 718-724, doi:10.1038/sj.ejcn.1601869 (2004).

42 Lin, H., Zhang, J. & Gao, P. Silent myocardial ischemia is associated with altered plasma phospholipids. *Journal of clinical laboratory analysis* **23**, 45-50, doi:10.1002/jcla.20288 (2009).

43 Paapstel, K. *et al.* Inverse relations of serum phosphatidylcholines and lysophosphatidylcholines with vascular damage and heart rate in patients with atherosclerosis. *Nutrition, metabolism, and cardiovascular diseases : NMCD* **28**, 44-52, doi:10.1016/j.numecd.2017.07.011 (2018).

44 Liepinsh, E. *et al.* Long-chain acylcarnitines determine ischaemia/reperfusion-induced damage in heart mitochondria. *The Biochemical journal* **473**, 1191-1202, doi:10.1042/bcj20160164 (2016).

45 Lopaschuk, G. D., Ussher, J. R., Folmes, C. D., Jaswal, J. S. & Stanley, W. C. Myocardial fatty acid metabolism in health and disease. *Physiol Rev* **90**, 207-258, doi:10.1152/physrev.00015.2009 (2010)

2.9 Supplementary data

1 Materials and methods

1.1 Sample size calculation

Though sample size determination is essential, the metabolic phenotyping which are usually characterized by high dimensions with hundreds of features limit the use of conventional techniques developed for other omics sciences like proteomics and genomics. Since our goal is to identify discriminating metabolites across the time course of ischemia/reperfusion injury, the effect size between the time points mainly determines the sample size. In our study, the largest effect (n=107, differential metabolites) was observed between 0 h and 48 h time points, and we chose those two time points to calculate the statistical power. The power analysis was done using MetaboAnalyst software v3.0. The MetaboAnalyst does power calculation based on two assumptions: 1) the effect is indeed present in the data, and 2) the test statistic follows a normal or near normal (Students't) distribution. A false discovery rate (FDR) of 0.1 was chosen as the significance criterion. The result (**Supplementary Figure.1**) indicated that power in our samples reaches an acceptable level (0.8) at a sample size of approximately 25.

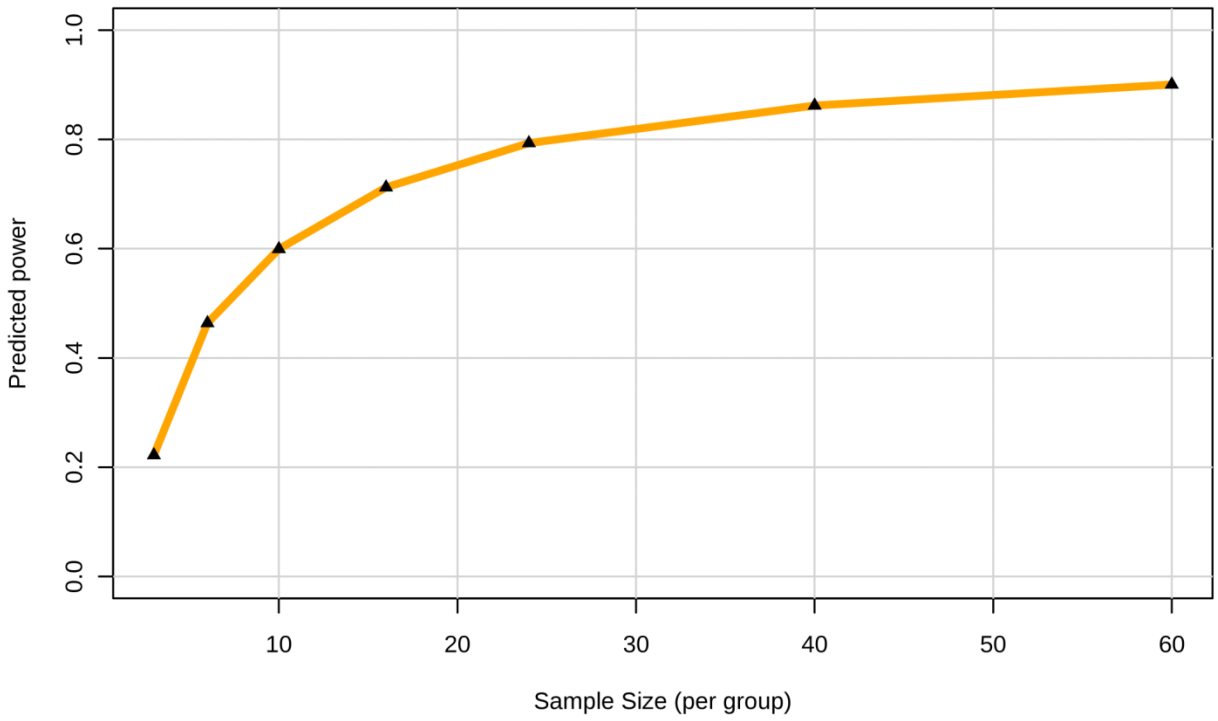

Supplementary Figure.1: Power vs. sample size, FDR = 0.1. The power analysis suggests that we will have over 80% power to detect discriminating metabolites using approximately 25 subjects in each group.

1.2 Chemicals

Acetonitrile and spectroscopic formic acid were purchased from Fisher Scientific (ON, Canada). Deionized ultrapure water was made in-house using Milli-Q System from Millipore Corporation (MA, USA). The ESI low concentration tuning mix and API-TOF reference mass solution containing Hexakisphosphazine (2.5 mM), Purine (5.0 mM) and Ammonium Trifluroacetate (100.00 mM) were obtained from Agilent Technologies (CA, USA).

1.3 Extraction of plasma metabolites

Briefly, plasma samples (100 microliters) were mixed with acetonitrile (200 microliters) in 1.5 millilitres Eppendorf tubes. The mixture is then vortexed vigorously for 30 seconds and was spun for 10 minutes (7378 x g at 4^{o}C). The supernatant was transferred into a new tube and dried under a gentle stream of nitrogen gas. The dried samples were reconstituted in 80% acetonitrile in deionized water (100 microliters). Each plasma sample was extracted in duplicate. The reconstituted samples were placed into a glass insert in an amber glass auto-sampler vial prior to LC-QTOF-MS analysis. A quality control (QC) mixture made of pooled plasma samples were extracted by the same method. This QC mixture was used to ensure the stability of LC -MS system. In order to ensure system stability, the pooled QC mixtures were analyzed in a random manner among all other samples. In addition to running the QC samples with all other plasma samples, six injections of pooled QC sample were carried out in both positive and negative mode before running the plasma samples to validate the extraction and LC-MS method.

1.4 Liquid chromatography separation

The metabolites were separated on a 1290 Infinity Agilent HPLC system from Agilent Technologies (CA, USA). The chromatographic separation for processed plasma was performed on a Zorbax Extend-C18 analytical column (2.1 mm × 50 mm I.D., particle size 1.8 µm, Agilent

Technologies, USA). Water was used as solvent A and acetonitrile was used as solvent B. All solvents for the LC system contained 0.1 % formic acid. Metabolites were eluted from the analytical column with a gradient of 0, 0.5, 12, 12.5 and 13 min with 30, 30, 100, 100 and 30% of solvent B respectively at a flow rate of 400 microliters/min. The column was immediately re-equilibrated at initial conditions (30% solvent B) for 2 min before injecting the next sample. The column temperature was kept at 55°C.

1.5 MS analysis

Mass spectral analysis of eluting peptides from the analytical column was carried out on a 6538 UHD Accurate Q-TOF LC/MS from Agilent Technologies (CA, USA) controlled by MassHunter Workstation Software (v 7.0). All analyses were performed in both positive and negative mode ESI employing a dual ionization source. These two sources will ensure that both polar and non-polar compounds are detected. The mass detection was done using reference ions of m/z 121.050873 and 922.009798 for positive mode and m/z 119.03632 and 1033.9881 for negative mode. The instrument settings were: gas temperature - 300 °C; drying N2 gas flow rate - 11 (litre/min); Nebulizer pressure - 50 psig; fragmentor voltage - 175 V; skimmer voltage – 50 V and OCTRF Vpp voltage - 750 V. The collision energy was applied by setting an appropriate equation having a slope value of 5 and offset value of 2.5. A full range mass scan from 50 to 1700 m/z with an extended dynamic range of 2 GHz standardized at 3200 was applied. Data acquisition rate was maintained at a rate of 2 spectra/second using a time frame of 500 milliseconds/spectra and a transient/spectrum ratio of 4057.

1.6 Data processing and statistical analysis

The acquired raw LC/MS data ('.d files') was preprocessed using Agilent MassHunter Qualitative Analysis (MHQ, vB.07) and Profinder (v B.06) software. Data processing was done by applying the "Find by Formula" (FBF) algorithm to the Total Ion Chromatogram (TIC) files by querying against the custom database to extract features, satisfying an absolute abundances of more than 5000 counts. The custom database was made by collecting information on numerous metabolites associated with cardiovascular disease from published literature and by combining reported metabolites in blood from Human Metabolome Database (HMDB). The FBF algorithm operates based on the compound's monoisotopic mass (in ppm), isotope spacing (in ppm) and isotope distribution (in %). During data processing, the match tolerance limit was set to ± 10 ppm for masses and ± 0.35 minutes for retention times. The parameters were chosen to provide information of the compound based on their isotope pattern, multiple charge states, the formation of dimer and adduct ions (+H, +Na, + K, +NH4 adducts in positive ion mode and -H, -HCOO and -CH3COO adducts in negative ion mode). The collected information summarizing retention time (RT), ion intensity, exact mass and possible chemical relationships (isotopes, adducts, dimers, multiple charge states) was converted into compound exchange format ('*.cef') files. The '*.cef' files were then imported to Agilent Mass Profiler Professional (MPP, v12.6) software for further data processing and statistical analysis. A frequency filtration was used to only accept features that were detected in at least one of the four conditions (time intervals). The ion intensities for each spectrum were normalized using a percentile shift algorithm set to 75 and were adjusted to the baseline values of the median of all samples. Repeated measures one way ANOVA ($p<0.001$) was used to identify metabolite changes over the four time intervals within the same subjects. The 'Bonferroni FWER' multiple testing correction method was used to adjust p-values derived from

multiple statistical tests and to correct for occurrences of false positives. The identified features satisfying the above conditions were then subjected to a recursive analysis using 'Batch Recursive Feature Extraction' algorithm in MPP to generate the final list of potential features. In recursive analysis, the list of features already identified by FBF algorithm was re-extracted once again by searching against the raw data files. The log-transformed metabolite concentrations (non-averaged) of the final entity list with 130 differential metabolites across the four time intervals (0 h ischemic condition (pre angioplasty), 2 h post reperfusion , 24 h post reperfusion and 48 h post reperfusion) were used for sample classification and further statistical analysis. The differential metabolites were classified based on their chemical taxonomy on HMDB and KEEG (*Kyoto* Encyclopedia of Genes and Genomes) databases.

Further statistical analysis and biomarker analysis were done using the MetaboAnalyst software v3.0 (McGill University, Quebec, Canada). In order to visualize the similarities and differences between each of the four time intervals in the plasma metabolome, the unsupervised multivariate pattern recognition technique, principal component analysis (PCA) was first employed on the metabolome data. In the PCA score plot, each point represents an individual sample. The loadings (weights) of the metabolites on the principal components indicate which among the four time points were similar, different or distinct. The supervised 3-dimensional partial least squares-discriminant analysis (PLS-DA) was then employed to maximize difference in metabolic profile between the time intervals. A cross comparison of the samples between different time intervals will help us to understand the early and late response in plasma metabolome in response to I/R injury by identifying the key metabolites involved at each junction. To accomplish this, a one-way analysis of variance (ANOVA) with p-value cut-off of 0.05, followed by Tukey's Honestly Significant Difference (Tukey's HSD) post hoc analysis was performed on the log-transformed

metabolite concentrations (non-averaged) of the final entity list with 130differential metabolites. Next, to examine the metabolomic pathways represented by these 130 differential metabolites, a pathway impact analysis was performed using MetPA (Metabolomics Pathway Analysis) tool (http://metpa.metabolomics.ca) based on KEGG database. The pathway impact was calculated as the sum of the importance measures of the matched metabolites normalized by the sum of the importance measures of all metabolites in each pathway. The differential metabolites identified from one-way ANOVA served as the input metabolite data set representing each time interval. To investigate the relationship of the 130 differential metabolites in the metabolite entity set, the pair-wise correlations (Pearson correlation coefficient) between the metabolites were calculated using correlation calculator from MetScape software v3.0 (http://metscape.ncibi.org) based on the log normalized intensities of the metabolites. Using group average values, only those metabolites satisfying a Pearson correlation coefficient, $|r| > 0.9$ were considered as highly correlated metabolites (n=37). The MetaboAnalyst v4.0 was used to plot the metabolite-metabolite interaction network plot to visualize and analyze biological relationships between the correlated metabolites. Next, to examine the underlying biochemical pathways reflected by this network correlation, a Metabolite Set Enrichment Analysis (MESA) was done on these correlated metabolites. MSEA is a metabolomic version of the popular GSEA (Gene Set Enrichment Analysis) software. MSEA has its own collection of metabolite set libraries (MetaboAnalyst v3.0 library contains 88 metabolite sets based on normal metabolic pathways). MSEA was implemented using the hypergeometric test to evaluate whether a particular metabolite set is represented more than expected by chance within the given compound list. The pathway significance was determined based on fold enrichment and p-value, by searching against the pathway-associated metabolite sets library. To further investigate the relationship between the plasma metabolites and

important clinical factors at baseline (0 h, time-1), correlations were also calculated for all pairs of metabolite-clinical factors using the R statistical package 'corrplot'. In addition, receiver operating characteristic (ROC) analysis was used to evaluate the diagnostic capability of metabolites which can serve as potential biomarkers. A summary of the metabolomic workflow was provided in **Supplementary Table.1**.

Supplementary Table.1 Summary of the metabolomic workflow
Step 1 Data processing
Non-targeted analysis of plasma samples in both ESI positive and ESI negative modes.
The processing of acquired raw LC/MS data ('.d files') using MHQ vB.07 and Profinder vB.06 software.
"Find by Formula" (FBF) algorithm was used to extract all detectable compounds. The entity list contained 765 and 670 compounds in ESI+ and ESI- modes, respectively.
'Batch Recursive Feature Extraction' algorithm in MPP v12.6.1 to remove false ± compounds. The entity list was reduced to 69 and 82 compounds in ESI+ and ESI- modes, respectively.
Repeated measures one way ANOVA followed by 'Bonferroni FWER' multiple testing correction method in MPP. After adjusting for p-value, the final list contained 130 significantly differential metabolites across all the four time points ($p<0.001$).
Step 2 Statistical analysis - MetaboAnalyst software v3.0
The supervised and unsupervised multivariate pattern recognition techniques, PCA and PLSDA were employed.
A one-way analysis of variance (ANOVA) with p-value cut-off of 0.05, followed by Tukey's Honestly Significant Difference (Tukey's HSD) post hoc analysis to identify significant metabolites at each junction in the time course.

Pathway impact analysis was performed using MetPA (Metabolomics Pathway Analysis) tool to identify biochemical pathways represented by the differential metabolites across different time points.
Step 3 Correlation network analysis
Pair-wise correlation analysis (Pearson correlation coefficient, |r|) to identify potential functional relationships between annotated metabolites - 37 metabolites were found with |r| >0.9 using MetScape software v3.0.
Heat map to visualize the highly correlated metabolite concentration across all the time points.
Metabolite Set Enrichment Analysis (MESA) to examine the underlying biochemical pathways reflected by this correlated metabolites.
The MetaboAnalyst v4.0 was used to plot the metabolite-metabolite interaction network plot using these highly correlated metabolites.
The statistical package 'corrplot' was used to plot the metabolite – clinical parameters correlation matrix.
Step 4 Diagnostic performance of metabolites
Three metabolites namely pentadecanoic acid, linoleoyl carnitine and 1-linoleoylglycerophosphocholine were selected to perform the ROC analysis.
Multivariate ROC plot based on random forests classification algorithm.

2 Results

2.1 Metabolites and different modes of ionization

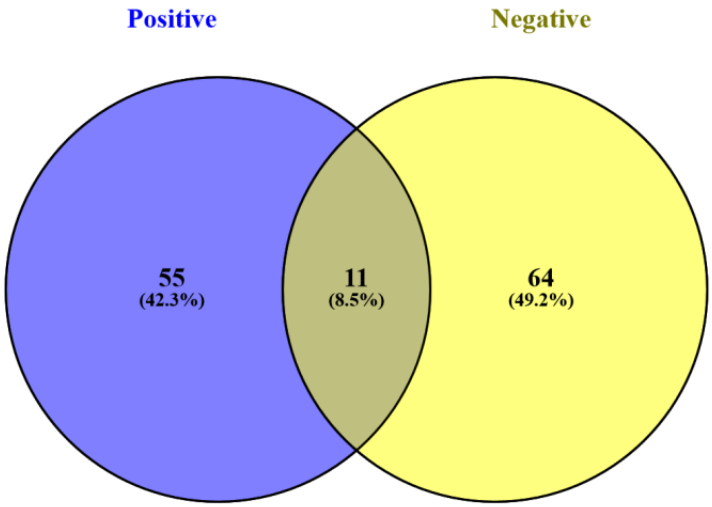

Supplementary Figure.2: The number of metabolites identified in different ionization modes.

Of the final 130 annotated compounds, 55 elements compounds were identified exclusively in "Positive" ESI mode, 64 compounds were identified exclusively in "Negative" ESI mode and 11 compounds were identified in both the modes.

2.2 Metabolites responsible for early and late response to reperfusion

The results from cross-comparison among different time intervals employing one-way ANOVA followed by Tukey's HSD identified the key set of metabolites responsible for early and late response to I/R injury. These metabolites were also responsible for the class separation observed with PCA and PLS-DA plots. In total, 11 metabolites were found to be significant between 0 h and 2 h comparison, 96 metabolites were found to be significant between 0 h and 24 h comparison, 107 metabolites were found to be significant between 0 h and 48 h comparison and were 16 metabolites found to be significant between 24 h and 48 h comparison. The numbers of metabolites involved at each time point were shown in below **Supplementary Figure.3**

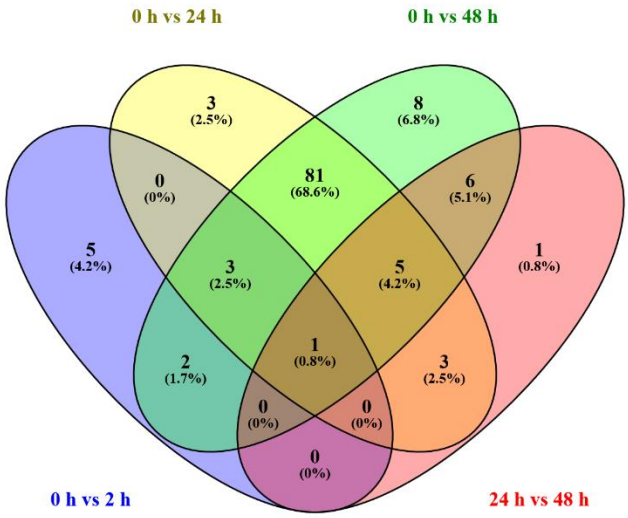

Supplementary Figure.3: The number of metabolites involved at each time point. The Venn diagram above depicts the number of metabolites shared among (or unique to) different groups (0 h ischemic condition (pre angioplasty), 2 h post angioplasty, 24 h post angioplasty and 48 h post angioplasty).

2.3 Troponin concentration and coronary artery

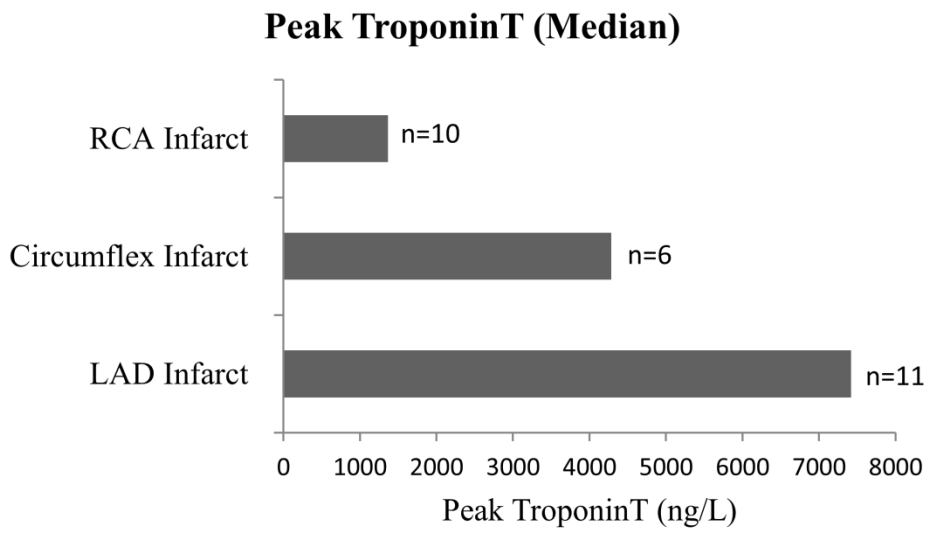

Supplementary Figure.4: LAD infarct vs RCA infarct vs Circumflex infarct. We compared the troponin values of LAD infarct with RCA infarct and Circumflex infarct. As expected, the median troponin value is largest for of LAD infarct compared to Circumflex infarct and RCA infarct.

Supplementary Table.2 Metabolites identified in different modes			
Sl.No	**55 elements identified exclusively in ESI + mode**	**64 elements identified exclusively in ESI - mode**	**11 common elements in ESI + and ESI -**
1	10-Hydroxydihydrosanguinarine	Benzaldehyde	LysoPC 18:3
2	Hydroxyisovaleroyl carnitine	5,8,11-Eicosatrienoic acid	Elaidic acid
3	Nudifloramide	PA 16:0/16:0	L Carnitine
4	Ribitol	PS 18:0/18:2	Dihomo-linoleate 20:2n6
5	2',3'-Cyclic AMP	LysoPC 20:3	Linolic acid
6	Palmitic acid	Dimethyl sulfone	Myo-inositol
7	1-palmitoyl-GPC	Sorbitol-6-phosphate	Eicosapentaenoic acid
8	LysoPE 18:3	Hydroxypropionylcarnitine	Leucine/Isoleucine
9	LysoPE 20:4	Pyroglutamic acid	Palmitoleic acid
10	1-methyladenosine	Docosapentaenoic acid	1-Methylhistamine
11	L-isoleucyl-L-Proline	3-Methoxytyramine	5'-methylthioadenosine
12	Dehydroascorbic acid	6-Hydroxygliclazide	
13	3-Octanone	Arachidonic acid	
14	LysoPE 22:1	Thienodihydropyridinium	

15	Linoleoyl carnitine	4-Aminophenol
16	PC 22:4/14:1	LysoPC 22:4
17	p-cresol	dCTP
18	Heptadecanoic acid	15-Keto-13,14-dihydroprostaglandin A2
19	Isovaleryl carnitine	3-Hydroxysuberic acid
20	LysoPC 22:6	D-Limonene
21	Orotic acid	N-Acetylserotonin
22	Xanthine	Mevalonic acid
23	1-Linoleoylglycerophosphocholine	Docosahexaenoic acid
24	Succinic acid	Glycyl-glycine
25	2-Nonynoic acid	Leucyl-phenylalanine
26	Ascorbic acid	11-Ketoetiocholanolone
27	LysoPC 24:0	N-Acetylaspartylglutamic acid
28	Xanthosine	3'-O-Methylepicatechin
29	Thromboxane B2	PG 18:0/18:1
30	2-hydroxyglutarate	L-Hexanoylcarnitine

31	Guanine	Thymidine
32	Propanoate	Calcitroic acid
33	Pyruvic acid	N-Acetylornithine
34	Acetate	Equol
35	gamma-Glutamylvaline	4-Ethylphenol
36	Malonic acid	3,5-Diiodothyronine
37	O-Phosphothreonine	Oleoyl glycine
38	Pyridoxamine 5'-phosphate	Homocysteine
39	3-Methoxy-4-Hydroxyphenylglycol sulfate	Acylcarnitine
40	Enterodiol	1,5-Anhydrosorbitol
41	5-Hydroxytryptophol	Enkephalin L
42	Dehydrogenated ticlopidine	Hydroxyphenylacetylglycine
43	3-Hydroxytetradecanedioate	Diacetylspermine
44	Normetanephrine	1,3,7-Trimethyluric acid
45	Hexanoylglycine	Benzoyl ecgonine
46	PC 16:0/16:0	Hypoxanthine

47	N-Desmethylpromazine	12,13-DiHODE
48	Retinylglucuronide	Protoprimulagenin A3
49	D-Pipecolic acid	O-Desmethylverapamil
50	SM d18:0/16:0	L-Tryptophan
51	Neopterin	dCMP
52	Aminoacetone	Pregnenolone sulfate
53	Deoxyadenosine	Citrulline
54	PG 18:0/22:4	Glycodesoxycholate
55	N-Desmethyleletriptan	Didodecylthiobispropanoate
56		Phenylacetylglutamine
57		Hydrocortisone
58		p-Hydroxyphenylacetate
59		Oxidized glutathione
60		Pentadecanoic acid
61		Biliverdin
62		Mannitol

63	PI 16:0/16:0
64	4-Hydroxybenzoic acid

Supplementary Table.3 Final list of 130 significant metabolites							
Sl.No	**Compound**	**P value**	**HMDB ID**	***m/z***	**Most abundant ionic species**	**RT**	**Pathways**
1	Benzaldehyde	5E-15	HMDB06115	151.0404	(M+HCOO)-	0.412	Phenylalanine metabolism
2	5,8,11-Eicosatrienoic acid	0.0004	HMDB10378	305.2483	(M-H)-	9.44	Arachidonic acid metabolism, Linoleic acid metabolism
3	PA 16:0/16:0	6E-08	HMDB00674	647.4623	(M-H)-	9.847	Glycerophospholipid metabolism
4	PS 18:0/18:2	0.0434	HMDB12380	832.5315	(M+HCOO)-	7.542	Glycerophospholipid metabolism
5	LysoPC 20:3	0.03	HMDB10393	590.3463	(M+HCOO)-	7.106	Glycerophospholipid metabolism
6	Dimethyl sulfone	0.0157	HMDB04983	187.0111	(2M-H)-	0.395	Sulfur metabolism
7	Sorbitol-6-phosphate	7E-17	HMDB05831	261.0378	(M-H)-	0.342	Fructose and mannose metabolism
8	Hydroxypropionyl carnitine	3E-05	HMDB13125	525.2693	(2M+CH3COO)-	0.393	Fatty acid metabolism
9	Pyroglutamic acid	0.0003	HMDB00267	128.0358	(M-H)-	0.337	Glutathione metabolism
10	Docosapentaenoic acid	6E-05	HMDB06528	329.2486	(M-H)-	9.19	Biosynthesis of unsaturated fatty acids, Linoleic acid metabolism
11	3-Methoxytyramine	1E-12	HMDB00022	379.1863	(2M+HCOO)-	9.856	Tyrosine metabolism
12	6-Hydroxygliclazide	1E-06	HMDB14028	398.1398	(M+CH3COO)-	9.009	Gliclazide Pathway
13	Arachidonic acid	0.0058	HMDB01043	303.2332	(M-H)-	8.931	Arachidonic acid metabolism, Linoleic acid metabolism
14	Thienodihydropyridinium	2E-22	HMDB13924	321.059	(M+CH3COO)-	0.355	NA

15	4-Aminophenol	0.0003	HMDB01169	263.1033	(2M+HCOO)-	0.351	Aminobenzoate degradation, Microbial metabolism in diverse environments
16	LysoPC 22:4	0.0062	HMDB10401	616.3621	(M+HCOO)-	7.697	Glycerophospholipid metabolism
17	dCTP	0.0032	HMDB00998	978.9779	(2M+HCOO)-	0.323	Pyrimidine metabolism
18	15-Keto-13,14-dihydroprostaglandin A2	2E-06	HMDB01244	667.4251	(2M-H)-	9.843	NA
19	3-Hydroxysuberic acid	3E-06	HMDB00325	379.1627	(2M-H)-	9.016	Fatty acid metabolism
20	D-Limonene	0.0001	HMDB03375	331.2648	(2M+CH3COO)-	9.862	Limonene and pinene degradation, Biosynthesis of terpenoids and steroids
21	N-Acetylserotonin	0.0002	HMDB01238	263.1033	(M+HCOO)-	0.351	Tryptophan metabolism
22	Mevalonic acid	1E-09	HMDB00227	355.161	(2M+CH3COO)-	9.564	Terpenoid backbone biosynthesis, Biosynthesis of terpenoids and steroids, Ferroptosis
23	Docosahexaenoic acid	0.0063	HMDB02183	327.233	(M-H)-	8.814	Biosynthesis of unsaturated fatty acids, Linoleic acid metabolism
24	Glycyl-glycine	0.0012	HMDB11733	263.0994	(2M-H)-	0.354	Glycine metabolism
25	LysoPC 18:3	0.0009	HMDB10388	562.3151	(M+HCOO)-	5.843	Glycerophospholipid metabolism

26	Leucyl-phenylalanine	0.0001	HMDB13243	277.1536	(M-H)-	5.6	Phenylalanine metabolism
27	11-Ketoetiocholanolone	1E-05	HMDB06031	667.4251	(2M+CH3COO)-	9.843	NA
28	N-Acetylaspartyl glutamic acid	7E-26	HMDB01067	653.1788	(2M+HCOO)-	3.086	Alanine, aspartate and glutamate metabolism
29	3'-O-Methylepicatechin	1E-31	HMDB29175	653.1906	(2M+HCOO)-	3.092	Flavonoid biosynthesis
30	PG 18:0/18:1	3E-08	HMDB10603	836.5805	(M+CH3COO)-	9.198	Glycerophospholipid metabolism
31	L-Hexanoylcarnitine	0.0256	HMDB00756	577.3737	(2M+CH3COO)-	10.617	Fatty acid metabolism
32	Thymidine	2E-08	HMDB00273	241.0836	(M-H)-	2.469	Pyrimidine metabolism
33	Calcitroic acid	2E-07	HMDB06472	433.2601	(M+CH3COO)-	9.893	NA
34	N-Acetylornithine	2E-11	HMDB03357	407.2144	(2M+CH3COO)-	0.518	Arginine and proline metabolism, Biosynthesis of amino acids
35	Equol	3E-12	HMDB02209	241.0873	(M-H)-	2.445	NA
36	4-Ethylphenol	0.0007	HMDB29306	121.0658	(M-H)-	0.501	Bisphenol degradation
37	3,5-Diiodothyronine	6E-14	HMDB00582	1108.8	(2M+CH3COO)-	8.807	Thyroid hormone synthesis
38	Oleoyl glycine	0.0153	HMDB13631	338.2707	(M-H)-	8.365	NA
39	Homocysteine	3E-10	HMDB00742	194.0501	(M+CH3COO)-	0.382	Homocysteine Degradation, Betaine Metabolism, Methionine Metabolism

40	Acylcarnitine	2E-08	HMDB01185	444.1451	(M+HCOO)-	8.628	Arginine and proline metabolism, Cysteine and methionine metabolism, Biosynthesis of amino acids
41	1,5-Anhydrosorbitol	6E-12	HMDB02712	327.1295	(2M-H)-	8.216	NA
42	Enkephalin L	3E-14	HMDB01045	1169.5576	(2M+CH3COO)-	0.326	Neuroactive ligand-receptor interaction
43	Hydroxyphenylacetylglycine	9E-29	HMDB00735	477.1525	(2M+CH3COO)-	4.111	Tyrosine metabolism
44	Diacetylspermine	0.0001	HMDB02172	345.249	(M+CH3COO)-	7.636	NA
45	1,3,7-Trimethyluric acid	2E-15	HMDB02123	255.0743	(M+HCOO)-	0.409	Caffeine metabolism
46	Benzoyl ecgonine	1E-06	HMDB41836	637.2768	(2M+CH3COO)-	6.592	NA
47	Hypoxanthine	0.0308	HMDB00157	181.0373	(M+HCOO)-	0.343	Purine metabolism, Caffeine metabolism
48	12,13-DiHODE	2E-09	HMDB10201	669.4582	(2M+HCOO)-	10.89	Linoleic acid metabolism
49	Protoprimulagenin A3	1E-14	HMDB33157	1147.5594	(M+HCOO)-	0.297	NA
50	O-Desmethylverapamil	0.0014	HMDB13961	499.2817	(M+CH3COO)-	5.411	(Drug metabolite)
51	[a]L-Tryptophan	1E-13	HMDB00929	263.1033	(M+CH3COO)-	0.351	Glycine, serine and threonine metabolism, Phenylalanine, tyrosine and tryptophan biosynthesis, Tryptophan metabolism, Biosynthesis of amino acids

52	[a]dCMP	9E-11	HMDB01202	352.0566	(M+HCOO)-	0.413	Pyrimidine metabolism
53	[a]Pregnenolone sulfate	0.0002	HMDB00774	395.1894	(M-H)-	3.184	Steroid hormone biosynthesis
54	[a]Citrulline	0.0007	HMDB00904	395.1894	(2M+HCOO)-	3.184	Arginine biosynthesis, Biosynthesis of amino acids
55	[a]Glycodesoxycholate	1E-05	HMDB00631	448.3072	(M-H)-	3.874	NA
56	[a]Didodecyl thiobispropanoate	7E-05	HMDB40172	1087.8188	(2M+CH3COO)-	9.202	NA
57	[a]Phenylacetylglutamine	8E-10	HMDB06344	263.1038	(M-H)-	0.35	Phenylalanine metabolism
58	[a]Hydrocortisone	2E-21	HMDB14879	407.2076	(M+HCOO)-	0.519	Bile secretion, Steroid hormone biosynthesis,
59	[a]p-Hydroxy phenylacetate	2E-24	HMDB00020	151.0402	(M-H)-	0.392	Phenylalanine metabolism, Tyrosine metabolism
60	[a]Oxidized glutathione	5E-14	HMDB03337	611.1449	(M-H)-	3.627	Glutathione metabolism, Ferroptosis
61	[a]Pentadecanoic acid	1E-05	HMDB00826	241.2174	(M-H)-	8.903	Fatty acid metabolism
62	[a]Biliverdin	2E-21	HMDB01008	581.2407	(M-H)-	10.53	Porphyrin and chlorophyll metabolism
63	[a]Mannitol	2E-21	HMDB00765	241.093	(M+CH3COO)-	2.415	Fructose and mannose metabolism
64	[a]PI 16:0/16:0	2E-21	HMDB09778	855.5254	(M+HCOO)-	8.738	Glycerophospholipid metabolism

65	[a]4-Hydroxybenzoic acid	4E-30	HMDB00500	137.0244	(M-H)-	0.525	Phenylalanine metabolism, Ubiquinone and other terpenoid-quinone biosynthesis
66	[a]10-Hydroxy dihydrosanguinarine	1E-06	NA	372.084	(M+Na)+	2.484	Isoquinoline alkaloid biosynthesis
67	[a]Elaidic acid	3E-13	HMDB00573	283.263	(M+H)+	10.011	Fatty acid biosynthesis, Biosynthesis of unsaturated fatty acids
68	[a]Hydroxyisovaleroyl carnitine	4E-26	HMDB62555	523.323	(2M+H)+	10.449	Fatty acid metabolism
69	[a]L Carnitine	2E-33	HMDB00062	162.1118	(M+H)+	0.331	Bile secretion
70	[a]dihomo-linoleate (20:2n6)	0.0005	HMDB61864	331.2629	(M+Na)+	9.374	Linoleic acid metabolism
71	[a]Linoleic acid	1E-07	HMDB00673	281.2473	(M+H)+	9.181	Linoleic acid metabolism
72	[a]Nudifloramide	0.0004	HMDB04193	153.0656	(M+H)+	0.371	Nicotinate and nicotinamide metabolism
73	[a]Ribitol	0.012	HMDB00508	153.0746	(M+H)+	0.353	Pentose and glucuronate interconversions, Riboflavin metabolism
74	[a]Myo-inositol	0.0085	HMDB00211	203.0526	(M+Na)+	0.324	Ascorbate and aldarate metabolism, Galactose metabolism
75	[a]2',3'-Cyclic AMP	7E-30	HMDB11616	347.0872	(M+NH4)+	0.424	Purine metabolism

76	[a]Palmitic acid	3E-11	HMDB00220	257.2473	(M+H)+	9.751	Fatty acid biosynthesis, Biosynthesis of unsaturated fatty acids
77	[a]1-palmitoyl glycerophosphocholine	2E-06	HMDB62541	519.3264	(M+Na)+	5.924	Glycerophospholipid metabolism
78	[a]Eicosapentaenoic acid	8E-14	HMDB01999	303.2314	(M+H)+	8.383	Biosynthesis of unsaturated fatty acids
79	[a]LysoPE 18:3	4E-15	HMDB11509	476.2761	(M+H)+	5.449	Glycerophospholipid metabolism
80	[a]Leucine/Isoleucine	1E-13	HMDB00687	132.1017	(M+H)+	0.341	Valine, leucine and isoleucine biosynthesis, Biosynthesis of amino acids
81	[a]LysoPE 20:4	0.0027	HMDB11517	502.2927	(M+H)+	6.145	Glycerophospholipid metabolism
82	[a]1-methyladenosine	0.0013	HMDB03331	299.1446	(M+NH4)+	0.38	NA
83	[a]L-isoleucyl-L-Proline	0.0006	HMDB11174	229.154	(M+H)+	0.334	NA
84	[a]Dehydroascorbic acid	5E-05	HMDB01264	366.0682	(2M+NH4)+	0.399	Ascorbate and aldarate metabolism, Glutathione metabolism
85	[a]3-Octanone	4E-11	HMDB31295	257.2475	(2M+H)+	9.759	NA
86	[a]LysoPE 22:1	0.0062	HMDB11521	536.3697	(M+H)+	8.544	Glycerophospholipid metabolism
87	[a]Linoleoyl carnitine	4E-08	HMDB06469	424.3415	(M+H)+	5.661	Fatty acid metabolism

88	[a]PC 22:4/14:1	6E-07	HMDB08624	780.5525	(M+H)+	9.758	Glycerophospholipid metabolism, Arachidonic acid metabolism, Linoleic acid metabolism
89	[a]p-cresol	0.0191	HMDB01858	126.0914	(M+NH4)+	0.354	Toluene degradation
90	[a]Heptadecanoic acid	1E-24	HMDB02259	271.2623	(M+H)+	10.367	Biosynthesis of unsaturated fatty acids
91	[a]Isovaleryl carnitine	6E-12	HMDB00688	268.1544	(M+Na)+	0.337	Leucine metabolism, Fatty acid metabolism
92	Palmitoleic acid	0.0196	HMDB03229	255.2315	(M+H)+	8.769	Fatty acid biosynthesis
93	[a]LysoPC 22:6	2E-06	HMDB10404	568.3398	(M+H)+	6.597	Glycerophospholipid metabolism
94	[a]Orotic acid	1E-05	HMDB00226	174.0524	(M+NH4)+	0.362	Pyrimidine metabolism
95	[a]Xanthine	5E-30	HMDB00292	153.0415	(M+H)+	0.363	Purine metabolism, Caffeine metabolism
96	[a]1-Linoleoyl glycerophosphocholine	8E-23	HMDB61692	1091.7001	(2M+Na)+	7.252	Glycerophospholipid metabolism
97	[a]Succinic acid	5E-30	HMDB00254	141.016	(M+Na)+	0.472	Phenylalanine metabolism, Tyrosine metabolism, Citrate cycle (TCA cycle), Butanoate metabolism, Alanine, aspartate and glutamate metabolism,

							Oxidative phosphorylation
98	[a]2-Nonynoic acid	5E-30	HMDB0032442	172.1333	(M+NH4)+	0.337	NA
99	[a]Ascorbic acid	0.0004	HMDB00044	194.0658	(M+NH4)+	0.695	Glutathione metabolism, Ascorbate and aldarate metabolism
100	[a]5'-methylthioadenosine	5E-30	HMDB01173	336.0508	(M+K)+	0.994	Cysteine and methionine metabolism
101	[a]LysoPC 24:0	8E-06	HMDB10405	646.4209	(M+K)+	9.842	Glycerophospholipid metabolism
102	[a]1-Methylhistamine	5E-30	HMDB00898	126.0994	(M+H)+	10.023	Histidine metabolism
103	[a]Xanthosine	3E-05	HMDB00299	285.0811	(M+H)+	0.695	Purine metabolism, Caffeine metabolism
104	[a]Thromboxane B2	0.0002	HMDB03252	741.4745	(2M+H)+	9.99	Arachidonic acid metabolism, Bile secretion
105	[a]2-hydroxyglutarate	5E-30	HMDB59655	193.0351	(M+HCOO)+	1.563	Butanoate metabolism
106	[a]Guanine	5E-30	HMDB00132	152.0562	(M+H)+	0.909	Purine metabolism
107	Propanoate	5E-30	NA	132.1016	(2M+NH4)+	0.332	Citrate cycle (TCA cycle)
108	[a]Pyruvic acid	0.0004	HMDB00243	201.0247	(2M+Na)+	0.674	Phenylalanine metabolism, Tyrosine metabolism, Citrate cycle (TCA cycle), Vitamin B6 metabolism,

109	[a]Acetate	5E-30	NA	141.016	(2M+Na)+	0.472	Citrate cycle (TCA cycle)
110	[a]gamma-Glutamylvaline	8E-10	HMDB11172	515.2332	(2M+Na)+	5.933	NA
111	[a]Malonic acid	5E-30	HMDB00691	267.0371	(2M+CH3COO)+	0.384	Pyrimidine metabolism
112	O-Phosphothreonine	0.0002	HMDB11185	200.0337	(M+H)+	0.419	Porphyrin and chlorophyll metabolism
113	Pyridoxamine 5'-phosphate	3E-07	HMDB01555	249.0614	(M+H)+	0.327	Vitamin B6 metabolism
114	3-Methoxy-4-Hydroxy phenylglycolsulfate	8E-16	HMDB03332	265.0352	(M+H)+	0.329	norepinephrine metabolism
115	Enterodiol	2E-13	HMDB05056	627.2916	(2M+Na)+	7.019	NA
116	5-Hydroxytryptophol	0.0011	HMDB01855	200.068	(M+Na)+	0.311	Serotonin degradation
117	Dehydrogenated ticlopidine	0.0253	HMDB13926	262.0451	(M+H)+	0.399	(Drug metabolite)
118	3-Hydroxytetra decanedioate	4E-07	HMDB00394	571.3446	(2M+Na)+	6.601	NA
119	Normetanephrine	5E-05	HMDB00819	367.1877	(2M+H)+	8.388	Tyrosine metabolism
120	Hexanoylglycine	0.0002	HMDB00701	347.2207	(2M+H)+	1.013	Fatty acid metabolism
121	PC 16:0/16:0	0.0418	HMDB00564	734.5682	(M+H)+	11.442	Glycerophospholipid metabolism
122	N-Desmethylpromazine	3E-07	HMDB13939	541.2479	(2M+H)+	5.518	(Drug metabolite)
123	Retinylglucuronide	0.0001	HMDB10340	480.2972	(M+NH4)+	6.157	(Drug metabolite)
124	D-Pipecolic acid	0.0233	HMDB05960	130.0862	(M+H)+	0.333	Lysine degradation
125	SM d18:0/16:0	0.0062	HMDB10168	744.557	(M+K)+	10.683	Sphingolipid metabolism
126	Neopterin	1E-22	HMDB00845	524.1952	(2M+NH4)+	4.445	Folate biosynthesis

127	Aminoacetone	4E-05	HMDB02134	169.0932	(2M+Na)+	0.379	Glycine, serine and threonine metabolism
128	Deoxyadenosine	2E-20	HMDB00101	525.1936	(2M+Na)+	4.429	Purine metabolism
129	PG 18:0/22:4	0.0013	HMDB10611	849.5645	(M+Na)+	9.955	Glycerophospholipid metabolism
130	N-Desmethyleletriptan	8E-12	HMDB13919	369.1627	(M+H)+	8.373	(Drug metabolite)

a - The compounds already reported in published literature known to be associated with either ischemia, myocardial infarction or other forms of CAD including non-obstructive coronary atherosclerosis, stable angina pectoris or unstable angina pectoris; P Value - P-values after 'Bonferroni FWER' multiple testing correction; HMDB ID - Human Metabolome Database ID; *m/z* – mass to charge ratio of the most abundant ion; RT – retention time

CHAPTER 3. Impact of myocardial reperfusion on human plasma lipidome

Rationale

Our previous non-targeted metabolomics demonstrated that lipid molecules represent the largest pool of altered metabolites during I/R injury. However, detailed knowledge about the disturbances in lipidome profiles during I/R injury has not been explored. Therefore, determining the changes in plasma lipidome and correlating these changes to clinical outcomes would offer new insight into the mechanisms of IR injury. The study of plasma lipidome is challenging, given the heterogenous chemical structure of lipids. This is why research in this area has focused primarily on abundant plasma lipids referred to as traditional lipids, such as cholesterol, triglycerides, high-density lipoprotein cholesterol, and low-density lipoprotein cholesterol, carried mainly by circulating lipoproteins. Only recently, with the advent of novel mass spectrometry approaches, we can truly identify and quantify a large pool of lipid molecules in plasma. We have developed a high-throughput analytical platform using a "triple quad (QqQ)" mass spectrometer that can perform a large-scale, detailed analysis of different lipids and provide insights into the lipid alterations involved in the onset and progression of I/R injury.

Published: iScience (2022), 25(2), 103828

Impact of myocardial reperfusion on human plasma lipidome

Arun Surendran BE, MBA[1,2,4], Negar Atefi BSc[1], Umar Ismail MD[3], Ashish Shah MD[2,3], Amir Ravandi MD PhD[1,2,3]

[1]Cardiovascular Lipidomics Laboratory, St. Boniface Hospital, Albrechtsen Research Centre, [2]Department of Physiology and Pathophysiology, Rady Faculty of Health Sciences, University of Manitoba, [3]Section of Cardiology, Department of Medicine, Rady Faculty of Health Sciences, University of Manitoba, [4]Mass Spectrometry and Proteomics Core Facility, Rajiv Gandhi Centre for Biotechnology, Kerala, India

Corresponding author & Lead Contact
Dr. Amir Ravandi MD PhD FRCPC
Interventional Cardiology
Cardiovascular Lipidomics Laboratory,
St. Boniface Hospital,
409 Tache Ave,
Winnipeg, MB Canada R2H 2A6

Phone.204-235-3206 and 204-235-3414
Fax.204-235-0793 and 204-235-0793

Email: aravandi@sbgh.mb.ca

3.1 Abstract

The primary aim of the study is to investigate the temporal changes in plasma lipidome before and after reperfusion in ST-segment elevation myocardial infarction (STEMI) patients and their association with myocardial injury. We found that 56% of the identified lipid species were significantly altered (corrected $p<0.05$) in the first 24 h following reperfusion in STEMI patients. Three lipid species, namely, acylcarnitine 18:2, TG 51:0, and LPC 17:1 were associated with change in troponin concentration (delta troponin) and in-hospital cardiovascular events. Of these, acylcarnitine 18:2, and LPC 17:1 and their respective whole class levels, were significantly higher ($p<0.05$) in the STEMI population than the age/sex-matched control subjects. Overall, our analyses show a large shift in plasma lipidome in patients that undergo myocardial reperfusion. The differences found for acylcarnitines and LPC species and their association with both cardiac markers and cardiac outcomes needs further validation.

Key words

Lipids, Lipidomics, Reperfusion injury, Ischemia/Reperfusion, STEMI, Myocardial Infarction

3.2 Graphical abstract

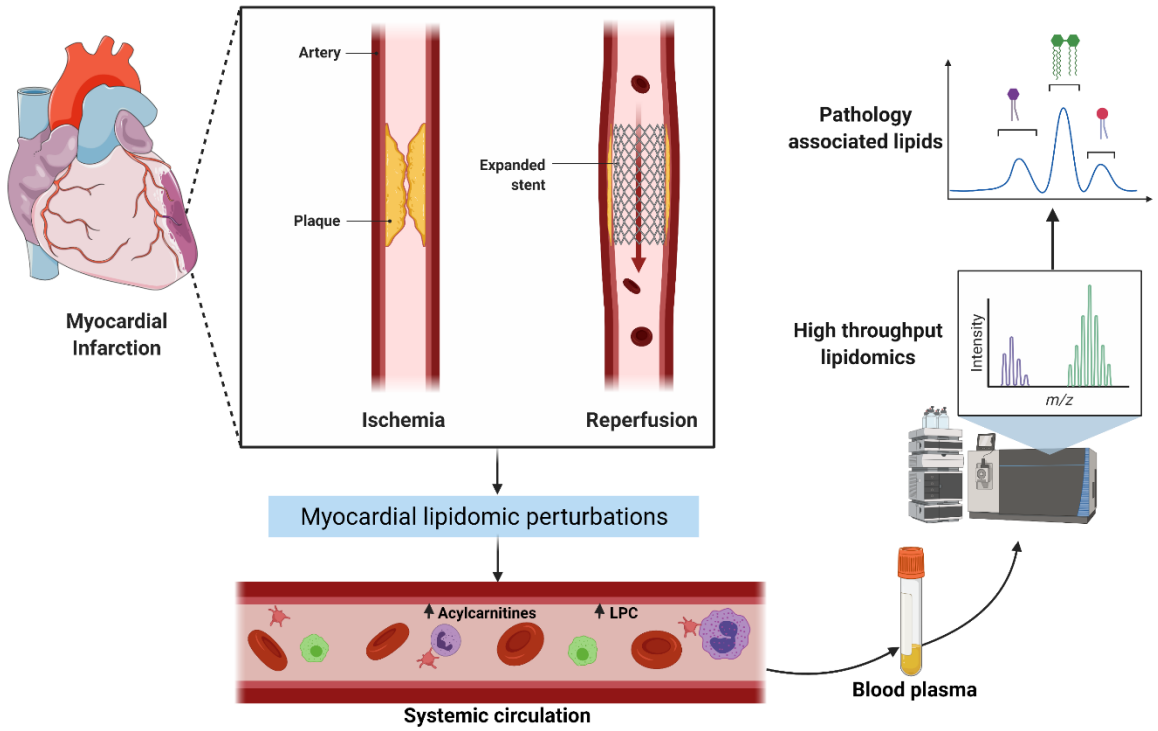

3.3 Abbreviations

STEMI, ST-segment elevation myocardial infarction; PCI, percutaneous coronary intervention; CVD, cardiovascular diseases; MI, myocardial infarction; IR, ischemia/reperfusion; CAD, coronary artery disease; LC/MS, liquid chromatography-mass spectrometry; ESI, electrospray ionization; MRM, multiple reaction monitoring; Δ cTnT, delta troponin; MACE, major adverse cardiovascular events; **Supplementary Table S1** contains the complete list of lipid abbreviations.

3.4 Introduction

Cardiovascular diseases (CVDs) accounted for ≈18.6 million deaths in 2019, 32% of all deaths globally[1]. Nearly 85% of these deaths were attributed to acute myocardial infarction (MI) and stroke[2]. After an acute MI, rapid coronary reperfusion using primary percutaneous coronary intervention (PCI), or intravenous fibrinolytic therapy is essential to restore blood flow and limit infarct size. Paradoxically, however, these treatment strategies can, in itself, induce additional myocardial injury, termed reperfusion injury, for which there is still no effective treatment options available[3]. Experimental models of myocardial ischemia and infarction suggest that reperfusion injury contributes nearly 50% of the final infarct size[4]. The biggest impact of ischemia/reperfusion (IR) injury in clinical settings arises in patients with ST-segment elevation (STEMI). Even after timely reperfusion, reperfused STEMI patients have a 30-day mortality rate of nearly 5%[5].

The conventional measurements for evaluating CVD risk include circulating lipid biomarkers such as cholesterol levels, triglycerides, high density lipoprotein (HDL), and low-density lipoprotein (LDL). However, these measurements provide limited information on the individual lipid species and their association with the disease. Human plasma lipidome is a tightly regulated environment, and its composition can reflect the underlying phenotype in health and disease states[6]. Latest developments in high-throughput liquid chromatography and mass spectrometry have enabled us to identify associations between plasma lipid species and disease states. In a large population-based study, Alshehry et al. identified 32 plasma lipids significantly associated with cardiovascular events and death[7]. Stegemann and colleagues showed that circulating lipid species outperform conventional lipid measures in CVD risk prediction[8]. Meikle et al. demonstrated the potential of plasma lipid profiling for the risk stratification of unstable coronary artery disease (CAD)[9]. From

all these results, it is now becoming more apparent that individual lipid species and classes can better reflect CVD risk and underlying pathophysiology than traditional lipid biomarkers.

Inflammation and oxidative stress accompanied by altered lipid metabolism are the prime drivers for the irreversible myocardial damage following ischemia and reperfusion[4,10-12]. However, little information is available about the changes in plasma lipidome in the setting of human myocardial IR injury. To better understand lipid biology during IR, it is necessary to assess lipid changes as a whole and not in individual parts accommodating both early and late reperfusion phases. Our recent non-targeted metabolomics study on STEMI patients showed that lipids formed the bulk of the altered plasma metabolome following reperfusion. Also, we identified specific lipid species that were highly correlative with the extent of myocardial injury[13]. In this report, we aim to investigate the changes in circulating plasma molecular lipids in the setting of a multifactorial process such as human myocardial reperfusion injury.

3.5 Results

3.5.1 Patient characteristics

Table 3.1 summarizes the clinical profile of the study participants. Overall, 67% of the STEMI cohort are male with an average age of 64 years (63.71 ± 12.21). The STEMI and control group participants were matched for conventional cardiovascular risk factors, including age, gender, and BMI, apart from smoking status and dyslipidemia. The medication use was also similar between the two groups. Heparin was administered intravenously before the coronary angiography procedure in all participants, including the control subjects. In our STEMI cohort, 36% had occlusion in the left anterior descending (LAD) coronary artery, 37% had occlusion in the right coronary artery (RCA), and 10% had occlusion in the circumflex coronary artery.

Table 3.1: Baseline characteristics of the study participants			
	Control (n=50)	**STEMI (n=80)**	**p value**
Age(years)	60.92 ± 10.72	63.71 ± 12.21	0.187
Male sex (%)	31 (62.0)	54 (67.5)	0.521
LVEF (%)	60 (58, 60)	60 (45, 70)	0.679
Body mass index (kg/m^2)	28.85 (26.17, 32.37)	27.67 (23.56, 32.40)	0.190
Comorbidity (%)			
Hypertension	23 (46.9)	37 (46.2)	0.939
Diabetes mellitus	7 (14.0)	16 (20.0)	0.383
Current smoker	6 (12.0)	22 (27.5)	0.036
Dyslipidemia	13 (26.0)	42 (52.5)	0.003
Hx of CAD	2 (4.0)	11 (13.8)	0.071
Laboratory data			
Triglyceride (mmol/l)	1.5 (1.0, 2.3)	1.3 (1.0, 2.1)	0.355
Cholesterol (mmol/l)	4.5 (3.9, 5.1)	4.8 (4.1, 5.3)	0.503
HDL cholesterol (mmol/l)	1.29 (0.9, 1.7)	1.10 (0.9, 1.37)	0.093
LDL cholesterol (mmol/l)	2.80 (1.93, 3.30)	2.80 (1.95, 3.45)	0.851
Creatinine (mmol/l)	78 (75, 84)	89 (71, 105.75)	0.086
Medications at baseline (%)			
ASA	8 (16.0)	18 (22.5)	0.367
ACEI/ARB	10 (20.0)	20 (25.0)	0.510
Beta blocker	9 (18.0)	8 (10.0)	0.188
Statin	8 (16.0)	20 (25.0)	0.225

Additional parameters		
Minutes from the onset of chest pain to reperfusion	*NA*	149.5 (86.25, 246.25)
Peak CK (Units/L)	*NA*	975 (372, 2335)
Peak TnT (ng/L)	*NA*	2029 (1102, 5943.50)
Culprit vessel (%)		
LAD Infarct (%)	*NA*	36 (45.0
RCA Infarct (%)	*NA*	37 (46.2)
Circumflex Infarct (%)	*NA*	10 (12.5)

Values are reported as mean ± standard deviation (SD), median (25th, 75th percentiles), or count (percentage) as applicable. The Chi-square test was used for categorical variables, while Student's t-test or Mann-Whitney U test was used for continuous variables to assess for statistical significance across sample groups as applicable based on data distribution.

Abbreviations: LVEF, left ventricular ejection fraction; Hx of CAD, history of coronary artery disease; HDL, high-density lipoprotein; LDL, low-density lipoprotein; ASA, Acetylsalicylic acid; ACEI, Angiotensin-converting enzyme (ACE) inhibitors; ARB, Angiotensin II receptor blockers; CK, Creatine kinase; TnT, troponin T; LAD, Left anterior descending coronary artery; RCA, Right coronary artery.

3.5.2 Time course of the plasma lipidome

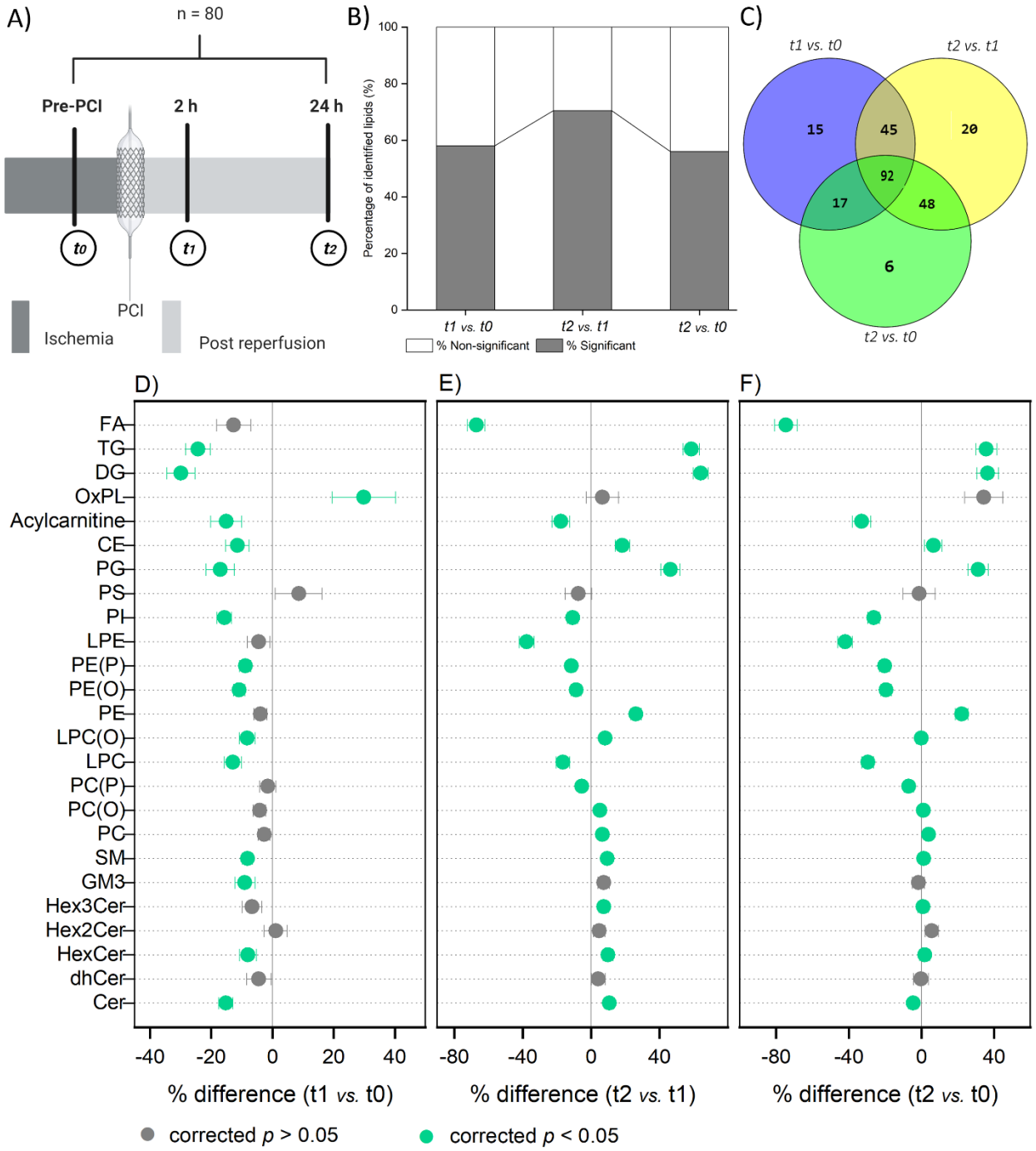

Figure-3.1: Temporal changes in plasma lipidome. (A) Study design: The samples were collected by venipuncture at three different time points; the first, after STEMI diagnosis but before primary PCI (*t0*); the second, 2 h post-PCI (*t1*) and the third, 24 h post-PCI(*t2*). (B) Percentage of statistically significant lipids (corrected $p<0.05$) at different time points, (C) Venn diagram showing the number of lipids shared or unique at different time points, (D-F) Forest plots showing total lipids expressed as percentage difference comparing each time point to one another. Data are represented as mean ± SEM. The corrected *p* values in (B), and (D)–(F) are obtained by repeated measures analysis of variance (ANOVA) followed by pairwise comparisons after Bonferroni correction. Grey circles represent the non-significant lipid classes/subclasses, and green circles represent the classes/subclasses with corrected $p<0.05$. **Supplementary Table S1** contains the list of lipid abbreviations.

First, to investigate the temporal changes in lipidome after PCI, lipid profiling was performed on plasma from STEMI patients at three time points (*t0, t1,* and *t2*). **Figure-3.1A** illustrates the study design. Overall, plasma lipidome was markedly altered in STEMI patients in the first 24 h after PCI. In the acute phase of reperfusion (*t1 vs. t0*), 58% of the identified lipids were significantly altered (corrected $p<0.05$), which increased to 70% with the increase in reperfusion time (*t2 vs. t1)* (**Figure-3.1B**). In total, 56% of the identified lipid species were altered in the first 24 h after PCI (*t2 vs. t0*). The Venn diagram (**Figure-3.1C**) shows that a panel of 92 lipids was significantly altered (corrected $p<0.05$) across all three time points. Also, each time point is characterized by its distinctive lipidomic feature (**Supplementary Table S5**). Six lipids, namely PC(O-36:3), CE 22:5, 16:0 acylcarnitine, 20:0 acylcarnitine, PGPC, and PONPC, signify the unique lipidomic difference between pre-PCI and 24 h post-PCI (*t2 vs. t0*).

Figure-3.1D-F highlights the differences in the whole lipid class amount at each interval. The lipid data is shown as a percentage difference in total lipids compared to other time points (**Supplementary Table S6-S8**). Compared with pre-PCI levels, the majority of lipid classes/subclasses (15 out of 25) were significantly lower (corrected $p<0.05$) in the acute reperfusion phase (*t1 vs. t0*) (**Figure-3.1D**). The only exception was the total oxidized phospholipid (OxPL) amount, whose levels increased significantly (29.87% higher, corrected $p=0.026$) after PCI treatment. Total DG and TG also displayed large differences in the acute reperfusion phase. Their levels were 29.92% and 24.28% lower at 2 h post-PCI relative to pre-PCI (corrected $p=5.2 \times 10^{-8}$, 2.91×10^{-7}, respectively). However, total DG and TG exhibited a reverse trend over the next 24 h (*t2 vs. t1).* Their levels increased by 64.06% and 58.62% (corrected $p=1.38 \times 10^{-21}$, 3.96×10^{-18}, respectively) at 24 h post-PCI relative to 2 h post-PCI (**Figure-3.1E**). Overall, between pre-PCI and 24 h post-PCI (**Figure-3.1F**), the total amount of circulating fatty acids (FA) showed the most notable difference (*t2 vs. t0)*. They were 74.5% lower in pre-PCI than 24 h post-PCI (corrected $p=4.49 \times 10^{-17}$).

3.5.3 Perturbations in molecular lipid species

Next, to attain a more in-depth view of the species level, forest plots were employed to visualize the change in individual lipid species at each time point. Consistent with the analysis of whole class amount, the majority of the individual lipid species were significantly lower (corrected *p<0.05*) in the acute reperfusion phase compared with pre-PCI levels (**Figure-3.2A and Supplementary Table S9-S11**). On the contrary, the levels of two OxPL species, namely, PGPC and PONPC, were 33.85% and 27.74% higher at 2 h post-PCI than pre-PCI. During this period (*t1 vs. t0),* the most remarkable change was observed for neutral lipid species, including DG and TG. On average, they were 30% lower at 2 h post-PCI than pre-PCI. However, over the next 24 h (*t2*

vs. t1), these neutral lipids shifted in the opposite direction (**Figure-3.2B).** Their mean values at 24 h post-PCI were around 58% higher than 2 h post-PCI. Overall, FA species displayed the greatest change in the first 24 h after reperfusion (*t2 vs. t0*). On average, the levels of each FA species at 24 h post-PCI were about 69% lower than pre-PCI (**Figure-3.2C**).

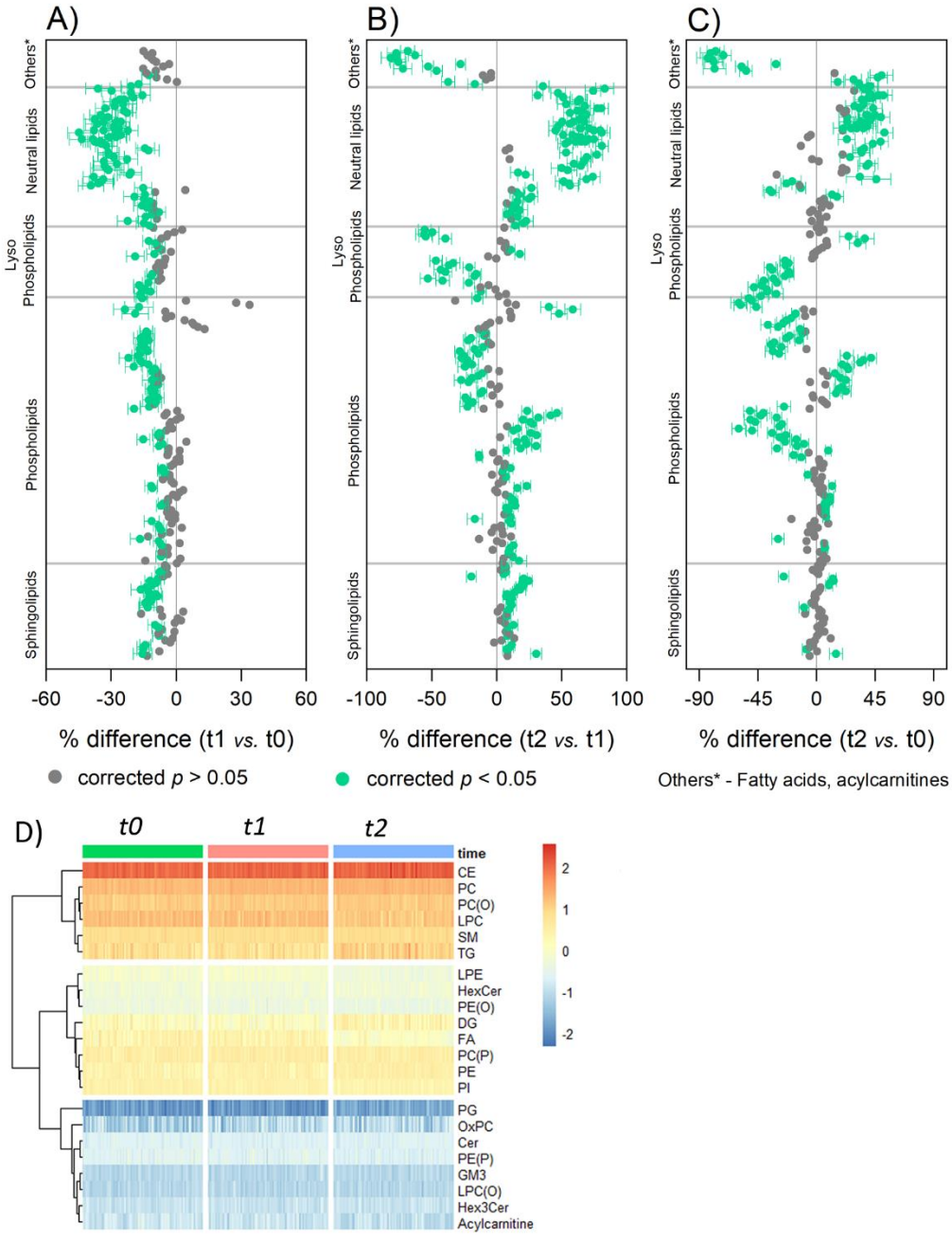

Figure-3.2: Perturbations in individual lipid species. (A-C) Forest plot showing individual lipid species expressed as percentage difference comparing each time point to one another. Data are represented as mean ± SEM. The corrected *p* values are obtained by repeated measures analysis of variance (ANOVA) followed by pairwise comparisons after Bonferroni correction. Grey circles represent the non-significant lipid species, and green circles represent the lipid species with corrected $p<0.05$. (D) Hierarchical heat map showing the abundance of the detected lipid species across different sampling time points. Color code indicates lipid concentration (log-transformed).

The hierarchical heatmap (**Figure-3.2D**) illustrates the similarities and disparities in lipid concentrations across different times. At the lipid class level, there is little difference in lipid concentrations across various time points. However, along the heatmap rows, three major clusters based on plasma lipid abundance can be identified. By lipid class, the top-5 lipid concentrations followed the next order: CE > PC > PC(O) > LPC > SM. Conversely, the bottom-5 least concentrated lipid classes in plasma were acylcarnitine, Hex3Cer, LPC(O), GM3, and PE(P). This ranking in lipid concentration remained unaffected before and after reperfusion.

3.5.4 Changes in lipidome by fatty acyl chain length and double-bond content

Next, we investigated whether there was any pattern in changes in lipid signals according to carbon atom numbers and degree of unsaturation (number of double bonds) before and after reperfusion. We focused our attention on major structural lipids, namely PC, PE, PI, and SM. **Figure-3.3A-D** demonstrates the relative concentration of lipid species at each time (*t1*, *t2*) compared to pre-PCI levels (*t0*). The values were normalized per sample to the total abundance within a lipid class. Based on the pattern of the number of carbon atoms and unsaturation degree, there was no alteration in concentration ratio in most of the PC species (**Figure-3.3A**) except for PC 36:6 and PC 34:4. These two species with higher double bond numbers were highly altered following

reperfusion. Among the PE species, two 40 carbon atoms species, PE 40:5, PE 40:6, characterized by a high degree of unsaturation, exhibited the most remarkable change (**Figure-3.3B**). Among the PI class, almost all species were altered in both directions (**Figure-3.3C)**. The most considerable change within the SM class was observed for the odd-numbered carbon atom with a double bond, namely SM 37:2 (**Figure-3.3D)**. Also, SM species with relatively low carbon atom numbers (31, 32, 33, and 34) were not altered at different sampling time points (*t0*, *t1*, *t2*).

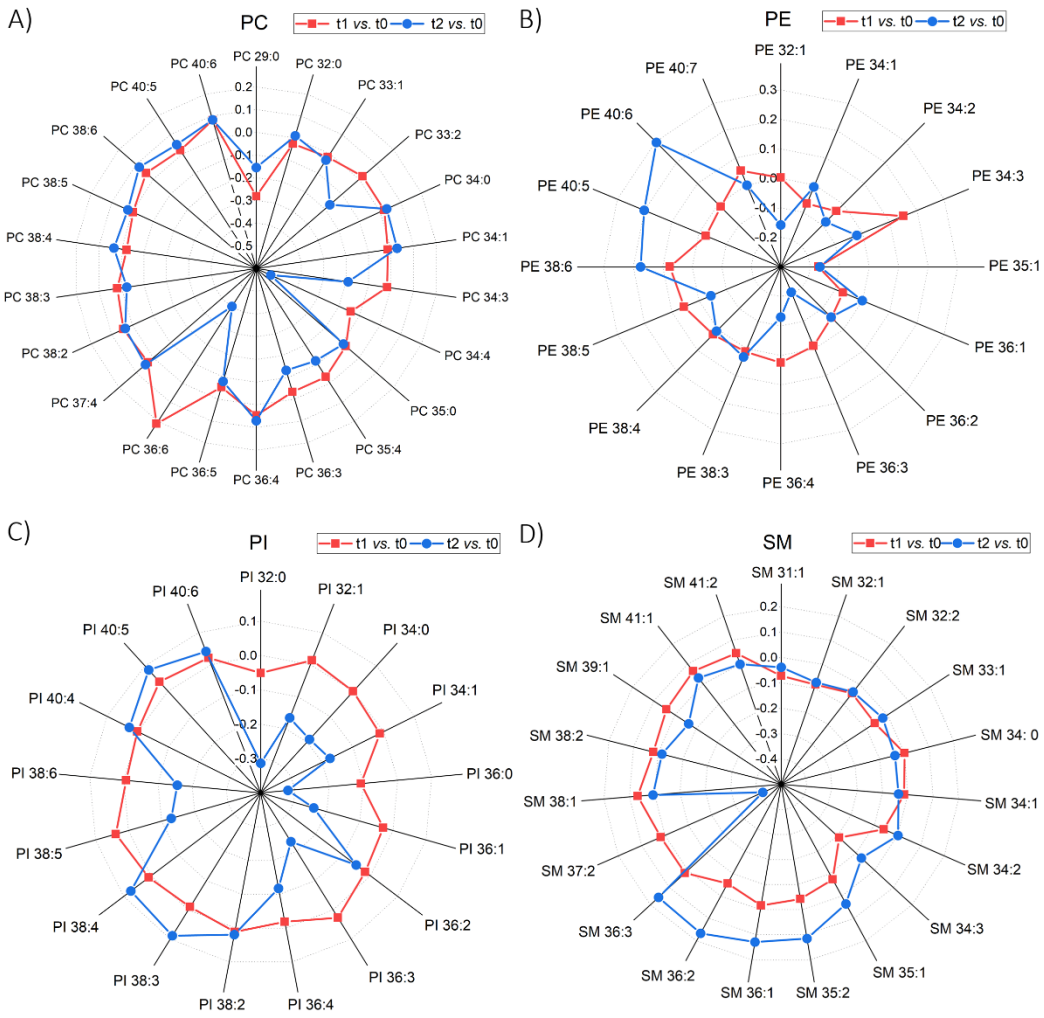

Figure-3.3: Alteration in lipid signal by the total number of carbon atoms and the degree of acyl chain saturation. (A-D) The relative concentration of lipids was expressed as the concentration of lipids per sample to the total abundance within (A) phosphatidylcholine, (B) phosphatidylethanolamine, (C) phosphatidylinositol, and (D) sphingomyelin classes. The red color indicates the log ratio of the relative concentration at 2 h post-PCI (*t1*) compared to pre-PCI (*t0*). The blue color indicates the log ratio of the relative concentration at 24 h post PCI (*t2*) compared to pre-PCI (*t0*). Abbreviations: PC, phosphatidylcholine; PE, phosphatidylethanolamine; PI, phosphatidylinositol; SM, sphingomyelin

3.5.5 Lipid signatures specific to IR injury

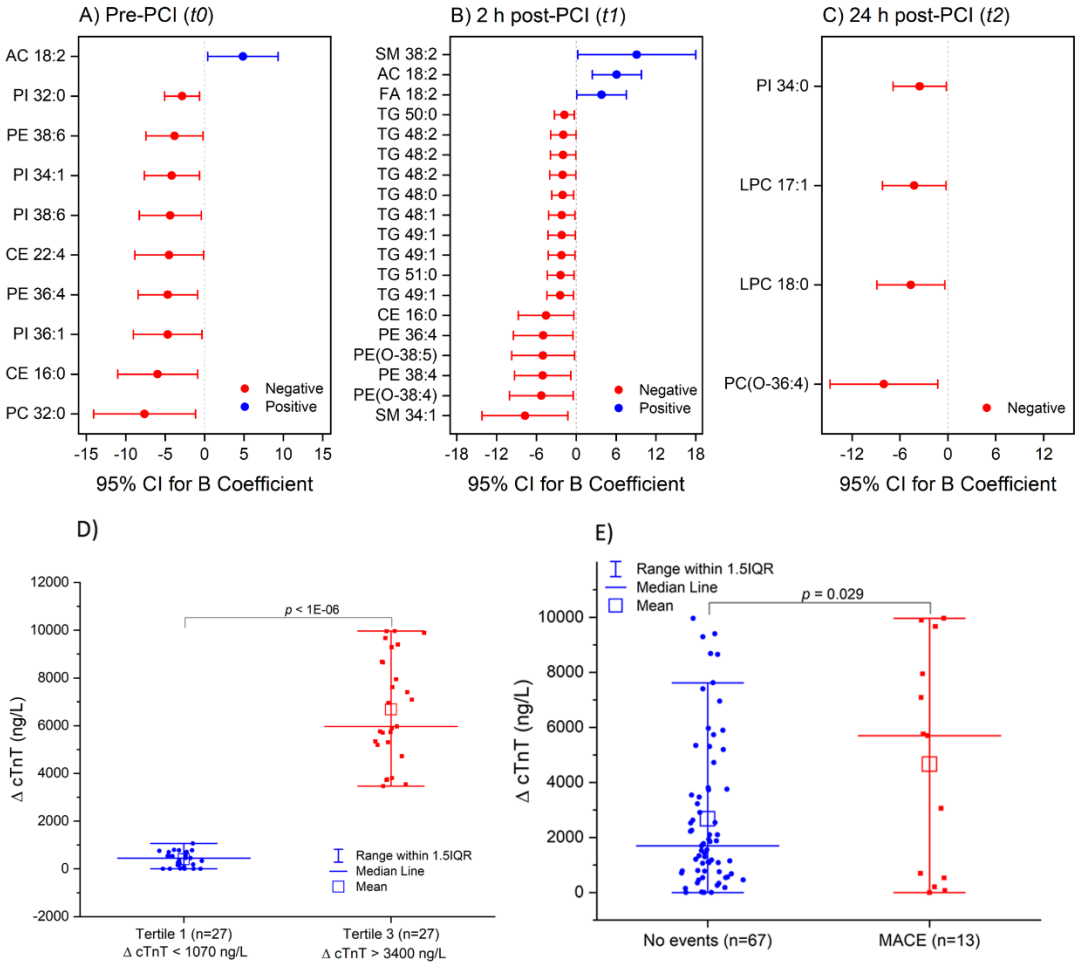

Figure-3.4: Association between delta troponin and plasma lipid species. Linear regression analysis between delta troponin and log-transformed concentrations of each lipid species was performed after adjusting for age, sex, body mass index (BMI), current smoking, diabetes history, and time from symptom onset to reperfusion. The unit of delta troponin is mg/L. The blue color shows significant positive correlations (p<0.05), and the red color shows significant negative correlations (p<0.05). Whiskers represent 95% confidence intervals (CI). (D) Delta troponin (Δ cTnT) amount in top (n = 27) and combined middle and bottom tertiles (n = 53). (E) Delta troponin (Δ cTnT) amount in MACE (n = 13) and 'No events' (n = 67) groups. *p* values in (D) and (E) are by Student's unpaired t-test. Abbreviations: B, Unstandardized B Coefficient; MACE, Major Adverse Cardiovascular Events; AC, Acylcarnitine.

Elevated cardiac troponin levels after PCI correlate with myocardial necrosis[14] and are also associated with worse 90-day clinical outcomes[15]. In our STEMI cohort, cardiac troponin T (cTnT) was measured daily for the first 72 h at regular intervals. Here, the delta troponin (Δ cTnT) value for each patient is defined as the absolute change in baseline (pre-PCI) troponin value from peak troponin value. A linear regression of delta troponin against lipid species was performed after adjusting for age, sex, body mass index (BMI), current smoking, diabetes history, and ischemic time (time from symptom onset to reperfusion) to investigate lipid changes specific to reperfusion injury (**Figure-3.4A-C, Supplementary Table S12-S14**). After adjustment of these major cardiovascular risk factors, ten lipid species were significantly associated (p<0.05) with delta troponin at pre-PCI (*t0*), 19 lipid species were significantly associated with delta troponin at 2 h post-PCI (*t1*), and four lipid species were significantly associated with delta troponin at 24 h post-PCI (*t2*). Notably, all the significant lipid associations at pre-PCI (*t0*) were negative except for acylcarnitine 18:2, which was positively associated with delta troponin (**Figure-3. 4A)**. Similarly,

except for three lipid species, namely acylcarnitine 18:2, FA 18:2, and SM 38:2, all other lipids were significantly negatively associated with delta troponin at 2 h post-PCI (**Figure-3.4B**). These included mainly TG, PE, and PE(O) classes. Only four lipid species (**Figure-3.4C)** were associated with delta troponin at 24 h post-PCI (*t2*), and among them, two were LPC species (LPC 17:1 and LPC 18:0). In total, 33 lipids were identified, which significantly associate (p<0.05) with delta troponin across three time points.

3.5.6 Lipids and the severity of myocardial IR injury

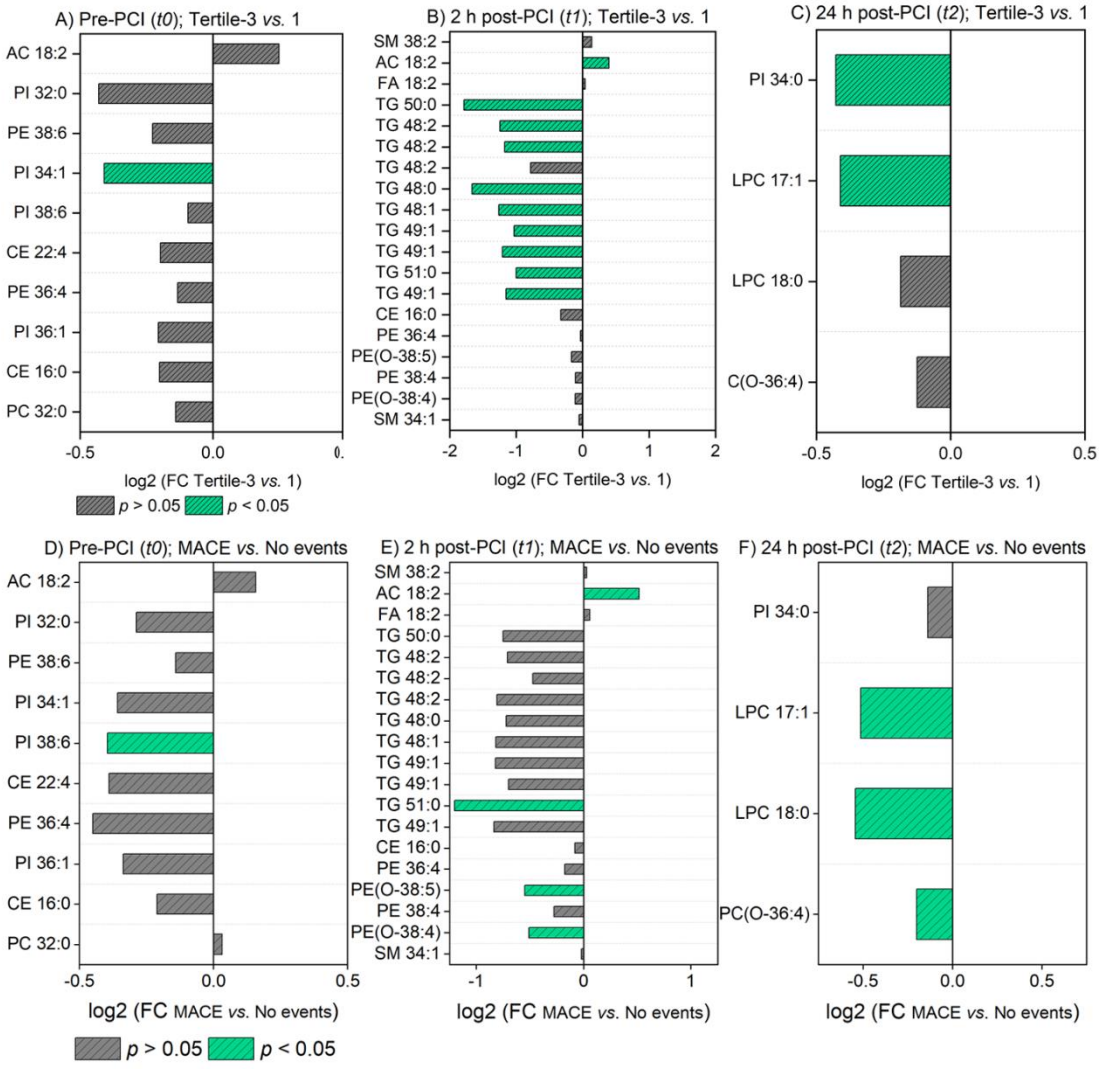

Figure-3.5: Lipid species and the extent of myocardial injury. (A-C) Log2 fold change of lipid abundance in top tertile (Tertile-3, n = 27) compared to lower tertiles (Tertile-1&2, n = 53) across different time points. (D-F) Log2 fold change of lipid abundance in MACE group (n = 13) compared to 'No events' group (n = 67) across different time points. The grey color represents the non-significant lipid species, and the green color represents the significant (p<0.05) lipid species. P values are by Student's unpaired t-test. Abbreviations: FC, fold change; AC, Acylcarnitine.

Next, we examined whether the delta troponin-associated lipids could determine the severity of myocardial injury in STEMI patients. In this regard, firstly, we classified the STEMI patients into two groups based on their delta troponin values (**Figure-3.4D and Supplementary Table S15)**. **Figure-3.5A-C** compares the direction, magnitude, and statistical significance of delta troponin-associated lipids between the top tertile (Δ cTnT >3400 ng/L) and the bottom (lower) tertile (≤ 1070 ng/L). Among the ten delta troponin-associated lipids at pre-PCI, only one lipid - acylcarnitine 18:2 - was higher in the top tertile (**Figure-3.5A**). The rest of the lipids (9/10) were lower in abundance in the top tertile, and among them, PI 34:1 was significantly lower (p<0.05) in the top tertile. Ten out of 19 delta troponin-associated lipids at 2 h post-PCI differed significantly between the two tertiles (**Figure-3.5B**). Of these 10 lipids, the level acylcarnitine 18:2 was significantly higher (p<0.05) in the top tertile. The rest, mainly comprising TG species, were significantly lower (p<0.05) in the top tertile. Amongst the four delta troponin-associated lipids identified at 24 h post-PCI (**Figure-3.5C**), two of them, namely PI 34:0, and LPC 17:1, were significantly lower (p<0.05) in the top tertile compared to the lower tertile. The significance of these lipids with delta troponin values holds true even after adjusting for differences in the HDL levels between top and bottom tertiles (**Supplementary Table S16**).

We then examined the role of these delta troponin-associated lipids in major adverse cardiovascular events (MACE). We calculated the incidences of MACE (cardiovascular death, re-hospitalization, myocardial infarction, and congestive heart failure) in our STEMI cohort. Accordingly, the STEMI patients were categorized into the MACE group (n=13) and the 'No events' group (n=67) (**Supplementary Table S17**). As shown in **Figure-3.4E**, the delta troponin values differed significantly (p<0.05) between the MACE and 'No events' groups. **Figure-3.5D-F** compares the direction, magnitude, and statistical significance of delta troponin-associated lipids between the two groups. Notably, except for one lipid– PC 32:0 – all other lipids followed the same direction (higher/lower) similar to the top *vs.* lower tertile comparison. Interestingly, two lipid species, namely acylcarnitine 18:2, and TG 51:0, which differed significantly (p<0.05) between the top and lower tertile of delta troponin at 2 h post-PCI (**Figure-3.5B**), exhibited a similar significant distinction (p<0.05) between MACE and the 'No events' group at the same period (**Figure-3.5E**). Likewise, LPC 17:1 which differed significantly (p<0.05) between the top and lower tertile of delta troponin at 24 h post-PCI (**Figure-3.5C**), followed the same trend in MACE *vs*. 'No events' comparison (**Figure-3.5F**). The above-described analysis based on delta troponin tertiles and MACE groups demonstrated that three lipid species, namely acylcarnitine 18:2, TG 51:0, and LPC 17:1, significantly associate (p<0.05) with delta troponin, and their levels differed significantly (p<0.05) between patients with sizeable myocardial injury and patients with lesser myocardial injury. The significance, timing, and direction of change of these cardiac-specific lipids remained the same in MACE *vs.* 'No events' comparison as well.

3.5.7 Early vs. late phase of reperfusion

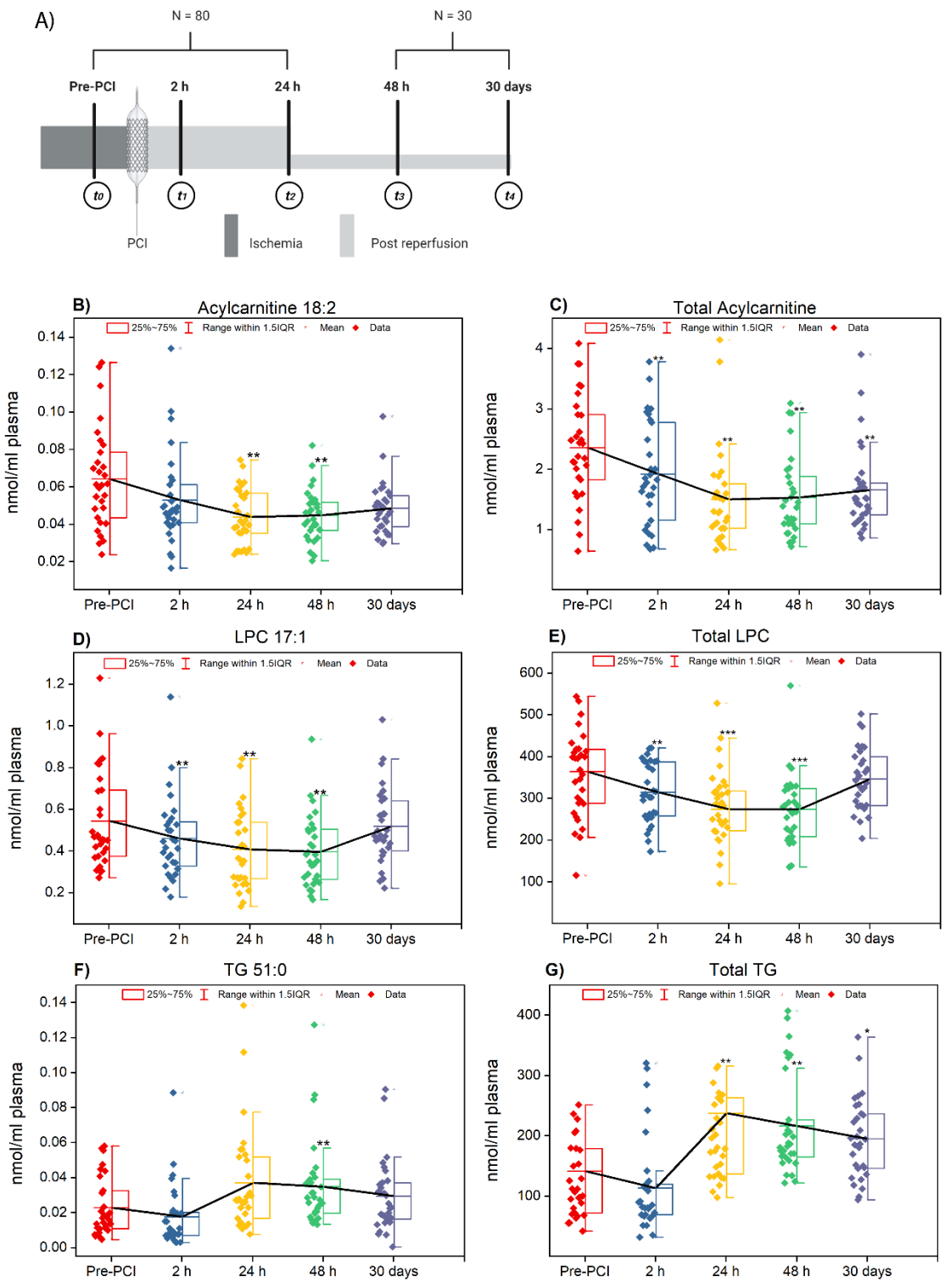

Figure-3.6: Lipid species at the late reperfusion phases. (A) Study design: In a subset of the population (n=30), the samples were collected by venipuncture at two additional time points; 48 h post- PCI (t3) and 30 days post-PCI (t4). (B-G) Distribution of specific lipid species and lipid classes in the early (pre-PCI, 2 h, 24 h) and late phases (48 h, 30 days) of reperfusion. The black line represents the mean of lipid species/classes. The *p* values were obtained by repeated measures analysis of variance (ANOVA) followed by pairwise comparisons after Bonferroni adjustment. Asterisks (∗, ∗∗ and ∗∗∗) indicate statistical significance at $p<0.05$, $p<0.01$, and $p<0.001$, respectively, to the baseline (pre-PCI).

We prospectively followed a subset of our cohort (n=30) for another 30 days (**Figure-3.6A**) to detect the changes in the three cardiac-specific lipids from early to late reperfusion. We observed that specific patterns characterize these lipids during early and late reperfusion phases. Except TG 51:0 and total TG, the levels of these cardiac-specific lipid species (acylcarnitine 18:2, LPC 17:1) as well as their respective whole class amount, including total acylcarnitine, and total LPC, progressively decreased up to 48 h after PCI before climbing again (**Figures-3.6B-E**). Though levels of TG 51:0 and total TG decreased immediately after PCI (**Figures-3.6F-G**), their levels sharply rose after 2 h of reperfusion, reached the maximum over the next 24 h (24 h post-PCI), and then plummeted again in the late phases of reperfusion (48 h and 30 days post-PCI). In short, the plasma lipid levels of acylcarnitine 18:2, LPC 17:1, and TG 51:0 as well as their respective whole class amount differed significantly ($p<0.05$) at late reperfusion phase (48 h post-PCI) compared with pre- PCI.

3.5.8 Comparison with controls subjects

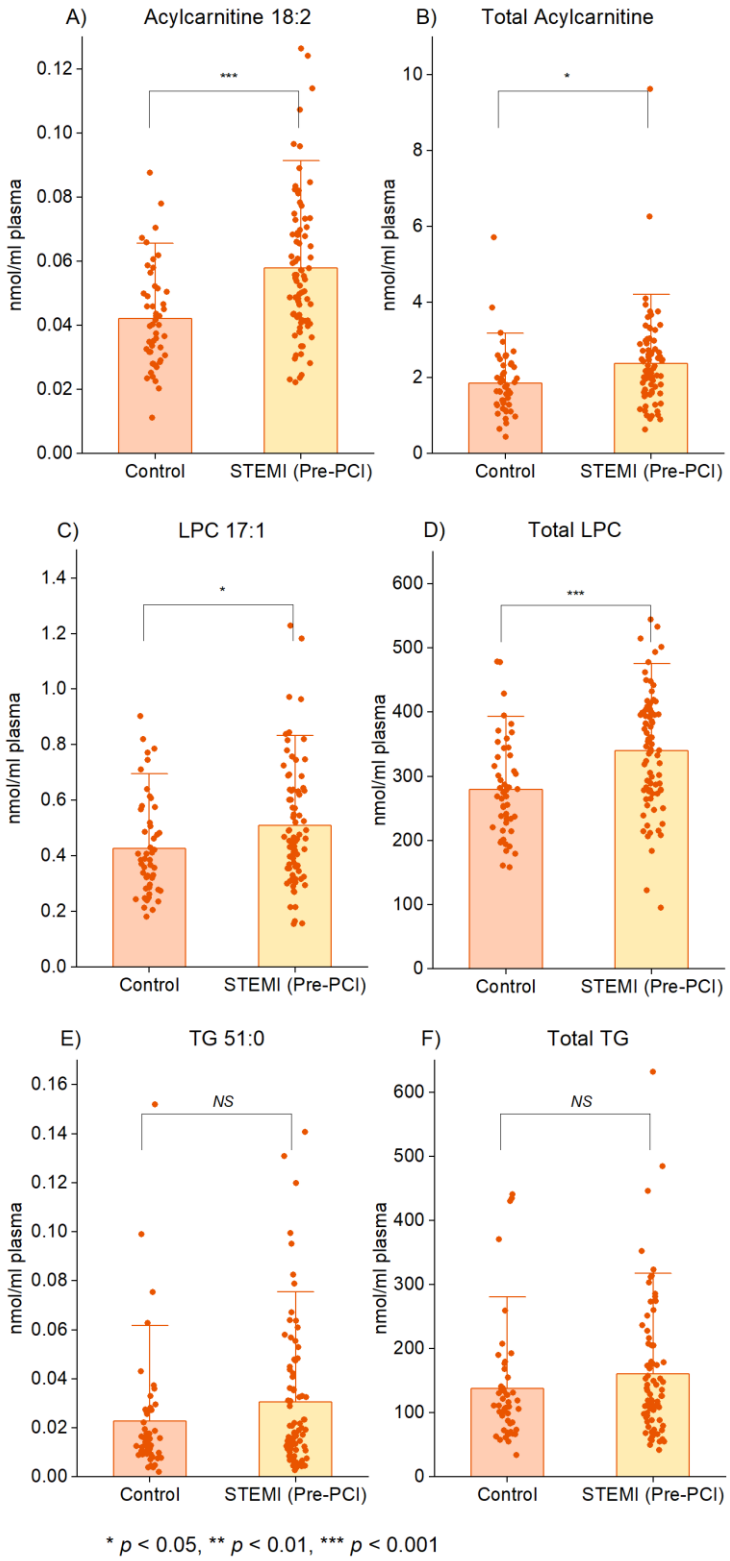

Figure-3.7: Significantly perturbed lipid species identified in patients with STEMI compared to controls. (A-F) Distribution of specific lipid species and lipid classes among the STEMI (pre-PCI) and control groups. P values are by Student's unpaired t-test. Asterisks (∗, ∗∗ and ∗∗∗) indicate statistical significance at $p<0.05$, $p<0.01$, and $p<0.001$, respectively, after Student's t-test.

Next, we examined whether the concentration of these cardiac-related lipid species/classes in the STEMI patients at the time of presentation (pre-PCI) is comparable with that of an age and gender-matched control population without any intervention. Based on Student's unpaired t-test, the levels of acylcarnitine 18:2 and total acylcarnitine were significantly higher ($p<0.05$) in the STEMI group relative to the control subjects (**Figure-3.7A-B**). Likewise, the concentration of individual LPC 17:1 , as well as the total LPC amount, were also significantly higher ($p<0.05$) in the STEMI group relative to the control subjects (**Figure-3.7C-D**). No significant differences were noted for TG 51:0, and its respective total class amount between the two groups (**Figure-3.7E-F**).

3.6 Discussion

This study elucidated a detailed lipidomic map of human plasma during myocardial ischemia and reperfusion. Given that there are currently no clinical therapies for reperfusion injury, we sought to understand the temporal changes in plasma lipids before and after reperfusion and their correlation with clinical markers of cardiac injury. The vast majority of research in the pathophysiology of ischemia/reperfusion (IR) injury has focused on the genetic and protein expression changes during reperfusion, with little to no attention given to the sizeable myocardial lipid pool that harbors profound biological activity. This may be why there are still no proven therapeutic options that allow for lowering the cardiotoxic effects of reperfusion injury. Our study is unique as it allows for the determination of the dynamic changes in circulating lipidome as a whole before and after reperfusion and its association with myocardial reperfusion injury. The IR

injury not only affects the ischemic organ alone (here, heart), but may also cause systemic damage to other organs, and can possibly lead to multiorgan dysfunction. Therefore, we have used cardiac biomarkers such as troponin and cardiovascular outcomes to select cardiac specific lipid molecules that are important during reperfusion and are less impacted by non-cardiac factors. Also, we employed a repeated measure study design in which the lipid values were measured on the same subject serially over time. In repeated measures designs, each subject serves as their own control. This helps control factors that cause variability between subjects, including diet and medications, and helps focus more precisely on the lipidomic changes due to intervention (PCI).

The most striking observation in this study was that myocardial ischemia followed by reperfusion results in significant shifts within the plasma lipidome. We found that 56% of the circulating lipid species were significantly altered (corrected $p<0.05$) in the first 24 h after PCI in STEMI patients. In the acute phase of reperfusion (*t1 vs. t0*), there was an overall decrease in the majority of lipid classes/subclasses, including phospholipids. In line with this notion is the observation that in animal models of cerebral ischemia/reperfusion, there is a significant reduction in blood plasma phospholipids during reperfusion[16]. The authors attributed it to oxidative stress and activation of phospholipases following reperfusion. In a study to examine the effects of ischemia/reperfusion on rat hearts, Paradies et al. demonstrated a similar reduction in plasma lipids. They ascribed it, in part, to lipid peroxidation of unsaturated fatty acids by oxygen free radicals[17]. The lone lipid class in our study that was significantly increased (corrected $p<0.05$) immediately after reperfusion was oxidized phospholipids (OxPL). In an *in vivo* model of renal IR injury, we previously showed that OxPL species are produced in kidney tissue during renal IR injury. Their levels increase with the increase in reperfusion time[11]. In patients with stable angina pectoris, Tsimikas and colleagues[18] showed that circulating OxPL levels were elevated immediately after PCI. OxPLs have been

recognized as toxic oxidative by-products of oxidative damage derived from sources of cellular injury such as plaque disruption and myocyte death[10]. The increased level of OxPL after reperfusion may reflect the increased oxidative stress immediately after reperfusion.

At the class level, the most substantial change in the first 24 h after PCI (*t2 vs. t0*) was observed for free fatty acids (FA), followed by neutral lipids (DG, TG) and oxidized phospholipids. The increase in circulating neutral lipids after PCI coincided with the decrease in free fatty acids (**Figure-3.1F, 2C**). The same trend was observed for individual molecular species from these lipid classes as well. This indicates the presence of an active triglyceride-fatty acid-triglyceride cycle during myocardial ischemia/reperfusion[19]. Our findings also agree with the work by Saddik et al., who showed significant enhancement in triglyceride synthesis during reperfusion of ischemic rat hearts. They showed that despite an initial burst of fatty acid β-oxidation, the rate of triglyceride lipolysis is not accelerated during reperfusion and was comparable to non-ischemic hearts [20]. This partly explains why triglyceride levels are not accompanied by a similar increase in circulating free fatty acids following reperfusion. Our results also showed that circulating fatty acids were elevated during ischemia (pre-PCI) compared to reperfusion (post-PCI). This observation is consistent with a recent study by Feng et al., which reported a decrease in circulating fatty acids with increased reperfusion time[21]. The heart is the most metabolically active organ in the human body, and under normal conditions, free fatty acids are the primary energy source for cardiac ATP production. However, during myocardial ischemia, these fatty acids are detrimental both clinically and experimentally. The detrimental effects are mainly due to inhibition of myocardial glucose utilization and accumulation of toxic intermediates of fatty acid metabolism, including long-chain acylcarnitines[22,23]. Mounting evidence suggests that the potential contributors to elevated levels of circulating fatty acids during myocardial ischemia are degradation of endogenous lipids such as

triacylglycerols or phospholipids and release of stress hormones such as epinephrine and catecholamines[12,20,24]. After acute MI, the elevated free fatty acids levels are of clinical importance related to reduced cardiac efficiency, increased risk of arrhythmias, and sudden death [20,22,23].

In most biological systems, the primary function of lipids is to serve as structural components of cell membranes. However, oxygen free radicals produced during reperfusion can cause membrane damage and contribute to reperfusion injury[25]. A comparison of saturation degree and chain length of fatty acids of major structural lipids (PC, PE, PI, and SM) before and after reperfusion can determine which lipid class is more prone to oxidation. Only a small number of PC species altered before and after reperfusion. Nevertheless, PE, PI, and SM showed great shifts between different time points during reperfusion (**Figure-3.3A-D**). This suggests that PC species are likely more resistant to oxidative stress than other membrane phospholipids and offer resistance to damage in order to maintain membrane integrity[26]. For PC species, the most extensive alteration was shown by 34–36 carbon atoms and 4–6 double bonds. For PE species, the most considerable alteration was shown by 40 carbon atoms and an unsaturation degree of 5–6. For PI species, all were altered; and for SM species, 37:2 showed the maximum diversity. We have previously shown that PI species are much more rapidly oxidized as LDL undergoes lipid oxidation. During 36 h of copper oxidation, there is a rapid loss of polyunsaturated PI species and the generation of oxidized PI species, which in terms of proportion are many folds higher than the generation of oxidized PC species within LDL[27]. This is in proportion to PIs' large polyunsaturated content compared to PCs. In this study, PC and PE species with a medium-to-long acyl chain (34-40) and four, five, or six double bonds have shown alteration following reperfusion, likely as a result of susceptibility to oxidative stress.

Because of its high sensitivity and specificity, cardiac troponins are considered "gold standard" biomarkers for myocardial damage[28]. In order to assess the ongoing myocardial tissue loss after reperfusion, we utilized the delta troponin post revascularization. This allowed us to determine the lipids that correlated with ongoing myocardial injury subsequent to revascularization. We found that 33 lipids associated with delta troponin at different time points (pre-PCI, 2h post-PCI, 24 h post-PCI) following adjustment for age, sex, BMI, current smoking status, diabetes history, and ischemic time (**Figure-3.4A-C**). Three of these lipids, namely, acylcarnitine 18:2, TG 51:0, and LPC 17:1, could also stratify patients based on the severity of cardiac injury (**Figure-3.5A-C**). They could also stratify those at increased risk of in-hospital cardiovascular events from regular ones (**Figure-3.5D-F**). Also, their levels in the late reperfusion phase (48 h post-PCI) were significantly different ($p<0.05$) from pre-PCI levels (**Figure-3.6B-G**). In addition, among these cardiac-related lipids, the levels of acylcarnitine 18:2, and LPC 17:1 as well as their respective whole class amount were significantly higher ($p<0.05$) in the STEMI population at the time of admission compared to the age and gender-matched control subjects (**Figure-3.7A-D**). This points to the fact that not all cardiac-related lipids identified as significant during reperfusion can be used as biomarkers to distinguish control subjects from STEMI patients. Of these, acylcarnitine 18:2 notably exhibited a positive association with delta troponin value at pre-PCI and 2 h post-PCI. Our previous non-targeted metabolomics study has shown that plasma levels of acylcarnitine 18:2 could determine the extent of cardiac injury in STEMI patients[13]. The long chain acylcarnitines are intermediates of fatty acid metabolism[29]. Their elevated circulating levels are widely used as diagnostic markers of fatty acid oxidation disorders[30]. A growing corpus of literature highlights the impacts of long-chain acylcarnitines on various aspects of cardiovascular pathophysiology, such as cardiovascular death, acute MI, and stroke[31,32]. In addition, it was shown that inhibition of

acylcarnitine accumulation could attenuate the incidence of lethal arrhythmias and contractile deficits following acute ischemia[33]. Many previous studies revealed that saturated long-chain fatty acids activate some pattern recognition receptors (PRRs), such as toll-like receptor 2 (TLR2) and TLR4[34,35]. These findings result in the conclusion that acylcarnitines have the potential to mediate inflammation. Rutkowsky et al. later confirmed this finding and showed that medium and long-chain acylcarnitines activate pro-inflammatory signaling pathways, including PRRs[36]. Our findings, therefore, fortify the role of acylcarnitines in cardiac injury and subsequent inflammation.

There are extensive in vitro and animal studies showing that reperfusion results in fatty acid accumulation. However, when the TG levels increase due to limited FA oxidation, as occurs in several pathological conditions, it can contribute to cardiac dysfunction and worsening contractile function[37]. Even though both plasma CE and TG are predictors of the development of CAD and poor outcomes, there are conflicting reports on the changes of plasma TG during acute MI[38] and specifically reperfusion. We identified ten triglyceride species with shorter carbon length and fewer double bonds (0,1,2) correlated with delta troponin at 2 h post-PCI. They were all negatively associated with delta troponin at 2 h post-PCI even after adjusting for clinical risk factors, including diabetes. TG 51:0 is also associated with the risk of adverse cardiovascular events. This finding agrees with prior studies demonstrating that specific triglycerides with a low carbon number and double-bond content were predictive of CVD[8,39]. The same triglyceride pattern was associated with BMI and abdominal adiposity in a metabolomics study among Framingham Offspring Cohort[40]. Together, these findings suggest a relationship between triglycerides acyl chain content with cardiac injury in the setting of IR injury.

Two LPC species at 24 h post-PCI, namely LPC 17:1 and LPC 18:0, displayed negative associations ($p<0.05$) with delta troponin. Supporting this observation, Meikle et al. have

previously shown that LPC species containing saturated fatty acids were strongly associated with CAD[9]. LPCs are a well-recognized group of pro-inflammatory lipids[41] whose levels in human circulation indicate atherosclerotic plaque inflammation and endothelial dysfunction[41,42]. Here, the levels of LPC 17:1, as well as the total LPC amount, were significantly higher ($p<0.05$) in the STEMI population (pre-PCI) compared to control subjects. Elevated levels of LPC in circulation can result from the increased degradation of PC on lipoprotein particles *via* the action of enzymes such as lipoprotein-associated phospholipase A2 (Lp-PLA2)[41,43]. Lp-PLA2, itself is a marker of vascular inflammation[44] and suggests a pro-inflammatory role for LPC in the setting of IR injury.

3.7 Limitations of the study

One limitation of our study is the small sample size. We have mitigated this by utilizing repeated measures analysis, which allows subjects to act as their control, mitigating the risk of confounding factors. The observed associations and relationships between cardiac-specific lipid markers in this manuscript should be considered hypothesis-generating. Hence, further confirmatory studies in independent cohorts and preclinical and clinical models of myocardial ischemia and reperfusion are needed to understand better the mechanistic link between the lipids identified in this report and reperfusion injury.

Conclusions

This study presents a detailed overview of the temporal changes in plasma lipidome in a clinical setting of myocardial reperfusion injury in humans. In short, reperfusion results in dramatic changes in the plasma lipidome. We identified significantly altered lipid classes/subclasses and lipid species before and after reperfusion. While a small number of the identified lipids have been previously shown to associate with coronary artery disease (e.g., PE(O-38:5)), most lipid changes are novel in the setting of human I/R injury. We also identified three lipids, representing three lipid

classes, associated with the severity of myocardial injury independent of other traditional CVD risk factors. These three lipids were also discriminatory for adverse cardiovascular events, suggesting their clinical relevance in the setting of IR injury, but further work is necessary to validate any of these findings.

Author contributions

Conceptualization, A.R. and A.S.; methodology, A.R. and A.S.; sample preparation, A.S. and N.A.; statistics, A.S.; formal analysis, A.S.; visualization, A.S.; writing - original draft, A.S.; writing - review & editing, A.R. and A.S.; supervision, A.R., U.I. and A.Shah. All authors have read and agreed to the published version of the manuscript.

Acknowledgments

The authors are indebted to Mrs. Kiran Atwal, Dr. Zahra Solati, Dr. Andrea Edel, and Dr. Pedram Hassan-Tash for their help with blood sample collection.

Declaration of interest

Dr. Ravandi is supported by a grant from Research Manitoba and Heart and Stroke Foundation of Canada. Mr. Surendran is supported by Research Manitoba Master's Studentship (2018), Bank of Montreal/Institute of Cardiovascular Sciences Studentship (2019), and Singal, Pawan K. Graduate Scholarship in Cardiovascular Sciences (2019). All authors declare no conflicts relevant to the contents of this paper.

3.8 STAR Methods

RESOURCE AVAILABILITY

Lead contact

Further information and requests for resources should be directed to and will be fulfilled by the Lead Contact, Dr. Amir Ravandi (aravandi@sbgh.mb.ca).

Materials availability

This study did not generate new unique reagents.

Data and code availability

The lipidomics data have been deposited to the publicly available EMBL-EBI MetaboLights database with the identifier MTBLS3839. This paper does not report original code. Any additional information required to reanalyze the data reported in this paper is available from the lead contact upon request.

3.8.1 Experimental model and subject details

Venous blood samples were collected from 80 patients undergoing primary PCI for STEMI between January 2017 and June 2018. The diagnosis of STEMI was based on presentation with chest pain, confirmation of ST-elevation on 12-lead ECG, and documentation of occluded coronary artery with coronary angiography. The samples were collected from STEMI patients (n=80) by venipuncture at three time points. The time points include the time of presentation at cardiac catheterization laboratory, but before reperfusion (pre-PCI), 2 h post successful reperfusion (2 h post-PCI), and 24 h post successful reperfusion (24 h post-PCI). To better understand the late response to reperfusion, in a sub-section of the STEMI cohort (n=30), blood samples were

prospectively collected at two additional time points, including 48 h after reperfusion (48 h post-PCI) and 30 days post successful reperfusion. For the age/sex-matched comparison population (n=50), blood from patients referred for diagnostic coronary angiography without any evidence of coronary disease was collected after angiography. Plasma was collected after centrifugation (2,500g, 5 min, 4°C) and was immediately stored at - 80°C until required. The average time between blood collection to plasma separation and aliquoting was less than 20 min. The study was approved by St. Boniface General Hospital and the University of Manitoba Research Ethics Board. Written informed consent was obtained from all study participants, and the study was conducted in compliance with the principles of the Declaration of Helsinki.

METHOD DETAILS

3.8.2 Lipid Standards and Solvents

Tetrahydrofuran, methanol (Optima LC/MS grade), and water were purchased from Fisher Chemical (Mississauga, ON). Ammonium formate and 1-butanol (analytical grade) were purchased from Sigma-Aldrich (St Louis, MO, USA). Chloroform (analytical grade) was purchased from Millipore Sigma (Oakville, ON). Lipid internal standards (ISTD) for dihydroceramide (dhCer 8:0), ceramide (Cer 17:0), sphingomyelin (SM 12:0), lysophosphatidylcholine (LPC 13:0), phosphatidylcholine (PC 13:0_13:0), oxidised phospholipids (PC 9:0_9:0), lysophosphatidylethanolamine (LPE 14:0), phosphatidylethanolamine (PE 17:0_17:0), phosphatidylglycerol (PG 17:0_17:0), and phosphatidylserine (PS 17:0_17:0) were purchased from Avanti Polar Lipids (Alabaster, AL, USA). Acylcarnitine (Acylcarnitine 3:0 (*d5*), Acylcarnitine 14:0 (*d3*)), cholesteryl ester (CE 18:0 (*d6*)), and fatty acid (FA 15:0 (*d3*)) were purchased from CDN Isotopes (Pointe-Claire, QC). Diacylglycerol (DG 15:0_15:0) was purchased from LGC Standards (Manchester, NH, USA). Monohexosylceramide (HexCer 16:0 (*d3*)),

dihexosylceramide (Hex2Cer 16:0 (*d3*)), and trihexosylceramide (Hex3Cer 17:0) were purchased from MJS BioLynx (Brockville, ON,). Triacylglycerol (TG 17:0_17:0_17:0) was purchased from Sigma-Aldrich (St Louis, MO, USA). Synthetic standards for phosphatidylcholines (PC) containing oxidized phospholipids (OxPL) such as 1-palmitoyl-2- (5-oxovaleroyl)-sn-glycero-3-phosphocholine (POVPC), 1-palmitoyl-2-(9-oxo)nonanoyl-sn-glycero-3-phosphocholine (PONPC), 1-palmitoyl-2-glutaroyl-sn-glycero-3-phosphocholine (PGPC), and 1-Palmitoyl-2-azelaoyl-sn-glycero-3-phosphocholine (PAzPC) were obtained from Avanti Polar Lipids. 1-(palmitoyl)-2-(5-keto-6-octene-dioyl)-3-phosphocholine (KOdiAPC), and 1-palmitoyl-2-(4-keto-dodec-3-ene-dioyl)-sn-glycero-3-phosphocholine (KDdiAPC) were purchased from Cayman Chemicals (Ann Arbor, MI, USA). Cholesteryl ester (CE) and fatty acid (FA) synthetic standards were purchased from Nu-Chek-Prep (Elysian, MN, USA).

3.8.3 Lipid Extraction

Lipid extraction was done using chloroform and methanol[9,45]. Briefly, plasma samples were thawed, and 10 µl of plasma was dispensed to a 1.5 ml polypropylene tube (Eppendorf). To the tube, 30 µl of lipid internal standards (ISTD) in chloroform/methanol (1:1, v/v) was added alongside 200 µl of chloroform/methanol (2:1, v/v). **Supplementary Table S1** contains the complete list of lipid abbreviations. ISTDs were either odd-chain or deuterated and are not present endogenously (**Supplementary Table S2**). The mixture was vortexed on a rotary mixer for 10 min and sonicated in a water bath at room temperature (RT) for 30 min. The mixture was subsequently allowed to settle for 20 min and then centrifuged (20,000g, 20 min, RT). The upper lipid-containing phase was transferred into a clean polypropylene tube and dried under a stream of nitrogen gas at room temperature. Lipids were reconstituted in 50 µl water-saturated 1-butanol and sonicated for 10 min. Finally, 50 µl of 10 mM ammonium formate in methanol was added to the

final lipid extract. The extract was centrifuged (10,000g, 10 min, RT), and 80 µl of the supernatant was transferred into the micro insert in sample vials for lipid analysis.

3.8.4 Lipid Separation

Lipids were separated on a reverse-phase liquid chromatography-electrospray ionization tandem mass spectrometry (LC/ESI-MS/MS) platform using a Prominence chromatographic system (Shimadzu Corporation, OR, USA). Instrument control and data processing were done with Analyst v1.6 and MultiQuant v2.1 software (AB Sciex, MA, USA). The separation was achieved on a Zorbax C18, 1.8 µm, 50 × 2.1 mm column (Agilent Technologies, Mississauga, ON). The flow rate was set to 300 µl/min using a linear gradient of mobile phase A and mobile phase B. Mobile phase A and B consisted of tetrahydrofuran, methanol, and water in the ratio 20:20:60 (v/v/v) and 75:20:5 (v/v/v), respectively. Both A and B contained 10 mM ammonium formate. The elution program was as follows: start with 0% solvent B; increase to 100% B at 8.00 min; maintained at 100% B for 2.5 min; and back to 0% B over 0.5 min. The column was finally re-equilibrated to the starting conditions (0% mobile phase B) for 3 min before the next sample injection. Diacylglycerol (DG) and triacylglycerol (TG) species were separated in an isocratic fashion (100 µl/min) by employing 85% mobile phase B over 8 min. The analytical column and autosampler were maintained at 50°C and 25°C, respectively, during the analysis. The injection volume was 5 µl.

3.8.5 Mass Spectral Analysis

Lipids eluted from the HPLC system were introduced into the AbSciex 4000 QTRAP triple quadrupole linear hybrid mass spectrometer. The mass spectrometer was operated in scheduled Multiple Reaction Monitoring (MRM) mode. In total, 322 unique lipids spanning 25 different lipid classes/subclasses were screened for targeted semi-quantitation (**Supplementary Tables S3**). All

lipid species other than fatty acids were scanned in positive electrospray ionization mode [ESI+] mode. The individual lipids in each lipid class were identified by lipid class-specific precursor ions or neutral losses (**Supplementary Table S2**). Lipids were then quantified by comparing the deisotoped lipid peak areas against those of the class-specific ISTDs added before lipid extraction. The linearity plot of lipid internal standards (ISTDs) in plasma is shown in **Supplementary Figures S1-S3.** Lipids were represented by the total carbon number of the fatty acids. The collision energy and declustering potential for each lipid class were fixed individually using flow injection analysis (**Supplementary Table S3**). In the ESI+ mode, the instrument settings were optimised as follows: curtain gas (psi), 26; collision gas (nitrogen), medium; ion spray voltage (V), 5500; temperature (°C), 500.0; ion source gas 1 (psi), 40.0; ion and source gas 2 (psi), 30.0. The MRM detection window was fixed between 45s and 90s depending upon the chromatographic peak width of the lipid class. Isobaric species within the same class, such as PC(O) and PC(P), exhibited clear separation in this method (**Supplementary Figure S4-A**). Also, molecular species within the same lipid class, which differ only in the number of double bonds, were well separated chromatographically (**Supplementary Figures S4-B, S4-C**). MRM transitions were established to detect phosphocholine (PC) containing oxidized phospholipids (OxPL) molecules in ESI+ mode using a product ion of 184.3 m/z, matching the cleaved phosphocholine moiety. Six commercially available OxPL standards (PONPC, POVPC, PGPC, PAzPC, KOdiAPC, and KDdiAPC) were injected, and accurate peak assignments were made based upon retention times and mass transitions (**Supplementary Figure S4-D**). Additionally, M+1/M+2 isotopes were scanned for high-intensity lipid species to prevent detection saturation. The detection of neutral lipids, including CE, DG, and TG species in ESI+ mode, was reported using ammonium salts generated in the presence of ammonium formate contained in the mobile phase.

Correction factors: Generally, lipid species of the same class have the same response factors. Certain lipid classes, including DG, TG, and CE, present with a rather complicated mass spectrum due to the fragmentation of ammoniated adducts, leading to the loss of fatty acid(s) and ammonia[45]. Due to the differential fragmentation efficiency of different acyl chain lengths, there is a considerable variation in response factors between species in these classes. Consequently, additional correction factors (CF) were applied for these lipid species (**Supplementary Table S3**). In DG species, if both fatty acyl chains in DG species were different, we applied a correction factor (CF) of 0.5. For TG species, if all the three fatty acyl chains were different, we applied a correction factor of 0.33. If two of the three acyl groups were the same in TG, we applied a correction factor of 0.66. To calculate the instrument response for CE, we prepared an equimolar mixture of seven commercially available CE species comprising three compounds varying in chain length (CE 16:0, CE 20:0, and CE 20:0), two monounsaturated species (CE 16:1 and CE 18:1), and two polyunsaturated species (CE 18:2 and CE 20:4). CE 23:0 was used as an internal standard (100 μM). After extrapolating for carbon chain length and double bonds, we found that saturated CE species were fitted by the following linear equation, y = 0.13x-0.71, where 'y' is the response factor, and 'x' is the carbon chain length. Monounsaturated species were characterized by the linear equation y=1.13x-0.23 and polyunsaturated species by y=-0.07x+1.54. Other lipid species were not corrected.

Fatty acids: Acidic compounds, namely free fatty acids (FA), were detected in the negative ESI mode (ESI-) using a "pseudo-molecular" multiple reaction monitoring (MRM) as previously described[46]. In the ESI- mode, ion source parameters including collision energy and declustering potential were optimized by flow injection analysis using commercially bought FA standards. Accordingly, the turbo ion spray voltage was set to −4500 V and the source temperature to 500

°C. Nitrogen was used as collision gas, and its pressure was set to "medium". The nebulizer gas was set to 40 psi, the auxiliary gas (GS2) to 30 psi, and the curtain gas to 26 psi. Thirteen commercially available FA standards were purchased, and accurate peak assignments were made based upon retention times and mass transitions. Two MRM transitions corresponding to the monoisotopic $[M-H]^-$ mass of the FA analyte were monitored for each FA. Though these MRM transitions have the same fragment and product ions, they differ in their collision cell parameters (**Supplementary Figure S5**). The first MRM transition with a low collision energy was used for quantification, while the second MRM transition with increased collision energy provided an unambiguous FA identification. In short, the second MRM for each FA served as a second qualification parameter.

3.8.6 Quality Control

The study followed the guidelines outlined by the lipidomics consortium for analytical quality assurance[47,48]. The plasma samples were randomized before analysis. The sample run order was given in **Supplementary Table S4**. Six injections of blank extracts, in the beginning, were used to identify the common contaminations. This study used two types of quality control (QC) samples to ensure analytical reproducibility and quality. A plasma quality control (PQC) sample was prepared by pooling equal aliquots (20 µl) from all samples. To assure the stability of the analytical platform, ten PQC samples were run at the beginning of each batch. In addition, PQC samples were intermittently injected throughout each batch to monitor and compensate for inter-batch analytical variability. Also, lipid extracts without matrix (plasma), referred to as technical quality control (TQC) samples, were analyzed at even intervals during the analytical batch. They were used to monitor the technical variation in LC/MS over time. Additionally, four replicate injections

of a global shared reference sample (NIST SRM 1950 plasma[47]) were included in each analytical batch to enable future comparison with different datasets.

3.8.7 Data Pre-Processing and Batch Alignment

The samples were run in multiple analytical batches, and each batch contained 60 study samples. There were twenty PQC samples within an analytical batch, six TQC samples, four SRM samples, and twelve blank extracts. The mass spectrometer's source was cleaned after two successive batches. To compensate for time-dependent drifts and batch variations, we used a PQC based normalization method known as systematic error removal using random forest (SERRF) as previously described[49]. The ratio of study samples to PQC samples was kept at 10:1. After batch correction, lipids were considered reproducible only if their coefficient of variation (CoV) among PQC samples was <20% and their highest mean was not in the blank extracts. Outliers with CoV <20% were removed (n=31), and only 291 lipid species were found eligible for subsequent downstream analysis. Principal component analysis (PCA) was used to evaluate the data consistency for all samples across all batches (**Supplementary Figure S6**). The tight clustering of identical samples (PQC, SRM) in the PCA plot validates the data quality after SERRF normalization.

3.8.8 Quantification and statistical analysis

Statistical analysis was done using the SPSS v24 (IBM Corporation, Armonk, NY, USA) software. Baseline participants' characteristics were presented as mean ± SD for continuous variables with normal distribution, median (25th, 75th percentiles) for continuous variables with non-normal distribution, and count (percentage) for categorical variables. The normality assumption of data was checked using the Shapiro-Wilk test. Based on the data distribution, the Chi-square test was used to assess differences in data across groups for categorical variables, and the Mann-Whitney

U test or Student's t-test was used for continuous variables as applicable. All tests were 2-sided, and p values <0.05 were considered statistically significant.

The lipid data were log-transformed before statistical analysis. A repeated measures analysis of variance (ANOVA) with a Greenhouse-Geisser correction was used to find the differentially regulated lipid species across time points. For pairwise comparisons, only corrected $p < 0.05$ were considered statistically significant. The "corrected p" denotes the false discovery rate (FDR) correction using the Bonferroni technique. The built-in 'pheatmap' package in R statistical software v3.5.2 (https://www.r-project.org) was used to compute and draw the clustered heatmap. The general linear regression model in SPSS employing the 'Enter' method was used to examine the associations between delta troponin (Δ cTnT) and lipid species, adjusting for the other covariates.

3.9 References

1 Virani, S. S. *et al.* Heart Disease and Stroke Statistics-2021 Update: A Report From the American Heart Association. *Circulation* **143**, e254-e743, doi:10.1161/cir.0000000000000950 (2021).

2 World Health Organization. *Cardiovascular diseases (CVDs)*, <https://www.who.int/en/news-room/fact-sheets/detail/cardiovascular-diseases-(cvds)> (2021).

3 Hausenloy, D. J. & Yellon, D. M. Myocardial ischemia-reperfusion injury: a neglected therapeutic target. *The Journal of Clinical Investigation* **123**, 92-100, doi:10.1172/JCI62874 (2013).

4 Yellon, D. M. & Hausenloy, D. J. Myocardial Reperfusion Injury. *New England Journal of Medicine* **357**, 1121-1135, doi:10.1056/NEJMra071667 (2007).

5 Lambert, L. *et al.* Association Between Timeliness of Reperfusion Therapy and Clinical Outcomes in ST-Elevation Myocardial Infarction. *JAMA* **303**, 2148-2155, doi:10.1001/jama.2010.712 (2010).

6 Burla, B. *et al.* MS-based lipidomics of human blood plasma: a community-initiated position paper to develop accepted guidelines. *J Lipid Res* **59**, 2001-2017, doi:10.1194/jlr.S087163 (2018).

7 Alshehry, Z. H. *et al.* Plasma Lipidomic Profiles Improve on Traditional Risk Factors for the Prediction of Cardiovascular Events in Type 2 Diabetes Mellitus. *Circulation* **134**, 1637-1650, doi:10.1161/circulationaha.116.023233 (2016).

8 Stegemann, C. *et al.* Lipidomics Profiling and Risk of Cardiovascular Disease in the Prospective Population-Based Bruneck Study. *Circulation* **129**, 1821-1831, doi:doi:10.1161/CIRCULATIONAHA.113.002500 (2014).

9 Meikle, P. J. *et al.* Plasma lipidomic analysis of stable and unstable coronary artery disease. *Arteriosclerosis, thrombosis, and vascular biology* **31**, 2723-2732, doi:10.1161/atvbaha.111.234096 (2011).

10 Yeang, C. *et al.* Reduction of myocardial ischaemia-reperfusion injury by inactivating oxidized phospholipids. *Cardiovasc Res* **115**, 179-189, doi:10.1093/cvr/cvy136 (2019).

11 Solati, Z., Edel, A. L., Shang, Y., O, K. & Ravandi, A. Oxidized phosphatidylcholines are produced in renal ischemia reperfusion injury. *PLoS One* **13**, e0195172, doi:10.1371/journal.pone.0195172 (2018).

12 Bilsen, M. v. *et al.* Lipid alterations in isolated, working rat hearts during ischemia and reperfusion: its relation to myocardial damage. *Circulation Research* **64**, 304-314, doi:doi:10.1161/01.RES.64.2.304 (1989).

13 Surendran, A., Aliani, M. & Ravandi, A. Metabolomic characterization of myocardial ischemia-reperfusion injury in ST-segment elevation myocardial infarction patients undergoing percutaneous coronary intervention. *Scientific Reports* **9**, 11742, doi:10.1038/s41598-019-48227-9 (2019).

14 Selvanayagam, J. B. *et al.* Troponin Elevation After Percutaneous Coronary Intervention Directly Represents the Extent of Irreversible Myocardial Injury. *Circulation* **111**, 1027-1032, doi:doi:10.1161/01.CIR.0000156328.28485.AD (2005).

15 Cantor, W. J. *et al.* Prognostic significance of elevated troponin i after percutaneous coronary intervention. *Journal of the American College of Cardiology* **39**, 1738-1744, doi:https://doi.org/10.1016/S0735-1097(02)01877-6 (2002).

16 Drgová, A., Likavcanová, K. & Dobrota, D. Changes of phospholipid composition and superoxide dismutase activity during global brain ischemia and reperfusion in rats. *Gen Physiol Biophys* **23**, 337-346 (2004).
17 Paradies, G. *et al.* Lipid peroxidation and alterations to oxidative metabolism in mitochondria isolated from rat heart subjected to ischemia and reperfusion. *Free Radical Biology and Medicine* **27**, 42-50, doi:https://doi.org/10.1016/S0891-5849(99)00032-5 (1999).
18 Tsimikas, S. *et al.* Percutaneous Coronary Intervention Results in Acute Increases in Oxidized Phospholipids and Lipoprotein(a). *Circulation* **109**, 3164-3170, doi:doi:10.1161/01.CIR.0000130844.01174.55 (2004).
19 Schoonderwoerd, K., Broekhoven-Schokker, S., Hülsmann, W. C. & Stam, H. Enhanced lipolysis of myocardial triglycerides during low-flow ischemia and anoxia in the isolated rat heart. *Basic Res Cardiol* **84**, 165-173, doi:10.1007/bf01907926 (1989).
20 Saddik, M. & Lopaschuk, G. D. Myocardial triglyceride turnover during reperfusion of isolated rat hearts subjected to a transient period of global ischemia. *Journal of Biological Chemistry* **267**, 3825-3831, doi:https://doi.org/10.1016/S0021-9258(19)50600-7 (1992).
21 Feng, L. *et al.* Lipid Biomarkers in Acute Myocardial Infarction Before and After Percutaneous Coronary Intervention by Lipidomics Analysis. *Med Sci Monit* **24**, 4175-4182, doi:10.12659/MSM.908732 (2018).
22 Hendrickson, S. C., St. Louis, J. D., Lowe, J. E. & Abdel-aleem, S. Free fatty acid metabolism during myocardial ischemia and reperfusion. *Molecular and Cellular Biochemistry* **166**, 85-94, doi:10.1023/A:1006886601825 (1997).
23 Lopaschuk, G. D. *et al.* Plasma fatty acid levels in infants and adults after myocardial ischemia. *Am Heart J* **128**, 61-67, doi:10.1016/0002-8703(94)90010-8 (1994).
24 Saponaro, C., Gaggini, M., Carli, F. & Gastaldelli, A. The Subtle Balance between Lipolysis and Lipogenesis: A Critical Point in Metabolic Homeostasis. *Nutrients* **7**, 9453-9474, doi:10.3390/nu7115475 (2015).
25 González-Montero, J., Brito, R., Gajardo, A. I. & Rodrigo, R. Myocardial reperfusion injury and oxidative stress: Therapeutic opportunities. *World J Cardiol* **10**, 74-86, doi:10.4330/wjc.v10.i9.74 (2018).
26 Piomelli, D., Astarita, G. & Rapaka, R. A neuroscientist's guide to lipidomics. *Nature Reviews Neuroscience* **8**, 743-754, doi:10.1038/nrn2233 (2007).
27 Hasanally, D., Edel, A., Chaudhary, R. & Ravandi, A. Identification of Oxidized Phosphatidylinositols Present in OxLDL and Human Atherosclerotic Plaque. *Lipids* **52**, 11-26, doi:10.1007/s11745-016-4217-y (2017).
28 Apple, F. S., Sandoval, Y., Jaffe, A. S. & Ordonez-Llanos, J. Cardiac Troponin Assays: Guide to Understanding Analytical Characteristics and Their Impact on Clinical Care. *Clin Chem* **63**, 73-81, doi:10.1373/clinchem.2016.255109 (2017).
29 Adams, S. H. *et al.* Plasma acylcarnitine profiles suggest incomplete long-chain fatty acid beta-oxidation and altered tricarboxylic acid cycle activity in type 2 diabetic African-American women. *J Nutr* **139**, 1073-1081, doi:10.3945/jn.108.103754 (2009).
30 McCoin, C. S., Knotts, T. A. & Adams, S. H. Acylcarnitines--old actors auditioning for new roles in metabolic physiology. *Nat Rev Endocrinol* **11**, 617-625, doi:10.1038/nrendo.2015.129 (2015).

31 Guasch-Ferré, M. *et al.* Plasma acylcarnitines and risk of cardiovascular disease: effect of Mediterranean diet interventions. *Am J Clin Nutr* **103**, 1408-1416, doi:10.3945/ajcn.116.130492 (2016).
32 Strand, E. *et al.* Serum Acylcarnitines and Risk of Cardiovascular Death and Acute Myocardial Infarction in Patients With Stable Angina Pectoris. *J Am Heart Assoc* **6**, e003620, doi:10.1161/JAHA.116.003620 (2017).
33 Corr, P. B., Creer, M. H., Yamada, K. A., Saffitz, J. E. & Sobel, B. E. Prophylaxis of early ventricular fibrillation by inhibition of acylcarnitine accumulation. *J Clin Invest* **83**, 927-936, doi:10.1172/jci113978 (1989).
34 Lee, J. Y., Sohn, K. H., Rhee, S. H. & Hwang, D. Saturated fatty acids, but not unsaturated fatty acids, induce the expression of cyclooxygenase-2 mediated through Toll-like receptor 4. *J Biol Chem* **276**, 16683-16689, doi:10.1074/jbc.M011695200 (2001).
35 Lee, J. Y. *et al.* Saturated fatty acid activates but polyunsaturated fatty acid inhibits Toll-like receptor 2 dimerized with Toll-like receptor 6 or 1. *J Biol Chem* **279**, 16971-16979, doi:10.1074/jbc.M312990200 (2004).
36 Rutkowsky, J. M. *et al.* Acylcarnitines activate proinflammatory signaling pathways. *Am J Physiol Endocrinol Metab* **306**, E1378-1387, doi:10.1152/ajpendo.00656.2013 (2014).
37 D'Souza, K., Nzirorera, C. & Kienesberger, P. C. Lipid metabolism and signaling in cardiac lipotoxicity. *Biochim Biophys Acta* **1861**, 1513-1524, doi:10.1016/j.bbalip.2016.02.016 (2016).
38 Cheng, K. H. *et al.* Lipid paradox in acute myocardial infarction-the association with 30-day in-hospital mortality. *Crit Care Med* **43**, 1255-1264, doi:10.1097/ccm.0000000000000946 (2015).
39 Toledo, E. *et al.* Plasma lipidomic profiles and cardiovascular events in a randomized intervention trial with the Mediterranean diet. *The American journal of clinical nutrition* **106**, 973-983, doi:10.3945/ajcn.116.151159 (2017).
40 Ho, J. E. *et al.* Metabolomic Profiles of Body Mass Index in the Framingham Heart Study Reveal Distinct Cardiometabolic Phenotypes. *PloS one* **11**, e0148361-e0148361, doi:10.1371/journal.pone.0148361 (2016).
41 Law, S.-H. *et al.* An Updated Review of Lysophosphatidylcholine Metabolism in Human Diseases. *International journal of molecular sciences* **20**, 1149, doi:10.3390/ijms20051149 (2019).
42 Lavi, S. *et al.* Local production of lipoprotein-associated phospholipase A2 and lysophosphatidylcholine in the coronary circulation: association with early coronary atherosclerosis and endothelial dysfunction in humans. *Circulation* **115**, 2715-2721, doi:10.1161/circulationaha.106.671420 (2007).
43 Packard, C. J. *et al.* Lipoprotein-associated phospholipase A2 as an independent predictor of coronary heart disease. West of Scotland Coronary Prevention Study Group. *N Engl J Med* **343**, 1148-1155, doi:10.1056/nejm200010193431603 (2000).
44 Lavi, S. *et al.* Local Production of Lipoprotein-Associated Phospholipase A₂ and Lysophosphatidylcholine in the Coronary Circulation. *Circulation* **115**, 2715-2721, doi:doi:10.1161/CIRCULATIONAHA.106.671420 (2007).
45 Weir, J. M. *et al.* Plasma lipid profiling in a large population-based cohort. *Journal of lipid research* **54**, 2898-2908, doi:10.1194/jlr.P035808 (2013).

46 Hellmuth, C., Weber, M., Koletzko, B. & Peissner, W. Nonesterified fatty acid determination for functional lipidomics: comprehensive ultrahigh performance liquid chromatography-tandem mass spectrometry quantitation, qualification, and parameter prediction. *Analytical chemistry* **84**, 1483-1490, doi:10.1021/ac202602u (2012).
47 Triebl, A. *et al.* Shared reference materials harmonize lipidomics across MS-based detection platforms and laboratories. *Journal of lipid research* **61**, 105-115, doi:10.1194/jlr.D119000393 (2020).
48 Burla, B. *et al.* MS-based lipidomics of human blood plasma: a community-initiated position paper to develop accepted guidelines1. *Journal of lipid research* **59**, 2001-2017, doi:https://doi.org/10.1194/jlr.S087163 (2018).
49 Fan, S. *et al.* Systematic Error Removal Using Random Forest for Normalizing Large-Scale Untargeted Lipidomics Data. *Analytical chemistry* **91**, 3590-3596, doi:10.1021/acs.analchem.8b05592 (2019).

3.10 Supplementary data

Supplementary Figure S1: Linearity plot of lipid internal standards (Cer 17:0, dhCer 8:0, PC 13:0_13:0, PE 17:0_17:0, LPC 13:0, LPE 14:0, PS 17:0_17:0 and PG 17:0_17:0) in plasma (related to STAR methods)

Serial dilutions of lipid internal standards (ISTDs) in a plasma quality control (PQC) sample were used to generate the response curves. **Supplementary Table S1** contains the complete list of lipid abbreviations.

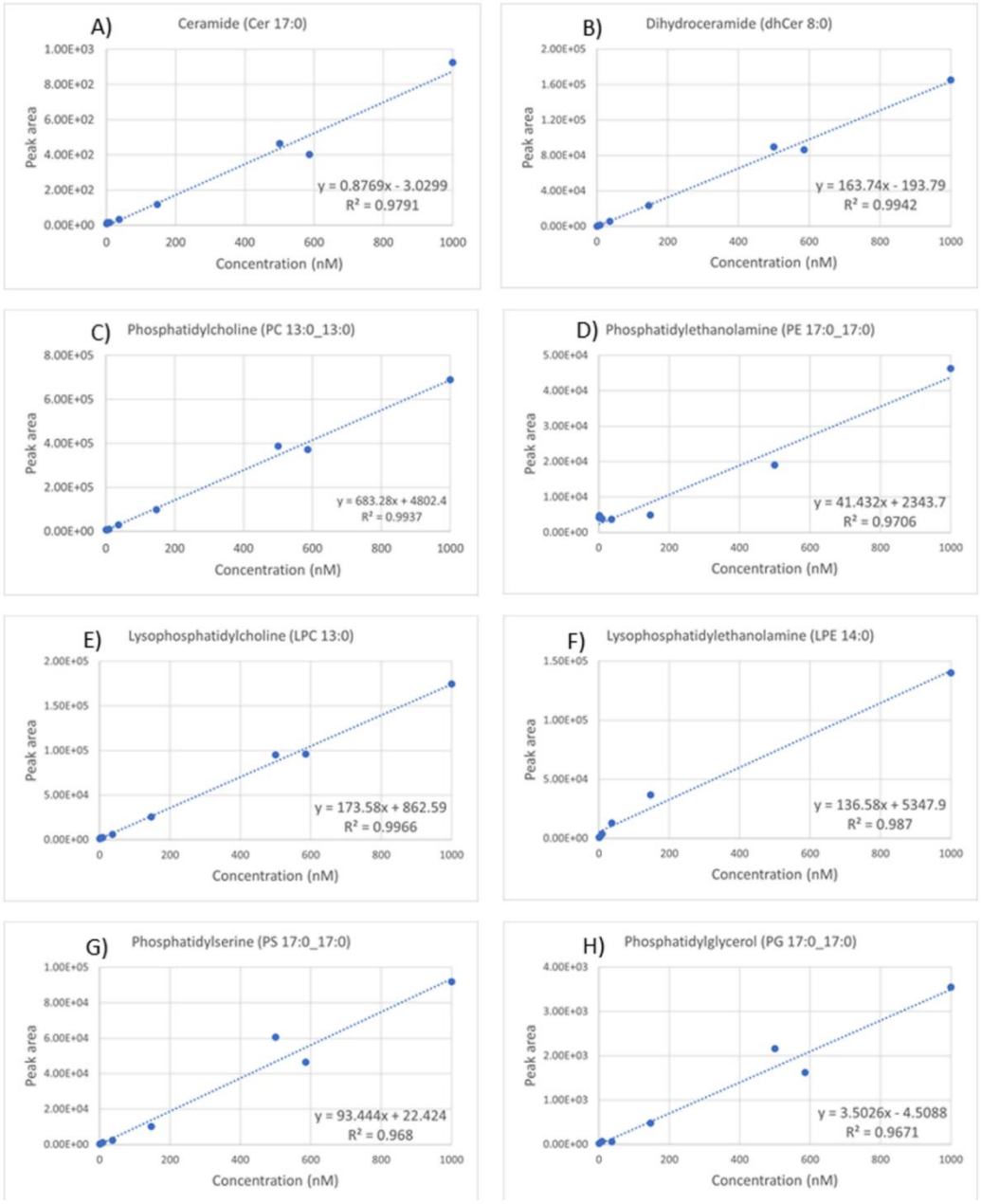

Supplementary Figure S2: Linearity plot of lipid internal standards (SM 12:0, HexCer 16:0 (d3), Hex2Cer 16:0 (d3), Hex3Cer 17:0, Acylcarnitine 3:0 (d5), Acylcarnitine 14:0 (d3), Diacylglycerol (DG 15:0_15:0) and Triacylglycerol (TG 17:0_17:0_17:0)) in plasma (related to STAR methods)

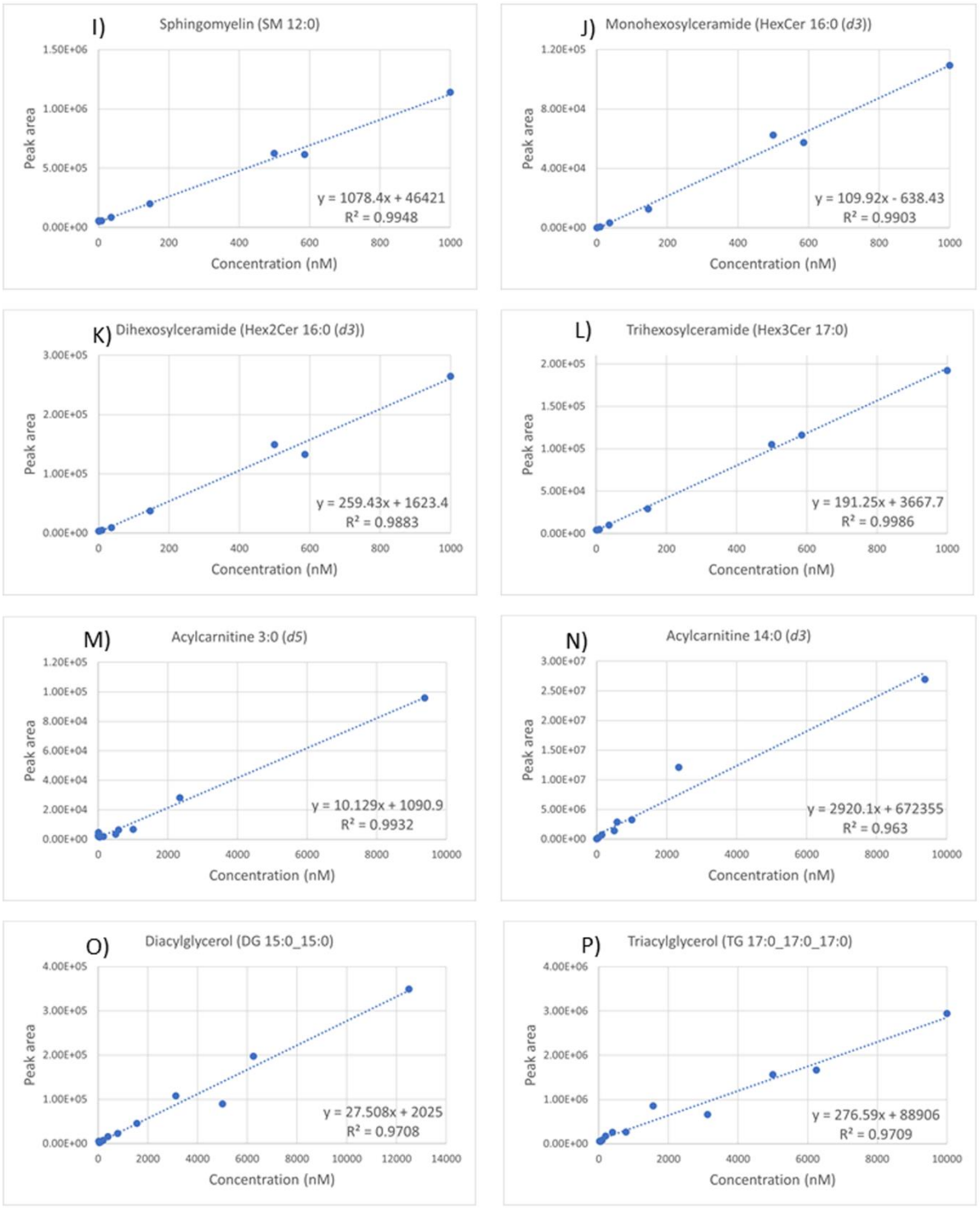

Supplementary Figure S3: Linearity plot of cholesteryl ester (CE 18:0 (d6)), and fatty acid (FA 15:0 (d3)) in plasma (related to STAR methods)

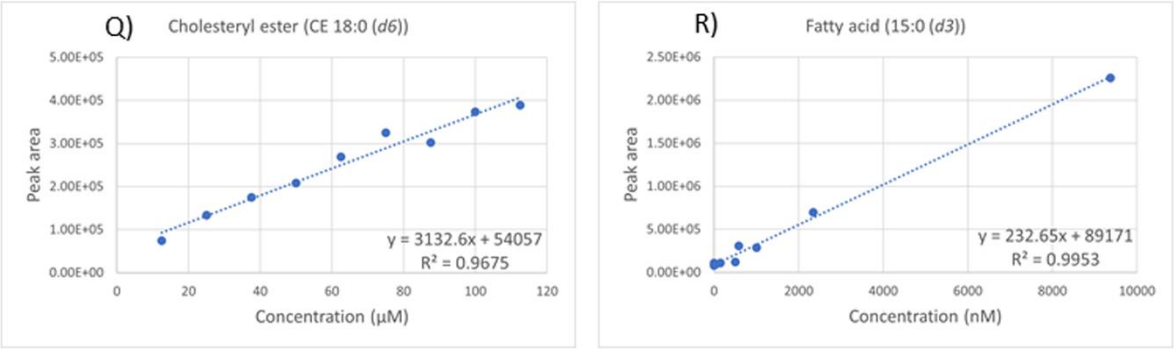

Supplementary Figure S4: Chromatographic separation of lipid species in ESI+ mode (related to STAR methods): Figure (A) shows separation of two isobaric species of PC in plasma scanned using the same transition 718.5/184.3, (B) shows separation of two acylcarnitine species in plasma differing in the number of carbon double bonds, (C) shows separation of two LPC species in plasma differing in the number of carbon double bonds and (D) shows separation of an equimolar mixture (100 µM) of six commercially bought oxidized phospholipids (OxPL) standards. **Supplementary Table S1** contains the complete list of lipid abbreviations.

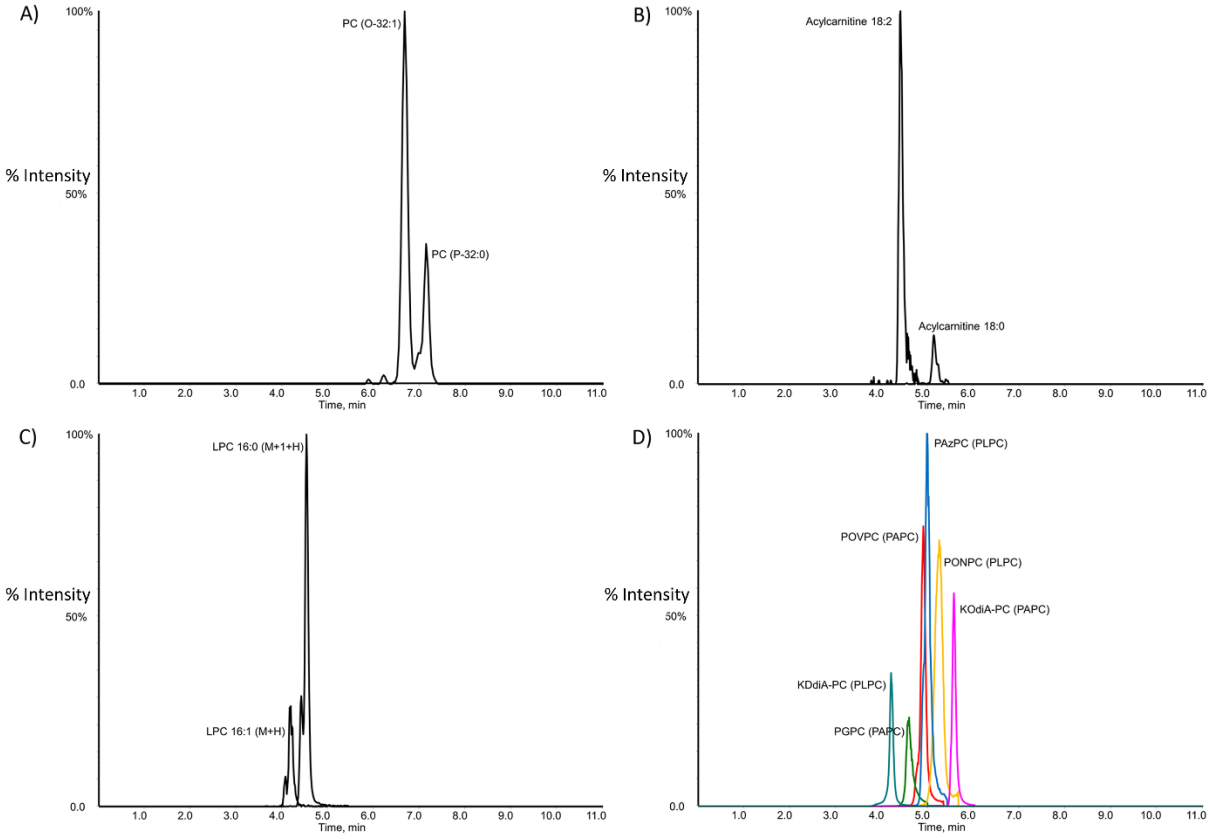

Supplementary Figure S5: Fatty acids in ESI- mode (related to STAR methods): The figure shows separation of c18 fatty acids in human plasma in ESI- mode. The quantifier ions with low collision energy are shown in blue, while the "pseudo-qualifier" ions with high collision energy are red.

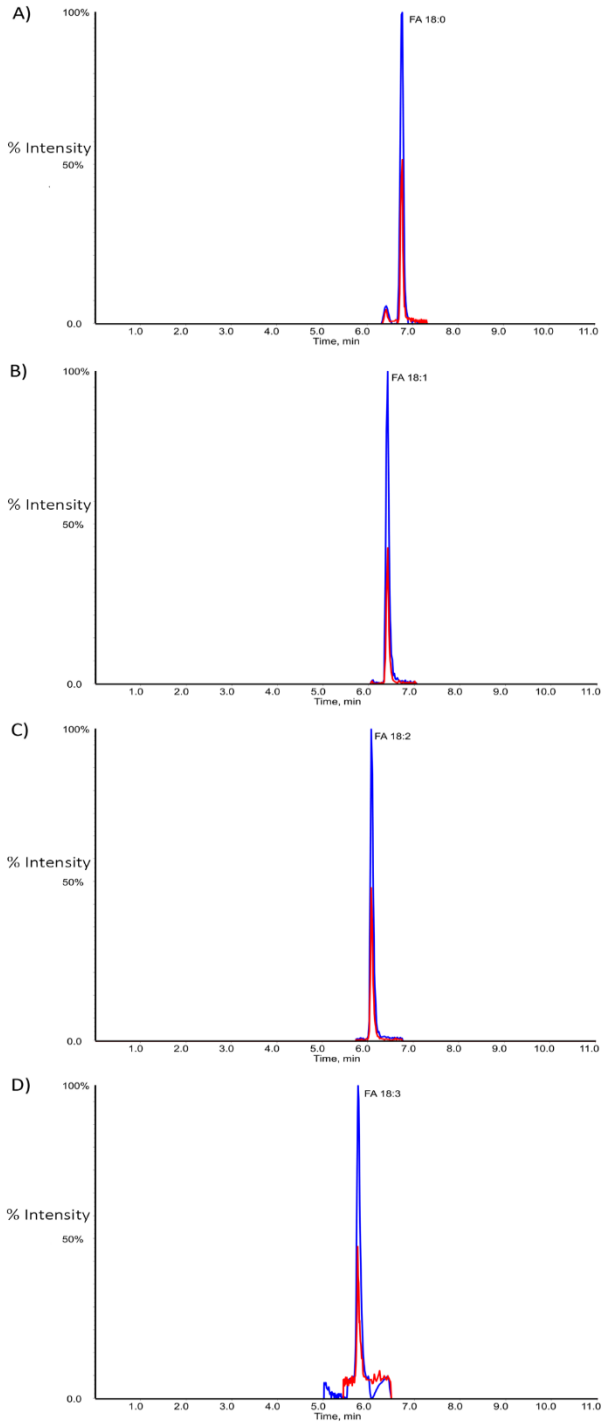

Supplementary Figure S6: Principal Component Analysis (PCA) plot (related to STAR methods): The tight clustering of the plasma quality control samples (PQC) and global shared reference samples (SRM) shows the data quality after SERRF normalization.

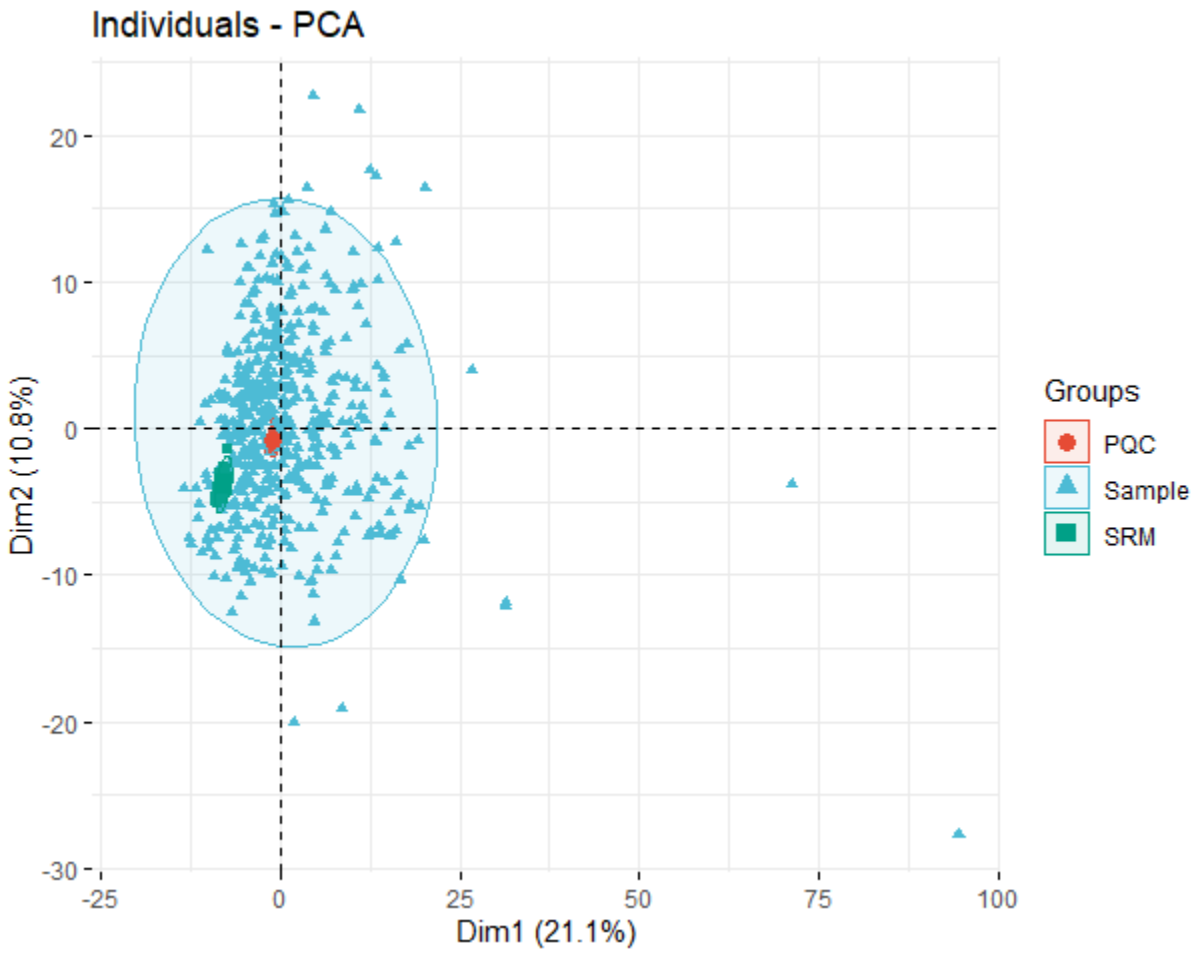

Supplementary Table S1: Abbreviations for lipids

Class	Abbreviation
Dihydroceramide	dhCer
Ceramide	Cer
Monohexosylceramide	HexCer
Dihexosylceramide	Hex2Cer
Trihexosylcermide	Hex3Cer
GM3 ganglioside	GM3
Sphingomyelin	SM
Phosphatidylcholine	PC
Oxidized phospholipids	OxPL
Alkylphosphatidylcholine	PC(O)
Phosphatidylcholine plasmalogen	PC(P)
Lysophosphatidylcholine	LPC
Lysoalkylphosphatidylcholine	LPC(O)
Phosphatidylethanolamine	PE
Alkylphosphatidylethanolamine	PE(O)
Phosphatidylethanolamine plasmalogen	PE(P)
Lysophosphatidylethanolamine	LPE
Phosphatidylinositol	PI
Phosphatidylserine	PS
Phosphatidylglycerol	PG
Cholesterol ester	CE
Diacylglycerol	DG
Triacylglycerol	TG
Fatty acids	FA
1-palmitoyl-2- (5-oxovaleroyl)-sn-glycero-3-phosphocholine	POVPC
1-palmitoyl-2-(9-oxo)nonanoyl-sn-glycero-3-phosphocholine	PONPC
1-palmitoyl-2-glutaroyl-sn-glycero-3-phosphocholine	PGPC
1-Palmitoyl-2-azelaoyl-sn-glycero-3-phosphocholine	PAzPC
1-(palmitoyl)-2-(5-keto-6-octene-dioyl)-3-phosphocholine	KOdiAPC
1- palmitoyl-2-(4-keto-dodec-3-ene-dioyl)-sn-glycero-3-phosphocholine	KDdiAPC

Supplementary Table S2: Experimental conditions for lipid identification and quantification

Lipid class	Lipid species	Internal Standard	Parent Ion	µM/ 30 µl	Fragmentation
dhCer	6	dhCer 8:0	[M+H]+	0.5	PIS, m/z 284.4
Cer	6	Cer 17:0	[M+H]+	5	PIS, *m/z* 264.4
HexCer	6	MHC 16:0 (*d3)*	[M+H]+	0.5	PIS, *m/z* 264.4
Hex2Cer	6	DHC 16:0 (*d3)*	[M+H]+	0.5	PIS, *m/z* 264.4
Hex3Cer	6	THC 17:0	[M+H]+	0.5	PIS, *m/z* 264.4
GM3	6	THC 17:0	[M+H]+	0.5	PIS, *m/z* 264.4
SM	20	SM 12:0	[M+H]+	0.5	PIS, *m/z* 184.3
PC	31	PC 13:0_13:0	[M+H]+	0.5	PIS, *m/z* 184.3
OxPL	6	PC 9:0_9:0	[M+H]+	0.5	PIS, *m/z* 184.3
PC(O)	14	PC 13:0_13:0	[M+H]+	0.5	PIS, *m/z* 184.3
PC(P)	6	PC 13:0_13:0	[M+H]+	0.5	PIS, *m/z* 184.3
LPC	19	LPC 13:0	[M+H]+	0.5	PIS, *m/z* 184.3
LPC(O)	6	LPC 13:0	[M+H]+	0.5	PIS, *m/z* 104.1
PE	18	PE 17:0_17:0	[M+H]+	0.5	NL, 141 Da
PE(O)	12	PE 17:0_17:0	[M+H]+	0.5	NL, 141 Da
PE(P)	7	PE 17:0_17:0	[M+H]+	0.5	NL, 141 Da
LPE	7	LPE 14:0	[M+H]+	0.5	NL, 141 Da
PI	17	PE 17:0_17:0	[M+NH4]+	0.5	NL, 277 Da
PS	7	PS 17:0_17:0	[M+H]+	0.5	NL, 185 Da
PG	4	PG 17:0_17:0	[M+NH4]+	0.5	NL, 189 Da
CE	20	CE 18:0 (*d6)*	[M+NH4]+	20	PIS, *m/z* 369.3
Acylcarnitine (<C14)	11	Acylcarnitine 3:0 (*d5*)	[M+H]+	5	PIS, *m/z* 85.0
Acylcarnitine (C>14)	5	Acylcarnitine 14:0 (*d3*)	[M+H]+	0.1	PIS, *m/z* 85.0
DG	20	DG 15:0_15:0	[M+NH4]+	5	NL, fatty acid
TG	43	TG 17:0_17:0_17:0	[M+NH4]+	5	NL, fatty acid
FA	13	FA 15:0 (*d3*)	[M-H]-	0.5	Pseudo MRM

Abbreviations: PIS, precursor ion scan; NL, neutral loss scan; MRM, Multiple reaction monitoring. **Supplementary Table S1** contains the complete list of lipid abbreviations.

Supplementary Table S3: LC/MS conditions for lipid identification in human plasma

No	Compound	Isotope	Q1	Q3	RT	DP	EP	CE	CXP	CF
1	IS dhCer 8:0	[M+H]+	428.6	284.4	6.47	120	10	30	11	-
2	IS Cer 17:0	[M+H]+	552.4	264.4	7.66	135	10	35	11	-
3	IS MHC 16:0 (*d3*)	[M+H]+	703.9	264.4	6.99	100	10	50	11	-
4	IS DHC 16:0 (*d3*)	[M+H]+	865.8	264.4	6.74	125	10	60	11	-
5	IS THC 17:0	[M+H]+	1038.7	264.4	6.69	105	10	60	11	-
6	IS SM 12:0	[M+1+H]+	648.5	185.3	5.8	100	10	35	11	-
7	IS SM 12:0	[M+2+H]+	649.5	186.3	5.8	100	10	35	11	-
8	IS SM 12:0	[M+H]+	647.5	184.3	5.8	100	10	22	11	-
9	IS PC 9:0-9:0	[M+H]+	538.6	184.3	4.64	100	10	22	11	-
10	IS PC 13:0-13:0	[M+1+H]+	651.5	185.3	6.43	100	10	35	11	-
11	IS PC 13:0-13:0	[M+2+H]+	652.5	186.3	6.43	100	10	35	11	-
12	IS PC 13:0-13:0	[M+H]+	650.5	184.3	6.43	100	10	22	11	-
13	IS LPC 13:0	[M+1+H]+	455.3	185.3	3.9	100	10	35	11	-
14	IS LPC 13:0	[M+H]+	454.3	184.3	3.9	100	10	53	11	-
15	IS PE 17:0_17:0	[M+H]+	720.6	579.5	7.38	100	10	30	11	-
16	IS LPE 14:0	[M+H]+	426.5	285.5	4.1	100	10	22	11	-
17	IS PS 17:0-17:0	[M+1+H]+	765.4	580.8	6.62	105	10	28	11	-
18	IS PS 17:0_17:0	[M+H]+	764.4	579.8	6.62	105	10	28	11	-
19	IS PG 17:0_17:0	[M+1+NH4]+	769.8	580.7	6.76	80	10	30	11	-
20	IS PG 17:0_17:0	[M+NH4]+	768.8	579.7	6.76	80	10	30	11	-
21	IS CE 18:0 (*d6* +1)	[M+1+NH4]+	677.7	376.5	9.46	52	10	22	11	-
22	IS CE 18:0 (*d6* +2)	[M+2+NH4]+	678.7	377.3	9.46	52	10	22	11	-
23	IS CE 18:0 (*d6*)	[M+NH4]+	676.7	375.4	9.46	52	10	22	11	-
24	IS AcylCarnitine 14:0 (*d3*)	[M+H]+	375.6	85	4.26	130	10	55	11	-
25	IS AcylCarnitine 3:0 (*d5*)	[M+H]+	223.2	85	0.39	130	10	55	11	-
26	IS DG 15:0_15:0	[M+NH4]+	558.5	299.3	2.33	50	10	22	11	-
27	IS TG 17:0_17:0_17:0	[M+NH4]+	866.8	579.5	6.5	100	10	55	11	-
28	IS TG 17:0_17:0_17:0	[M+1+NH4]+	867.8	580.5	6.5	100	10	55	11	-
29	IS PC 9:0	[M-CH3]-	522.3	522.3	4.45	-140	-10	-8	-7	-
30	IS PC 9:0*	[M-CH3]-	522.4	522.4	4.45	-140	-10	-25	-7	-
31	IS FA 15:0 (*d3*)	[M-H]-	243.8	243.8	5.78	-75	-10	-20	-7	-
32	IS FA 15:0* (*d3*)	[M-H]-	243.9	243.9	5.78	-75	-10	-25	-7	-
33	Cer 16:0	[M+H]+	538.5	264.4	6.73	135	10	35	11	-
34	Cer 18:0	[M+H]+	566.6	264.4	7.8	135	10	35	11	-
35	Cer 20:0	[M+H]+	594.6	264.4	8.01	135	10	35	11	-
36	Cer 22:0	[M+H]+	622.6	264.4	8.22	135	10	35	11	-

37	Cer 24:0	[M+H]+	650.7	264.4	8.39	135	10	35	11	-
38	Cer 24:1	[M+H]+	648.6	264.4	8.22	135	10	35	11	-
39	dhCer 16:0	[M+H]+	540.5	284.4	7.7	120	10	30	11	-
40	dhCer 18:0	[M+H]+	568.6	284.4	7.88	120	10	30	11	-
41	dhCer 20:0	[M+H]+	596.6	284.4	8.08	120	10	30	11	-
42	dhCer 22:0	[M+H]+	624.6	284.4	8.3	120	10	30	11	-
43	dhCer 24:0	[M+H]+	652.7	284.4	8.46	120	10	30	11	-
44	dhCer 24:1	[M+H]+	650.7	284.4	8.3	120	10	30	11	-
45	HexCer 16:0	[M+H]+	700.6	264.4	6.99	100	10	50	11	-
46	HexCer 18:0	[M+H]+	728.6	264.4	7.37	100	10	50	11	-
47	HexCer 20:0	[M+H]+	756.6	264.4	7.51	100	10	50	11	-
48	HexCer 22:0	[M+H]+	784.7	264.4	7.75	100	10	50	11	-
49	HexCer 24:0	[M+H]+	812.7	264.4	7.94	100	10	50	11	-
50	HexCer 24:1	[M+H]+	810.7	264.4	7.87	100	10	50	11	-
51	Hex2Cer 16:0	[M+H]+	862.6	264.4	6.74	125	10	60	11	-
52	Hex2Cer 18:0	[M+H]+	890.7	264.4	7.04	125	10	60	11	-
53	Hex2Cer 20:0	[M+H]+	918.7	264.4	7.26	125	10	60	11	-
54	Hex2Cer 22:0	[M+H]+	946.7	264.4	7.5	125	10	60	11	-
55	Hex2Cer 24:0	[M+H]+	974.8	264.4	7.71	125	10	60	11	-
56	Hex2Cer 24:1	[M+H]+	972.7	264.4	7.52	125	10	60	11	-
57	Hex3Cer 16:0	[M+H]+	1024.7	264.4	6.56	105	10	60	11	-
58	Hex3Cer 18:0	[M+H]+	1052.7	264.4	6.83	105	10	60	11	-
59	Hex3Cer 20:0	[M+H]+	1080.7	264.4	7.1	105	10	60	11	-
60	Hex3Cer 22:0	[M+H]+	1108.8	264.4	7.32	105	10	60	11	-
61	Hex3Cer 24:0	[M+H]+	1136.8	264.4	7.56	105	10	60	11	-
62	Hex3Cer 24:1	[M+H]+	1134.8	264.4	7.33	105	10	60	11	-
63	GM3 16:0	[M+H]+	1153.7	264.4	5.86	105	10	60	11	-
64	GM3 18:0	[M+H]+	1181.8	264.4	6.15	105	10	60	11	-
65	GM3 20:0	[M+H]+	1209.8	264.4	6.39	105	10	60	11	-
66	GM3 22:0	[M+H]+	1237.8	264.4	6.66	105	10	60	11	-
67	GM3 24:0	[M+H]+	1265.9	264.4	6.88	105	10	60	11	-
68	GM3 24:1	[M+H]+	1263.8	264.4	6.67	105	10	60	11	-
69	SM 31:1	[M+H]+	661.5	184.3	5.94	100	10	22	11	-
70	SM 32:1	[M+1+H]+	676.6	185.3	6.14	100	10	35	11	-
71	SM 32:2	[M+H]+	673.5	184.3	5.91	100	10	22	11	-
72	SM 33:1	[M+1+H]+	690.6	185.3	6.28	100	10	35	11	-
73	SM 34: 0	[M+H]+	705.3	185.3	6.46	100	10	22	11	-
74	SM 34:1	[M+2+H]+	705.6	186.3	6.45	100	10	35	11	-
75	SM 34:2	[M+1+H]+	702.6	185.3	6.25	100	10	35	11	-
76	SM 34:3	[M+H]+	699.5	184.3	6.06	100	10	22	11	-
77	SM 35:1	[M+H]+	717.6	184.3	6.59	100	10	22	11	-
78	SM 35:2	[M+H]+	715.6	184.3	6.39	100	10	22	11	-
79	SM 36:1	[M+1+H]+	732.6	185.3	6.75	100	10	35	11	-

80	SM 36:2	[M+1+H]+	730.6	185.3	6.55	100	10	35	11	-
81	SM 36:3	[M+H]+	727.6	184.3	6.38	100	10	22	11	-
82	SM 37:2	[M+H]+	743.5	184.3	6.94	100	10	22	11	-
83	SM 38:1	[M+1+H]+	760.6	185.3	6.87	100	10	35	11	-
84	SM 38:2	[M+H]+	757.6	184.3	6.84	100	10	22	11	-
85	SM 39:1	[M+H]+	773.7	184.3	7.16	100	10	22	11	-
86	SM 41:1	[M+H]+	801.7	184.3	7.39	100	10	22	11	-
87	SM 41:2	[M+H]+	799.7	184.3	7.22	100	10	22	11	-
88	SM 42:1	[M+1+H]+	816.7	185.3	7.51	100	10	35	11	-
89	PC 29:0	[M+H]+	692.5	184.3	6.33	100	10	22	11	-
90	PC 31:0	[M+H]+	720.6	184.3	6.84	100	10	22	11	-
91	PC 32:0	[M+H]+	734.6	184.3	7	100	10	22	11	-
92	PC 33:0	[M+H]+	748.6	184.3	7.08	100	10	22	11	-
93	PC 33:1	[M+H]+	746.6	184.3	6.94	100	10	22	11	-
94	PC 33:2	[M+H]+	744.6	184.3	6.76	100	10	22	11	-
95	PC 34:0	[M+H]+	762.6	184.3	7.07	100	10	22	11	-
96	PC 34:1	[M+1+H]+	761.6	185.3	7.07	100	10	35	11	-
97	PC 34:2	[M+2+H]+	760.6	186.3	6.88	100	10	35	11	-
98	PC 34:3	[M+H]+	756.6	184.3	6.71	100	10	22	11	-
99	PC 34:4	[M+H]+	754.5	184.3	6.62	100	10	22	11	-
100	PC 35:0	[M+H]+	776.6	184.3	7.19	100	10	22	11	-
101	PC 35:2	[M+H]+	772.6	184.3	7	100	10	22	11	-
102	PC 35:3	[M+H]+	770.6	184.3	6.83	100	10	22	11	-
103	PC 35:4	[M+H]+	768.6	184.3	6.7	100	10	22	11	-
104	PC 36:2	[M+2+H]+	788.6	186.3	7.16	100	10	35	11	-
105	PC 36:3	[M+1+H]+	785.6	185.3	6.95	100	10	35	11	-
106	PC 36:4	[M+2+H]+	784.6	186.3	6.88	100	10	35	11	-
107	PC 36:5	[M+H]+	780.6	184.3	6.74	100	10	22	11	-
108	PC 36:6	[M+H]+	778.5	184.3	6.58	100	10	22	11	-
109	PC 37:4	[M+H]+	796.6	184.3	7.03	100	10	22	11	-
110	PC 37:5	[M+H]+	794.6	184.3	7.05	100	10	22	11	-
111	PC 37:6	[M+H]+	792.6	184.3	7.01	100	10	22	11	-
112	PC 38:2	[M+H]+	814.6	184.3	7.33	100	10	22	11	-
113	PC 38:3	[M+H]+	812.6	184.3	7.14	100	10	22	11	-
114	PC 38:4	[M+H]+	810.6	184.3	7.13	100	10	22	11	-
115	PC 38:5	[M+H]+	808.6	184.3	6.96	100	10	22	11	-
116	PC 38:6	[M+H]+	806.6	184.3	6.84	100	10	22	11	-
117	PC 40:5	[M+H]+	836.6	184.3	7.19	100	10	22	11	-
118	PC 40:6	[M+H]+	834.6	184.3	7.13	100	10	22	11	-
119	PC 40:7	[M+H]+	832.6	184.3	6.93	100	10	22	11	-
120	PC(O-30:0)	[M+H]+	692.5	184.3	6.7	100	10	53	11	-
121	PC(O-32:0)	[M+H]+	720.6	184.3	7.06	100	10	53	11	-
122	PC(O-32:1)	[M+H]+	718.5	184.3	6.6	100	10	53	11	-

123	PC(O-32:2)	[M+H]+	716.6	184.3	6.41	100	10	53	11	-
124	PC(O-34:0)	[M+H]+	748.6	184.3	7.32	100	10	53	11	-
125	PC(O-34:1)	[M+H]+	746.6	184.3	7.1	100	10	53	11	-
126	PC(O-34:2)	[M+H]+	744.6	184.3	6.99	100	10	53	11	-
127	PC(O-36:1)	[M+H]+	774.6	184.3	7.18	100	10	53	11	-
128	PC(O-36:3)	[M+H]+	770.6	184.3	7.03	100	10	53	11	-
129	PC(O-36:4)	[M+H]+	768.6	184.3	6.9	100	10	53	11	-
130	PC(O-36:5)	[M+H]+	766.5	184.3	6.98	100	10	53	11	-
131	PC(O-38:4)	[M+H]+	796.6	184.3	7.23	100	10	53	11	-
132	PC(O-38:5)	[M+H]+	794.6	184.3	7.2	100	10	53	11	-
133	PC(O-40:7)	[M+H]+	818.6	184.3	7.5	100	10	53	11	-
134	PC(P-32:0)	[M+H]+	718.5	184.3	7.05	100	10	53	11	-
135	PC(P-32:1)	[M+H]+	716.6	184.3	6.87	100	10	53	11	-
136	PC(P-34:1)	[M+H]+	744.6	184.3	7.13	100	10	53	11	-
137	PC(P-34:2)	[M+H]+	742.5	184.3	6.93	100	10	53	11	-
138	PC(P-36:2)	[M+H]+	770.6	184.3	7.22	100	10	53	11	-
139	PC(P-40:5)	[M+H]+	820.6	184.3	7.2	100	10	53	11	-
140	LPC 14:0	[M+H]+	468.3	184.3	4.3	100	10	53	11	-
141	LPC 15:0	[M+H]+	482.3	184.3	4.5	100	10	53	11	-
142	LPC 16:0	[M+1+H]+	497.3	185.3	4.7	100	10	35	11	-
143	LPC 16:1	[M+H]+	494.3	184.3	4.4	100	10	53	11	-
144	LPC 17:0	[M+H]+	510.4	184.3	5	100	10	53	11	-
145	LPC 17:1	[M+H]+	508.3	184.3	4.7	100	10	53	11	-
146	LPC 18:0	[M+H]+	524.4	184.3	5.2	100	10	53	11	-
147	LPC 18:1	[M+H]+	522.4	184.3	4.9	100	10	53	11	-
148	LPC 18:2	[M+H]+	520.3	184.3	4.6	100	10	53	11	-
149	LPC 18:3	[M+H]+	518.3	184.3	4.4	100	10	53	11	-
150	LPC 20:0	[M+H]+	552.4	184.3	5.6	100	10	53	11	-
151	LPC 20:1	[M+H]+	550.4	184.3	5.3	100	10	53	11	-
152	LPC 20:2	[M+H]+	548.4	184.3	5	100	10	53	11	-
153	LPC 20:3	[M+H]+	546.4	184.3	4.8	100	10	53	11	-
154	LPC 20:4	[M+H]+	544.3	184.3	4.7	100	10	53	11	-
155	LPC 20:5	[M+H]+	542.3	184.3	4.4	100	10	53	11	-
156	LPC 22:4	[M+H]+	572.4	184.3	4.82	100	10	53	11	-
157	LPC 22:6	[M+H]+	568.3	184.3	4.7	100	10	53	11	-
158	LPC 24:0	[M+H]+	608.5	184.3	6.3	100	10	53	11	-
159	LPC(O-20:0)	[M+H]+	538.4	104.3	5.3	100	10	53	11	-
160	LPC(O-22:0)	[M+H]+	566.5	104.3	6	100	10	53	11	-
161	LPC(O-22:1)	[M+H]+	564.4	104.3	5.7	100	10	53	11	-
162	LPC(O-24:0)	[M+H]+	594.5	104.3	6.4	100	10	53	11	-
163	LPC(O-24:1)	[M+H]+	592.5	104.3	6	100	10	53	11	-
164	LPC(O-24:2)	[M+H]+	590.5	104.3	5.8	100	10	53	11	-
165	PE 32:1	[M+H]+	690.5	549.5	6.93	100	10	30	11	-

166	PE 34:1	[M+H]+	718.5	577.5	7.19	100	10	30	11	-
167	PE 34:2	[M+H]+	716.5	575.5	7.02	100	10	30	11	-
168	PE 34:3	[M+H]+	714.5	573.5	6.86	100	10	30	11	-
169	PE 35:1	[M+H]+	732.6	591.5	7.3	100	10	30	11	-
170	PE 35:2	[M+H]+	730.5	589.5	7.14	100	10	30	11	-
171	PE 36:1	[M+H]+	746.6	605.6	7.44	100	10	30	11	-
172	PE 36:2	[M+H]+	744.6	603.5	7.27	100	10	30	11	-
173	PE 36:3	[M+H]+	742.5	601.5	7.09	100	10	30	11	-
174	PE 36:4	[M+H]+	740.5	599.5	7.03	100	10	30	11	-
175	PE 36:5	[M+H]+	738.5	597.5	6.88	100	10	30	11	-
176	PE 38:3	[M+H]+	770.6	629.6	7.37	100	10	30	11	-
177	PE 38:4	[M+H]+	768.6	627.5	7.29	100	10	30	11	-
178	PE 38:5	[M+H]+	766.5	625.5	7.09	100	10	30	11	-
179	PE 38:6	[M+H]+	764.5	623.5	7.01	100	10	30	11	-
180	PE 40:5	[M+H]+	794.6	653.6	7.31	100	10	30	11	-
181	PE 40:6	[M+H]+	792.6	651.5	7.27	100	10	30	11	-
182	PE 40:7	[M+H]+	790.5	649.5	7.08	100	10	30	11	-
183	PE(O-34:1)	[M+H]+	704.6	563.5	7.27	100	10	30	11	-
184	PE(O-34:2)	[M+H]+	702.5	561.5	7.12	100	10	30	11	-
185	PE(O-36:2)	[M+H]+	730.5	589.5	7.37	100	10	30	11	-
186	PE(O-36:3)	[M+H]+	728.6	587.5	7.19	100	10	30	11	-
187	PE(O-36:4)	[M+H]+	726.5	585.5	7.12	100	10	30	11	-
188	PE(O-36:5)	[M+H]+	724.5	583.5	7.1	100	10	30	11	-
189	PE(O-38:4)	[M+H]+	754.6	613.6	7.38	100	10	30	11	-
190	PE(O-38:5)	[M+H]+	752.6	611.5	7.16	100	10	30	11	-
191	PE(O-38:6)	[M+H]+	750.5	609.5	7.13	100	10	30	11	-
192	PE(O-40:5)	[M+H]+	780.6	639.6	7.41	100	10	30	11	-
193	PE(O-40:6)	[M+H]+	778.5	637.5	7.22	100	10	30	11	-
194	PE(O-40:7)	[M+H]+	776.6	635.5	7.19	100	10	30	11	-
195	PE(P-34:1)	[M+H]+	702.5	561.5	7.11	100	10	30	11	-
196	PE(P-34:2)	[M+H]+	700.5	559.5	7.08	100	10	30	11	-
197	PE(P-36:2)	[M+H]+	728.6	587.5	7.34	100	10	30	11	-
198	PE(P-38:4)	[M+H]+	752.6	611.5	7.34	100	10	30	11	-
199	PE(P-38:6)	[M+H]+	748.5	607.5	7.06	100	10	30	11	-
200	PE(P-40:5)	[M+H]+	778.5	637.5	7.31	100	10	30	11	-
201	PE(P-40:6)	[M+H]+	776.6	635.5	7.36	100	10	30	11	-
202	LPE 16:0	[M+H]+	454.3	313.3	4.6	100	10	22	11	-
203	LPE 18:0	[M+H]+	482.3	341.3	5.1	100	10	22	11	-
204	LPE 18:1	[M+H]+	480.3	339.3	4.7	100	10	22	11	-
205	LPE 18:2	[M+H]+	478.3	337.3	4.4	100	10	22	11	-
206	LPE 18:3	[M+H]+	476.3	335.3	4.4	100	10	22	11	-
207	LPE 20:4	[M+H]+	502.3	361.3	4.5	100	10	22	11	-
208	LPE 22:6	[M+H]+	526.3	385.3	4.5	100	10	22	11	-

209	PI 32:0	[M+NH4]+	828.6	551.6	6.3	100	10	30	11	-
210	PI 32:1	[M+NH4]+	826.5	549.5	6.1	100	10	30	11	-
211	PI 34:0	[M+NH4]+	856.6	579.6	6.4	100	10	30	11	-
212	PI 34:1	[M+NH4]+	854.6	577.6	6.39	100	10	30	11	-
213	PI 36:0	[M+NH4]+	884.6	607.6	6.64	100	10	30	11	-
214	PI 36:1	[M+NH4]+	882.6	605.6	6.64	100	10	30	11	-
215	PI 36:2	[M+NH4]+	880.6	603.6	6.49	100	10	30	11	-
216	PI 36:3	[M+NH4]+	878.6	601.6	6.32	100	10	30	11	-
217	PI 36:4	[M+NH4]+	876.6	599.6	6.24	100	10	30	11	-
218	PI 38:2	[M+NH4]+	908.6	631.6	6.58	100	10	30	11	-
219	PI 38:3	[M+NH4]+	906.6	629.6	6.58	100	10	30	11	-
220	PI 38:4	[M+NH4]+	904.6	627.6	6.51	100	10	30	11	-
221	PI 38:5	[M+NH4]+	902.6	625.6	6.34	100	10	30	11	-
222	PI 38:6	[M+NH4]+	900.6	623.6	6.22	100	10	30	11	-
223	PI 40:4	[M+NH4]+	932.6	655.6	6.69	100	10	30	11	-
224	PI 40:5	[M+NH4]+	930.6	653.6	6.54	100	10	30	11	-
225	PI 40:6	[M+NH4]+	928.6	651.6	6.49	100	10	30	11	-
226	PS 36:1	[M+H]+	790.6	605.6	6.72	105	10	28	11	-
227	PS 36:2	[M+H]+	788.5	603.5	6.54	105	10	28	11	-
228	PS 38:3	[M+H]+	814.6	629.6	6.65	105	10	28	11	-
229	PS 38:4	[M+H]+	812.5	627.5	6.57	105	10	28	11	-
230	PS 38:5	[M+H]+	810.5	625.5	6.4	105	10	28	11	-
231	PS 40:5	[M+H]+	838.6	653.6	6.6	105	10	28	11	-
232	PS 40:6	[M+H]+	836.5	651.5	6.57	105	10	28	11	-
233	PG 34:1	[M+NH4]+	766.6	577.5	6.53	80	10	30	11	-
234	PG 34:2	[M+NH4]+	764.5	575.5	6.37	80	10	30	11	-
235	PG 36:1	[M+NH4]+	794.6	605.6	6.81	80	10	30	11	-
236	PG 36:2	[M+NH4]+	792.6	603.5	6.65	80	10	30	11	-
237	CE 14:0	[M+NH4]+	614.6	369.5	9.27	52	10	22	11	1.15
238	CE 16:0	[M+NH4]+	642.6	369.5	9.38	52	10	22	11	1.4
239	CE 16:1	[M+NH4]+	640.6	369.5	9.25	52	10	22	11	0.6
240	CE 16:2	[M+NH4]+	638.6	369.5	9.14	52	10	22	11	0.34
241	CE 17:0	[M+NH4]+	656.6	369.5	9.4	52	10	22	11	1.55
242	CE 17:1	[M+NH4]+	654.6	369.5	9.32	52	10	22	11	0.52
243	CE 18:0	[M+NH4]+	670.7	369.5	9.36	52	10	22	11	1.65
244	CE 18:1	[M+NH4]+	668.6	369.5	9.36	52	10	22	11	0.44
245	CE 18:2	[M+2+NH4]+	668.6	371.5	9.25	52	10	22	11	0.18
246	CE 18:3	[M+NH4]+	664.6	369.5	9.17	52	10	22	11	0.18
247	CE 20:0	[M+NH4]+	698.7	369.3	9.46	52	10	22	11	1.95
248	CE 20:2	[M+NH4]+	694.7	369.5	9.3	52	10	22	11	0.02
249	CE 20:3	[M+NH4]+	692.6	369.5	9.21	52	10	22	11	0.02
250	CE 20:4	[M+1+NH4]+	691.6	370.5	9.17	52	10	22	11	0.02
251	CE 20:5	[M+NH4]+	688.6	369.5	9.1	52	10	22	11	0.02

252	CE 22:0	[M+NH4]+	726.7	369.3	9.52	52	10	22	11	2.2
253	CE 22:1	[M+NH4]+	724.7	369.5	9.35	52	10	22	11	0.14
254	CE 22:4	[M+NH4]+	718.7	369.5	9.26	52	10	22	11	0.02
255	CE 22:5	[M+NH4]+	716.6	369.5	9.2	52	10	22	11	0.02
256	CE 22:6	[M+NH4]+	714.6	369.5	9.12	52	10	22	11	0.02
257	Carnitine	[M+H]+	162.2	85	0.39	130	10	55	11	-
258	Acylcarnitine 2:0	[M+H]+	204.2	85	0.39	130	10	55	11	-
259	Acylcarnitine 3:0	[M+H]+	218.2	85	0.39	130	10	55	11	-
260	Acylcarnitine 4:0	[M+H]+	232.3	85	0.39	130	10	55	11	-
261	Acylcarnitine 5:0	[M+H]+	247.3	85	0.38	130	10	55	11	-
262	Acylcarnitine (C4-Methyl)	[M+H]+	246.3	85	0.38	130	10	55	11	-
263	Acylcarnitine (C4-Methyl-OH)	[M+H]+	262.3	85	0.38	130	10	55	11	-
264	Acylcarnitine 6:0	[M+H]+	260.3	85	0.38	130	10	55	11	-
265	Acylcarnitine 8:0	[M+H]+	288.4	85	0.36	130	10	55	11	-
266	Acylcarnitine 10:0	[M+H]+	316.5	85	0.36	130	10	55	11	-
267	Acylcarnitine (C10-OH)	[M+H]+	318.3	85	0.36	130	10	55	11	-
268	Acylcarnitine 14:0	[M+H]+	372.6	85	3.84	130	10	55	11	-
269	Acylcarnitine 16:0	[M+H]+	400.6	85	4.42	130	10	55	11	-
270	Acylcarnitine 18:0	[M+H]+	428.7	85	4.96	130	10	55	11	-
271	Acylcarnitine 18:2	[M+H]+	424.4	85	4.28	130	10	55	11	-
272	Acylcarnitine 20:0	[M+H]+	456.4	85	5.48	130	10	55	11	-
273	POVPC	[M+H]+	594.6	184.3	4.83	125	10	53	11	-
274	PGPC	[M+H]+	610.6	184.3	4.49	125	10	53	11	-
275	PONPC	[M+H]+	650.6	184.3	5.16	125	10	53	11	-
276	PAzPC	[M+H]+	666.6	184.3	4.92	125	10	53	11	-
277	KOdiA-PC	[M+H]+	664.6	184.3	5.52	125	10	53	11	-
278	KDdiA-PC	[M+H]+	720.6	184.3	4.1	125	10	53	11	-
279	DG 14:0_16:0	[M+NH4]+	558.5	313.3	2.28	50	10	22	11	0.5
280	DG 14:0_18:1	[M+NH4]+	584.5	285.2	2.25	50	10	22	11	0.5
281	DG 14:0_18:2	[M+NH4]+	582.5	285.2	2.11	50	10	22	11	0.5
282	DG 16:0_16:0	[M+NH4]+	586.5	313.3	2.38	50	10	22	11	1
283	DG 16:0_18:1	[M+NH4]+	612.6	339.3	2.4	50	10	22	11	0.5
284	DG 16:0_18:2	[M+NH4]+	610.5	313.3	2.26	50	10	22	11	0.5
285	DG 16:0_20:3	[M+NH4]+	636.6	313.3	2.34	50	10	22	11	0.5
286	DG 16:0_20:4	[M+NH4]+	634.5	313.3	2.26	50	10	22	11	0.5

287	DG 16:0_22:5	[M+NH4]+	660.6	313.3	2.18	50	10	22	11	0.5
288	DG 16:0_22:6	[M+NH4]+	658.5	313.3	2.21	50	10	22	11	0.5
289	DG 16:1_18:1	[M+NH4]+	610.5	339.3	2.26	50	10	22	11	0.5
290	DG 18:0_18:1	[M+NH4]+	640.6	339.3	2.57	50	10	22	11	0.5
291	DG 18:0_18:2	[M+NH4]+	638.6	341.3	2.41	50	10	22	11	0.5
292	DG 18:0_20:4	[M+NH4]+	662.6	341.3	1.53	50	10	22	11	0.5
293	DG 18:1_18:1	[M+NH4]+	638.6	339.3	2.42	50	10	22	11	1
294	DG 18:1_18:2	[M+NH4]+	636.6	339.3	2.29	50	10	22	11	0.5
295	DG 18:1_18:3	[M+NH4]+	634.5	339.3	2.14	50	10	22	11	0.5
296	DG 18:1_20:3	[M+NH4]+	662.6	339.3	2.33	50	10	22	11	0.5
297	DG 18:1_20:4	[M+NH4]+	660.6	339.3	2.26	50	10	22	11	0.5
298	DG 18:2_18:2	[M+NH4]+	634.5	337.3	2.17	50	10	22	11	1
299	TG 48:1	[M+NH4]+	822.8	523.5	5.03	100	10	55	11	0.33
300	TG 48:2	[M+NH4]+	820.8	547.5	4.58	100	10	55	11	0.33
301	TG 48:2	[M+NH4]+	820.8	521.5	4.55	100	10	55	11	0.33
302	TG 48:3	[M+NH4]+	818.8	521.5	4.09	100	10	55	11	0.33
303	TG 49:1	[M+NH4]+	836.8	537.5	5.23	100	10	55	11	0.33
304	TG 50:1	[M+NH4]+	850.8	605.6	5.01	100	10	55	11	0.33
305	TG 50:4	[M+NH4]+	844.8	599.5	4.14	100	10	55	11	0.67
306	TG 48:2	[M+NH4]+	820.8	577.6	4.56	100	10	55	11	0.33
307	TG 48:2	[M+NH4]+	820.8	549.5	4.54	100	10	55	11	0.33
308	TG 50:3	[M+NH4]+	846.8	603.6	4.59	100	10	55	11	0.33
309	TG 50:3	[M+NH4]+	846.8	547.5	4.56	100	10	55	11	0.67
310	TG 49:1	[M+NH4]+	836.8	577.5	5.23	100	10	55	11	0.33
311	TG 51:2	[M+NH4]+	862.8	603.6	5.23	100	10	55	11	0.33
312	TG 48:0	[M+NH4]+	824.8	551.5	5.56	100	10	55	11	1
313	TG 50:0	[M+NH4]+	852.8	551.5	6.19	100	10	55	11	0.67
314	TG 50:1	[M+1+NH4]+	851.8	552.5	5.56	100	10	55	11	0.67
315	TG 50:2	[M+NH4]+	848.8	551.5	5.03	100	10	55	11	0.67
316	TG 49:1	[M+NH4]+	836.8	563.5	5.22	100	10	55	11	0.33
317	TG 50:2	[M+1+NH4]+	849.8	550.5	4.99	100	10	55	11	0.33
318	TG 51:0	[M+NH4]+	866.8	593.6	5.86	100	10	55	11	0.33
319	TG 51:1	[M+NH4]+	864.8	565.5	5.78	100	10	55	11	0.33
320	TG 51:2	[M+NH4]+	862.8	589.6	5.23	100	10	55	11	0.33
321	TG 52:1	[M+NH4]+	878.8	577.5	6.19	100	10	55	11	0.33
322	TG 52:2	[M+1+NH4]+	877.8	604.6	5.54	100	10	55	11	0.67
323	TG 52:3	[M+1+NH4]+	875.8	578.6	5.03	100	10	55	11	0.33
324	TG 52:4	[M+NH4]+	872.8	599.6	4.58	100	10	55	11	0.67
325	TG 48:3	[M+NH4]+	818.8	547.5	4.07	100	10	55	11	1
326	TG 50:2	[M+NH4]+	848.8	547.5	5.01	100	10	55	11	0.33
327	TG 50:3	[M+NH4]+	846.8	575.6	4.55	100	10	55	11	0.67
328	TG 51:2	[M+NH4]+	862.8	563.5	5.22	100	10	55	11	0.33
329	TG 52:3	[M+NH4]+	874.8	603.6	4.99	100	10	55	11	0.67

330	TG 52:4	[M+NH4]+	872.8	573.6	4.57	100	10	55	11	0.33
331	TG 53:2	[M+NH4]+	890.8	603.6	5.83	100	10	55	11	0.67
332	TG 54:1	[M+NH4]+	906.9	607.6	6.19	100	10	55	11	0.67
333	TG 54:2	[M+NH4]+	904.9	603.6	6.19	100	10	55	11	0.67
334	TG 54:4	[M+NH4]+	900.8	599.5	5.06	100	10	55	11	0.67
335	TG 54:3	[M+1+NH4]+	903.9	604.6	5.52	100	10	55	11	1
336	TG 54:4	[M+NH4]+	900.9	603.9	5	100	10	55	11	0.67
337	TG 56:6	[M+NH4]+	924.9	603.6	4.87	100	10	55	11	0.67
338	TG 58:8	[M+NH4]+	948.9	603.7	4.58	100	10	55	11	0.67
339	TG 54:5	[M+NH4]+	898.9	599.6	4.58	100	10	55	11	0.67
340	TG 54:6	[M+NH4]+	896.9	599.6	4.15	100	10	55	11	1
341	TG 56:8	[M+NH4]+	920.9	599.6	4.03	100	10	55	11	0.67
342	FA 15:0	[M-H]-	241	241.2	5.78	-75	-10	-20	-7	-
343	FA 15:0*	[M-H]-	241	241.1	5.78	-75	-10	-25	-7	-
344	FA 16:0	[M-H]-	255	255	6.13	-80	-10	-35	-7	-
345	FA 16:0*	[M-H]-	255	255.1	6.13	-80	-10	-37	-7	-
346	FA 16:1	[M-H]-	253	253	5.74	-78	-10	-30	-7	-
347	FA 16:1*	[M-H]-	253	253.1	5.74	-78	-10	-34	-7	-
348	FA 17:0	[M-H]-	269	269.1	6.36	-85	-10	-20	-7	-
349	FA 17:0*	[M-H]-	269	269	6.36	-85	-10	-25	-7	-
350	FA 18:0	[M-H]-	283.1	283.1	6.59	-87	-10	-35	-7	-
351	FA 18:0*	[M-H]-	283.1	283.2	6.59	-87	-10	-37	-7	-
352	FA 18:1	[M-H]-	281.1	281.1	6.35	-80	-10	-37	-7	-
353	FA 18:1*	[M-H]-	281.1	281	6.35	-80	-10	-39	-7	-
354	FA 18:2	[M-H]-	279	279.1	5.89	-80	-10	-32	-7	-
355	FA 18:2*	[M-H]-	279	279	5.89	-80	-10	-34	-7	-
356	FA 18:3	[M-H]-	277.1	277.1	5.67	-75	-10	-20	-7	-
357	FA 18:3*	[M-H]-	277.1	277	5.67	-75	-10	-25	-7	-
358	FA 20:3	[M-H]-	305.1	305.1	6.15	-80	-10	-8	-7	-
359	FA 20:3*	[M-H]-	305.1	305	6.15	-80	-10	-26	-7	-
360	FA 20:4	[M-H]-	303.1	303.1	5.94	-70	-10	-10	-7	-
361	FA 20:4*	[M-H]-	303.1	303	5.94	-70	-10	-21	-7	-
362	FA 20:5	[M-H]-	301.1	301.1	5.64	-70	-10	-10	-7	-
363	FA 20:5*	[M-H]-	301.1	301.2	5.64	-70	-10	-21	-7	-
364	FA 22:5	[M-H]-	329.1	329	6.03	-40	-10	-6	-7	-
365	FA 22:5*	[M-H]-	329.1	329.1	6.03	-40	-10	-15	-7	-
366	FA 22:6	[M-H]-	327.1	327	5.89	-40	-10	-6	-7	-
367	FA 22:6*	[M-H]-	327.1	327.1	5.89	-40	-10	-15	-7	-

Abbreviations: IS, internal standard; Q1, precursor ion; Q3, product ion; RT, retention time; DP, declustering potential; EP, entrance potential; CE, collision energy; CXP, exit potential; CF, correction factor; [M+1+H]+, isotope with one mass unit increase; [M+2+H]+, isotope with two mass unit increase; * denotes the MRM transition with higher collision energy in negative mode.

Supplementary Table S4: Sample run order

Injection No	Sample type	
1	Extracted blank-1	Six blank injections in the beginning of each batch.

5	Extracted blank-6	
6	System conditioning QC-1	Ten PQC in the beginning of each batch for system equilibration.

15	System conditioning QC-10	
16	PQC-1	Injecting various QC samples (PQC, TQC and SRM) to monitor system stability and technical variation.
17	PQC-2	
18	TQC-1	
19	TQC-2	
20	SRM-1	
21	SRM-2	
22	PQC-3	
23	Study sample-1	Study sample injection starts
24	Study sample-2	

32	Study sample-10	
33	Extracted blank-6	Blank injection after 10 consecutive study samples injection.
34	PQC-4	
35	Study sample-11	

44	Study sample-20	
45	Extracted blank-7	
46	PQC-5	PQC injection after 20 study samples injection.
47	TQC-3	TQC injection after 20 study samples injection.

Abbreviations: PQC, plasma quality control; TQC, technical quality control; SRM, NIST SRM 1950 plasma

Supplementary Table S5: Lipids shared or unique between different time points.
(Related to Figure-3.1C**)**
A:92 common lipids in "*t1 vs. t0*", "*t2 vs. t1*" and "*t2 vs. t0*"
B:15 lipids exclusive to "*t1 vs. t0*"
C:20 lipids exclusive to "*t2 vs. t1*"
D:6 lipids exclusive to "*t2 vs. t0*"

No	A	B	C	D
1	Acylcarnitine 2:0	DG 18:0_20:4	CE 18:2	Acylcarnitine 16:0
2	CE 22:6	DG 18:1_20:3	CE 22:4	Acylcarnitine 20:0
3	Cer 18:0	DG 18:1_20:4	Cer 24:0	CE 22:5
4	Cer 22:0	LPC(O-24:1)	GM3 16:0	PC(O-36:3)
5	DG 16:0_18:1	LPE 16:0	LPC (O-24:0)	PGPC
6	DG 16:0_18:2	LPE 18:0	PC 29:0	PONPC
7	DG 16:0_22:5	PC 34:3	PC 33:1	
8	DG 16:1_18:1	PC 35:4	PC 36:4	
9	DG 18:0_18:1	PC 36:3	PC 36:6	
10	DG 18:0_18:2	PC(O-36:4)	PC 37:5	
11	DG 18:1_18:1	PE 35:2	PC 37:6	
12	DG 18:1_18:2	PE(O-36:2)	PC 38:3	
13	DG 18:1_18:3	PE(O-40:6)	PC(O-34:1)	
14	DG 18:2_18:2	PE(P-40:5)	PC(O-36:1)	
15	LPC 14:0	SM 39:1	PC(O-38:5)	
16	LPC 16:1		PC(O-40:7)	
17	LPC 18:1		PE 36:3	
18	LPC 20:0		SM 38:1	
19	LPC 20:1		SM 41:2	
20	PC 34:1		THC 16:0	
21	PC 38:4			
22	PC 38:5			
23	PC(O-32:2)			
24	PE 34:1			
25	PE 34:2			
26	PE 36:1			
27	PE 36:2			
28	PE(O-34:2)			
29	PE(O-36:3)			
30	PE(O-36:4)			
31	PE(O-36:5)			
32	PE(O-38:5)			
33	PE(O-38:6)			
34	PE(P-34:2)			
35	PE(P-38:4)			
36	PG 34:1			
37	PG 36:1			

38	PG 36:2
39	PI 32:0
40	PI 32:1
41	PI 34:0
42	PI 34:1
43	PI 36:0
44	PI 36:1
45	PI 36:2
46	PI 36:3
47	PI 36:4
48	PI 38:2
49	PI 38:5
50	PI 38:6
51	PI 40:4
52	PI 40:6
53	SM 36:1
54	SM 36:2
55	SM 36:3
56	TG 48:2
57	TG 48:2
58	TG 48:2
59	TG 48:2
60	TG 48:3
61	TG 48:3
62	TG 49:1
63	TG 49:1
64	TG 49:1
65	TG 50:1
66	TG 50:1
67	TG 50:2
68	TG 50:2
69	TG 50:3
70	TG 50:3
71	TG 50:3
72	TG 50:4
73	TG 51:0
74	TG 51:1
75	TG 51:2
76	TG 51:2
77	TG 51:2
78	TG 52:1
79	TG 52:2
80	TG 52:3
81	TG 52:3

82	TG 52:4
83	TG 52:4
84	TG 53:2
85	TG 54:2
86	TG 54:3
87	TG 54:4
88	TG 54:4
89	TG 54:5
90	TG 54:6
91	TG 56:6
92	TG 58:8

Supplementary Table S6. Plasma lipid classes differentially regulated in 2 h post-PCI (*t1*) vs. pre-PCI (*t0*) (Related to Figure-3.1D).

No	Lipid Class	Percentage difference, *t1 vs. t0* (%)	SEM	p-value	p-value (Bonferroni)*
1	Cer	-15.2324	2.310853	1.64E-08	1.95E-08
2	dhCer	-4.43055	4.005675	0.456165	0.788089
3	HexCer	-7.98452	2.738544	0.001249	0.014076
4	Hex2Cer	1.068409	3.74162	0.226997	1
5	Hex3Cer	-6.62879	3.257072	0.028895	0.162756
6	GM3	-8.99302	3.355359	0.019449	0.028177
7	SM	-8.13677	1.602941	1.51E-08	7.79E-06
8	PC	-2.6724	1.950236	0.003502	0.537792
9	PC(O)	-4.16148	2.050878	0.021878	0.149576
10	PC(P)	-1.55904	2.690074	0.02455	1
11	LPC	-12.9599	2.777559	1.14E-12	6.61E-05
12	LPC(O)	-8.2038	2.556478	0.001856	0.007021
13	PE	-3.9156	2.05952	3.05E-12	1.81E-01
14	PE(O)	-10.895	1.889008	4.11E-09	4.67E-07
15	PE(P)	-8.86941	1.827694	8.52E-11	1.96E-05
16	LPE	-4.50767	3.689748	5.53E-20	6.62E-01
17	PI	-15.7131	2.402064	1.89E-13	2.30E-08
18	PS	8.600936	7.631153	0.573445	1
19	PG	-17.0643	4.698144	1.44E-12	1.89E-03
20	CE	-11.4486	3.850719	0.000361	0.011194
21	Acylcarnitine	-15.0511	5.075217	1.58E-08	0.013253
22	**OxPL**	**29.87915**	10.40869	0.001854	0.026933
23	**DG**	**-29.9244**	4.591791	4.35E-20	5.21E-08
24	**TG**	**-24.2858**	4.048233	1.74E-18	2.91E-07
25	FA	-12.6519	5.572163	6.35E-25	1.11E-01

p-value: Repeated measures ANOVA with a Greenhouse-Geisser correction.
*: Corrected p-value after adjustment for multiple comparisons using Bonferroni. Corrected $p<0.05$ are highlighted in light red.
Abbreviation: SEM, Standard Error Mean

Supplementary Table S7. Plasma lipid classes differentially regulated in 24 h post-PCI (*t2*) vs. 2 h post-PCI (*t1*) (Related to Figure-3.1E**).**

No	Lipid Class	Percentage difference, *t2 vs. t1* (%)	SEM	*p*-value	*p*-value (Bonferroni)*
1	Cer	10.74667427	2.553694	1.64E-08	2.12E-04
2	dhCer	4.220715251	4.020922	0.456165	0.869953095
3	HexCer	9.862223428	2.868704	0.001249	0.002968361
4	Hex2Cer	4.803903456	3.390393	0.226997	0.494423818
5	Hex3Cer	7.358663075	2.741552	0.028895	0.027425159
6	GM3	7.406122737	3.380285	0.019449	0.09786463
7	SM	9.409117388	1.522558	1.51E-08	8.17E-08
8	PC	6.676782089	1.817695	0.003502	0.001288246
9	PC(O)	5.195524759	1.470115	0.021878	0.002083447
10	PC(P)	-5.412763068	1.715756	0.02455	0.006849897
11	LPC	-16.50162822	3.909369	1.14E-12	2.50E-04
12	LPC(O)	8.206641183	2.453838	0.001856	0.003996552
13	PE	26.24691618	3.013101	3.05E-12	1.81E-12
14	PE(O)	-8.808699977	2.901976	4.11E-09	1.50E-02
15	PE(P)	-11.56217023	2.596377	8.52E-11	1.18E-04
16	LPE	-37.71380088	4.330246	5.53E-20	2.85E-12
17	PI	-10.86240355	3.105658	1.89E-13	2.33E-03
18	PS	-7.454027394	7.782289	0.573445	0.924246429
19	PG	46.3960175	5.62962	1.44E-12	1.10E-10
20	CE	18.22884219	4.286609	0.000361	0.000224955
21	Acylcarnitine	-17.70756971	5.250324	1.58E-08	0.00340701
22	OxPL	6.568571315	9.565957	0.001854	1
23	**DG**	**64.06186107**	4.376867	4.35E-20	1.38E-21
24	**TG**	**58.62646089**	4.712544	1.74E-18	3.96E-18
25	FA	-67.16443932	5.154134	6.35E-25	1.45E-19

p-value: A repeated measures ANOVA with a Greenhouse-Geisser correction.
*: Corrected p-value after adjustment for multiple comparisons using Bonferroni. Corrected $p<0.05$ are highlighted in light red.
Abbreviation: SEM, Standard Error Mean

Supplementary Table S8. Plasma lipid classes differentially regulated in 24 h post-PCI (*t2*) vs. pre-PCI (*t0*) (Related to Figure-3.1F)**.**

No.	Lipid Class	Percentage difference, *t2 vs. t0* (%)	SEM	*p*-value	*p*-value (Bonferroni)*
1	Cer	-4.526299642	2.478114	1.64E-08	2.12E-01
2	dhCer	-0.34516639	4.135659	0.456165	1
3	HexCer	1.820989799	2.736293	0.001249	1
4	Hex2Cer	5.756988877	3.691018	0.226997	0.348735355
5	Hex3Cer	0.819684699	2.695072	0.028895	1
6	GM3	-1.632415004	3.339083	0.019449	1
7	SM	1.281943359	1.657817	1.51E-08	1.00E+00
8	PC	4.021011798	2.071708	0.003502	0.166790008
9	PC(O)	1.020522411	2.056684	0.021878	1
10	PC(P)	-6.911862204	2.694342	0.02455	0.048811061
11	LPC	-29.51797428	3.225649	1.14E-12	2.48E-13
12	LPC(O)	-0.081773174	2.665744	0.001856	1
13	PE	22.18783761	3.599431	3.05E-12	1.53E-07
14	PE(O)	-19.44120266	2.888806	4.11E-09	1.28E-08
15	PE(P)	-20.23525445	2.855516	8.52E-11	2.28E-09
16	LPE	-42.03891566	4.123581	5.53E-20	4.75E-15
17	PI	-26.2434024	3.251004	1.89E-13	2.86E-11
18	PS	-1.307566634	8.828938	0.573445	1
19	PG	31.24636087	5.577051	1.44E-12	8.11E-06
20	CE	6.588666817	4.799165	0.000361	0.484606778
21	Acylcarnitine	-32.87063766	5.070422	1.58E-08	2.83639E-08
22	OxPL	34.23184598	10.45401	0.001854	0.004596785
23	DG	36.4753469	5.901769	4.35E-20	1.41E-06
24	TG	35.74365838	5.674479	1.74E-18	3.30E-07
25	**FA**	**-74.55166213**	6.240169	6.35E-25	4.49E-17

p-value: A repeated measures ANOVA with a Greenhouse-Geisser correction.
*: Corrected p-value after adjustment for multiple comparisons using Bonferroni. Corrected $p<0.05$ are highlighted in light red.
Abbreviation: SEM, Standard Error Mean

Supplementary Table S9. Plasma individual lipids differentially regulated in 2 h post-PCI (*t1*) vs. pre-PCI (*t0*) (Related to Figure-3.2A).

No.	Lipid Class	Percentage difference, *t1 vs. t0* (%)	SEM	*p*-value	*p*-value (Bonferroni)*
1	Cer 16:0	-13.36087786	5.677068	0.077681	0.069418473
2	Cer 18:0	-15.45947941	4.309848	1.04E-08	0.001688144
3	Cer 20:0	-7.813614918	3.892171	0.072423	0.144973166
4	Cer 22:0	-15.23882737	2.769255	1.22E-06	2.19127E-06
5	Cer 24:0	-15.26474331	2.837304	1.22E-06	4.21074E-06
6	Cer 24:1	-14.21006595	2.469355	8.82E-07	5.41967E-07
7	dhCer 22:0	-2.740055311	6.093331	0.83629	1
8	dhCer 24:0	-5.042062748	4.970712	0.580476	0.951858547
9	dhCer 24:1	-1.650250979	5.965113	0.062301	1
10	HexCer 16:0	-7.926053214	3.038307	0.012992	0.032153792
11	HexCer 18:0	-8.2897251	5.334673	0.202552	0.386487544
12	HexCer 20:0	-0.75089937	4.933584	0.209607	1
13	HexCer 22:0	-6.468272351	3.502657	0.046545	0.219406394
14	HexCer 24:0	-8.371202007	2.911954	0.008823	0.015818196
15	HexCer 24:1	-9.785458118	3.26196	0.00031	0.012004379
16	Hex2Cer 22:0	-0.704197638	5.032147	0.409507	1
17	Hex2Cer 24:0	2.252846531	5.134634	0.614799	1
18	Hex2Cer 24:1	0.716070434	4.054063	0.203082	1
19	Hex3Cer 16:0	-6.551362751	3.398011	0.022641	0.191294967
20	Hex3Cer 18:0	-16.25508627	6.469913	0.064513	0.069316471
21	Hex3Cer 24:1	3.308642488	6.414145	0.760688	1
22	GM3 16:0	-7.474919845	3.645038	0.023075	0.142456557
23	GM3 18:0	-13.08370803	4.212485	0.012046	0.007663082
24	SM 31:1	-13.5609402	3.351764	0.000288	0.000357793
25	SM 32:1	-14.28726706	2.446343	3.17E-07	4.13497E-07
26	SM 32:2	-11.56868346	2.569968	3.71E-05	7.76491E-05
27	SM 33:1	-12.49402869	2.214345	6.6E-09	7.9062E-07
28	SM 34: 0	-8.612160032	2.351874	0.000429	0.001385325
29	SM 34:1	-9.318590317	2.589943	0.002072	0.001656389
30	SM 34:2	-12.69385795	2.500933	7.21E-09	8.34986E-06
31	SM 34:3	-16.33585497	4.454411	0.000206	0.002209034
32	SM 35:1	-13.94698951	2.369544	2.44E-11	2.91066E-07
33	SM 35:2	-11.11910771	2.831617	1.93E-11	0.000596416
34	SM 36:1	-9.263629513	2.255265	6.97E-15	0.000301438
35	SM 36:2	-11.90936341	2.573755	9.68E-18	4.68974E-05
36	SM 36:3	-8.365970237	2.961575	1.37E-10	0.017146014
37	SM 37:2	-5.939848642	3.478166	9.92E-10	0.319937722
38	SM 38:1	-3.876511021	1.738642	0.008016	0.085285311

39	SM 38:2	-7.63271404	2.063984	0.000832	0.001220659
40	SM 39:1	-6.030913483	1.973551	0.014868	0.009413916
41	SM 41:1	-4.335250964	2.495929	0.029194	0.258706176
42	SM 41:2	-5.143016206	2.189058	0.024385	0.062788188
43	SM 42:1	0.297681416	2.635737	0.151453	1
44	PC 29:0	-14.2601283	6.014448	0.011738	0.056750614
45	PC 31:0	1.997030131	4.169469	0.145688	1
46	PC 32:0	-6.880265655	2.386546	3.08E-06	0.015994455
47	PC 33:0	-3.865797533	4.856895	0.116837	1
48	PC 33:1	-6.778844378	2.830264	0.001594	0.066303907
49	PC 33:2	-4.178176288	2.561069	0.037572	0.341433534
50	PC 34:0	-3.903668376	2.019395	1.61E-05	0.172743062
51	PC 34:1	-6.841457231	2.072778	6.5E-08	0.004494856
52	PC 34:2	1.653079809	2.988474	0.124377	1
53	PC 34:3	-8.088527054	2.324151	0.010214	0.002512421
54	PC 34:4	-16.59266491	4.516628	1.61E-07	0.001743735
55	PC 35:0	-12.87100527	5.502131	0.040745	0.066552645
56	PC 35:2	-6.652784601	2.879553	0.057026	0.071298262
57	PC 35:3	-2.924462566	2.852748	0.062573	0.993495494
58	PC 35:4	-7.007459056	2.495345	0.028825	0.019778044
59	PC 36:2	2.644047358	3.397357	0.68516	1
60	PC 36:3	-8.079429025	2.321103	0.004531	0.002607605
61	PC 36:4	-2.163293235	3.466568	0.004753	1
62	PC 36:5	-11.38132639	3.464167	0.001413	0.004732222
63	PC 36:6	-0.407451266	6.76363	0.024088	1
64	PC 37:4	-3.416826068	2.467048	7.1E-05	0.509426642
65	PC 37:5	-0.550595596	3.071118	0.07761	1
66	PC 37:6	-4.230121535	3.437837	0.041734	0.729293555
67	PC 38:2	-2.210638424	2.603034	0.001212	1
68	PC 38:3	-4.166790754	2.148837	0.00781	0.173346214
69	PC 38:4	-6.927451774	2.190731	6.53E-08	0.006830533
70	PC 38:5	-6.014340417	2.339089	5.07E-06	0.036190826
71	PC 38:6	-3.783910409	2.273637	3.76E-07	0.300705059
72	PC 40:5	-3.736179041	3.134266	0.00052	0.718495647
73	PC 40:6	0.400373372	2.946499	0.000532	1
74	PC 40:7	-1.45026098	3.286348	0.114407	1
75	PC(O-30:0)	1.555479117	4.303124	0.701206	1
76	PC(O-32:0)	3.229157977	3.000665	0.39211	0.763743256
77	PC(O-32:1)	-10.93803476	2.080049	7.33E-09	3.87154E-06
78	PC(O-32:2)	-11.56953138	2.874078	1.51E-12	0.000428374
79	PC(O-34:0)	-1.060349261	2.439136	0.764094	1
80	PC(O-34:1)	-2.026416941	2.372334	0.087056	1
81	PC(O-34:2)	-6.17697534	2.602561	0.067565	0.058477811
82	PC(O-36:1)	-3.112549155	2.267525	0.011747	0.547353184

83	PC(O-36:3)	-3.040861622	2.300893	0.016139	0.62714506
84	PC(O-36:4)	-5.693818176	2.185997	0.03319	0.036659213
85	PC(O-36:5)	-6.316856519	2.298043	0.028041	0.025691502
86	PC(O-38:4)	-6.328059076	1.995771	5.73E-07	0.006666519
87	PC(O-38:5)	-2.508075311	2.495304	0.051926	1
88	PC(O-40:7)	-1.156705733	3.557119	0.101686	1
89	PC(P-32:0)	1.680279977	3.598321	0.628526	1
90	PC(P-32:1)	0.239659908	4.165277	0.683476	1
91	PC(P-34:1)	1.386152137	3.247139	0.000183	1
92	PC(P-34:2)	-4.050798173	3.118611	3.91E-07	0.707027713
93	PC(P-36:2)	-3.501298083	2.243839	0.037497	0.413973102
94	PC(P-40:5)	1.664960313	2.784616	0.001071	1
95	PE 32:1	-3.471519514	3.836333	0.000196	1
96	PE 34:1	-7.958571341	2.459929	1E-13	0.005280435
97	PE 34:2	-6.304643088	2.357938	5.21E-09	0.027009339
98	PE 34:3	4.71195349	3.865	0.000157	0.647898515
99	PE 35:1	-15.17044868	2.906575	1.12E-05	4.34018E-06
100	PE 35:2	-7.685750262	2.348778	0.196603	0.005033532
101	PE 36:1	-8.34275884	2.654869	4.93E-11	0.007061673
102	PE 36:2	-7.705192041	2.276364	5.83E-10	0.003496223
103	PE 36:3	-4.508804798	2.592596	0.001738	0.255003756
104	PE 36:4	-1.720128448	2.468316	2.06E-05	1
105	PE 36:5	-2.77064951	3.437667	0.188135	1
106	PE 38:3	-3.093512665	2.73161	4.32E-13	0.767388821
107	PE 38:4	-2.407022849	2.526574	1.5E-11	1
108	PE 38:5	0.125505963	2.515846	1.7E-08	1
109	PE 38:6	1.943964019	3.070229	1.32E-13	1
110	PE 40:5	-5.418796851	3.040186	3.34E-21	0.23717388
111	PE 40:6	-4.354336685	2.901143	6.76E-21	0.411599926
112	PE 40:7	0.406535003	3.532629	2.48E-07	1
113	PE(O-34:1)	-19.40291661	2.924856	7.58E-08	1.35405E-08
114	PE(O-34:2)	-12.43361452	4.134237	4.43E-07	0.011509191
115	PE(O-36:2)	-9.982769311	2.762845	0.08791	0.001703112
116	PE(O-36:3)	-9.32346919	2.57876	1.17E-06	0.001718002
117	PE(O-36:4)	-12.62580652	2.785747	1.48E-20	7.68175E-05
118	PE(O-36:5)	-8.604088626	2.943263	6.41E-14	0.014491584
119	PE(O-38:4)	-10.09362825	2.560518	4.08E-05	0.000550985
120	PE(O-38:5)	-10.93696276	2.36903	9.25E-14	4.50707E-05
121	PE(O-38:6)	-9.819898852	2.423554	7.2E-08	0.000354104
122	PE(O-40:5)	-11.52619971	2.668878	0.003014	0.000137619
123	PE(O-40:6)	-10.628426	2.277521	0.004924	3.76074E-05
124	PE(O-40:7)	-8.24953465	2.493242	0.000207	0.005084927
125	PE(P-34:1)	-8.677659616	4.364979	8.14E-05	0.241069144
126	PE(P-34:2)	-11.1827187	4.489923	3.77E-10	0.045723424

127	PE(P-36:2)	-6.89829299	2.970822	2.91E-07	0.069700896
128	PE(P-38:4)	-9.11199854	2.29624	8.05E-15	0.000507678
129	PE(P-38:6)	-8.432257603	3.810696	8.43E-06	0.094968561
130	PE(P-40:5)	-10.94576527	2.24842	0.003732	1.80173E-05
131	PE(P-40:6)	-9.764385242	2.679946	2.12E-06	0.00152684
132	PI 32:0	-19.53791812	3.99115	5.41E-12	2.00428E-05
133	PI 32:1	-12.79699521	3.266558	1.08E-07	0.000597362
134	PI 34:0	-15.75596997	3.497887	6.15E-14	0.000109312
135	PI 34:1	-16.61352337	2.879249	2.45E-16	7.35312E-07
136	PI 36:0	-22.03545383	4.182904	5.31E-20	4.82184E-06
137	PI 36:1	-17.6009454	2.825363	5.79E-22	1.14763E-07
138	PI 36:2	-16.67435223	2.723465	1.12E-13	1.30846E-07
139	PI 36:3	-13.06017401	2.807838	1.91E-18	6.29448E-05
140	PI 36:4	-16.74650021	2.62604	8.8E-13	4.48769E-08
141	PI 38:2	-14.61669735	2.930095	7.53E-10	1.27653E-05
142	PI 38:3	-16.16199515	2.419741	2.85E-10	1.17302E-08
143	PI 38:4	-14.91062013	2.737185	2.73E-09	2.06266E-06
144	PI 38:5	-12.66013542	2.541354	9.76E-15	1.38891E-05
145	PI 38:6	-16.34615486	3.28941	5.07E-13	1.38176E-05
146	PI 40:4	-14.79281489	3.122806	8.57E-09	3.03905E-05
147	PI 40:5	-13.29981437	3.33821	2.62E-07	0.000499117
148	PI 40:6	-13.7819749	2.889937	1.19E-07	2.61152E-05
149	PS 36:1	13.1622479	8.079125	0.227424	0.615448144
150	PS 36:2	10.03558166	8.163065	0.436706	0.90049811
151	PS 38:3	8.277831116	7.70838	0.571359	1
152	PS 38:4	7.493703094	7.694037	0.734873	1
153	PS 38:5	3.838783491	8.796013	0.962394	1
154	PS 40:5	-4.630940972	6.837087	0.327891	1
155	PS 40:6	-2.28798428	6.478175	0.238195	1
156	PG 34:1	-18.86697695	6.201374	2.71E-11	0.013358676
157	PG 34:2	-4.985103669	8.300167	0.360281	1
158	PG 36:1	-23.58438677	5.296658	1.72E-12	8.05159E-05
159	PG 36:2	-17.15232383	6.519126	2.49E-07	0.037325037
160	**PGPC**	**33.8502037**	**11.60509**	**0.000429**	0.05560076
161	**PONPC**	**27.74920429**	**10.76198**	**0.003632**	0.061686124
162	KDdiA-PC	4.573590237	9.338225	0.05731	1
163	LPC 14:0	-15.6928103	2.726432	1.89E-10	7.81325E-07
164	LPC 15:0	-16.39234607	2.721037	7.56E-06	2.43541E-07
165	LPC 16:0	-16.44586937	2.855262	3.04E-05	1.13051E-06
166	LPC 16:1	-11.74523115	2.75933	1.46E-07	0.000266775
167	LPC 17:0	-14.48175332	2.899057	2.84E-05	1.45711E-05
168	LPC 17:1	-16.26049968	3.472311	1.64E-07	5.29187E-05
169	LPC 18:0	-17.10799609	2.554378	1.14E-09	2.08097E-08
170	LPC 18:1	-12.81558781	2.791252	1.44E-14	8.30014E-05

171	LPC 18:2	-8.086593808	3.624101	8.02E-19	0.096314885
172	LPC 18:3	-7.011729386	4.538045	1.35E-21	0.403161253
173	LPC 20:0	-11.52901294	2.897625	3.85E-09	0.000544181
174	LPC 20:1	-11.08541261	2.41466	2.76E-09	5.18942E-05
175	LPC 20:2	-7.660223346	3.409902	9.43E-20	0.090136593
176	LPC 20:3	-8.022181904	4.402682	9.79E-19	0.21450697
177	LPC 20:4	-9.168946476	3.883937	1.77E-10	0.062587091
178	LPC 20:5	-5.670564599	4.641403	2.2E-14	0.620380397
179	LPC 22:4	-8.079490899	4.337133	3.23E-14	0.208153343
180	LPC 22:6	-5.38742787	4.294962	1.2E-21	0.699149233
181	LPC 24:0	-4.971636645	2.979508	0.180127	0.295436865
182	LPC(O-20:0)	-18.8968018	4.010996	9.21E-06	3.47544E-05
183	LPC(O-22:0)	-10.10730931	3.386025	9.95E-06	0.010978029
184	LPC(O-22:1)	-2.470261086	4.564703	0.201897	1
185	LPC(O-24:0)	-6.702902028	3.581754	0.008607	0.224108348
186	LPC(O-24:1)	-8.252471207	3.161246	0.036488	0.041267779
187	LPC(O-24:2)	-8.915027333	5.735147	0.221322	0.2855937
188	LPE 16:0	-9.395033721	2.971553	0.036294	0.007634625
189	LPE 18:0	-12.55467778	2.942106	0.003487	0.000235301
190	LPE 18:1	-6.733498871	3.99479	2.49E-19	0.282260478
191	LPE 18:2	-4.335692234	4.262479	3.55E-23	0.983270003
192	LPE 18:3	-3.856634764	5.275667	2.44E-19	1
193	LPE 20:4	-0.854842098	4.619352	2.27E-21	1
194	LPE 22:6	2.830216945	4.487282	1.77E-20	1
195	CE 14:0	-10.49197216	4.772125	0.098708	0.088523273
196	CE 16:0	-12.30846948	2.910796	3.53E-06	0.000195541
197	CE 16:1	-14.96901764	3.391329	5.25E-06	0.000114831
198	CE 16:2	-22.25264047	4.83716	7.02E-05	6.15524E-05
199	CE 17:0	-8.962935851	5.143237	0.064176	0.308523789
200	CE 17:1	-14.03283794	3.772745	0.000607	0.001103196
201	CE 18:0	-11.30240595	2.675172	0.000388	0.00019242
202	CE 18:1	-7.96135098	2.998393	0.006568	0.028147086
203	CE 18:2	-10.10912986	5.486178	0.011103	0.20858636
204	CE 18:3	-13.5036706	4.416604	0.003661	0.01291561
205	CE 20:0	-15.62145106	4.016587	0.000862	0.000690423
206	CE 20:2	-10.44074074	4.345938	0.162221	0.055209221
207	CE 20:3	-12.36534353	3.404118	0.001727	0.001763992
208	CE 20:4	-14.9401873	4.05511	3.8E-06	0.001626487
209	CE 20:5	-19.31747119	4.934342	4.46E-06	0.001101095
210	CE 22:1	-14.37262196	3.448195	2.63E-05	0.00023522
211	CE 22:4	-9.645283186	4.313483	0.01219	0.084980888
212	CE 22:5	4.177525506	5.153908	0.005241	1
213	CE 22:6	-15.25009169	3.988527	2E-07	0.000905177
214	DG 14:0_18:1	**-39.3962084**	5.905454	7.55E-11	9.5155E-08

215	DG 14:0_18:2	**-35.9967588**	7.118291	7.37E-09	6.12943E-05
216	DG 16:0_16:0	**-34.63721986**	5.378295	1.9E-09	1.3162E-07
217	DG 16:0_18:1	**-33.67749111**	5.045831	8.61E-19	3.4569E-08
218	DG 16:0_18:2	**-37.99145825**	4.952523	4.9E-19	4.09468E-10
219	DG 16:0_20:3	**-21.54276367**	5.537187	0.001007	0.000963011
220	DG 16:0_20:4	**-20.90197749**	5.006609	0.002869	0.000273559
221	DG 16:0_22:5	**-31.23080442**	7.254937	5.3E-10	0.000273984
222	DG 16:0_22:6	**-32.3322112**	7.091315	1.52E-07	0.000296729
223	DG 16:1_18:1	**-33.00337321**	4.964271	7.05E-18	2.75952E-08
224	DG 18:0_18:1	**-27.35159593**	5.205325	3.43E-16	7.74868E-06
225	DG 18:0_18:2	**-33.29971891**	5.046184	5.34E-18	5.01811E-08
226	DG 18:0_20:4	**-22.6946504**	4.934256	0.000119	0.000193893
227	DG 18:1_18:1	**-28.73492622**	4.796368	5.25E-22	3.61483E-07
228	DG 18:1_18:2	**-31.14582317**	4.833562	1.66E-24	4.87197E-08
229	DG 18:1_18:3	**-31.24942701**	4.938337	1.77E-13	2.05774E-07
230	DG 18:1_20:3	**-12.81823813**	4.984517	0.036249	0.033287504
231	DG 18:1_20:4	**-14.36853986**	4.35415	0.014759	0.004500795
232	DG 18:2_18:2	**-32.2684937**	5.104436	1.01E-21	7.32855E-08
233	TG 48:1	**-34.48154996**	4.891523	2.98E-10	2.54051E-08
234	TG 48:2	**-36.80254452**	5.112077	1.32E-12	1.80956E-08
235	TG 48:2	**-37.53956043**	5.358106	1.08E-09	6.7951E-08
236	TG 48:3	**-43.50625983**	5.712554	5.85E-11	2.86027E-08
237	TG 49:1	**-27.83033812**	4.966872	4.17E-13	4.07457E-06
238	TG 50:1	**-28.04605098**	4.944651	2.08E-13	2.34743E-06
239	TG 50:4	**-44.89334369**	5.274218	3.72E-16	3.7659E-10
240	TG 48:2	**-34.82888931**	5.975013	4.52E-11	1.37721E-06
241	TG 48:2	**-35.04103057**	5.144722	1.43E-14	3.45304E-08
242	TG 50:3	**-22.41369896**	4.860139	6.98E-11	0.000146778
243	TG 50:3	**-37.88462157**	4.829666	5.05E-18	4.51619E-10
244	TG 49:1	**-27.70530012**	4.904809	2.7E-14	2.84274E-06
245	TG 51:2	**-28.40432138**	4.362971	2.19E-22	4.19323E-08
246	TG 48:0	**-28.69861733**	5.34345	5.37E-07	8.50374E-06
247	TG 50:0	**-36.18723917**	5.716264	6.64E-08	7.44201E-06
248	TG 50:1	**-25.61198499**	4.118726	2.24E-15	1.28567E-07
249	TG 50:2	**-25.63077223**	4.284111	6.73E-16	3.06419E-07
250	TG 49:1	**-30.79482479**	4.961523	7.9E-13	3.88717E-07
251	TG 50:2	**-27.50340936**	4.248575	7.36E-17	4.77487E-08
252	TG 51:0	**-37.5965425**	5.079713	3.42E-15	3.73202E-09
253	TG 51:1	**-31.58077471**	4.851454	8.9E-16	1.92376E-07
254	TG 51:2	**-27.82356633**	4.70549	5.33E-18	5.05888E-07
255	TG 52:1	**-34.75262342**	5.218812	2.36E-13	1.38443E-06
256	TG 52:2	**-22.64377914**	4.198582	1.33E-18	2.97182E-06
257	TG 52:3	**-24.14862419**	3.870441	1.26E-21	1.16242E-07
258	TG 52:4	**-32.72601367**	4.595224	1.91E-19	6.31698E-09

259	TG 48:3	**-38.35225978**	5.587038	1.08E-16	3.01484E-08
260	TG 50:2	**-33.2665485**	5.727052	2.65E-09	2.97822E-06
261	TG 50:3	**-33.51450002**	4.694142	1.96E-20	4.304E-09
262	TG 51:2	**-26.37397817**	4.804093	2.18E-18	2.60404E-06
263	TG 52:3	**-23.87262274**	3.89401	1.08E-21	1.53581E-07
264	TG 52:4	**-32.70083471**	4.662889	5.85E-21	1.28526E-08
265	TG 53:2	**-28.33863325**	4.930014	3.62E-21	2.09172E-06
266	TG 54:1	**-24.46370143**	6.271693	3.78E-05	0.001684635
267	TG 54:2	**-27.92846295**	5.974715	6.42E-13	0.000174659
268	TG 54:4	**-25.97467912**	4.278795	2.98E-14	3.05919E-07
269	TG 54:3	**-19.67866835**	4.301806	3.49E-15	5.83552E-05
270	TG 54:4	**-23.96923751**	3.97006	5.82E-17	2.21058E-07
271	TG 56:6	**-15.59266184**	3.707663	4.29E-10	0.00032529
272	TG 58:8	**-20.88505038**	4.286781	1.36E-11	3.05932E-05
273	TG 54:5	**-29.79635895**	4.659563	2.06E-16	1.80194E-07
274	TG 54:6	**-36.1155596**	5.607667	4.08E-13	1.8732E-07
275	TG 56:8	**-20.87311041**	4.576324	2.45E-08	0.000231533
276	Acylcarnitine 2:0	-17.26255211	5.321312	3.37E-08	0.005717609
277	Acylcarnitine 14:0	0.391086777	4.042283	4.39E-08	1
278	Acylcarnitine 16:0	-4.204139981	2.392157	0.001984	0.247295889
279	Acylcarnitine 18:0	-9.058669186	6.403981	0.309563	0.98085061
280	Acylcarnitine 18:2	-12.56412319	3.254449	1.42E-06	0.000736997
281	Acylcarnitine 20:0	-13.67626378	6.390464	0.030609	0.089296182
282	FA 16:0	-9.374169733	4.130457	3.85E-24	0.08654597
283	FA 16:1	-15.27355747	7.401252	8.4E-17	0.216356392
284	FA 17:0	-5.957587333	3.903234	9.81E-28	0.435282021
285	FA 18:0	-3.217720533	3.507798	1.12E-15	1
286	FA 18:1	-9.237106635	6.055771	1.92E-21	0.6519238
287	FA 18:2	-10.6405886	6.375857	2.79E-21	0.511560732
288	FA 18:3	-11.57471153	7.132081	2.91E-20	0.58640482
289	FA 20:4	-13.28284986	5.566611	6.98E-25	0.07926609
290	FA 20:5	-11.06334151	6.497335	3.31E-23	0.445842761
291	FA 22:6	-15.06163481	5.898277	5.8E-23	0.055553849

p-value: A repeated measures ANOVA with a Greenhouse-Geisser correction.
*: Corrected *p*-value after adjustment for multiple comparisons using Bonferroni. Corrected $p<0.05$ are highlighted in light red.
SEM: Standard Error Mean

Supplementary Table S10. Plasma individual lipids differentially regulated in 24 h post-PCI (*t2*) vs. 2 h post-PCI (*t1*) (Related to Figure-3.2B).

No.	Lipid Class	Percentage difference, *t2 vs. t1* (%)	SEM	*p*-value	*p*-value (Bonferroni)*
1	Cer 16:0	8.434657743	5.428734	0.077681	0.381156477
2	Cer 18:0	30.41025418	4.31123	1.04E-08	3.36116E-09
3	Cer 20:0	8.428349073	4.016974	0.072423	0.108981356
4	Cer 22:0	7.447273838	2.847545	1.22E-06	0.032277048
5	Cer 24:0	10.11538195	2.929408	1.22E-06	0.002836692
6	Cer 24:1	11.52541594	2.736855	8.82E-07	0.000211069
7	dhCer 22:0	-1.949028419	5.951021	0.83629	1
8	dhCer 24:0	3.725347567	5.011386	0.580476	1
9	dhCer 24:1	13.43960825	5.666619	0.062301	0.068699466
10	HexCer 16:0	8.360895779	2.920141	0.012992	0.017254837
11	HexCer 18:0	10.09206841	5.762457	0.202552	0.293312026
12	HexCer 20:0	6.940060249	3.814672	0.209607	0.205913351
13	HexCer 22:0	8.420803169	3.739348	0.046545	0.084285744
14	HexCer 24:0	8.917495538	3.302977	0.008823	0.025697355
15	HexCer 24:1	12.82460775	3.381908	0.00031	0.001056624
16	Hex2Cer 22:0	6.173293792	5.037675	0.409507	0.655205479
17	Hex2Cer 24:0	3.087430891	4.550207	0.614799	1
18	Hex2Cer 24:1	5.494545835	3.692446	0.203082	0.41753586
19	Hex3Cer 16:0	8.174419058	2.834433	0.022641	0.014836225
20	Hex3Cer 18:0	7.747280127	6.551992	0.064513	0.783107689
21	Hex3Cer 24:1	0.773597723	6.396034	0.760688	1
22	GM3 16:0	9.535897132	3.392905	0.023075	0.019525343
23	GM3 18:0	3.31008746	4.975652	0.012046	1
24	SM 31:1	11.7206804	3.610756	0.000288	0.005266745
25	SM 32:1	10.4463963	2.032923	3.17E-07	6.05673E-06
26	SM 32:2	9.848328506	2.625847	3.71E-05	0.001000464
27	SM 33:1	11.92556734	1.925743	6.6E-09	8.4111E-08
28	SM 34: 0	7.188905296	2.347741	0.000429	0.008791766
29	SM 34:1	8.063276067	2.611057	0.002072	0.008522152
30	SM 34:2	14.05249974	1.864831	7.21E-09	2.33142E-10
31	SM 34:3	18.08138333	4.353748	0.000206	0.00032499
32	SM 35:1	17.10435871	2.533268	2.44E-11	7.82775E-09
33	SM 35:2	20.77253024	2.623862	1.93E-11	5.02197E-11
34	SM 36:1	19.59783523	2.205918	6.97E-15	6.3052E-13
35	SM 36:2	24.93903923	2.439087	9.68E-18	1.77755E-15
36	SM 36:3	20.73953346	2.944957	1.37E-10	2.229E-09
37	SM 37:2	-19.55197034	3.622122	9.92E-10	2.38232E-06
38	SM 38:1	5.270326239	1.672982	0.008016	0.00703979

39	SM 38:2	7.343334947	2.467864	0.000832	0.011509054
40	SM 39:1	3.16057081	2.254545	0.014868	0.511142871
41	SM 41:1	7.254427557	3.010166	0.029194	0.053720872
42	SM 41:2	6.19581742	2.48397	0.024385	0.043685129
43	SM 42:1	4.495201405	2.729678	0.151453	0.313980946
44	PC 29:0	17.31962009	5.658762	0.011738	0.009607809
45	PC 31:0	5.252663692	3.27611	0.145688	0.349266437
46	PC 32:0	12.43267022	2.004768	3.08E-06	7.69988E-08
47	PC 33:0	9.23002405	3.893822	0.116837	0.056969654
48	PC 33:1	9.193767375	2.242294	0.001594	0.000314805
49	PC 33:2	-2.979467759	2.333015	0.037572	0.596592533
50	PC 34:0	10.54780779	2.185094	1.61E-05	2.08045E-05
51	PC 34:1	12.92061367	2.061404	6.5E-08	5.76955E-08
52	PC 34:2	4.184786829	2.535801	0.124377	0.310934051
53	PC 34:3	0.136678089	3.048276	0.010214	1
54	PC 34:4	-13.6364676	5.107068	1.61E-07	0.062784007
55	PC 35:0	11.06173763	5.788969	0.040745	0.162295573
56	PC 35:2	4.75278885	2.60217	0.057026	0.217686271
57	PC 35:3	-3.868606432	2.184898	0.062573	0.242967203
58	PC 35:4	4.090926391	2.253815	0.028825	0.221520629
59	PC 36:2	-1.714848674	3.109974	0.68516	1
60	PC 36:3	3.385024735	2.254405	0.004531	0.404337303
61	PC 36:4	11.35681414	2.998989	0.004753	0.000908116
62	PC 36:5	9.739359634	3.461878	0.001413	0.018376217
63	PC 36:6	-16.86331121	5.854653	0.024088	0.021273453
64	PC 37:4	10.78188044	2.398035	7.1E-05	7.61556E-05
65	PC 37:5	5.748739584	2.149498	0.07761	0.027364267
66	PC 37:6	8.002249283	2.553829	0.041734	0.007251575
67	PC 38:2	9.077873312	2.116713	0.001212	0.000158268
68	PC 38:3	7.086560251	2.167664	0.00781	0.004823236
69	PC 38:4	14.39129068	2.255233	6.53E-08	4.3975E-08
70	PC 38:5	12.30174291	2.470213	5.07E-06	1.2906E-05
71	PC 38:6	13.73363557	2.582321	3.76E-07	3.39437E-06
72	PC 40:5	11.99864027	2.996858	0.00052	0.000424104
73	PC 40:6	10.02838767	3.079585	0.000532	0.00512149
74	PC 40:7	6.848621076	3.546057	0.114407	0.164161218
75	PC(O-30:0)	0.304434138	3.276848	0.701206	1
76	PC(O-32:0)	-1.171657482	2.168514	0.39211	1
77	PC(O-32:1)	15.88861271	2.559124	7.33E-09	9.13584E-08
78	PC(O-32:2)	23.30381152	2.970774	1.51E-12	1.23644E-10
79	PC(O-34:0)	1.561160124	1.898778	0.764094	1
80	PC(O-34:1)	4.800651669	1.801487	0.087056	0.028055767
81	PC(O-34:2)	4.833090728	2.788653	0.067565	0.252298303
82	PC(O-36:1)	7.336641778	2.53868	0.011747	0.015310161

83	PC(O-36:3)	-3.755076191	1.633152	0.016139	0.071892324
84	PC(O-36:4)	4.080706565	1.725908	0.03319	0.062566392
85	PC(O-36:5)	4.776594013	1.921409	0.028041	0.045029107
86	PC(O-38:4)	10.8241694	1.79147	5.73E-07	1.53003E-07
87	PC(O-38:5)	5.747824361	1.796179	0.051926	0.006223604
88	PC(O-40:7)	6.401744781	2.395589	0.101686	0.02681707
89	PC(P-32:0)	0.350792861	2.345256	0.628526	1
90	PC(P-32:1)	1.570820667	2.318657	0.683476	1
91	PC(P-34:1)	-13.23591311	2.27148	0.000183	4.29919E-07
92	PC(P-34:2)	-13.74837897	2.52522	3.91E-07	1.83819E-06
93	PC(P-36:2)	-2.72901547	1.852487	0.037497	0.433834824
94	PC(P-40:5)	7.29047102	2.103922	0.001071	0.00261569
95	PE 32:1	18.34685899	4.757245	0.000196	0.00063849
96	PE 34:1	30.54108372	3.400132	1E-13	4.65551E-13
97	PE 34:2	23.31620357	3.578824	5.21E-09	2.82891E-08
98	PE 34:3	15.66636898	4.589285	0.000157	0.003200664
99	PE 35:1	21.47858707	4.009688	1.12E-05	3.36405E-05
100	PE 35:2	2.687826749	3.698352	0.196603	1
101	PE 36:1	30.79510667	3.353931	4.93E-11	3.49331E-13
102	PE 36:2	26.23207608	3.072156	5.83E-10	3.99872E-12
103	PE 36:3	12.90437979	3.464395	0.001738	0.001166657
104	PE 36:4	16.08044592	3.332957	2.06E-05	2.54014E-05
105	PE 36:5	8.162626054	4.824328	0.188135	0.275640683
106	PE 38:3	27.68153814	3.214584	4.32E-13	2.37819E-12
107	PE 38:4	25.80703014	3.331879	1.5E-11	1.21743E-10
108	PE 38:5	20.09988189	3.35888	1.7E-08	2.22162E-07
109	PE 38:6	32.13029014	4.190549	1.32E-13	2.14901E-10
110	PE 40:5	41.48023236	3.56667	3.34E-21	5.70537E-18
111	PE 40:6	46.43058888	3.980771	6.76E-21	8.1145E-18
112	PE 40:7	23.42324198	4.254227	2.48E-07	1.577E-06
113	PE(O-34:1)	-10.07665707	4.47937	7.58E-08	0.096582868
114	PE(O-34:2)	-22.45923011	5.781093	4.43E-07	0.002058264
115	PE(O-36:2)	2.083956293	4.013347	0.08791	1
116	PE(O-36:3)	-18.60424428	4.534262	1.17E-06	0.000861353
117	PE(O-36:4)	-22.91160671	3.223381	1.48E-20	1.84103E-09
118	PE(O-36:5)	-24.14234809	3.784386	6.41E-14	4.42004E-08
119	PE(O-38:4)	-3.330440819	2.86015	4.08E-05	0.756688744
120	PE(O-38:5)	-12.49114137	2.818953	9.25E-14	9.29007E-05
121	PE(O-38:6)	-11.04144787	3.518182	7.2E-08	0.010398761
122	PE(O-40:5)	0.430125699	3.661445	0.003014	1
123	PE(O-40:6)	1.907148666	3.370005	0.004924	1
124	PE(O-40:7)	-4.59613978	3.126257	0.000207	0.53060075
125	PE(P-34:1)	-21.74090595	5.976318	8.14E-05	0.0173797
126	PE(P-34:2)	-27.41287354	5.275906	3.77E-10	1.7992E-05

127	PE(P-36:2)	-19.1131129	4.189425	2.91E-07	0.00012043
128	PE(P-38:4)	-14.17126619	2.654329	8.05E-15	2.65592E-06
129	PE(P-38:6)	-11.23133074	3.822385	8.43E-06	0.012771319
130	PE(P-40:5)	1.946852896	3.141816	0.003732	1
131	PE(P-40:6)	-6.519138714	3.082292	2.12E-06	0.147545937
132	PI 32:0	-24.50517632	5.339832	5.41E-12	4.97065E-05
133	PI 32:1	-19.01187038	5.081118	1.08E-07	0.001148556
134	PI 34:0	-22.91783037	4.606186	6.15E-14	1.20663E-05
135	PI 34:1	-22.62455409	3.910804	2.45E-16	4.45884E-07
136	PI 36:0	-27.18678471	4.343363	5.31E-20	8.95308E-08
137	PI 36:1	-25.58102566	3.580303	5.79E-22	1.43641E-09
138	PI 36:2	-14.17843082	3.497442	1.12E-13	0.000370775
139	PI 36:3	-28.56013408	3.790926	1.91E-18	2.46961E-10
140	PI 36:4	-17.11534399	3.920911	8.8E-13	0.000131017
141	PI 38:2	-10.3241558	3.616515	7.53E-10	0.016659244
142	PI 38:3	-4.48205911	3.109109	2.85E-10	0.462470786
143	PI 38:4	-6.426878396	3.245627	2.73E-09	0.152718669
144	PI 38:5	-21.92952799	3.63823	9.76E-15	1.67897E-07
145	PI 38:6	-19.85998625	4.241849	5.07E-13	3.25896E-05
146	PI 40:4	-9.551926487	3.828237	8.57E-09	0.042092427
147	PI 40:5	-8.193456268	3.785454	2.62E-07	0.099855502
148	PI 40:6	-10.57086526	4.034903	1.19E-07	0.032697226
149	PS 36:1	-13.98575466	8.474148	0.227424	0.26368898
150	PS 36:2	-9.174051325	7.60129	0.436706	0.631679191
151	PS 38:3	-7.788999644	7.573254	0.571359	0.844105368
152	PS 38:4	-4.940756855	7.929189	0.734873	1
153	PS 38:5	2.007045039	8.59272	0.962394	1
154	PS 40:5	11.0321747	6.690476	0.327891	0.334627187
155	PS 40:6	11.42905446	6.799574	0.238195	0.290981173
156	PG 34:1	48.05018377	6.240193	2.71E-11	1.39115E-09
157	PG 34:2	10.35189898	9.449391	0.360281	0.634399746
158	PG 36:1	58.5962308	6.114189	1.72E-12	1.65895E-12
159	PG 36:2	40.06611019	6.209808	2.49E-07	2.14315E-07
160	PGPC	14.92846309	10.17279	0.000429	0.332128491
161	PONPC	8.40244408	9.494489	0.003632	1
162	KDdiA-PC	-31.91876907	10.11426	0.05731	0.110152274
163	LPC 14:0	-14.91061132	4.209732	1.89E-10	0.001997725
164	LPC 15:0	1.439466573	3.814912	7.56E-06	1
165	LPC 16:0	7.162829657	3.670665	3.04E-05	0.184668516
166	LPC 16:1	-12.32398578	4.345656	1.46E-07	0.018552358
167	LPC 17:0	-1.040389183	3.915816	2.84E-05	1
168	LPC 17:1	-12.50421979	5.225459	1.64E-07	0.068121561
169	LPC 18:0	-6.383087596	3.748581	1.14E-09	0.27185121
170	LPC 18:1	-21.49941571	4.123086	1.44E-14	5.94164E-06

171	LPC 18:2	-41.57652091	5.21017	8.02E-19	9.30385E-11
172	LPC 18:3	-52.90755361	5.882996	1.35E-21	1.17373E-12
173	LPC 20:0	-17.03917036	4.383976	3.85E-09	0.00090285
174	LPC 20:1	-15.74903249	3.957601	2.76E-09	0.000585434
175	LPC 20:2	-39.39496202	4.799323	9.43E-20	2.49393E-11
176	LPC 20:3	-42.88798054	5.4797	9.79E-19	1.30833E-10
177	LPC 20:4	-21.22436965	4.601333	1.77E-10	7.20709E-05
178	LPC 20:5	-36.86170806	5.513935	2.2E-14	2.66309E-08
179	LPC 22:4	-33.5172393	5.194635	3.23E-14	3.87855E-08
180	LPC 22:6	-46.74957357	4.882257	1.2E-21	4.69956E-14
181	LPC 24:0	-0.337303689	3.339924	0.180127	1
182	LPC(O-20:0)	-6.694703898	5.382687	9.21E-06	0.633871688
183	LPC(O-22:0)	17.84921416	3.906894	9.95E-06	5.30811E-05
184	LPC(O-22:1)	8.721046947	4.57451	0.201897	0.206646787
185	LPC(O-24:0)	10.7628519	3.311395	0.008607	0.005263552
186	LPC(O-24:1)	6.15200236	3.135297	0.036488	0.164827327
187	LPC(O-24:2)	6.986391449	6.495529	0.221322	0.87465285
188	LPE 16:0	6.790290466	3.858067	0.036294	0.260590359
189	LPE 18:0	2.808543139	4.029923	0.003487	1
190	LPE 18:1	-39.59081483	4.791969	2.49E-19	2.44162E-11
191	LPE 18:2	-54.59111824	5.292681	3.55E-23	9.57101E-15
192	LPE 18:3	-56.08090573	6.180973	2.44E-19	1.39459E-12
193	LPE 20:4	-49.48366049	4.870986	2.27E-21	8.02873E-15
194	LPE 22:6	-55.52788756	4.962543	1.77E-20	1.82109E-16
195	CE 14:0	5.857594508	5.128701	0.098708	0.838188759
196	CE 16:0	14.30148317	2.990454	3.53E-06	2.85363E-05
197	CE 16:1	20.43062997	3.572112	5.25E-06	6.88042E-07
198	CE 16:2	22.55152122	5.612248	7.02E-05	0.000611944
199	CE 17:0	11.26152019	4.758303	0.064176	0.066301922
200	CE 17:1	16.28420165	4.325128	0.000607	0.000921278
201	CE 18:0	7.609804677	2.653333	0.000388	0.016926149
202	CE 18:1	11.17624772	3.538415	0.006568	0.00760856
203	CE 18:2	17.89057644	5.886244	0.011103	0.009189538
204	CE 18:3	15.21169266	4.412189	0.003661	0.00277575
205	CE 20:0	10.95394859	4.370659	0.000862	0.049272579
206	CE 20:2	7.610310531	5.393864	0.162221	0.774720727
207	CE 20:3	16.04437078	3.981026	0.001727	0.000634687
208	CE 20:4	24.73578846	4.365825	3.8E-06	8.37445E-07
209	CE 20:5	26.66669563	5.128965	4.46E-06	6.24753E-06
210	CE 22:1	17.08006148	4.002574	2.63E-05	0.000169007
211	CE 22:4	15.4601741	5.095746	0.01219	0.01514939
212	CE 22:5	11.68469038	4.811525	0.005241	0.051538826
213	CE 22:6	26.60958147	4.65768	2E-07	8.10961E-07
214	DG 14:0_18:1	**56.35335256**	6.443164	7.55E-11	3.60497E-12

215	DG 14:0_18:2	**55.8003156**	7.557895	7.37E-09	2.27576E-09
216	DG 16:0_16:0	**51.61611082**	6.44308	1.9E-09	5.07891E-11
217	DG 16:0_18:1	**69.00173373**	5.061926	8.61E-19	2.93993E-20
218	DG 16:0_18:2	**73.95859548**	5.451312	4.9E-19	9.32165E-19
219	DG 16:0_20:3	**22.28061693**	6.023743	0.001007	0.001741988
220	DG 16:0_20:4	**16.36582641**	5.822454	0.002869	0.01704698
221	DG 16:0_22:5	**54.36016803**	7.404307	5.3E-10	8.41013E-09
222	DG 16:0_22:6	**49.87137654**	7.805049	1.52E-07	2.78596E-07
223	DG 16:1_18:1	**64.8645229**	5.117854	7.05E-18	1.09028E-18
224	DG 18:0_18:1	**59.25186261**	5.10751	3.43E-16	9.82443E-17
225	DG 18:0_18:2	**67.10933723**	5.270792	5.34E-18	3.0707E-17
226	DG 18:0_20:4	**10.10900731**	4.814548	0.000119	0.135135196
227	DG 18:1_18:1	**69.2716883**	4.466658	5.25E-22	4.73126E-23
228	DG 18:1_18:2	**77.11833898**	4.465456	1.66E-24	1.34586E-23
229	DG 18:1_18:3	**53.39720457**	5.015605	1.77E-13	5.29763E-15
230	DG 18:1_20:3	**6.815043353**	4.805895	0.036249	0.507075356
231	DG 18:1_20:4	**9.776277053**	4.843758	0.014759	0.135879105
232	DG 18:2_18:2	**80.98091681**	4.794477	1.01E-21	3.14901E-20
233	TG 48:1	**52.96079133**	5.968836	2.98E-10	4.18729E-12
234	TG 48:2	**65.17972136**	6.25058	1.32E-12	4.36696E-15
235	TG 48:2	**60.55341997**	7.151843	1.08E-09	2.01096E-11
236	TG 48:3	**70.57148555**	7.455133	5.85E-11	3.25329E-13
237	TG 49:1	**62.21278063**	5.997664	4.17E-13	6.52077E-15
238	TG 50:1	**51.28546536**	5.452637	2.08E-13	4.13405E-13
239	TG 50:4	**80.95797514**	6.423591	3.72E-16	7.18149E-17
240	TG 48:2	**54.97307962**	6.123847	4.52E-11	1.22779E-12
241	TG 48:2	**68.17281512**	5.751939	1.43E-14	5.93122E-17
242	TG 50:3	**45.42298457**	5.488978	6.98E-11	2.70859E-11
243	TG 50:3	**74.58659221**	5.55266	5.05E-18	1.30245E-19
244	TG 49:1	**64.47016064**	5.815081	2.7E-14	2.69948E-16
245	TG 51:2	**71.01436346**	4.905245	2.19E-22	3.546E-21
246	TG 48:0	**47.19020239**	7.216366	5.37E-07	2.62923E-08
247	TG 50:0	**56.31668659**	7.520188	6.64E-08	4.28471E-10
248	TG 50:1	**58.16798933**	4.860891	2.24E-15	3.03938E-17
249	TG 50:2	**67.35466806**	5.670552	6.73E-16	4.82924E-17
250	TG 49:1	**61.88091003**	5.975964	7.9E-13	6.47767E-15
251	TG 50:2	**59.11837146**	4.75789	7.36E-17	1.21425E-17
252	TG 51:0	**63.6462466**	5.727321	3.42E-15	2.87016E-15
253	TG 51:1	**66.06175543**	5.234899	8.9E-16	1.36741E-18
254	TG 51:2	**64.72117042**	4.889756	5.33E-18	9.64854E-20
255	TG 52:1	**68.72976331**	5.70207	2.36E-13	1.80365E-17
256	TG 52:2	**56.30083587**	4.633924	1.33E-18	1.59476E-17
257	TG 52:3	**65.8582955**	4.837237	1.26E-21	1.13257E-19
258	TG 52:4	**80.32787065**	5.44812	1.91E-19	9.49333E-20

259	TG 48:3	**74.69594414**	6.021554	1.08E-16	5.91821E-18
260	TG 50:2	**50.38422874**	6.90297	2.65E-09	1.12296E-09
261	TG 50:3	**79.63484404**	5.363449	1.96E-20	9.1994E-22
262	TG 51:2	**64.03708644**	5.284246	2.18E-18	6.73359E-18
263	TG 52:3	**61.9051861**	4.828925	1.08E-21	8.54316E-19
264	TG 52:4	**77.37295689**	5.321546	5.85E-21	2.33546E-21
265	TG 53:2	**67.80922111**	4.399375	3.62E-21	6.37059E-22
266	TG 54:1	**53.50517392**	6.636105	3.78E-05	2.97144E-05
267	TG 54:2	**62.28506197**	5.923508	6.42E-13	1.389E-14
268	TG 54:4	**63.8704544**	5.75178	2.98E-14	1.57993E-14
269	TG 54:3	**51.37964524**	5.280662	3.49E-15	1.243E-13
270	TG 54:4	**63.60821078**	5.598379	5.82E-17	7.57024E-16
271	TG 56:6	**31.66906818**	4.009746	4.29E-10	1.26688E-10
272	TG 58:8	**47.28947948**	5.682446	1.36E-11	2.86707E-11
273	TG 54:5	**74.04826208**	6.004758	2.06E-16	4.68116E-17
274	TG 54:6	**83.06572133**	6.800357	4.08E-13	4.92615E-15
275	TG 56:8	**35.67171863**	4.682958	2.45E-08	2.21354E-10
276	Acylcarnitine 2:0	-16.81922905	5.635961	3.37E-08	0.010926882
277	Acylcarnitine 14:0	-37.38662089	4.984038	4.39E-08	1.32534E-06
278	Acylcarnitine 16:0	-8.102652004	3.537137	0.001984	0.075790903
279	Acylcarnitine 18:0	-4.545140683	6.329638	0.309563	1
280	Acylcarnitine 18:2	-10.78174088	4.515606	1.42E-06	0.056200887
281	Acylcarnitine 20:0	-4.515993143	7.608949	0.030609	1
282	FA 16:0	-46.14896196	4.274456	3.85E-24	6.1707E-16
283	FA 16:1	-72.17848823	7.033576	8.4E-17	4.58645E-14
284	FA 17:0	-52.76630486	4.207399	9.81E-28	4.43612E-19
285	FA 18:0	-27.88081303	3.793123	1.12E-15	1.17157E-09
286	FA 18:1	-75.60903217	6.038568	1.92E-21	7.22885E-18
287	FA 18:2	-76.45101293	6.146303	2.79E-21	8.53985E-18
288	FA 18:3	-81.66158282	7.098033	2.91E-20	1.66647E-16
289	FA 20:4	-62.7869665	5.231273	6.98E-25	5.13766E-18
290	FA 20:5	-77.19599495	6.911246	3.31E-23	2.13696E-16
291	FA 22:6	-68.50094096	5.477855	5.8E-23	2.95283E-18

p-value: A repeated measures ANOVA with a Greenhouse-Geisser correction.
*: Corrected *p*-value after adjustment for multiple comparisons using Bonferroni. Corrected $p<0.05$ are highlighted in light red.
SEM: Standard Error Mean

Supplementary Table S11. Plasma individual lipids differentially regulated in 24 h post-PCI (*t2*) vs. pre-PCI (*t0*) (Related to Figure-3.2C).

No.	Lipid Class	Percentage difference, *t2 vs. t0* (%)	SEM	*p*-value	*p*-value (Bonferroni)*
1	Cer 16:0	-5.171404043	6.38604	0.077681	1
2	Cer 18:0	14.9646175	5.102478	1.04E-08	0.013605277
3	Cer 20:0	0.537886458	4.224372	0.072423	1
4	Cer 22:0	-7.921812406	2.73655	1.22E-06	0.014744501
5	Cer 24:0	-5.326617424	2.643737	1.22E-06	0.14396977
6	Cer 24:1	-2.682417554	2.868859	8.82E-07	1
7	dhCer 22:0	-4.86796659	6.259403	0.83629	1
8	dhCer 24:0	-1.298256255	4.999661	0.580476	1
9	dhCer 24:1	10.9854119	5.716114	0.062301	0.180678251
10	HexCer 16:0	0.307761889	3.338827	0.012992	1
11	HexCer 18:0	1.816116639	5.926974	0.202552	1
12	HexCer 20:0	6.190512215	4.171817	0.209607	0.388752195
13	HexCer 22:0	1.909307397	3.133626	0.046545	1
14	HexCer 24:0	0.608792163	3.246761	0.008823	1
15	HexCer 24:1	3.104382842	2.822177	0.00031	0.825053719
16	Hex2Cer 22:0	5.132235018	5.006033	0.409507	0.866214424
17	Hex2Cer 24:0	5.316904899	5.11128	0.614799	1
18	Hex2Cer 24:1	6.194562957	3.700569	0.203082	0.273984238
19	Hex3Cer 16:0	1.704899746	2.850657	0.022641	1
20	Hex3Cer 18:0	-8.72429582	6.215452	0.064513	0.635952548
21	Hex3Cer 24:1	3.803670563	6.829334	0.760688	1
22	GM3 16:0	1.968495741	3.657395	0.023075	1
23	GM3 18:0	-9.639496442	3.963813	0.012046	0.048788619
24	SM 31:1	-1.812855439	3.59453	0.000288	1
25	SM 32:1	-3.860866758	2.769338	3.17E-07	0.481407083
26	SM 32:2	-1.761087627	2.796301	3.71E-05	1
27	SM 33:1	-0.57151095	2.229722	6.6E-09	1
28	SM 34: 0	-1.414221443	2.114967	0.000429	1
29	SM 34:1	-1.220848422	3.054374	0.002072	1
30	SM 34:2	1.320828234	2.363282	7.21E-09	1
31	SM 34:3	2.593150228	4.281823	0.000206	1
32	SM 35:1	3.213898545	2.154844	2.44E-11	0.41755521
33	SM 35:2	9.65437425	2.66275	1.93E-11	0.001515943
34	SM 36:1	10.41569308	1.825477	6.97E-15	5.92803E-07
35	SM 36:2	13.08968427	2.284714	9.68E-18	5.52744E-07
36	SM 36:3	12.41043434	2.582372	1.37E-10	2.31251E-05
37	SM 37:2	-25.32338631	4.002717	9.92E-10	1.12862E-07
38	SM 38:1	1.380769952	1.769408	0.008016	1

39	SM 38:2	-0.209624257	2.00474	0.000832	1
40	SM 39:1	-2.881487243	1.722794	0.014868	0.295978277
41	SM 41:1	3.005057793	2.562366	0.029194	0.729391672
42	SM 41:2	1.164528883	2.461505	0.024385	1
43	SM 42:1	4.767158385	2.886777	0.151453	0.298114427
44	PC 29:0	3.099612951	6.005954	0.011738	1
45	PC 31:0	7.619456522	4.205899	0.145688	0.211197332
46	PC 32:0	5.547426015	2.504723	3.08E-06	0.0871524
47	PC 33:0	5.293817252	4.379605	0.116837	0.66828025
48	PC 33:1	2.510696518	2.432574	0.001594	0.910363511
49	PC 33:2	-7.202080095	3.057766	0.037572	0.076213954
50	PC 34:0	6.704483988	2.314072	1.61E-05	0.014632956
51	PC 34:1	6.084666088	2.22023	6.5E-08	0.022399512
52	PC 34:2	5.781741183	3.130555	0.124377	0.204302595
53	PC 34:3	-7.8026757	3.21062	0.010214	0.05137323
54	PC 34:4	-29.53183868	4.765164	1.61E-07	1.04914E-07
55	PC 35:0	-1.494726424	5.230756	0.040745	1
56	PC 35:2	-1.964303224	2.9551	0.057026	1
57	PC 35:3	-6.707661995	3.07062	0.062573	0.105775476
58	PC 35:4	-2.917680679	2.865448	0.028825	0.951161162
59	PC 36:2	1.002133038	3.521297	0.68516	1
60	PC 36:3	-4.681581313	2.593042	0.004531	0.232725835
61	PC 36:4	8.975884842	3.745267	0.004753	0.06070717
62	PC 36:5	-1.531824222	2.569386	0.001413	1
63	PC 36:6	-19.34453559	6.299316	0.024088	0.056883426
64	PC 37:4	7.420441556	2.476454	7.1E-05	0.011235772
65	PC 37:5	5.222387757	2.856492	0.07761	0.203380382
66	PC 37:6	3.746981972	3.069947	0.041734	0.642582721
67	PC 38:2	6.798385285	2.593034	0.001212	0.031483583
68	PC 38:3	2.961368438	2.403774	0.00781	0.657514749
69	PC 38:4	7.539815928	2.536441	6.53E-08	0.012157386
70	PC 38:5	6.383936317	2.352451	5.07E-06	0.025693894
71	PC 38:6	10.07514105	2.516767	3.76E-07	0.000456055
72	PC 40:5	8.307861641	3.135755	0.00052	0.028961234
73	PC 40:6	10.42187397	2.809575	0.000532	0.001208933
74	PC 40:7	5.482576381	3.632674	0.114407	0.411071728
75	PC(O-30:0)	2.726143471	4.060817	0.701206	1
76	PC(O-32:0)	2.309939491	2.786883	0.39211	1
77	PC(O-32:1)	5.064841926	2.560519	7.33E-09	0.156278927
78	PC(O-32:2)	11.98087566	2.654399	1.51E-12	6.82446E-05
79	PC(O-34:0)	0.492509275	2.404025	0.764094	1
80	PC(O-34:1)	2.809520662	2.165723	0.087056	0.582724279
81	PC(O-34:2)	-1.377083604	2.93281	0.067565	1
82	PC(O-36:1)	4.254194933	2.44784	0.011747	0.254912157

83	PC(O-36:3)	-6.777518456	2.500607	0.016139	0.029569971
84	PC(O-36:4)	-1.621642207	2.423594	0.03319	1
85	PC(O-36:5)	-1.64374522	2.635765	0.028041	1
86	PC(O-38:4)	4.5076721	1.973245	5.73E-07	0.074240837
87	PC(O-38:5)	3.192501409	2.411145	0.051926	0.546755655
88	PC(O-40:7)	5.5199937	3.143538	0.101686	0.233035778
89	PC(P-32:0)	2.268427335	3.483473	0.628526	1
90	PC(P-32:1)	2.026450192	3.767588	0.683476	1
91	PC(P-34:1)	-11.80912068	3.462988	0.000183	0.005703614
92	PC(P-34:2)	-17.643597	3.402326	3.91E-07	7.91274E-06
93	PC(P-36:2)	-6.189114645	2.650577	0.037497	0.075961145
94	PC(P-40:5)	9.047542018	2.356664	0.001071	0.00077418
95	PE 32:1	15.09361642	4.878654	0.000196	0.008087488
96	PE 34:1	22.63381051	3.835184	1E-13	3.25809E-07
97	PE 34:2	17.18425484	3.699776	5.21E-09	5.12306E-05
98	PE 34:3	19.8129087	5.24654	0.000157	0.001114612
99	PE 35:1	6.844735209	4.140004	1.12E-05	0.27236028
100	PE 35:2	-5.116907495	4.236865	0.196603	1
101	PE 36:1	22.44941537	4.501624	4.93E-11	1.25254E-05
102	PE 36:2	18.50900046	4.004782	5.83E-10	5.92612E-05
103	PE 36:3	8.409729646	3.90744	0.001738	0.108039297
104	PE 36:4	14.14682167	3.897558	2.06E-05	0.001723428
105	PE 36:5	5.002961551	5.066057	0.188135	0.865213664
106	PE 38:3	24.49953527	3.904331	4.32E-13	6.88736E-08
107	PE 38:4	23.27444666	3.897102	1.5E-11	2.56883E-07
108	PE 38:5	19.91956438	3.801731	1.7E-08	6.26594E-06
109	PE 38:6	33.52748957	4.377373	1.32E-13	6.90004E-10
110	PE 40:5	35.98644804	4.110683	3.34E-21	2.02091E-12
111	PE 40:6	41.83273855	4.34063	6.76E-21	2.06586E-13
112	PE 40:7	23.31419111	4.905071	2.48E-07	4.28036E-05
113	PE(O-34:1)	-28.81208616	4.781276	7.58E-08	5.82364E-07
114	PE(O-34:2)	-33.62615349	5.877475	4.43E-07	1.82146E-06
115	PE(O-36:2)	-7.716201432	4.367764	0.08791	0.657580076
116	PE(O-36:3)	-27.1718925	4.982506	1.17E-06	3.86755E-06
117	PE(O-36:4)	-35.0149514	3.248326	1.48E-20	2.85683E-16
118	PE(O-36:5)	-32.39734154	4.024833	6.41E-14	3.81864E-11
119	PE(O-38:4)	-13.26317045	3.224603	4.08E-05	0.000312174
120	PE(O-38:5)	-23.28164699	2.744556	9.25E-14	5.26548E-12
121	PE(O-38:6)	-20.5597611	3.314014	7.2E-08	9.11132E-08
122	PE(O-40:5)	-10.80018079	3.741691	0.003014	0.02228062
123	PE(O-40:6)	-8.529213792	3.276134	0.004924	0.058377213
124	PE(O-40:7)	-12.60536354	2.992275	0.000207	0.000247512
125	PE(P-34:1)	-29.56686226	5.642562	8.14E-05	2.71858E-05
126	PE(P-34:2)	-37.37499452	5.565699	3.77E-10	1.74387E-08

127	PE(P-36:2)	-25.60650025	4.742409	2.91E-07	4.26921E-06
128	PE(P-38:4)	-23.11967306	2.659765	8.05E-15	1.97848E-12
129	PE(P-38:6)	-19.68038625	4.064653	8.43E-06	2.14229E-05
130	PE(P-40:5)	-8.792668769	3.461976	0.003732	0.065831649
131	PE(P-40:6)	-16.15506301	3.059314	2.12E-06	5.16604E-06
132	PI 32:0	-42.87922103	5.561893	5.41E-12	3.27343E-10
133	PI 32:1	-30.9413374	5.343632	1.08E-07	5.33184E-07
134	PI 34:0	-37.99633289	4.327769	6.15E-14	2.42189E-12
135	PI 34:1	-38.28712314	4.098478	2.45E-16	1.73804E-13
136	PI 36:0	-48.16853796	4.488686	5.31E-20	5.97138E-16
137	PI 36:1	-42.35440791	3.697948	5.79E-22	2.67733E-17
138	PI 36:2	-30.27951783	3.696453	1.12E-13	1.90721E-11
139	PI 36:3	-40.7107515	4.118292	1.91E-18	1.36317E-14
140	PI 36:4	-33.1487489	4.08698	8.8E-13	3.09117E-11
141	PI 38:2	-24.52580547	3.703597	7.53E-10	1.47734E-08
142	PI 38:3	-20.46201083	3.110318	2.85E-10	1.68197E-08
143	PI 38:4	-21.12768259	3.417474	2.73E-09	9.02233E-08
144	PI 38:5	-34.00103354	3.940151	9.76E-15	2.54442E-12
145	PI 38:6	-35.64496802	4.515226	5.07E-13	6.45084E-11
146	PI 40:4	-23.9820029	3.861958	8.57E-09	9.12214E-08
147	PI 40:5	-21.35893787	3.801946	2.62E-07	1.4403E-06
148	PI 40:6	-24.08958163	4.242294	1.19E-07	7.34112E-07
149	PS 36:1	-3.390172251	9.482532	0.227424	1
150	PS 36:2	-1.813375779	8.690321	0.436706	1
151	PS 38:3	-2.670448486	9.100372	0.571359	1
152	PS 38:4	-0.482347476	8.869061	0.734873	1
153	PS 38:5	1.801104537	9.295265	0.962394	1
154	PS 40:5	4.62578788	7.361331	0.327891	1
155	PS 40:6	8.348175292	7.304867	0.238195	0.731431135
156	PG 34:1	31.63119117	6.319587	2.71E-11	1.92636E-05
157	PG 34:2	7.755168093	9.183676	0.360281	0.834978525
158	PG 36:1	37.1334209	7.013142	1.72E-12	6.41366E-05
159	PG 36:2	24.56712677	6.91736	2.49E-07	0.006661599
160	PGPC	45.93533072	11.17546	0.000429	0.000464618
161	PONPC	33.33465117	10.51473	0.003632	0.006129852
162	KDdiA-PC	-30.7387448	10.23838	0.05731	0.239693423
163	LPC 14:0	-30.38592736	4.151781	1.89E-10	1.02272E-09
164	LPC 15:0	-14.96817647	3.572595	7.56E-06	0.000221716
165	LPC 16:0	-9.508800192	3.615327	3.04E-05	0.029797197
166	LPC 16:1	-24.01235264	3.794647	1.46E-07	4.83286E-08
167	LPC 17:0	-15.60285296	3.542669	2.84E-05	0.000117163
168	LPC 17:1	-28.47252151	4.355973	1.64E-07	2.18249E-08
169	LPC 18:0	-23.63081443	3.259069	1.14E-09	1.27474E-09
170	LPC 18:1	-34.15296781	3.499627	1.44E-14	1.77302E-14

171	LPC 18:2	-49.39086227	4.456011	8.02E-19	8.29407E-17
172	LPC 18:3	-59.8533558	5.120999	1.35E-21	9.10081E-18
173	LPC 20:0	-28.44403408	4.053033	3.85E-09	4.83794E-09
174	LPC 20:1	-26.48213909	3.80609	2.76E-09	5.72557E-09
175	LPC 20:2	-46.99649079	4.046257	9.43E-20	1.46343E-17
176	LPC 20:3	-50.71699043	4.854946	9.79E-19	1.36362E-15
177	LPC 20:4	-30.60658368	3.948099	1.77E-10	1.01896E-10
178	LPC 20:5	-42.75723175	4.624901	2.2E-14	2.16141E-13
179	LPC 22:4	-40.84646604	4.897447	3.23E-14	1.16266E-11
180	LPC 22:6	-51.10736719	4.946473	1.2E-21	2.77281E-15
181	LPC 24:0	-5.231841773	3.051397	0.180127	0.282237675
182	LPC(O-20:0)	-24.85863575	5.271857	9.21E-06	3.74455E-05
183	LPC(O-22:0)	7.925292673	3.301832	9.95E-06	0.05702014
184	LPC(O-22:1)	6.156085141	5.086565	0.201897	0.654426995
185	LPC(O-24:0)	4.091324737	3.363114	0.008607	0.659509899
186	LPC(O-24:1)	-2.273780353	3.269757	0.036488	1
187	LPC(O-24:2)	-2.787625902	5.752431	0.221322	1
188	LPE 16:0	-2.643564768	4.040519	0.036294	1
189	LPE 18:0	-9.537391411	4.019332	0.003487	0.056940434
190	LPE 18:1	-46.2325892	4.425228	2.49E-19	3.97876E-15
191	LPE 18:2	-58.37629794	5.091889	3.55E-23	5.82428E-17
192	LPE 18:3	-59.8568143	6.005582	2.44E-19	5.52428E-14
193	LPE 20:4	-49.85002648	5.088631	2.27E-21	2.25657E-14
194	LPE 22:6	-51.87577617	5.75814	1.77E-20	7.71319E-13
195	CE 14:0	-5.039079108	4.803532	0.098708	0.87896784
196	CE 16:0	1.895561514	2.946023	3.53E-06	1
197	CE 16:1	5.445082627	4.528607	5.25E-06	0.758974377
198	CE 16:2	0.097484181	6.036662	7.02E-05	1
199	CE 17:0	2.160008508	4.759943	0.064176	1
200	CE 17:1	2.457442316	4.863839	0.000607	1
201	CE 18:0	-3.733488564	3.032671	0.000388	0.668331911
202	CE 18:1	3.111427867	3.801752	0.006568	1
203	CE 18:2	7.723586062	6.309651	0.011103	0.566572248
204	CE 18:3	1.206286734	5.223887	0.003661	1
205	CE 20:0	-4.994562047	3.988165	0.000862	0.674158815
206	CE 20:2	-3.008736357	5.801933	0.162221	1
207	CE 20:3	3.983741143	4.830236	0.001727	1
208	CE 20:4	10.12821816	5.102764	3.8E-06	0.214042624
209	CE 20:5	6.937525286	5.388956	4.46E-06	0.727051777
210	CE 22:1	2.641258345	3.972524	2.63E-05	1
211	CE 22:4	5.831542866	5.18902	0.01219	0.948588209
212	CE 22:5	15.69991043	4.939214	0.005241	0.005627857
213	CE 22:6	12.01398372	4.706688	2E-07	0.049432304
214	DG 14:0_18:1	19.24833711	8.049075	7.55E-11	0.164538205

215	DG 14:0_18:2	22.95791116	8.699296	7.37E-09	0.078701435
216	DG 16:0_16:0	19.97287742	7.683366	1.9E-09	0.142261088
217	DG 16:0_18:1	38.48183955	6.558215	8.61E-19	8.24242E-06
218	DG 16:0_18:2	40.15463103	6.915211	4.9E-19	5.07602E-06
219	DG 16:0_20:3	1.834435677	6.958992	0.001007	1
220	DG 16:0_20:4	-3.311908823	6.802796	0.002869	1
221	DG 16:0_22:5	25.67603328	7.617851	5.3E-10	0.00992384
222	DG 16:0_22:6	20.15112393	8.479431	1.52E-07	0.194234054
223	DG 16:1_18:1	34.67125432	6.628113	7.05E-18	2.85787E-05
224	DG 18:0_18:1	34.18598797	6.411108	3.43E-16	3.24475E-05
225	DG 18:0_18:2	36.65192181	6.620858	5.34E-18	1.12721E-05
226	DG 18:0_20:4	-11.99476135	5.024887	0.000119	0.052770527
227	DG 18:1_18:1	43.30994925	6.01164	5.25E-22	3.09313E-08
228	DG 18:1_18:2	49.19778728	6.121486	1.66E-24	9.72233E-10
229	DG 18:1_18:3	23.23057572	6.393994	1.77E-13	0.005560982
230	DG 18:1_20:3	-6.712095827	5.458722	0.036249	0.643245991
231	DG 18:1_20:4	-4.465630946	5.506689	0.014759	1
232	DG 18:2_18:2	52.25926499	6.433739	1.01E-21	2.65091E-09
233	TG 48:1	20.07617198	7.709503	2.98E-10	0.065692611
234	TG 48:2	30.75121869	8.025695	1.32E-12	0.003440104
235	TG 48:2	26.5543103	8.794203	1.08E-09	0.040655738
236	TG 48:3	30.91369093	9.444807	5.85E-11	0.021856533
237	TG 49:1	36.43240802	7.345799	4.17E-13	0.000153591
238	TG 50:1	23.67960008	6.419241	2.08E-13	0.001691672
239	TG 50:4	41.32699537	8.392284	3.72E-16	0.000116009
240	TG 48:2	20.66500977	7.767929	4.52E-11	0.048318797
241	TG 48:2	36.00457605	7.419666	1.43E-14	0.000244942
242	TG 50:3	23.67033236	6.38794	6.98E-11	0.002307643
243	TG 50:3	39.57415541	7.315263	5.05E-18	1.21987E-05
244	TG 49:1	38.37172219	7.312397	2.7E-14	3.31613E-05
245	TG 51:2	44.92665536	6.042331	2.19E-22	4.22883E-09
246	TG 48:0	21.06196675	8.322869	5.37E-07	0.144724787
247	TG 50:0	22.88181337	9.14226	6.64E-08	0.26681224
248	TG 50:1	34.12975983	6.143348	2.24E-15	1.20558E-05
249	TG 50:2	43.6623663	6.879351	6.73E-16	3.60729E-07
250	TG 49:1	33.02284224	7.355212	7.9E-13	0.000644764
251	TG 50:2	33.05216328	5.967834	7.36E-17	8.5588E-06
252	TG 51:0	29.14372179	6.819464	3.42E-15	0.001604389
253	TG 51:1	36.25534976	6.895097	8.9E-16	6.23963E-05
254	TG 51:2	38.29618273	6.387623	5.33E-18	1.76358E-06
255	TG 52:1	36.24039413	7.727465	2.36E-13	0.001243569
256	TG 52:2	34.91282021	5.400522	1.33E-18	2.45202E-07
257	TG 52:3	43.4739614	5.536346	1.26E-21	6.5084E-10
258	TG 52:4	51.51328988	6.862181	1.91E-19	2.11955E-08

259	TG 48:3	39.20961164	7.777756	1.08E-16	6.09843E-05
260	TG 50:2	18.05206067	7.943798	2.65E-09	0.156204614
261	TG 50:3	49.53232068	6.84555	1.96E-20	3.49644E-08
262	TG 51:2	39.30362869	6.250062	2.18E-18	5.20055E-07
263	TG 52:3	40.08264539	5.426333	1.08E-21	1.67408E-09
264	TG 52:4	47.9874062	6.681223	5.85E-21	3.87675E-08
265	TG 53:2	40.67217065	6.084799	3.62E-21	1.16425E-07
266	TG 54:1	28.88089797	8.058882	3.78E-05	0.145305171
267	TG 54:2	36.44454051	7.44791	6.42E-13	0.00028465
268	TG 54:4	40.08932226	6.842778	2.98E-14	2.43273E-06
269	TG 54:3	32.90503571	5.754264	3.49E-15	1.22806E-06
270	TG 54:4	41.50967796	6.187477	5.82E-17	3.96452E-08
271	TG 56:6	16.1944959	4.747271	4.29E-10	0.004714227
272	TG 58:8	28.33771259	6.271178	1.36E-11	0.00018474
273	TG 54:5	47.10381007	7.415272	2.06E-16	5.07055E-07
274	TG 54:6	50.07667626	8.707169	4.08E-13	1.28941E-05
275	TG 56:8	14.02521608	5.938154	2.45E-08	0.10568385
276	Acylcarnitine 2:0	-34.41950693	5.453055	3.37E-08	5.86583E-08
277	Acylcarnitine 14:0	-36.00464132	4.980773	4.39E-08	1.98993E-09
278	Acylcarnitine 16:0	-12.00517575	3.623203	0.001984	0.003880578
279	Acylcarnitine 18:0	-13.15864978	6.696838	0.309563	0.466927048
280	Acylcarnitine 18:2	-23.1248284	4.191424	1.42E-06	1.42828E-06
281	Acylcarnitine 20:0	-18.87260681	6.883796	0.030609	0.036978367
282	**FA 16:0**	**-54.12694866**	4.812023	3.85E-24	8.17032E-17
283	**FA 16:1**	**-78.44260637**	8.784793	8.4E-17	5.23713E-12
284	**FA 17:0**	**-57.65872801**	4.773403	9.81E-28	1.61968E-18
285	**FA 18:0**	**-31.26102102**	3.446169	1.12E-15	2.94867E-13
286	**FA 18:1**	**-78.84930588**	7.32569	1.92E-21	1.342E-14
287	**FA 18:2**	**-79.9401206**	7.502264	2.79E-21	1.52994E-14
288	**FA 18:3**	**-83.60263573**	8.343885	2.91E-20	7.12808E-14
289	**FA 20:4**	**-71.73697958**	6.11231	6.98E-25	4.18117E-17
290	**FA 20:5**	**-81.68809902**	7.508042	3.31E-23	7.87015E-16
291	**FA 22:6**	**-77.44447498**	6.575896	5.8E-23	4.42145E-16

p-value: A repeated measures ANOVA with a Greenhouse-Geisser correction.
*: Corrected *p*-value after adjustment for multiple comparisons using Bonferroni. Corrected $p<0.05$ are highlighted in light red.
SEM: Standard Error Mean

Supplementary Table S12: Association of lipid species with delta troponin at pre-PCI (*t0*). Related to Figure-3.4A

		Unstandardized Coefficients		**Standardized Coefficients**	**t-value**	***p*-value**	**95.0% CI for B**	
No	Lipids	B	Std. Error	Beta			Lower	Upper
1	**Acylcarnitine 18:2**	**4.87**	**2.23**	**0.28**	**2.182**	**0.033**	**0.41**	**9.32**
2	PI 32:0	-2.85	1.11	-0.33	-2.564	0.013	-5.07	-0.63
3	PE 38:6	-3.80	1.81	-0.28	-2.098	0.040	-7.42	-0.18
4	PI 34:1	-4.15	1.75	-0.30	-2.369	0.021	-7.64	-0.65
5	PI 38:6	-4.35	1.98	-0.31	-2.200	0.031	-8.29	-0.40
6	CE 22:4	-4.49	2.18	-0.26	-2.056	0.044	-8.85	-0.13
7	PE 36:4	-4.65	1.90	-0.29	-2.445	0.017	-8.46	-0.85
8	PI 36:1	-4.68	2.18	-0.27	-2.147	0.035	-9.03	-0.33
9	CE 16:0	-5.95	2.55	-0.28	-2.333	0.023	-11.03	-0.86
10	PC 32:0	-7.61	3.24	-0.29	-2.345	0.022	-14.09	-1.13

Linear regression (delta troponin) - adjusted for age, sex, body mass index (BMI), current smoking, diabetes history, and ischemic time (time from symptom onset to reperfusion)
Positive associations are shown in bold.

Supplementary Table S13: Association of lipid species with delta troponin at 2 h post-PCI (*t1*). Related to Figure-3.4B

		Unstandardized Coefficients		**Standardized Coefficients**	**t-value**	***p*-value**	**95.0% CI for B**	
No	Lipids	B	Std. Error	Beta			Lower	Upper
1	**SM 38:2**	**9.12**	**4.45**	**0.25**	**2.049**	**0.044**	**0.23**	**18.00**
2	**Acylcarnitine 18:2**	**6.10**	**1.85**	**0.40**	**3.295**	**0.002**	**2.40**	**9.79**
3	**FA 18:2**	**3.81**	**1.87**	**0.26**	**2.044**	**0.045**	**0.09**	**7.54**
4	TG 50:0	-1.79	0.75	-0.34	-2.387	0.020	-3.28	-0.29
5	TG 48:2	-1.94	0.95	-0.28	-2.035	0.046	-3.85	-0.04
6	TG 48:2	-1.97	0.96	-0.28	-2.051	0.044	-3.89	-0.05
7	TG 48:2	-2.03	0.99	-0.29	-2.053	0.044	-4.01	-0.06
8	TG 48:0	-2.04	0.83	-0.34	-2.455	0.017	-3.69	-0.38
9	TG 48:1	-2.17	0.99	-0.32	-2.181	0.033	-4.15	-0.18
10	TG 49:1	-2.18	1.04	-0.30	-2.106	0.039	-4.25	-0.11
11	TG 49:1	-2.21	1.01	-0.31	-2.179	0.033	-4.23	-0.19
12	TG 51:0	-2.34	1.01	-0.33	-2.322	0.023	-4.35	-0.33
13	TG 49:1	-2.43	1.00	-0.35	-2.423	0.018	-4.42	-0.43
14	CE 16:0	-4.54	2.10	-0.26	-2.160	0.034	-8.73	-0.34
15	PE 36:4	-4.97	2.25	-0.27	-2.213	0.030	-9.46	-0.49
16	PE(O-38:5)	-5.00	2.37	-0.26	-2.113	0.038	-9.73	-0.28
17	PE 38:4	-5.06	2.11	-0.29	-2.393	0.020	-9.28	-0.84
18	PE(O-38:4)	-5.25	2.41	-0.26	-2.182	0.033	-10.06	-0.45
19	SM 34:1	-7.72	3.24	-0.28	-2.383	0.020	-14.19	-1.25

Linear regression (delta troponin) - adjusted for age, sex, body mass index (BMI), current smoking, diabetes history, and ischemic time (time from symptom onset to reperfusion)
Positive associations are shown in bold.

Supplementary Table S14: Association of lipid species with delta troponin at 24 h post-PCI (*t2*). Related to Figure-3.4C

		Unstandardized Coefficients		Standardized Coefficients	t-value	p-value	95.0% CI for B	
No	Lipids	B	Std. Error	Beta			Lower	Upper
1	PI 34:0	-3.52	1.67	-0.27	-2.107	0.039	-6.86	-0.18
2	LPC 17:1	-4.21	1.99	-0.28	-2.113	0.038	-8.19	-0.23
3	LPC 18:0	-4.65	2.13	-0.27	-2.180	0.033	-8.90	-0.39
4	PC(O-36:4)	-8.02	3.39	-0.29	-2.367	0.021	-14.78	-1.26

Linear regression (delta troponin) - adjusted for age, sex, body mass index (BMI), current smoking, diabetes history, and ischemic time (time from symptom onset to reperfusion)

Supplementary Table S15: Clinical demographics for subgroup comparison based on change in troponin concentration ((Δ cTnT)			
	Low Tertile (n=27)	Top Tertile (n=27)	*p* value
Age(years)	63.44 (12.5)	68.14 (12.03)	0.165
Male sex (%)	20 (74.1)	16 (59.3)	0.248
LVEF (%)	58.5 (41.25, 69.25)	50 (40, 64)	0.438
Body mass index (kg/m^2)	26.77 (23.18, 34.71)	26.92(23.40, 28.70)	0.392
Comorbidity (%)			
Hypertension	15 (55.6)	12 (44.44)	0.414
Diabetes mellitus	6 (22.2)	2 (7.40)	0.125
Current smoker	10 (37)	7 (25.9)	0.379
Dyslipidemia	18 (66.7)	13 (48.1)	0.169
Hx of CAD	5 (18.5)	3 (11.1)	0.444
Laboratory data			
Triglyceride (mmol/l)	1.4 (0.85, 3.15)	1.2 (0.87, 1.42)	0.161
Cholesterol (mmol/l)	4.7 (4.15, 5.6)	4.95 (4.05, 5.70)	0.752
HDL cholesterol (mmol/l)	0.9 (0.7, 1.15)	1.2 (1.05, 1.55)	*0.019*
LDL cholesterol (mmol/l)	2.7 (2.2, 3.5)	3.0 (2.22, 3.55)	0.48
Creatinine (mmol/l)	86 (70, 104)	89 (78, 109)	0.368
Medications at baseline (%)			
ASA	7 (25.9)	5 (18.5)	0.513
ACEI/ARB	9 (33.3)	7 (25.9)	0.551
Beta blocker	4 (14.8)	4 (14.8)	1
Statin	9 (33.3)	8 (29.6)	0.77
Additional parameters			
Minutes from the onset of chest pain to reperfusion	161 (104, 395)	135 (80, 218)	0.426
Peak CK (Units/L)	331 (237.25, 578.5)	2679 (1803, 3450)	*<0.001*
Peak TnT (ng/L)	762 (499, 1145)	7175 (5740, 10000)	*<0.001*
Culprit vessel (%)			
LAD Infarct (%)	13 (48.1)	16 (59.3)	0.413
RCA Infarct (%)	12 (44.4)	8 (29.6)	0.26
Circumflex Infarct (%)	2 (7.4)	3 (11.1)	0.639

Values are reported as mean ± standard deviation (SD), median (25th, 75th percentiles), or count (percentage) as applicable. The Chi-square test was used for categorical variables, while Student's t-test or Mann-Whitney U test was used for continuous variables to assess for statistical significance across sample groups as applicable based on data distribution. Abbreviations: LVEF = left ventricular ejection fraction; Hx of CAD = history of coronary artery disease; HDL = high-density lipoprotein; LDL = low-density lipoprotein; ASA = Acetylsalicylic acid; ACEI = Angiotensin-converting enzyme (ACE) inhibitors; ARB = Angiotensin II receptor blockers; CK = Creatine kinase; TnT = troponin T; LAD = Left anterior descending coronary artery; RCA = Right coronary artery.

Supplementary Table S16: Logistic regression analysis
Dependent Variable: Delta troponin (two groups: "low (T1)" and "high (T3)" tertile)

								95% C.I.for EXP(B)	
Sl.No	**Time**	**Lipid**	**B**	**S.E.**	**Wald**	**p-value**	**Exp(B)**	**Lower**	**Upper**
1	*t0*	PI 34:1	-0.56	0.27	4.38	*0.036*	0.57	0.34	0.96
2	*t1*	AC 18:2	41.58	17.65	5.55	*0.018*	1.15E+18	1087.76	1.20964E+33
3	*t1*	TG 48:1	-1.46	0.60	5.93	*0.015*	0.23	0.07	0.75
4	*t1*	TG 48:2	-3.41	1.46	5.46	*0.019*	0.03	0.00	0.58
5	*t1*	TG 49:1	-6.20	2.69	5.30	*0.021*	0.00	0.00	0.40
6	*t1*	TG 48:2	-14.67	6.84	4.60	*0.032*	0.00	0.00	0.28
7	*t1*	TG 49:1	-12.37	5.32	5.42	*0.020*	0.00	0.00	0.14
8	*t1*	TG 48:0	-0.43	0.18	5.65	*0.017*	0.65	0.46	0.93
9	*t1*	TG 50:0	-1.28	0.58	4.91	*0.027*	0.28	0.09	0.86
10	*t1*	TG 49:1	-5.96	2.51	5.66	*0.017*	0.00	0.00	0.35
11	*t1*	TG 51:0	-47.62	20.64	5.32	*0.021*	0.00	0.00	0.00
12	*t2*	LPC 17:1	-3.85	1.95	3.88	*0.049*	0.02	0.00	0.98
13	*t2*	PI 34:0	-7.20	3.24	4.93	*0.026*	0.00	0.00	0.43

A logistic regression was performed to ascertain the effects of HDL on delta troponin groups. All models are adjusting for HDL. **Abbreviation**: Wald, Wald chi-square test; B, intercept; S.E, standard error; Exp(B), exponentiation of the B coefficient

Supplementary Table S17: Clinical demographics for subgroup comparison based on major adverse cardiovascular event (MACE)			
	No MACE (n=67)	MACE (n=13)	*p value*
Age(years)	63.01 ± 12.28	67.30 ± 11.62	0.249
Male sex (%)	44 (65.7)	10 (76.9)	0.428
LVEF (%)	61 (55, 70)	35 (34.25, 43.75)	<0.001
Body mass index (kg/m^2)	28 (24.55, 32.59)	23.70 (21.82, 30.84)	0.077
Comorbidity (%)			
Hypertension	32 (47.8)	5 (38.5)	0.538
Diabetes mellitus	15 (22.4)	1 (7.7)	0.225
Current smoker	15 (22.4)	7 (53.8)	0.02
Dyslipidemia	33 (49.3)	9 (69.2)	0.187
Hx of CAD	9 (13.4)	2 (15.4)	0.852
Laboratory data			
Triglyceride (mmol/l)	1.4 (1.0, 2.22)	1.0 (0.8, 1.47)	0.133
Cholesterol (mmol/l)	4.85 (4.1, 5.42)	4.3 (2.95, 5.12)	0.225
HDL cholesterol (mmol/l)	1.1 (0.9, 1.30)	1.3 (0.77, 1.57)	0.351
LDL cholesterol (mmol/l)	2.8 (2.02, 3.47)	2.4 (1.25, 3.15)	0.27
Creatinine (mmol/l)	89 (71, 104)	86 (64, 118)	0.819
Medications at baseline (%)			
ASA	13 (19.4)	5 (38.5)	0.132
ACEI/ARB	16 (23.9)	4 (30.8)	0.6
Beta blocker	5 (7.5)	3 (23.1)	0.086
Statin	15 (22.4)	5 (38.5)	0.221
Additional parameters			
Minutes from the onset of chest pain to reperfusion	146 (86, 99)	166 (250, 217)	0.896
Peak CK (Units/L)	906 (373.5, 1516.5)	3450 (352.0, 5836.5)	0.036
Peak TnT (ng/L)	1889 (994, 3867)	5813 (1997, 10000)	0.016
Culprit vessel (%)			
LAD Infarct (%)	27 (40.3)	9 (69.2)	0.055
RCA Infarct (%)	33 (49.3)	4 (30.8)	0.221
Circumflex Infarct (%)	10 (14.9)	0 (0)	0.136

Values are reported as mean ± standard deviation (SD), median (25th, 75th percentiles), or count (percentage) as applicable. The Chi-square test was used for categorical variables, while Student's t-test or Mann-Whitney U test was used for continuous variables to assess for statistical significance across sample groups as applicable based on data distribution. Abbreviations: LVEF = left ventricular ejection fraction; Hx of CAD = history of coronary artery disease; HDL = high-density lipoprotein; LDL = low-density lipoprotein; ASA = Acetylsalicylic acid; ACEI = Angiotensin-converting enzyme (ACE) inhibitors; ARB = Angiotensin II receptor blockers; CK = Creatine kinase; TnT = troponin T; LAD = Left anterior descending coronary artery; RCA = Right coronary artery.

CHAPTER 4. Lipidomic predictors of coronary no-reflow

Rationale

Despite re-opening the culprit epicardial coronary artery, a group of STEMI patients may experience inadequate myocardial perfusion, known as no-reflow. No-reflow is associated with adverse clinical events, including death. This unique phenomenon is still poorly understood, and no single effective treatment for no-reflow exists.

No-reflow begins with ischemic insult and intensifies at the reperfusion time. Our previous non-targeted and targeted metabolomics analysis demonstrated that lipid-related disturbances play a vital role in myocardial ischemia and reperfusion. Also, since lipids play a role in vasoreactivity, platelet activity, and thrombus formation, we aimed to understand the role of lipid molecules in the no-reflow phenomenon. Herein, mass spectrometry-based lipid profiling was used to investigate the lipid changes associated with no-reflow and correlate these changes with clinical parameters representing coronary no-reflow in the clinical setting.

Lipidomic predictors of coronary no-reflow

Arun Surendran[1,3,4], Umar Ismail[4,6], Negar Atefi[1], Ashim K Bagchi[5], Pawan K Singal[4], Ashish Shah[4,6], Michel Aliani[2], and Amir Ravandi[1,4,6]

[1]Cardiovascular Lipidomics Laboratory, St. Boniface Hospital, Albrechtsen Research Centre, Winnipeg, Canada, [2]Faculty of Agricultural and Food Sciences, University of Manitoba, Winnipeg, Canada, [3]Mass Spectrometry and Proteomics Core Facility, Rajiv Gandhi Centre for Biotechnology, Kerala, India, [4]Department of Physiology and Pathophysiology, Rady Faculty of Health Sciences, University of Manitoba, Winnipeg, Canada, [6]Department of Internal Medicine, University of Arkansas for Medical Sciences, Arkansas, USA. [6]Section of Cardiology, Department of Medicine, Rady Faculty of Health Sciences, University of Manitoba, Winnipeg, Canada,

Submitted: Journal of Lipid Research

Corresponding author & Lead Contact
Dr. Amir Ravandi MD PhD FRCPC
Interventional Cardiology
Cardiovascular Lipidomics Laboratory,
St. Boniface Hospital,
409 Tache Ave,
Winnipeg, MB Canada R2H 2A6

Phone.204-235-3206 and 204-235-3414
Fax.204-235-0793 and 204-235-0793

Email: aravandi@sbgh.mb.ca

4.1 Abstract

Background: The 'no-reflow' phenomenon (NRP) after primary percutaneous coronary intervention (PCI) is a serious complication among acute ST-segment elevation myocardial infarction (STEMI) patients. Lipidomic profiling offers the prospect of revealing no-reflow-associated lipid signatures and improving risk assessment.

Methods: A comprehensive lipidomics approach was used to quantify over 300 distinct molecular species in circulating plasma from 126 patients with ST-elevation myocardial infarction (STEMI) before and after primary PCI. The patients were grouped into normal flow and no-reflow based on their corrected TIMI frame count (CTFC) after PCI.

Results: Three lipid classes: phosphatidylcholine (PC), alkylphosphatidylcholine (PC(O)), and sphingomyelin (SM), were significantly elevated ($p<0.05$) in no-reflow patients before primary PCI. The levels of individual fatty acids and total fatty acid levels were significantly lower ($p<0.05$) in no-reflow subjects after PCI. The grouping of patients based on ECG ST-segment resolution (STR) also demonstrated the same trend, confirming the possible role of these differential lipids in the setting of no-reflow. Time-dependent analysis showed that ten of these lipids were also significantly different ($p<0.05$) between pre-PCI and post-PCI time intervals. Sphingomyelin species, SM 41:1 and SM 41:2 were invariably positively correlated with CTFC at pre-PCI and post-PCI. The plasma levels of SM 42:1 exhibited an inverse association ($p<0.05$) consistently with tumor necrosis factor-alpha (TNF-α) at pre-PCI and post-PCI, implying a role for sphingomyelin species in the regulation of immune response in no-reflow.

Conclusions: Our study identified plasma lipid profiles that distinguish individuals at risk of no-reflow and provided novel insights into how dyslipidemia may contribute to NRP after primary PCI.

4.2 Graphical abstract

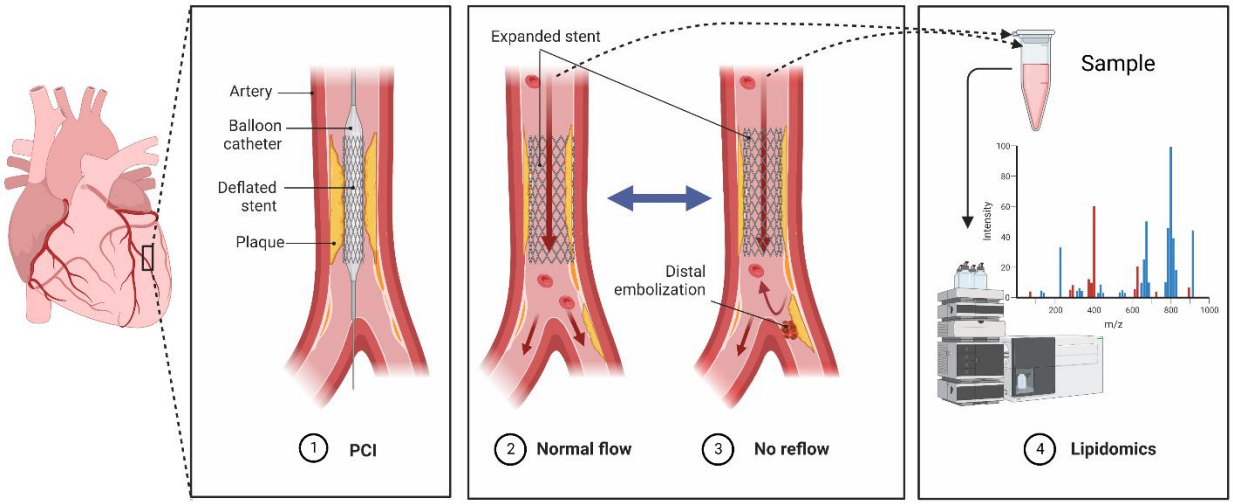

Keywords: No-reflow, lipidomics, sphingomyelin, ether-lipids

4.3 Abbreviations

NRP, ‘no-reflow’ phenomenon; PCI, primary percutaneous coronary intervention; STEMI, ST-segment elevation myocardial infarction; TIMI, thrombolysis in myocardial infarction; CTFC, corrected TIMI frame count; PC, phosphatidylcholine; PC(O), alkylphosphatidylcholine; SM, sphingomyelin; STR, ST-segment resolution; TNF-α, tumor necrosis factor-alpha; IR, ischemia/reperfusion

4.4 Introduction

Primary percutaneous coronary intervention (PCI) is the choice of revascularisation strategy for ST-segment elevation myocardial infarction (STEMI) patients. Nevertheless, myocardial tissue fails to perfuse normally in a small proportion of patients despite the infarct-related artery reopening, a phenomenon known as 'no-/slow-reflow.' No-reflow after PCI results in larger infarct size[1] and is influenced by the duration of ischemia and reperfusion[2]. According to various reports, no-reflow occurs in more than 30% of all patients after PCI[3,4]. Once it happens, it attenuates the beneficial effect of reperfusion therapy and hurts clinical outcomes. To date, the exact pathophysiological mechanisms underlying no-reflow phenomenon (NRP) remains incomplete.

The NRP is associated with several factors, including atherosclerotic plaque rupture, atheroembolism, ischemic injury, reperfusion injury, and vascular endothelial dysfunction[5]. Previous intravascular imaging studies have demonstrated that the lipid burden of the atherosclerotic plaque is a major discriminator between no-reflow and normal flow in STEMI patients[6]. Furthermore, it has also been reported that the release of plaque contents, including cholesterol crystals, results in embolization of the distal vessels and contributes to no-reflow[7]. This evidence shows that lipid-related disturbances are closely associated with the initiation and progression of no-reflow, and thus, NRP is a suitable candidate for lipidomics studies.

It is now well established that plasma lipids outperform traditional lipid measures (total cholesterol, HDL-C, LDL-C, and total triglycerides) as markers for cardiovascular risk[8,9]. Our previous non-targeted metabolomics analysis in STEMI patients showed that lipids formed the bulk of the altered metabolomic profile in a clinical setting of ischemia/reperfusion (IR) injury[10]. Also, we showed that selected lipid species could serve as markers of myocardial infarct size. More recently, in lipidomics on the plasma of STEMI patients, we showed that human plasma

lipidome rapidly shifts during myocardial ischemia and reperfusion, and specific lipids could predict future cardiovascular events[11]. These studies show that lipid metabolism is perturbed in STEMI patients following PCI. However, no studies have investigated the association between circulating lipids and NRP in STEMI patients after PCI. Here, we aim to do an in-depth lipidomics analysis of human plasma to understand lipids' role in a no-reflow clinical setting.

4.5 Materials and methods

4.5.1 Study population

A total of 126 patients undergoing PCI for STEMI in St. Boniface Hospital between January 2017 and June 2020 were included in the study. Venous blood samples were taken from each patient at the time of presentation (pre-PCI) and 2 h post successful reperfusion (2 h post-PCI). Patients were diagnosed as STEMI based on chest pain onset, confirmation of ST-elevation on 12 lead surface EKG on admission, and documentation of occluded coronary artery with coronary angiography. Blood samples were collected into tubes containing EDTA, and after centrifugation (2,500 × g, 5 min, 4 °C), the extracted plasma samples were immediately stored at −80 °C until needed. The mean time from blood collection to storage at −80 °C was under 20 min. The informed consent was obtained from all patients. The University of Manitoba and the St. Boniface Hospital Research ethics boards accepted the study protocol and complied with the Declaration of Helsinki.

For each patient, the no-reflow was defined using the corrected TIMI frame count (CTFC) and surface electrocardiography (ECG). The CTFC method, first described by Gibson et al., provides a quantitative assessment of the coronary artery flow[13]. The number of cine frames (at a fluoroscopic rate of 30 frames per second) required for the contrast agent to reach a standardized anatomic landmark in the infarct-related artery was referred to as the CTFC[13]. The cine angiographic examination was initially recorded in the cardiac catheterization laboratory at a rate

of 7.5 and 15 frames per second. It was then corrected to 30 frames per second to obtain the CTFC value.

4.5.2 Lipid analysis

Frozen plasma samples were thawed for nearly 20 min. Lipids were extracted using chloroform and methanol as previously described[11,14]. Briefly, 10 µl of plasma was added to 200 µl of chloroform/methanol (2:1, v/v) along with 30 µl of internal lipid standards (ISTD) in Eppendorf tubes, vortexed for 10 min, and sonicated in a water bath at room temperature (RT) for 30 min. The mixture was allowed to settle for 20 min, after which it was centrifuged at 20,000g for 20 min at RT. The lipid-containing top layer was later transferred to a new Eppendorf tube and dried under a gentle stream of nitrogen gas (~1 h). The dried samples were then resuspended in 50 µl of water-saturated 1-butanol and sonicated for 10 min, followed by adding 50 µl of 10 mM ammonium formate in methanol. Finally, the extract was spun (10,000g for 10 min at RT), and the supernatant (80 µL) was transferred into glass vials with inserts. The samples were randomized prior to LC/MS analysis. The lipidomic profiling was performed using a Prominence chromatographic system (Shimadzu Corporation, OR, USA) coupled with an AbSciex 4000 QTRAP triple quadrupole mass spectrometer. The entire LC/MS methodology for this work, including details of ISTD, quality control, and data processing, are described in detail in our previously published work[11].

4.5.3 Cytokine analysis

Plasma cytokine levels were determined using a custom Meso Scale Discovery kit (MSD, Meso Scale Diagnostics, Rockville, MD, United States) according to the instructions by the manufacturer. The assays were done in 96-well formats, with ten spots per well. The multiplex panel used a single protocol for the simultaneous quantification of 10 analytes, including interleukins (IL) -1β, 6, 8, 10, tumor necrosis factor-alpha (TNF-α), interferon (IFN)-γ,

macrophage inflammatory protein (MIP-1α), interferon-γ-induced protein (IP-10), monocyte chemoattractant protein (MCP-1) and stromal cell-derived factor-1α (SDF-1α). Plates were read with an MSD instrument, and the final values were obtained in pg/ml. Samples with values outside assay range were excluded from the analysis.

4.5.4 Data normalization

The pre-normalized data was imported into the Mass Profiler Professional (MPP; 12.6) software, and the data were normalized using the 'percentile shift' normalization procedure (default 75th percentile). This is a global normalization procedure in which all intensity values in a sample are adjusted. The data was further filtered by omitting the low-intensity values. To this effect, the upper and lower cut-off values for normalized intensity values were set to 100 percent and 20 percent, respectively.

4.5.5 Statistical analysis

The baseline demographics and clinical characteristics of patients in **Table-4.1** are represented as mean value plus or minus standard deviation (SD) for continuous variables with normal distribution, median (25th, 75th percentiles) for continuous variables with non-normal distribution, and count (%) for categorical variables. The data normality was tested with the Shapiro-Wilk test. Differences in means of these parameters were examined using a student's t-test or Mann-Whitney test (for continuous variables), or Chi-square test (for categorical variables) where applicable.

Lipid concentrations were log-transformed before the statistical analysis. The differences in plasma lipid levels between normal and no-reflow subjects were assessed from an independent Student's t-test. The adjustment for multiple testing was made using a false discovery rate (FDR) approach using the Benjamini-Hochberg method[15]. The adjusted p-value (Q-value) cut-off was set to 0.2. All statistical analyses were conducted using the IBM Statistical Package for the Social

Sciences (SPSS v24), and a p-value < 0.05 was considered statistically significant unless stated otherwise.

4.6 Results

4.6.1 Baseline characteristics

Table-4.1 shows the study participants' demographic, clinical, and laboratory characteristics stratified by CTFC. The subjects were divided into the normal flow and no-reflow groups according to the top CTFC tertile (≥30 frames/second) versus combined middle and bottom tertiles (CTFC <30 frames/second). Patients in the no-reflow group were well balanced compared with the normal flow group for age, sex, BMI, and other risk factors (frequency of hypertension, diabetes mellitus, current smoking, dyslipidemia). Similarly, baseline lipid profile and concomitant medications (frequency of acetylsalicylic acid, angiotensin-converting enzyme inhibitor, β-blockers, statin) were comparable between the two groups. As expected, the no-reflow patients have a significantly longer time from symptom onset to PCI and a much higher post-PCI CTFC. The two groups also had comparable blood plasma levels of creatine kinase (peak CK) and cardiac troponin T (peak TnT), biomarkers of myocardial tissue injury.

Table-4.1: Baseline characteristics of the study participants			
	Normal flow	**No-reflow**	
	Tertile-1&2 (n=83)	**Tertile-3 (n=43)**	**p value**
Age(years)	62 (51, 74)	62 (58, 69)	0.75
Male sex (%)	61 (73.5)	36 (83.7)	0.196
LVEF (%)	60 (44.7, 68.2)	58.5 (43, 66.2)	0.431
Body mass index (kg/m^2)	27.4 (23.5, 31.2)	28.8 (26.3, 32.8)	0.148
Comorbidity (%)			
Hypertension	29 (34.9)	21 (48.8)	0.131
Diabetes mellitus	17 (20.5)	7 (16.3)	0.569
Current smoker	29 (34.9)	10 (23.3)	0.179
Dyslipidemia	43 (51.8)	17 (39.5)	0.191
Hx of CAD	17 (20.5)	6 (14.0)	0.368
Laboratory data			
Triglyceride (mmol/l)	1.4 (1, 2.3)	1.2 (1, 1.9)	0.421
Cholesterol (mmol/l)	4.58 ± 1.15	4.62 ± 1.16	0.889
HDL cholesterol (mmol/l)	1.1 (0.9, 1.4)	1.0 (0.85, 1.3)	0.589
LDL cholesterol (mmol/l)	2.6 (1.7, 3.3)	2.8 (2.1, 3.5)	0.244
Creatinine (mmol/l)	85.5 (72, 102.5)	94 (78, 114)	0.113
Medications at baseline (%)			
ASA	21 (25.3)	9 (20.9)	0.585
ACEI/ARB	17 (20.5)	11 (25.6)	0.514

Beta blocker	10 (12)	3 (7)	0.375
Statin	23 (27.7)	7 (16.3)	0.153
Additional parameters			
CTFC (frames)	20 (16, 24)	40 (35.3, 49.4)	*<0.0001*
Ischemic time (min)	163 (105, 244)	247 (125, 479)	*0.027*
Peak CK (Units/L)	949 (373, 2591)	1224 (676, 3092)	0.213
Peak TnT (ng/L)	2259 (882, 5791)	3575 (1229, 8689)	0.093
Culprit vessel (%)			
LAD Infarct (%)	35 (42.2)	22 (51.2)	0.336
RCA Infarct (%)	43 (51.8)	12 (27.9)	*0.01*
Circumflex Infarct (%)	7 (8.4)	10 (23.3)	*0.021*

Values are reported as mean ± standard deviation (SD), median (25th, 75th percentiles), or count (percentage) as applicable. The Chi-square test was used for categorical variables, while Student's t-test or Mann-Whitney U test was used for continuous variables to assess for statistical significance across sample groups as applicable based on data distribution.

Abbreviations: CTFC = corrected TIMI frame count; LVEF = left ventricular ejection fraction; Hx of CAD = history of coronary artery disease; HDL = high-density lipoprotein; LDL = low-density lipoprotein; ASA = Acetylsalicylic acid; ACEI = Angiotensin-converting enzyme (ACE) inhibitors; ARB = Angiotensin II receptor blockers; CK = Creatine kinase; TnT = troponin T; LAD = Left anterior descending coronary artery; RCA = Right coronary artery.

4.6.2 Plasma lipidome alterations in the setting of the NRP

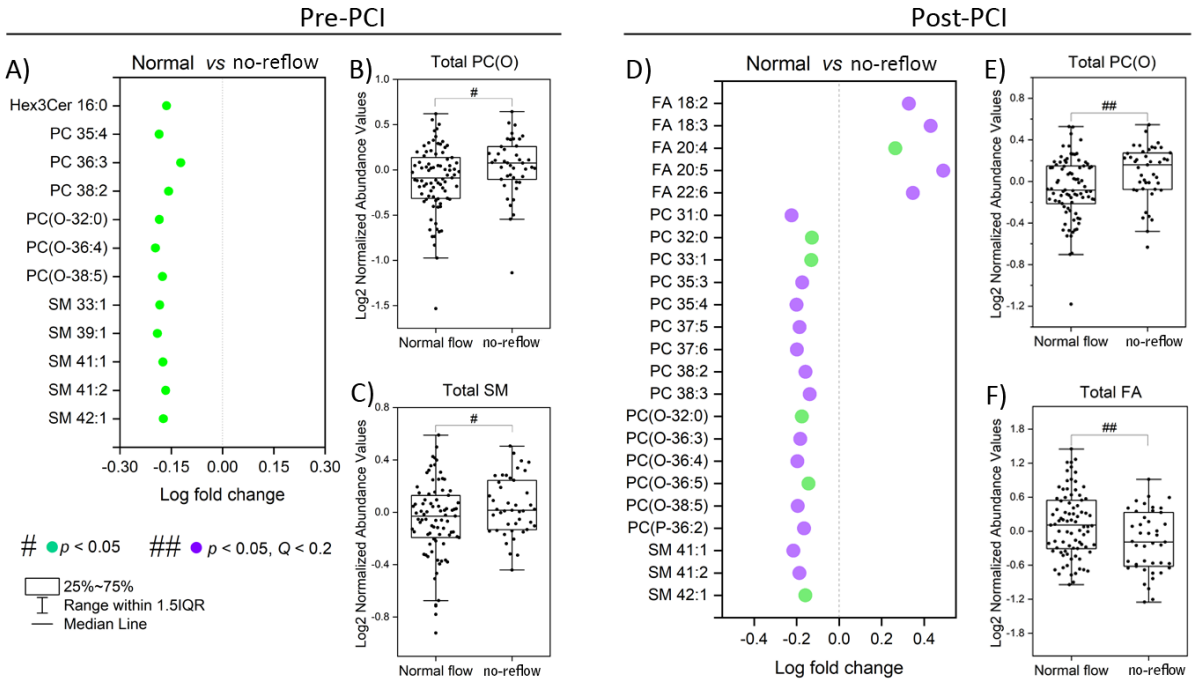

Figure-4.1: Altered lipid species and classes during the coronary no-reflow phenomenon. (A) The significantly altered lipid species between normal and no-reflow subjects at pre-PCI. (B, C) Boxplots of the abundance of lipid classes significantly differed between normal and no-reflow subjects at pre-PCI. (D) The significantly altered lipid species between normal and no-reflow subjects at post-PCI. (E, F) Boxplots of the abundance of lipid classes significantly differed between normal and no-reflow subjects at post-PCI. Green circles show lipid species with $p < 0.05$, and purple circles show lipid species with Q (corrected p) < 0.2 after independent Student's t-test. # and ## represent statistical significance at $p < 0.05$ and $Q < 0.2$ after independent Student's t-test.

Figure-4.1 shows the lipids significantly perturbed ($p<0.05$) in no-reflow patients compared to normal flow patients at pre-PCI and post-PCI. Twelve lipid species were elevated considerably ($p<0.05$) in no-reflow patients compared to normal flow patients at pre-PCI (**Figure-4.1A**). They

mainly belong to phosphatidylcholine (PC), alkylphosphatidylcholine (PC(O)), and sphingomyelin (SM) classes. In addition, the total amount of two lipid classes, PC(O) and SM, was significantly higher ($p<0.05$) in no-reflow patients than in normal flow patients (**Figure-4.1B, 4.1C**). Consistent with pre-PCI, 17 lipid species belonging to PC, PC(O), and SM lipid classes were also significantly elevated in no-reflow patients at post-PCI (**Figure-4.1D**). Surprisingly, fatty acids (FA) exhibited a reverse trend at post-PCI. The levels of five fatty acids (FA 18:2, FA 18:3, FA 20:4, FA 20:5, and FA 22:6), as well as the total fatty acid amount (**Figure-4.1D, 4.1F**), were significantly lower ($p<0.05$) in no-reflow patients than normal flow patients at post-PCI, even after correction for multiple testing ($Q<0.2$).

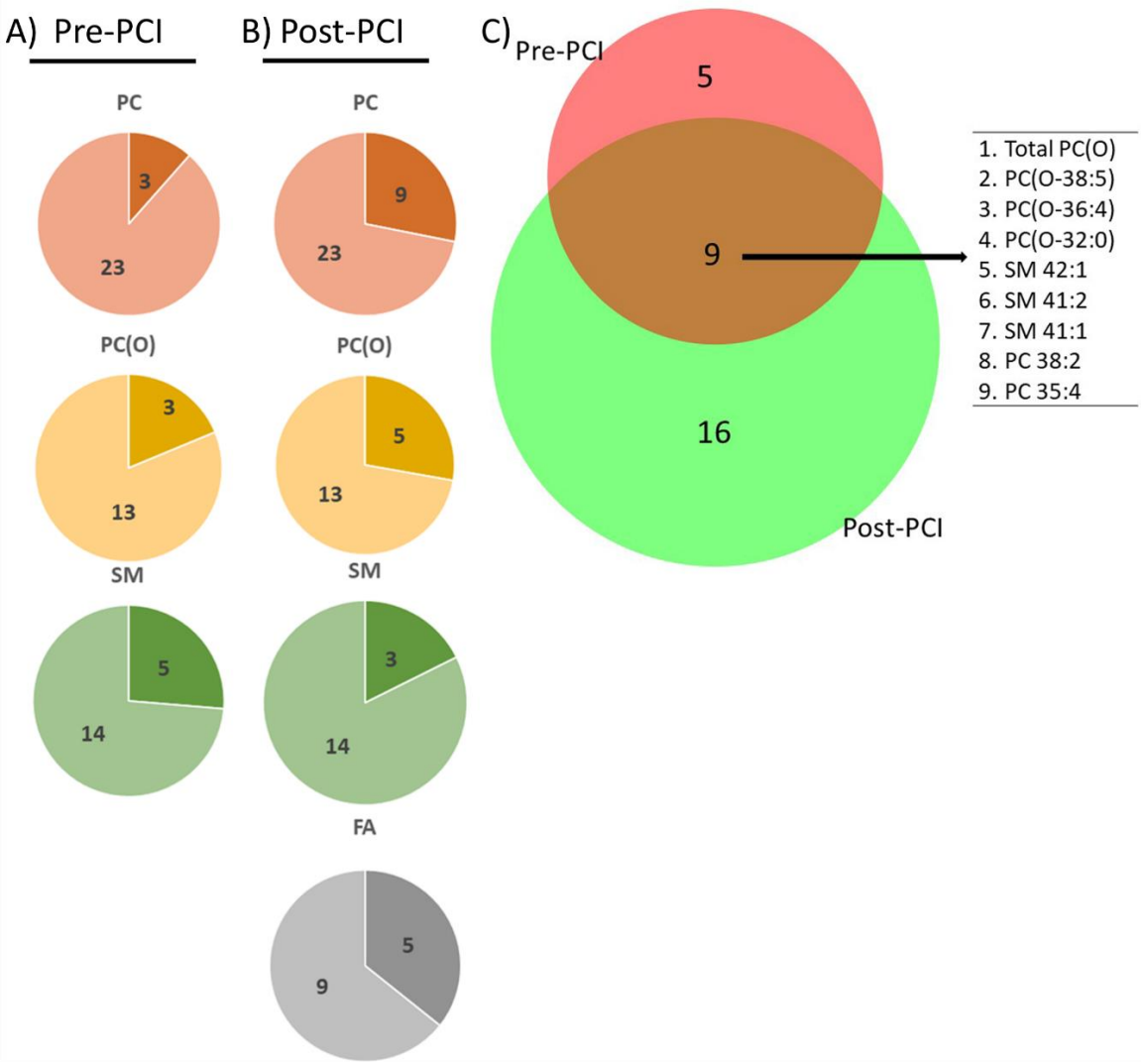

Figure-4.2: Lipids at pre- and post-PCI. The number of significantly altered lipid species (shown in a darker shade) at (A) pre-PCI and (B) post-PCI as parts of the corresponding whole lipid class between normal and no-reflow patients. Here, the number shown in the lighter shade represents the total number of lipid species in that particular class. (C) Venn diagram shows the number of significantly altered lipid species ($p < 0.05$) unique or common between pre-PCI and post-PCI.

At pre-PCI and post-PCI, we detected 12 and 23 differentially expressed lipid species between normal and no-reflow patients, amounting to less than 1 % of all measured lipid species (322

lipids). On the species level, 13% of PC, 23% of PC(O), and 35% of SM were altered at pre-PCI (**Figure-4.2A**), whereas 39% of PC, 38% of PC(O), 21% of SM, and 55% of FA were altered at post-PCI (**Figure-4.2B**). Notably, eight lipid species (excluding total PC (O)), including two PC species (PC 35:4 and PC 38:2), three SM species (SM 41:1, SM 41:2, and SM 42:1), and three PC(O) species (PC(O-32:0), PC(O-36:4), and PC(O-38:5)) were significantly altered ($p<0.05$) between normal and no-reflow patients at both pre-PCI and post-PCI time intervals (**Figure-4.2C**). The total PC(O) amount is also significantly altered at pre-PCI and post-PCI (**Figure-4.2C**).

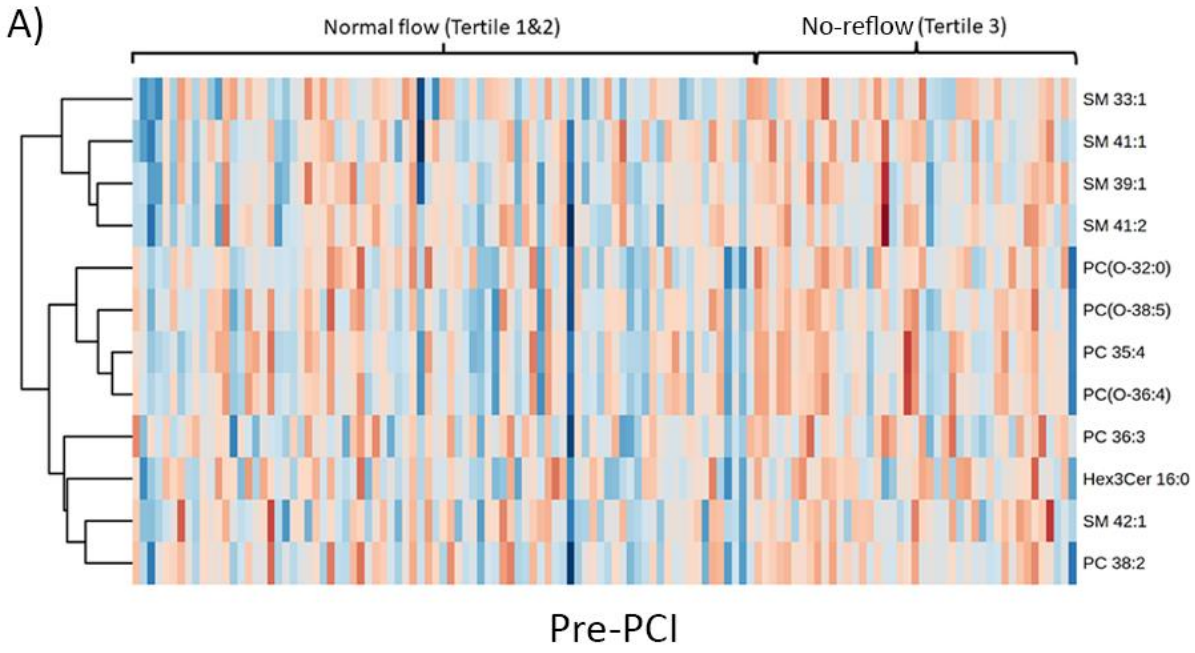

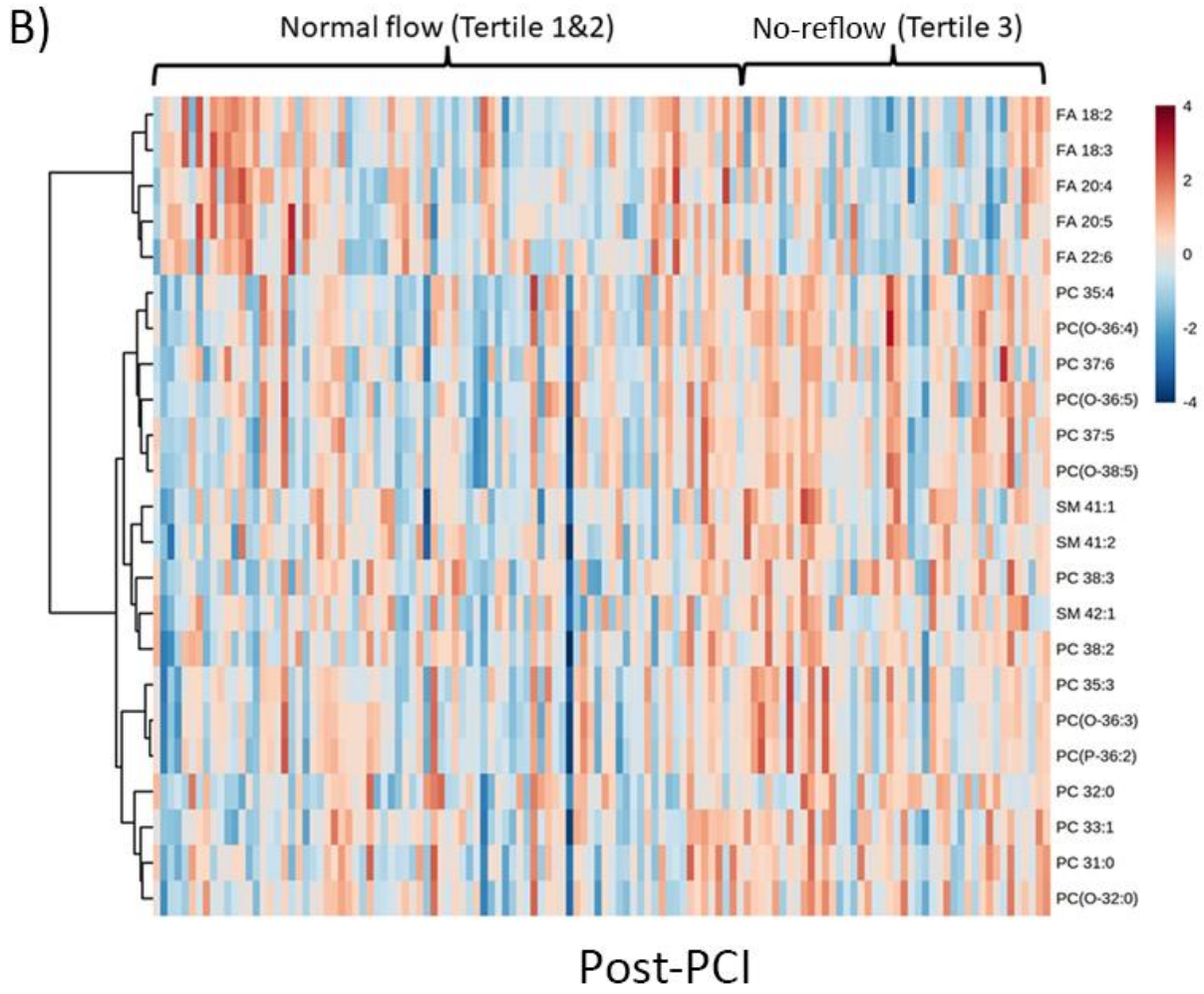

Figure-4.3: Clustered heatmap of significantly altered lipid species. A hierarchically clustered heat map representing significantly altered lipid species ($p < 0.05$) between normal and no-reflow subjects at (A) pre-PCI and (B) at post-PCI. Data were normalized, log-transformed, and auto scaled.

A heatmap of statistically significant lipids (**Figure-4.3**) was constructed to visualize the intensity variations between the normal and no-reflow patients at pre-PCI and post-PCI. The heatmap was generated (using default parameters) using the web-based tool MetaboAnalyst (www.metaboanalyst.ca). Except for fatty acids, the levels of all other lipids were generally higher

in the no-reflow group than in the normal flow group during both periods (**Figure-4.3A, 4.3B**). Interestingly, the fatty acid profile was distinct from the rest of the lipids at post-PCI. In the heatmap, related lipids are grouped by hierarchical clustering. Notably, all the fatty acids exhibited a tight clustering post-PCI (**Figure-4.3B**), indicating their similarity in action after reperfusion.

4.6.3 Association of clinical parameters of no-reflow with circulating lipids

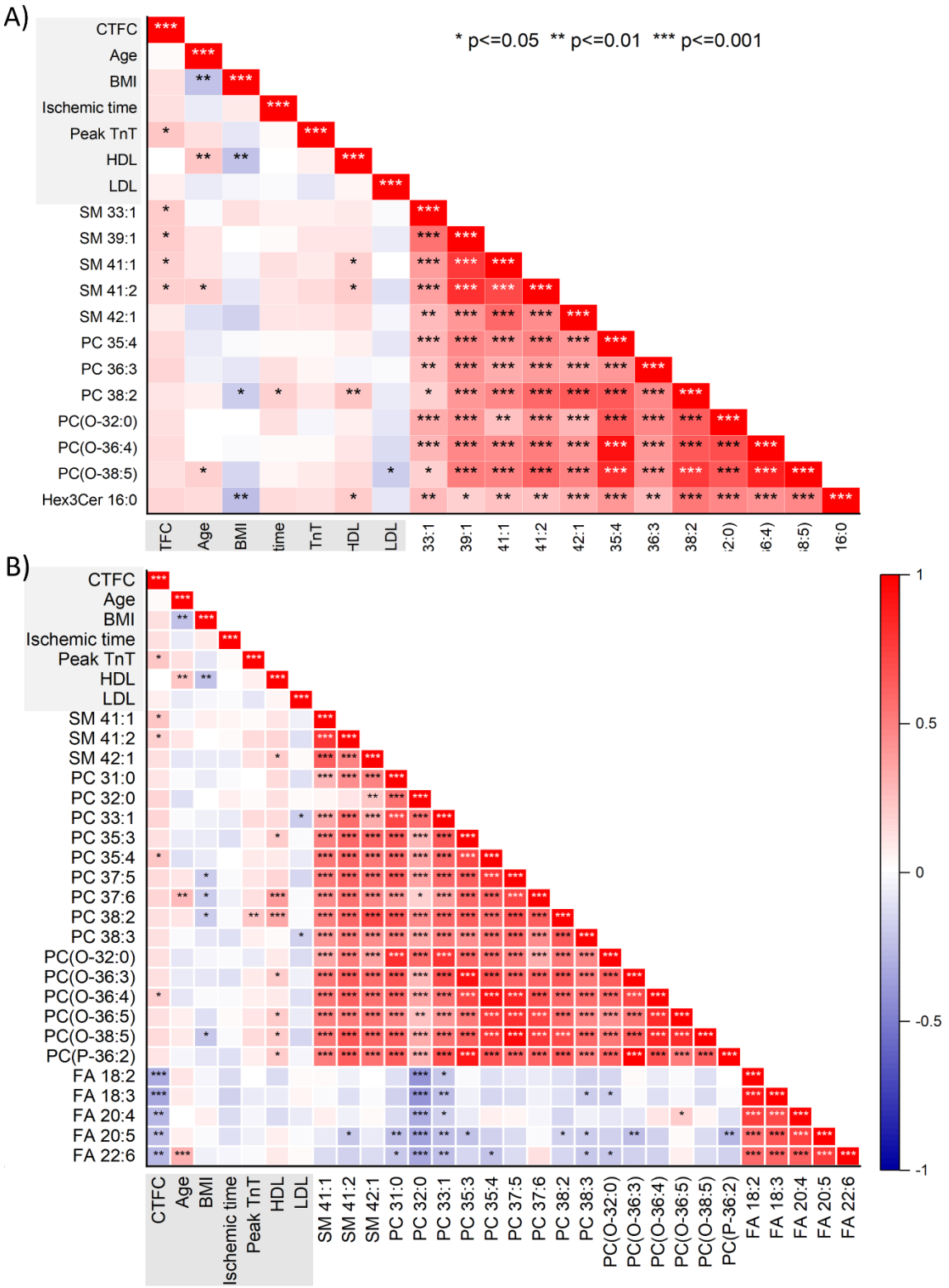

Figure-4.4: Correlation between lipid species and clinical parameters. The correlation plots depict the strength of the relationship (Pearson correlation) between significantly altered lipid species ($p < 0.05$) in the no-reflow patients and clinical parameters at (A) pre-PCI and (B) post-PCI. Positive correlations are displayed in red and negative correlations in blue. *, **, *** represents the significant level at $p < 0.05$, 0.01, 0.001 respectively.

The results of correlation analysis (Pearson correlation) between circulating lipids and the clinical factors associated with no-reflow were illustrated as a correlation matrix (**Figure-4.4)**. The correlation analysis displayed two clusters, 1) a cluster with all no-reflow-associated PC, PC(O), and SM species and 2) a cluster with fatty acids alone. The PC, PC(O), and SM species were positively associated ($p< 0.001$) with each other and among themselves at pre-PCI and post-PCI. The fatty acids were positively associated ($p< 0.001$) with each other at post-PCI but not with other no-reflow-associated lipids. The correlation analysis also revealed a significant ($p<0.05$) positive correlation between CTFC and two SM species, namely SM 41:1 and 41:2 at pre-PCI and post-PCI. The post-PCI levels of all fatty acids exhibited inverse correlations with CTFC ($p<0.01$).

4.6.4 Temporal perturbations in no-reflow associated lipid species

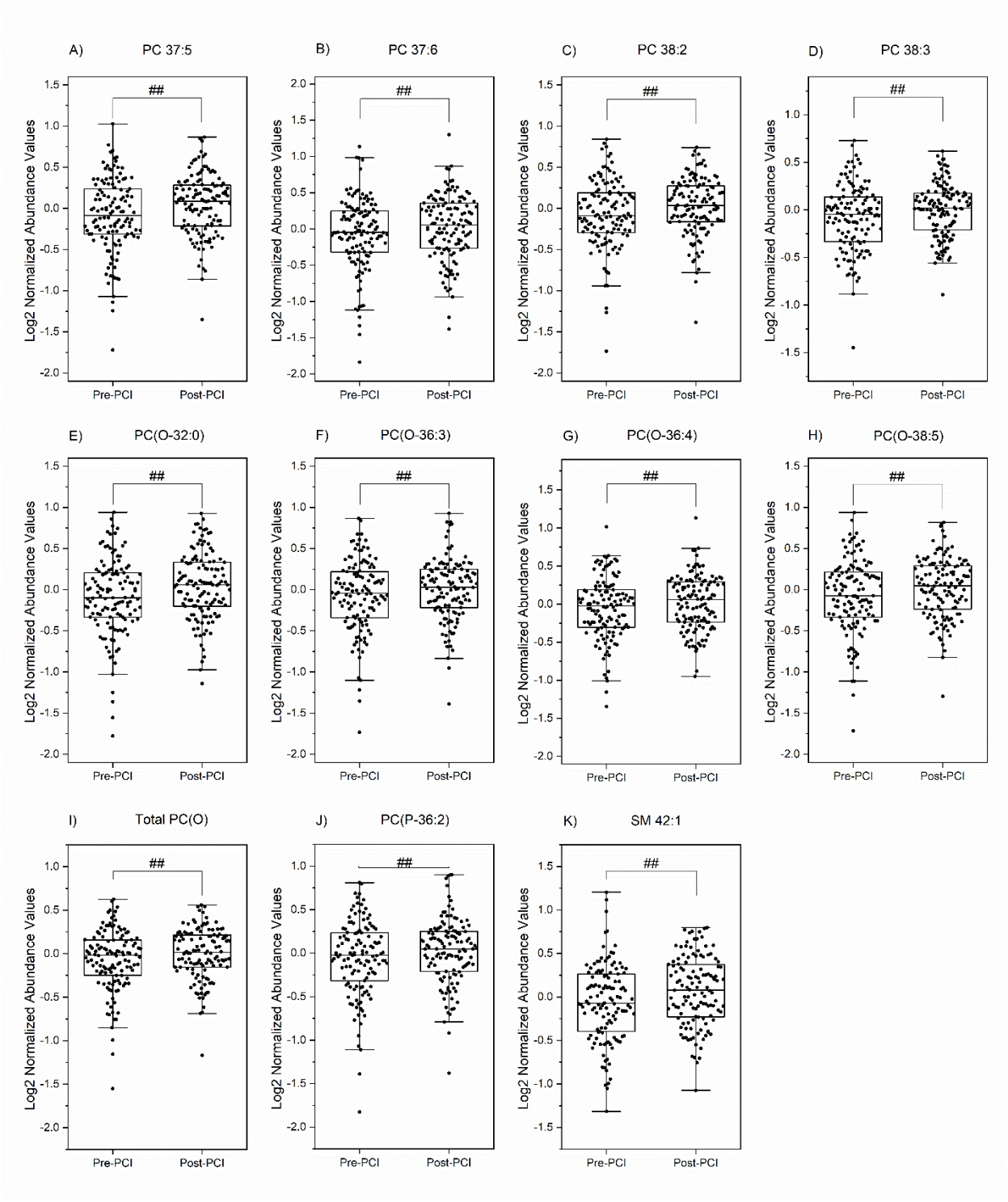

Figure-4.5: Time-dependent changes in no-reflow associated lipid species. The box plots show the significantly altered lipid species ($p < 0.05$) in time (between pre-PCI and post-PCI). A paired

t-test was run on the list of 26 lipids and four lipid classes (significantly different between normal and no-reflow patients) to determine whether there was a statistically significant difference in time. ## represents the significant level at Q (corrected p) < 0.05.

We next investigated the changes over time in select lipid species which were predicted to play essential roles in the setting of NRP. Of the total 26 lipids that were differentially abundant between normal and no-reflow patients based on CTFC, ten lipids were also significantly different (Q < 0.05) between pre- and post-PCI (**Figure-4.5)**. Interestingly, these included four PC species (PC 37:5, PC 37:6, PC 38:2, and PC 38:3) and four PC(O) species (PC(O-32:0), PC(O-36:3), PC(O-36:4), and PC(O-38:5))). The total PC(O) amount is also significantly altered between pre- and post-PCI.

4.6.5 Association of lipids with ST-segment resolution (STR)

ST-segment monitoring in serial ECG is another simple means of assessing myocardial perfusion following PCI[16]. ST-segment resolution (STR) is increasingly used in clinical research as a marker of no-reflow. We then explored whether the lipids associated with CTFC were also associated with STR. Based on STR, we again categorized the patients into two groups, normal and no-reflow. Those with STR <50% were classified as no-flow patients, and those with STR>50% were grouped into normal-flow patients. Based on STR classification, seven of the 12 differential lipids identified via CTFC classification at pre-PCI significantly differed between normal and no-reflow patients (**Figure-4.6)**. Similarly, nine out of 23 differential lipids were common in post-PCI CTFC and STR classifications. Interestingly, all the differential lipids exhibited the same trend regarding increment or decrement of their amounts in no-reflow and normal flow patients with both groupings.

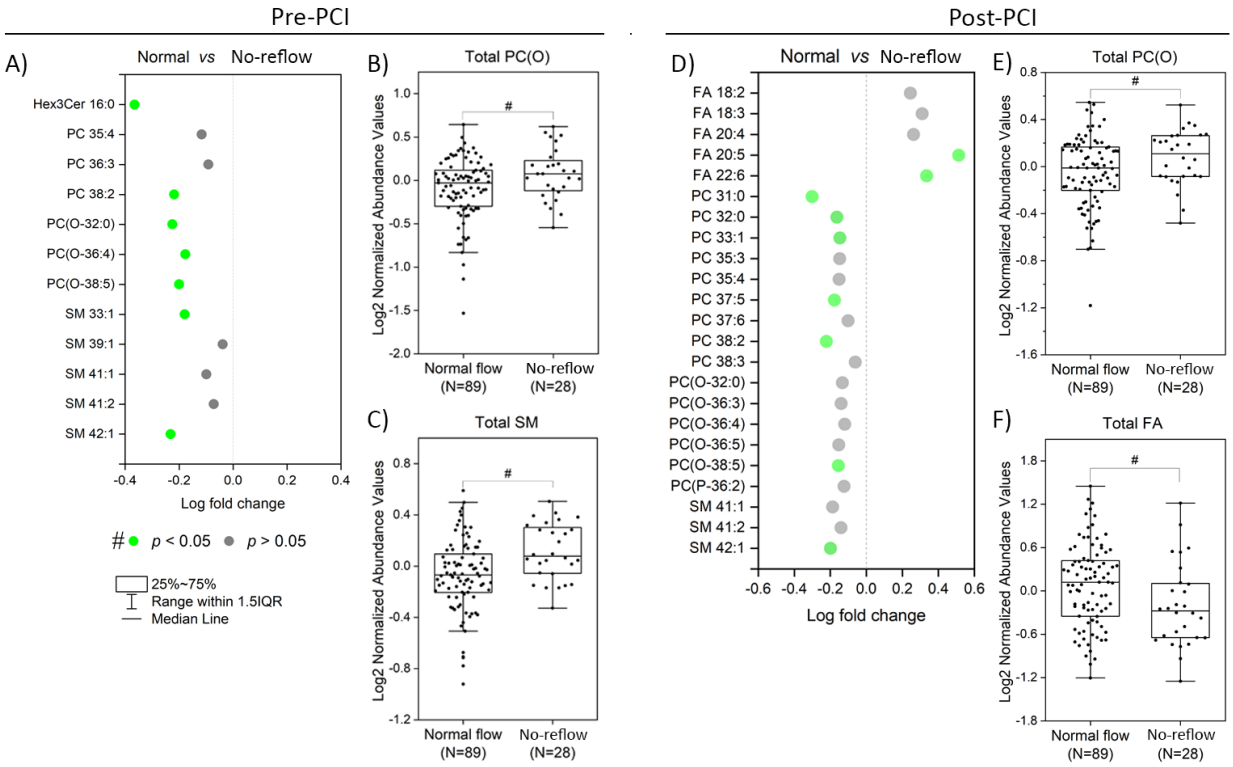

Figure-4.6: Altered lipid species and classes based on ST segment resolution (A) The significantly altered lipid species between normal and no-reflow subjects (ST resolution <50%) at pre-PCI. (B, C) Boxplots of the abundance of lipid classes significantly differed between normal and no-reflow subjects (ST resolution <50%) at pre-PCI. (D) The significantly altered lipid species between normal and no-reflow subjects (ST resolution <50%) at post-PCI. (E, F) Boxplots of the abundance of lipid classes significantly differed between normal and no-reflow subjects (ST resolution <50%) at post-PCI. Green circles show lipid species with $p < 0.05$, and grey circles show lipid species with $p > 0.05$ after independent Student's t-test. # represent statistical significance at $p < 0.05$ after independent Student's t-test.

4.6.6 Correlations between plasma cytokine levels and no-reflow-associated lipids

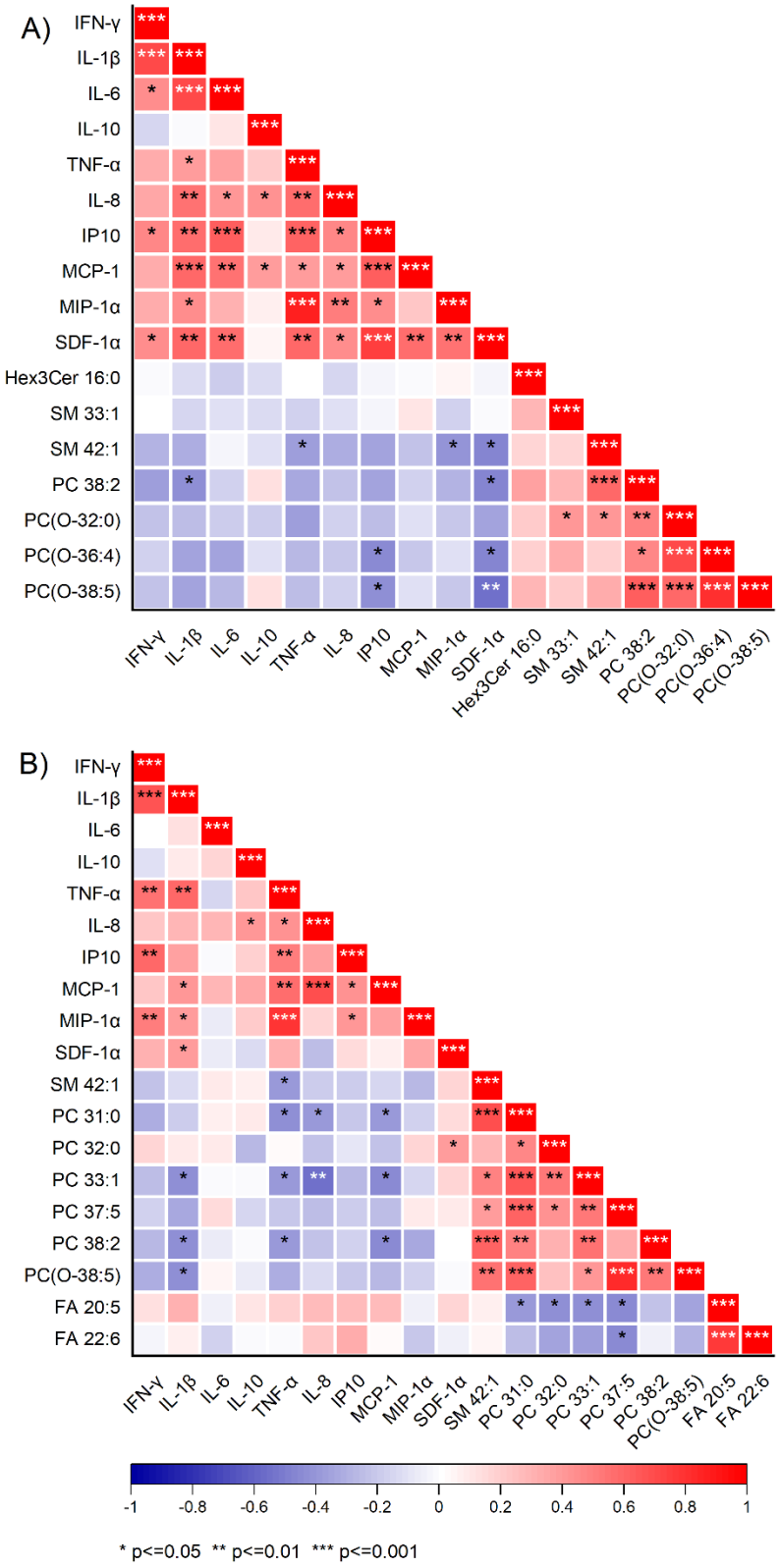

Figure-4.7: Correlation of cytokines with lipid species. The plot shows the association of significantly altered lipids based on both corrected TIMI frame count (CTFC) and ST-segment resolution with ten cytokines at pre-PCI (A) and post-PCI (B) for 28 subjects. The red color symbolizes positive correlation, and the blue color symbolizes negative correlation. *, **, *** represents the significant level at $p < 0.05$, 0.01, 0.001, respectively.

Inflammation is an essential component of myocardial ischemia/reperfusion (IR) injury that underlies no-reflow development[17]. Therefore, we decided to assess the interactions between lipid metabolism and immune response in our cohort (in a subset of 28 STEMI patients). To this end, we choose a panel of 10 cytokines and chemokines associated with inflammatory responses during IR injury. A correlation matrix is displayed in **Figure-4.7**. Two chemokines, namely stromal cell-derived factor 1α (SDF-1α) and interferon-γ-induced protein-10 (IP-10), were correlated inversely ($p<0.05$) with two ether-linked PCs, namely PC(O-36:4), and PC(O-38:5) at pre-PCI (**Figure-4.7A)**. Our data also showed inverse correlation ($p<0.05$) between two PC species, namely PC 33:1 and PC 38:2, and circulating levels of three pro-inflammatory cytokines, namely interleukin 1 beta (IL-1β), tumor necrosis factor-alpha (TNF-α), and monocyte chemoattractant protein-1(MCP-1) at post-PCI (**Figure-4.7B)**. SM 42:1 exhibited an inverse correlation ($p<0.05$) with TNF-α at pre-PCI and post-PCI. Notably, none of the no-reflow-associated lipids were associated with the anti-inflammatory cytokine IL-10 at both intervals.

4.7 Discussion

Our study describes the detailed changes in human plasma lipidome in the setting of NRP in patients undergoing primary PCI. Our results revealed that STEMI patients who develop no-reflow have a distinct lipidomic signature compared to those with normal flow. We found that 1) levels of specific species of phosphatidylcholine (PC), alkylphosphatidylcholine (PC(O)), and

sphingomyelin (SM) were significantly elevated ($p<0.05$) in no-reflow patients; 2) the levels of circulating fatty acids were markedly lower ($p<0.05$) in the no-reflow group than the normal flow group at post-PCI; 3) no-reflow associated lipids were significantly perturbed ($p<0.05$) before and after reperfusion; and 4) specific SM species exhibited a positive association with CTFC and an inverse association with TNF-α, a pro-inflammatory cytokine.

The levels of PC (O-32:0), PC(O-36:4), and PC(O-38:5), as well as total PC(O) levels, were significantly higher ($p<0.05$) in the no-reflow group compared to the normal flow group. This persists even after correction for multiple comparisons at post-PCI ($Q<0.2$). PC(O) is an ether-linked phospholipid in which an ether bond attaches the hydrocarbon chain at the *sn-1* position of the glycerol backbone instead of the more common ester bond[18]. In addition to their structural roles (e.g., lipid packing), ether-linked PCs exert diverse functions ranging from regulating cell differentiation to lipid signaling and inflammation[18,19]. There is also evidence that ether lipids protect against oxidative damage by functioning as endogenous antioxidants[18]. This is particularly interesting in the setting of NRP, where oxidative stress plays a key role[24]. No-reflow is a process that starts with lethal ischemia and increases during reperfusion[5,25]. Within the first few minutes of reperfusion, oxygen-free radicals are produced in excess through multiple pathways, leading to additional myocardial damage, known as myocardial ischemia/reperfusion injury[26,27]. Our findings show a marked increase in the levels of ether-linked PCs in the reperfused state (post-PCI) compared to the ischemic state (pre-PCI). In the current study, the paradoxical increase in circulating levels of ether-linked PCs in no-reflow patients and at reperfused state might be an antioxidant response to increased oxidative stress under these conditions.

Our analysis also revealed that the elevated phospholipids (PC, PC(O), and SM) levels in no-reflow patients at post-PCI are accompanied by a relative reduction in free fatty acid levels,

including arachidonic acid (AA; C20:4) and docosahexaenoic acid (DHA; C22:6). These fatty acids were also significantly (negative) correlated with CTFC at post-PCI. Ether-linked PCs such as those identified in the current study (36:4, 36:5, 38:5) are highly unsaturated and comprise AA as the major fatty acid moiety at the *sn-2* position. Polyunsaturated fatty acids (PUFAs) can be released due to increased phospholipase A2 (PLA2) activity[28]. AA can then be enzymatically oxidized to form bioactive signaling lipids known as eicosanoids, which have recently been implicated in many human diseases, including diabetes and cardiovascular disease (CVD)[29]. They also serve essential functions in cardiovascular homeostasis, such as regulating vascular tone[30]. Since AA is found almost entirely in phospholipids, our current study's observed decrease in arachidonate suggests reduced PLA2 activity in no-reflow patients after coronary intervention. However, it is yet to be seen whether this deficit of arachidonic acid in no-reflow patients leads to reduced biotransformation of arachidonate to AA-derived eicosanoids.

We found that plasma sphingomyelin levels (SM 41:1, SM 41:2, and SM 42:1) were consistently elevated in the no-reflow group at pre-PCI and post-PCI. Of these, the levels of SM 41:1 and SM 41:2 were also positively associated with the levels of CTFC at pre-PCI and post-PCI. This data agrees with two recent reports which have demonstrated that sphingolipids are increased in atherosclerotic plaques compared with normal arteries and that the major source is plasma lipoproteins[31-33]. A lipidomic analysis on the plaques isolated from hypercholesterolemic rabbits showed that SM was present in relatively higher amounts within the atherosclerotic lesions[31]. Consistent with this is the observation that levels of several sphingolipids, including SM, are elevated in symptomatic human atherosclerotic plaques[32]. In another study involving human patients, Tanaka et al.[34] demonstrated that lipid content from culprit plaques is an independent predictor of no-reflow. These data suggest that elevated plasma SM levels in no-reflow patients

likely reflect the higher SM content in the lipid-rich atherosclerotic plaque. The physical destruction of this plaque during PCI may induce an outflow of soluble factors, including lipids from the culprit lesion, into the coronary circulation[34] and may trigger no-reflow.

Our data failed to show any association between plasma levels of inflammatory cytokines and coronary no-reflow, as assessed by CTFC (data not shown). This finding is in line with a previous interventional study[35] which showed that baseline systemic inflammation, as assessed by serum CRP, is not associated with NRP. In general, the correlation between levels of cytokines and no-reflow-associated lipids was inconsistent at pre-PCI and post-PCI. Strikingly, the levels of TNF-α were consistently significantly correlated ($p<0.05$) with levels of SM 42:1 at pre-PCI and post-PCI. TNF-α is a key regulator of MI and IR injury[36] through several signaling pathways, including the production of reactive oxygen species (ROS), synthesis of nitric oxide (NO), or activating sphingomyelinase[36]. TNF-α also participates in regulating lipid metabolism, including sphingolipid metabolism[36,37]. There is evidence that the action TNF-α, in part, is mediated by the SM signal transduction pathway[38,39]. TNF-α is a known agonist of sphingomyelinase, which hydrolyze SM to generate ceramides[40]. This conversion is fast and depends on the cell types involved. The association between SM 42:1 and TNF-α suggests the regulation of immune responses by sphingomyelins during no-reflow in STEMI patients after PCI.

4.8 Study limitations

Firstly, though the present investigation demonstrated novel lipid signatures associated with no-reflow, the molecular basis of these findings remains elusive. Translating these results (body fluid readouts) to target tissues (here, the myocardium) is challenging. One way to address this issue is by combining animal models of no-reflow with omics platforms, such as proteomics, metabolomics, and lipidomics. This approach will help to unravel specific mechanisms and also

help to establish the causal link between circulating lipids and NRP. Secondly, the current study was a single-center study with a relatively small sample size and lacked external validation. Therefore, our primary focus in the future should be to use an independent validation cohort to strengthen our current findings.

Conclusions

In conclusion, by simultaneously quantifying over 300 lipid species in plasma, we identified lipid species and lipid pathways dysregulated in a clinical setting of no-reflow. Our data showed that lipid abnormalities, mainly involving PC, PC(O), SM, and fatty acid species, were associated with no-reflow development. Our results highlight the value of lipidomics in identifying new biomarkers of disease risk and offer a better understanding of the underlying mechanisms involved in disease pathogenesis.

Acknowledgments

The authors are indebted to Mrs. Kiran Atwal, Dr. Zahra Solati, Dr. Andrea Edel, and Dr. Pedram Hassan-Tash for their help with blood sample collection.

Author contributions

Conceptualization, A.R.; methodology, A.R., U.I., A.B., A.S.; sample preparation, A.S., N.A.; statistics, A.S., M.A.; formal analysis, A.S, U.I.; visualization, A.S.; writing - original draft, A.S.; writing - review & editing, A.S, A.R. and M.A.; supervision, A.R., A.Shah, M.A., and P.S.

Declaration of interests

All authors declare no conflicts relevant to the contents of this article.

4.9 References

1 Gupta, S. & Gupta, M. M. No reflow phenomenon in percutaneous coronary interventions in ST-segment elevation myocardial infarction. *Indian Heart Journal* **68**, 539-551, doi:https://doi.org/10.1016/j.ihj.2016.04.006 (2016).

2 Reffelmann, T., Hale, S. L., Li, G. & Kloner, R. A. Relationship between no reflow and infarct size as influenced by the duration of ischemia and reperfusion. *Am J Physiol Heart Circ Physiol* **282**, H766-772, doi:10.1152/ajpheart.00767.2001 (2002).

3 Tanaka, A. *et al.* No-Reflow Phenomenon and Lesion Morphology in Patients With Acute Myocardial Infarction. *Circulation* **105**, 2148-2152, doi:doi:10.1161/01.CIR.0000015697.59592.07 (2002).

4 Fajar, J. K., Heriansyah, T. & Rohman, M. S. The predictors of no reflow phenomenon after percutaneous coronary intervention in patients with ST elevation myocardial infarction: A meta-analysis. *Indian Heart Journal* **70**, S406-S418, doi:https://doi.org/10.1016/j.ihj.2018.01.032 (2018).

5 Rezkalla, S. H. & Kloner, R. A. No-Reflow Phenomenon. *Circulation* **105**, 656-662, doi:doi:10.1161/hc0502.102867 (2002).

6 Soeda, T. *et al.* Morphological predictors for no reflow phenomenon after primary percutaneous coronary intervention in patients with ST-segment elevation myocardial infarction caused by plaque rupture. *European Heart Journal - Cardiovascular Imaging* **18**, 103-110, doi:10.1093/ehjci/jev341 (2016).

7 Katayama, Y. *et al.* No-reflow phenomenon and in vivo cholesterol crystals combined with lipid core in acute myocardial infarction. *Int J Cardiol Heart Vasc* **38**, 100953, doi:10.1016/j.ijcha.2022.100953 (2022).

8 Alshehry, Z. H. *et al.* Plasma Lipidomic Profiles Improve on Traditional Risk Factors for the Prediction of Cardiovascular Events in Type 2 Diabetes Mellitus. *Circulation* **134**, 1637-1650, doi:doi:10.1161/CIRCULATIONAHA.116.023233 (2016).

9 Stegemann, C. *et al.* Lipidomics Profiling and Risk of Cardiovascular Disease in the Prospective Population-Based Bruneck Study. *Circulation* **129**, 1821-1831, doi:doi:10.1161/CIRCULATIONAHA.113.002500 (2014).

10 Surendran, A., Aliani, M. & Ravandi, A. Metabolomic characterization of myocardial ischemia-reperfusion injury in ST-segment elevation myocardial infarction patients undergoing percutaneous coronary intervention. *Sci Rep* **9**, 11742, doi:10.1038/s41598-019-48227-9 (2019).

11 Surendran, A., Atefi, N., Ismail, U., Shah, A. & Ravandi, A. Impact of myocardial reperfusion on human plasma lipidome. *iScience* **25**, 103828, doi:https://doi.org/10.1016/j.isci.2022.103828 (2022).

12 Bouleti, C., Mewton, N. & Germain, S. The no-reflow phenomenon: State of the art. *Archives of Cardiovascular Diseases* **108**, 661-674, doi:https://doi.org/10.1016/j.acvd.2015.09.006 (2015).

13 Gibson, C. M. *et al.* TIMI Frame Count. *Circulation* **93**, 879-888, doi:doi:10.1161/01.CIR.93.5.879 (1996).

14 Weir, J. M. *et al.* Plasma lipid profiling in a large population-based cohort[S]. *Journal of Lipid Research* **54**, 2898-2908, doi:https://doi.org/10.1194/jlr.P035808 (2013).

15 Benjamini, Y. & Hochberg, Y. Controlling the False Discovery Rate: A Practical and Powerful Approach to Multiple Testing. *Journal of the Royal Statistical Society: Series B (Methodological)* **57**, 289-300, doi:https://doi.org/10.1111/j.2517-6161.1995.tb02031.x (1995).

16 de Lemos, J. A. & Braunwald, E. ST segment resolution as a tool for assessing the efficacy of reperfusion therapy. *Journal of the American College of Cardiology* **38**, 1283-1294, doi:https://doi.org/10.1016/S0735-1097(01)01550-9 (2001).

17 Jaffe, R., Charron, T., Puley, G., Dick, A. & Strauss, B. H. Microvascular Obstruction and the No-Reflow Phenomenon After Percutaneous Coronary Intervention. *Circulation* **117**, 3152-3156, doi:doi:10.1161/CIRCULATIONAHA.107.742312 (2008).

18 Dean, J. M. & Lodhi, I. J. Structural and functional roles of ether lipids. *Protein Cell* **9**, 196-206, doi:10.1007/s13238-017-0423-5 (2018).

19 Donovan, E. L., Pettine, S. M., Hickey, M. S., Hamilton, K. L. & Miller, B. F. Lipidomic analysis of human plasma reveals ether-linked lipids that are elevated in morbidly obese humans compared to lean. *Diabetol Metab Syndr* **5**, 24, doi:10.1186/1758-5996-5-24 (2013).

20 Snyder, F., Cress, E. A. & Stephens, N. An unidentified lipid prevalent in tumors. *Lipids* **1**, 381-386, doi:10.1007/bf02532540 (1966).

21 Albert, D. H. & Anderson, C. E. Ether-linked glycerolipids in human brain tumors. *Lipids* **12**, 188-192, doi:10.1007/bf02533292 (1977).

22 Benjamin, D. I. *et al.* Ether lipid generating enzyme AGPS alters the balance of structural and signaling lipids to fuel cancer pathogenicity. *Proc Natl Acad Sci U S A* **110**, 14912-14917, doi:10.1073/pnas.1310894110 (2013).

23 Eisinger, K. *et al.* Lipidomic analysis of the liver from high-fat diet induced obese mice identifies changes in multiple lipid classes. *Experimental and Molecular Pathology* **97**, 37-43, doi:https://doi.org/10.1016/j.yexmp.2014.05.002 (2014).

24 Gür, M. *et al.* Paraoxonase-1 activity and oxidative stress in patients with anterior ST elevation myocardial infarction undergoing primary percutaneous coronary intervention

with and without no-reflow. *Atherosclerosis* **234**, 415-420, doi:10.1016/j.atherosclerosis.2014.03.005 (2014).

25 Ambrosio, G., Weisman, H. F., Mannisi, J. A. & Becker, L. C. Progressive impairment of regional myocardial perfusion after initial restoration of postischemic blood flow. *Circulation* **80**, 1846-1861, doi:doi:10.1161/01.CIR.80.6.1846 (1989).

26 Xiang, M. *et al.* Role of Oxidative Stress in Reperfusion following Myocardial Ischemia and Its Treatments. *Oxid Med Cell Longev* **2021**, 6614009, doi:10.1155/2021/6614009 (2021).

27 Bolli, R. *et al.* Direct evidence that oxygen-derived free radicals contribute to postischemic myocardial dysfunction in the intact dog. *Proc Natl Acad Sci U S A* **86**, 4695-4699, doi:10.1073/pnas.86.12.4695 (1989).

28 Sonnweber, T., Pizzini, A., Nairz, M., Weiss, G. & Tancevski, I. Arachidonic Acid Metabolites in Cardiovascular and Metabolic Diseases. *International Journal of Molecular Sciences* **19**, 3285 (2018).

29 Dennis, E. A. & Norris, P. C. Eicosanoid storm in infection and inflammation. *Nat Rev Immunol* **15**, 511-523, doi:10.1038/nri3859 (2015).

30 Schrör, K. Prostaglandins, other eicosanoids and endothelial cells. *Basic Res Cardiol* **80**, 502-514, doi:10.1007/bf01907914 (1985).

31 Bojic, L. A. *et al.* Lipidome of atherosclerotic plaques from hypercholesterolemic rabbits. *Int J Mol Sci* **15**, 23283-23293, doi:10.3390/ijms151223283 (2014).

32 Edsfeldt, A. *et al.* Sphingolipids Contribute to Human Atherosclerotic Plaque Inflammation. *Arteriosclerosis, Thrombosis, and Vascular Biology* **36**, 1132-1140, doi:doi:10.1161/ATVBAHA.116.305675 (2016).

33 Jiang, X.-c. *et al.* Plasma Sphingomyelin Level as a Risk Factor for Coronary Artery Disease. *Arteriosclerosis, Thrombosis, and Vascular Biology* **20**, 2614-2618, doi:doi:10.1161/01.ATV.20.12.2614 (2000).

34 Tanaka, A. *et al.* Lipid-rich plaque and myocardial perfusion after successful stenting in patients with non-ST-segment elevation acute coronary syndrome: an optical coherence tomography study. *Eur Heart J* **30**, 1348-1355, doi:10.1093/eurheartj/ehp122 (2009).

35 Niccoli, G. *et al.* Baseline systemic inflammatory status and no-reflow phenomenon after percutaneous coronary angioplasty for acute myocardial infarction. *International Journal of Cardiology* **117**, 306-311, doi:https://doi.org/10.1016/j.ijcard.2006.05.012 (2007).

36 Tian, M., Yuan, Y. C., Li, J. Y., Gionfriddo, M. R. & Huang, R. C. Tumor necrosis factor-α and its role as a mediator in myocardial infarction: A brief review. *Chronic Dis Transl Med* **1**, 18-26, doi:10.1016/j.cdtm.2015.02.002 (2015).

37 Maceyka, M. & Spiegel, S. Sphingolipid metabolites in inflammatory disease. *Nature* **510**, 58-67, doi:10.1038/nature13475 (2014).

38 Kim, M. Y., Linardic, C., Obeid, L. & Hannun, Y. Identification of sphingomyelin turnover as an effector mechanism for the action of tumor necrosis factor alpha and gamma-interferon. Specific role in cell differentiation. *J Biol Chem* **266**, 484-489 (1991).

39 Lecour, S. *et al.* Identification of a novel role for sphingolipid signaling in TNF alpha and ischemic preconditioning mediated cardioprotection. *J Mol Cell Cardiol* **34**, 509-518, doi:10.1006/jmcc.2002.1533 (2002).

40 Dressler, K. A., Mathias, S. & Kolesnick, R. N. Tumor necrosis factor-alpha activates the sphingomyelin signal transduction pathway in a cell-free system. *Science* **255**, 1715-1718, doi:10.1126/science.1313189 (1992).

CHAPTER 5. Discussion

Cardiovascular disease (CVD) is the world's leading cause of morbidity and mortality[1]. According to the latest WHO data, it is accountable for over 30% of all global deaths, most of which were due to heart attacks (myocardial infarction)[1]. Therefore, the early diagnosis of CVD is essential for better management of the disease. Significant advances have been made in treating myocardial infarction (MI) over the past two decades. In particular, timely restoration of blood flow to the myocardium during ischemia, named reperfusion, using percutaneous coronary interventions (PCI) or thrombolytic approaches, has been a significant step forward.

Nevertheless, while 'reperfusion' is the primary therapeutic aim for limiting the myocardial infarct size and bettering the clinical outcome, the process of ischemia, followed by reperfusion, can also induce additional injury, a phenomenon termed myocardial ischemia/reperfusion (I/R) injury. In a clinical setting, the largest impact of I/R injury is in patients presenting with an acute ST-segment elevation myocardial infarction (STEMI) who undergo revascularization. Even after early and fast reperfusion, the 30-day mortality rate for these patients is nearly $5\%^{2}$. Not only is there scant information on the metabolic changes within human plasma during I/R but there are also currently no therapies available to attenuate the devastating clinical impact of I/R injury.

Non-targeted metabolomics analysis

The first objective was to complete a comprehensive non-targeted metabolomics analysis of plasma from STEMI patients undergoing primary PCI. This allowed us to determine the metabolic patterns that highlight altered metabolic pathways during I/R and its clinical relevance. Plasma samples were collected from 27 STEMI patients before primary PCI; and at three time points after PCI (2 h, 24 h, and 48 h).

Our analysis discovered 130 metabolites in plasma that were significantly perturbed ($p < 0.001$) in the setting of I/R injury during the first 48 hours[3]. Interestingly, **lipid molecules represent the largest pool of metabolites changing over the first 48 h**. The visualizing plots, principal component analysis (PCA), and partial least square discriminant analysis (PLS-DA) demonstrated that the initial time intervals (0 h, 2 h) and final time intervals were well separated. This suggests that **sudden revascularization employing PCI introduced significant changes within the human plasma metabolome**. The pathway analysis revealed the perturbed metabolic pathways during I/R injury. The altered metabolic pathways indicative of the early reaction to reperfusion (2 h after reperfusion) were associated with valine, leucine, and isoleucine biosynthesis, vitamin B6 metabolism, and glutathione metabolism. Also, the altered pathways (24 h and 48 h after reperfusion) indicative of the late response to reperfusion were associated with phenylalanine metabolism, tyrosine metabolism, linoleic acid metabolism, and glycerophospholipid metabolism. Notably, the metabolic pathways indicative of the early reaction to reperfusion were quite different from those representing the late response to reperfusion. The ROC analysis identified three lipid species, namely pentadecanoic acid (15:0), linoleoyl carnitine (18:2 carnitine), and 1-linoleoylglycerophosphocholine (18:2 LPC), that **can predict the extent of myocardial infarction at 48 h based on the initial blood sampling**. This suggests that these three lipids' levels at admission are a marker of myocardial infarct size following primary PCI.

Targeted lipidomics analysis

The large inventory of perturbed lipid molecules found in blood plasma (plasma lipidome) from our non-targeted metabolomic analysis offers insights into the disturbances in lipid metabolism in STEMI patients following reperfusion. **The second objective builds upon our initial findings from the non-targeted research by moving it into the next stage – the targeted analysis of**

lipids in a clinical setting of myocardial reperfusion injury in humans. We looked at over 300 lipid species spanning 25 different lipid classes/subclasses semi-quantitatively. This helped to determine the lipid molecules that exhibited a significant difference ($p<0.05$) before primary PCI and in the follow-up time points and to correlate these changes to clinical outcomes. The samples were collected from 80 STEMI patients undergoing primary PCI from multiple time points until 30 days.

In agreement with our previous results, the lipidomics analysis showed that **sudden reperfusion using PCI brings about significant changes within the plasma lipidome**. Barring oxidized phospholipids (OxPL), the total amount of most of the lipid classes was markedly reduced immediately after reperfusion. The higher OxPL content after PCI may suggest increased oxidative stress in the wake of reperfusion. The circulating free fatty acids (FA) exhibited the most extensive change in the first 24 h after PCI. This was followed by neutral lipids (DG, TG) and OxPLs. The levels of FAs decreased, while neutral lipids increased after reperfusion. This suggests the likely involvement of an active triglyceride-FA-triglyceride cycle in reperfusion injury. At the species level, a few phosphatidylcholine (PC) species were affected due to reperfusion. However, all phosphatidylinositol (PI) species were altered before and after reperfusion. This shows the resistance offered by PC species against oxidative damage to maintain membrane fluidity.

We identified **three lipids, acylcarnitine 18:2, TG 51:0, and LPC 17:1, which have the potential to predict clinical outcomes in STEMI patients after PCI**. These three lipids could also distinguish STEMI patients with less cardiac injury from those with sizeable cardiac injury. In addition, these three lipids were also associated with future cardiovascular events. Among these three lipids, the baseline levels of acylcarnitine 18:2, and LPC 17:1 as well as their respective whole class amount were significantly higher ($p< 0.05$) in the STEMI population compared to the

age and gender-matched control subjects. Of these, acylcarnitine 18:2 deserves special attention as it is one among the three lipids identified by our initial non-targeted metabolomics analysis as a marker of myocardial injury following reperfusion. These results suggest that dysregulation in lipid metabolism plays a vital role in the onset and progression of reperfusion injury.

Lipidomic predictors of coronary no-reflow in STEMI patients

No-reflow in STEMI patients initiates during the ischemic period and then progresses during reperfusion[4]. Our previous results showed that lipid-related disturbances play a critical role during ischemia and reperfusion. Therefore, our third objective was to investigate the changes within human plasma lipidome during coronary no-reflow in STEMI patients and to correlate these changes with clinical parameters that represent no-reflow, including ST-segment resolution difference (from ECG) and corrected TIMI frame count (CTFC, from coronary angiography). Our cohort consisted of 126 STEMI patients undergoing PCI, and they were categorized into normal flow and no-reflow based on their CTFC after PCI.

We identified an **increased abundance of phosphatidylcholine (PC), alkylphosphatidylcholine (PC(O)), and sphingomyelin (SM) species in no-reflow patients at the time of admission**. The total PC(O) level remains elevated pre- and post-PCI. PC(O) is an ether lipid characterized by the presence of an ether linkage. Ether lipids play a protective role against oxidative damage by functioning as endogenous antioxidant[5]. Therefore, the observed abundance of ether lipids in no-reflow patients might be an antioxidant response to increased oxidative stress at reperfused state. Interestingly, the increased amounts of phospholipids (PC, PC(O), and SM) at post-PCI coincided with the decreased abundance of FAs. In addition, these FAs exhibited an inverse correlation with CTFC at post-PCI. We propose that the observed decreased abundance of FAs might result from the reduced activity of the enzyme phospholipase A2 (PLA2) in no-reflow patients. The level of

several sphingomyelin species was significantly higher ($p<0.05$) in the no-reflow group compared to the normal flow group at pre- and post-PCI. Moreover, their levels (e.g., SM 42:1) significantly correlate ($p<0.05$) with the level of tumor necrosis factor-alpha (TNF-α), a mediator of immune functions, at pre- and post-PCI. This suggests the role played by sphingomyelins in regulating immune responses during coronary no-reflow in STEMI patients. To the best of this author's knowledge, this is the first study to investigate over 300 circulating lipids using a lipidomics approach in a setting of coronary no-reflow in STEMI patients. We showed associations of novel plasma lipids with coronary no-reflow and mined perturbed lipid pathways in the setting of no-reflow.

Significance

Limiting reperfusion injury in STEMI patients after revascularization is an active study area. Unfortunately, the success has been limited to classic models of experimental reperfusion injury. Many factors are responsible for this, including poorly designed experimental design, lack of statistical robustness and validity, and, most importantly, the complexness of the human *in vivo* model. Most other studies in the setting of I/R injury focussed on a single metabolite, a specific metabolite class (e.g., fatty acids or eicosanoids), or a single pathway (e.g., BCAA metabolism). To our knowledge, this is the first study attempting to incorporate time course analyses in the setting of human I/R injury. This helped us better understand the dynamic changes and metabolic pathways involved in human I/R injury. Our analysis provided new insights into the metabolic and lipid disturbances that are operative in the pathogenesis of I/R injury. We uncovered novel metabolites and metabolic pathways that accompany I/R injury in human subjects. These findings will move us closer to our ultimate goal of improving diagnostic capability and treatment strategies for STEMI patients.

Limitations of study and future directions

We took several precautions to minimize biases while designing this study. We employed a serial blood sampling in which each patient is sampled at different time points, thereby minimizing the inter-individual biological variability. However, there are certain caveats when interpreting the results of this study. First of all, this single-center study lacks a replication cohort. Therefore, extrapolation of the current findings to other populations is challenging. One way to overcome this is by conducting independent metabolomics studies in diverse STEMI cohorts (multi-centric) to evaluate our results. The use of multiple analytical platforms (triple quadrupole, quadrupole and time-of-flight MS systems) has its inherent merits and drawbacks. While we covered a broad spectrum of circulating metabolites and lipids, some metabolite categories and classes were still missing from our analysis (e.g., bile acids). Our lipidomics platform does not resolve fatty acyl chains' sn-position (composition and position of fatty acyl chain) on the glycerol backbone. Therefore, there is the likelihood that identified lipid markers are not unique molecules but represent a mixture of molecular isomers (e.g., SM 42:1). The determination of acyl chain composition requires extensive chromatographic or ion-mobility separations or derivatization methods.

We also lack information on the dietary habits and feeding history of our STEMI patients. This could probably be a confounder for our analysis since dietary patterns profoundly impact the endogenous metabolome. Identifying metabolites related to the intake of foods and diets among study subjects can help identify more meaningful biological variations in future studies.

We highlight that we analyzed venous plasma samples, not coronary sinus or myocardial tissue samples. Hence, translating our findings at the myocardial level is challenging. The observed associations of metabolites with each other and established clinical markers (e.g., troponin) in this

study should be considered hypothesis-generating. One way to address this issue is to use animal models of myocardial I/R injury by integrating metabolomics with genomics and proteomics. This will help to establish a causal link between metabolites of interest and disease pathogenesis. Also, further studies should be directed to assess the metabolite concentrations in arterial blood and the coronary sinus as it will provide more accurate information on the metabolic changes within the heart.

References

1 Organization, W. H. *Cardiovascular diseases*, <https://www.who.int/news-room/fact-sheets> (2021).

2 Lambert, L. *et al.* Association between timeliness of reperfusion therapy and clinical outcomes in ST-elevation myocardial infarction. *Jama* **303**, 2148-2155, doi:10.1001/jama.2010.712 (2010).

3 Surendran, A., Aliani, M. & Ravandi, A. Metabolomic characterization of myocardial ischemia-reperfusion injury in ST-segment elevation myocardial infarction patients undergoing percutaneous coronary intervention. *Sci Rep* **9**, 11742, doi:10.1038/s41598-019-48227-9 (2019).

4 Rezkalla, S. H. & Kloner, R. A. No-Reflow Phenomenon. *Circulation* **105**, 656-662, doi:doi:10.1161/hc0502.102867 (2002).

5 Dean, J. M. & Lodhi, I. J. Structural and functional roles of ether lipids. *Protein Cell* **9**, 196-206, doi:10.1007/s13238-017-0423-5 (2018).